In vivo functional genetic analysis of cytochromes P450 involved in insecticide resistance in the malaria vector *Anopheles gambiae*

Thesis submitted in accordance with the requirements of the University of Liverpool for the degree of Doctor in Philosophy by

Adriana Adolfi

Primary supervisor: Dr. Gareth J. Lycett

Secondary supervisor: Prof. Hilary Ranson

July 2017

Declaration

Statement 1

This work has not previously been accepted in substance for any degree and is not being currently submitted in candidature for any degree.

Signed …… 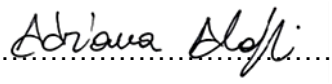 ……(Candidate)

Date……13/07/2017……

Statement 2

This thesis is the result of my own investigation, except where otherwise stated. Other sources are acknowledged and bibliography appended.

Signed …… 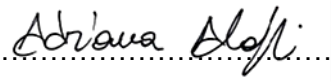 ……(Candidate)

Date……13/07/2017……

Statement 3

I hereby give my consent for this thesis, if accepted, to be available for photocopying and for inter-library loan, and for the title and summary to be made available to outside organisations.

Signed …… 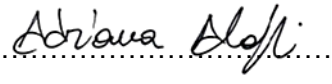 ……(Candidate)

Date……13/07/2017……

“*Above all, don’t fear difficult moments. The best comes from them.*”

Rita Levi-Montalcini (Italian neurobiologist, 1909-2012)

Nobel Prize in Physiology or Medicine (1986)

Acknowledgments

I would like to express my sincere gratitude to my supervisor, Gareth Lycett, whose patience, encouragement and expertise guided me through this project.
I am grateful for the numerous stimulating conversations that inspired me to look at things from different perspectives and helped me maturing as a researcher. He pushed me beyond my limits and encouraged me to be curious, inquisitive, and to be critical about science.
I appreciate the praise I received as well as the criticism. Thanks for sitting in the audience of all my presentations and saying 'well done' at the end; for taking me out for dinner when I got my first transgenics; for bringing coffee and food during my long weekend hours.
I am most grateful for his genuine interest in my development as a researcher and in my future career prospects.
Gareth's support was there every step of the way. Without his encouragement, patience, and enthusiasm it would have been impossible to complete this work, and certainly it would not have been as exciting and formative as it has been.

My gratitude goes to Hilary Ranson for supporting the project and me personally, and for being an outstanding example of women in science.

I am sincerely thankful to Martin Donnelly, whose office door was always open for advice and who challenged and supported me through the years.

This work would have been considerably harder without the help of members of the Lycett group with whom I shared insectary weekend duties. Thanks to Amy Lynd, who was there from day one of my PhD, when everything was new and I had to learn it quickly. She thought me most of what I know about mosquito rearing and molecular cloning and she was there to answer my questions, for that I am grateful. Thanks to Amalia Anthousi, for her help with mosquito rearing, her constant support, and the endless provisions of Cretan delicacies.

I also owe thanks to Angela Hughes, who helped me with anything I needed in the lab, and to Vicky Ingham, Eva Caamaño and Arturas Grauslys for advice on data analysis.

This PhD would have not been the same without my current and past colleagues, but above all friends – Angela Hughes, Glauber Pacelli Gomes de Lima, Grazia Camarda, Amalia Anthousi, Cristina Yunta Yanes, Jacob Riveron Miranda, Nelson Grisales Alzate, Chris Spencer, Eva Caamaño and Eilidh Carrington – with whom I shared the most fun times of my stay in the UK. I must reserve a special thanks to Grazia, Cristina, Ange, Glauber and Jacob for their support and for being always available for a coffee or a chat.

Thanks to everybody in the Vector Group for unforgettable annual Christmas parties and Lab days out.

Lunch breaks would not have been the same without the “LSTM Italian club” – Martina Savio, Arianna Braccioni, Grazia Camarda, Federica Guglielmo, Corrado Minetti, and Luca Facchinelli. Thanks for good chats in my beautiful native language.

Thanks to my friends from home – Chiara Franzonello, Elina Conti, Annalú Mirone, Chiara Brunetto, Giuliana Pennisi, Renata Scalia – for making all my trips back to Catania a joy and for always making me feel close to home.

My ultimate gratitude goes to my tireless and biggest supporters, Mum and Dad. I could not have made it through without their encouragement. Thanks for believing in me and for supporting my dreams, even if it meant going far away from home. Also thanks to my sister Ale, my brother Salvo and my niece Irene, for keeping me smile every day. Grazie di cuore.

Lastly, I wish to express my most sincere gratitude to my fiancé, Peter Shum, who has shared the ups and downs of my PhD since the very beginning. His understanding of my long working hours, his endless encouragement, support, and reassurance were invaluable and made this journey truly special.

Abstract

Insecticide-based vector control strategies have greatly contributed to malaria control, yet their success is hindered by the spread of resistance. It is thus essential to discover the molecular basis of resistance to use the current insecticides effectively and to search for new ones informatively. In *Anopheles gambiae*, overexpression of single detoxifying enzymes of the P450 (CYP) family has been strongly associated with resistance, yet *in vivo* analysis has only been performed in the fruit fly. Furthermore, patterns of P450 overexpression that lead to resistance, which are crucial to identify detoxification pathways, remain unclear. This study aims to investigate the role of two genes, *Cyp6m2* and *Cyp6p3*, in conferring resistance *in vivo* in *An. gambiae* when overexpressed tissue-specifically in the midgut, oenocytes, or Malpighian tubules or in multiple tissues.

To obtain spatially-controlled gene overexpression the GAL4/UAS system was employed. Responder lines for the expression of *Cyp6s* were created by PhiC31-RMCE and crossed with two tissue-specific drivers specific for the midgut or the oenocytes. Resistance phenotype assessment, conducted according to WHO guidelines, revealed no difference in mortality between mosquitoes overexpressing *Cyp6* genes and controls after exposure to four different insecticides, suggesting that overexpression confined to these tissues is not sufficient to drive resistance.

We therefore aimed to examine overexpression in the Malpighian tubules and in multiple tissues. Since promoters for these locations had not been characterised, putative regulatory regions were isolated from genes showing desired patterns of expression. Two main candidates, PUBc and GPI, were chosen after assessing their activity by luciferase assay in mosquito cells, and were used to create driver lines using the piggyBac transposon. Random insertion was chosen to identify single genomic sites able to sustain widespread expression and at the same time create new PhiC31 docking lines at these permissive sites. Patterns of expression induced by PUBc drivers carrying single insertions were investigated by crossing with a responder UAS:mCherry line. Two drivers were isolated that induced multi-tissue expression in all life stages and both sexes at relatively higher (A10) and lower (A8) levels. In similar experiments, the ubiquitous GPI and the Malpighian-specific VATG candidate promoters did not show visible mCherry expression.

The PUBc driver lines were finally used to assess resistance resulting from multi-tissue overexpression. Ubiquitous expression of *Cyp6m2* under the control of the A10 driver correlated with acquisition of WHO levels of resistance to pyrethroids, while that of *Cyp6p3* with resistance to pyrethroids and bendiocarb; DDT resistance was not affected. Lower levels of overexpression driven by A8 did not significantly alter the resistance phenotype except for permethrin resistance when *Cyp6m2* is overexpressed. Furthermore, *Cyp6* overexpression driven by A10 or A8 caused an increase in susceptibility to the pro-insecticide malathion, supporting the role of specific CYP6s in providing negative cross-resistance between insecticide classes.

This study provides the first *in vivo* evidence of the role of *Cyp6s* in causing WHO-defined resistance in *An. gambiae*, suggesting that location and level of overexpression are critical. Overall, this work contributed to the optimisation of a system for *in vivo* functional analysis in transgenic *An. gambiae* through the characterisation of a novel ubiquitous promoter and the ability to modulate level of expression using alternative drivers. Such a system is physiologically more relevant than the current *Drosophila*-based system for *in vivo* validation of mosquito resistance gene. In addition, metabolically resistant lines created here can be included alongside field-caught populations for screening new insecticides.

Table of Contents

List of Figures

List of Tables

List of Abbreviations

An.	*Anopheles*
WHO	World Health Organisation
Ae.	*Aedes*
C.	*Culex*
D.	*Drosophila*
B.	*Bombyx*
P.	*Plutella*
T.	*Tribolium*
DDT	Dichloro-Diphenyl-Trichloroethane
VGSC	Voltage-Gated Sodium Channel
ITN	Insecticide Treated Net
LLIN	Long Lasting Insecticidal Net
PBO	Piperonyl Butoxide
PPF	Pyriproxyfen
IRS	Indoor Residual Spraying
Kdr	Knock-Down Resistance
AchE, Ace-1	Acetylcholinesterase
GABA	Gamma-Aminobutyric acid
Rdl	Resistance to Dieldrin
GST	Glutathione S-Transferase
CCE	Carboxyl/Choline Esterase
P450	Cytochrome P450 monooxygenase
CYP6	Cytochrome P450 family 6
RMCE	Recombinase-Mediated Cassette Exchange
UAS	Upstream Activating Sequence
PCR	Polymerase Chain Reaction
LD	Lethal Dose
YFP	Yellow Fluorescent Protein
CFP	Cyan Fluorescent Protein
DsRed	*Discosoma sp.* red fluorescent protein

Chapter 1

Introduction

1.1 Malaria and mosquito vectors

1.1.1 The disease

Malaria is a parasitic vector-borne disease which imposes a major human health burden in tropical and subtropical regions of the world. In 2015 transmission was active in 91 countries with 212 million cases and 429,000 deaths estimated, 92% of which occurred in Sub-Saharan Africa (WHO, 2016a).

The disease is caused by protozoa of the *Plasmodium* genus and transmitted to humans by female *Anopheles* mosquitoes. Five *Plasmodium* species are responsible for human infections: *P. falciparum*, *P. vivax*, *P. ovale*, *P. malariae*, and *P. knowlesi*. *P. falciparum* is responsible for most malaria-related deaths and is predominant in the African continent, but it is also extensively found in South-East Asia (Sinka et al., 2011). Outside Africa, *P. vivax* is the most common malaria parasite (WHO, 2016a), with almost half of the worldwide population at risk of *P. vivax* infection living in India (Sinka et al., 2011).

For the parasite life cycle to complete, it must encompass two hosts, a human and a mosquito. In the human host, asexual replication takes place in the liver (asymptomatic stage) and in red blood cells (symptomatic stage). Blood stage replication recurs cyclically and determines erythrocyte lysis which causes peaks of fever characteristic of the disease. In the most severe *P. falciparum* cases where the parasitic load is high, asexual forms can clog brain capillaries (cerebral malaria) causing neurological complications and death. In the mosquito host, sexual reproduction occurs with the formation of mature gametes that fuse forming a mobile ookinete which attaches to the outer epithelium of the mosquito midgut forming an oocyst. The infective stage sporozoites develop within the oocyst before bursting out and migrating to the salivary glands where they are transmitted to a human host via an infectious bite from a female. The parasite life cycle in the mosquito (sporogonic cycle) typically lasts 10-18 days depending on ambient temperature (CDC, 2015a).

1.1.2 The vectors

Vectors responsible for human malaria transmission are mosquitoes of the genus *Anopheles* (order Diptera, family Culicidae, sub-genus *Cellia*) and, while there are over 400 species of anophelines, only 41 are known to transmit human malaria (Hay et al., 2010).

Anopheles species are distributed worldwide (Figure 1.1). In Africa, the dominant vector species are members of the *An. gambiae* complex (*An. gambiae sensu stricto*, *An. coluzzi*, *An. arabiensis*, *An. merus*, *An. melas*) as well as *An. funestus*, *An. moucheti* and *An. nili* (Sinka et al., 2010a). Dominant vector species in the Asian-Pacific region are difficult to define due to the complex co-existence of multiple species including *An. stephensi*, *An. dirus*, *An. minimus,* and *An. sinensis* (Sinka et al., 2011). Anophelines most commonly found in the Americas are *An. albimanus*, *An. darling* and *An. freeborni* (Sinka et al., 2010b). In European and Middle-Eastern regions, where malaria transmission is rare, *An. messeae* shows the largest distribution across northern countries (Sinka et al., 2010a).

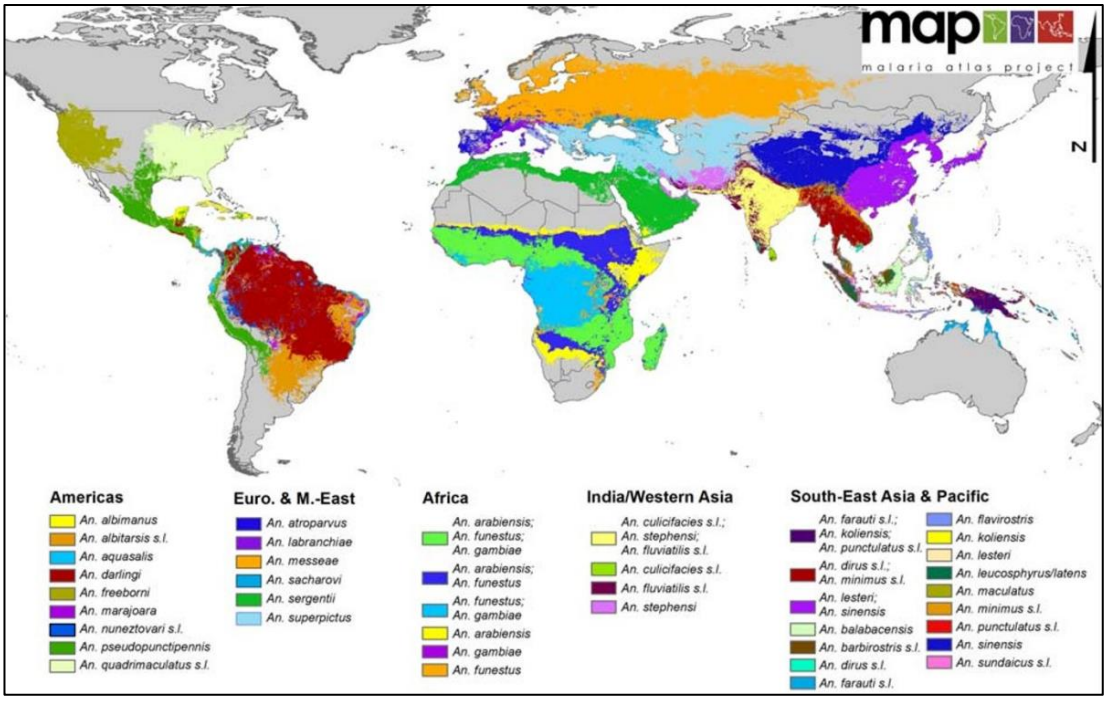

Figure 1.1 Worldwide distribution of malaria vectors (taken from Sinka et al., 2012).

Only adult females are responsible for disease transmission as they inoculate sporozoites while taking a blood meal that is essential for egg production. Therefore,

transmission dynamics are largely dependent on the number of infective bites received, which, in turn, changes with mosquito population size. This is overall dependent on weather conditions (temperature, humidity, rainfall) suitable for successful development of mosquitoes through egg, larva, and pupa stages into adults, as well as the longevity of females for completion of the sporogonic cycle. Part of the reason why Africa accounts for the highest malaria morbidity and mortality is that it hosts the most effective vectors that transmit *P. falciparum*, *An. gambiae* mosquitoes. These exist in close contact with humans as they are primarily attracted by human blood (anthropophilic) and preferentially feed at night and rest indoor (endophagic and endophilic) (CDC, 2015b).

A remarkable amount of financial resources (US$ 2.9 billion in 2015) and efforts have been spent in malaria control programs with the aim of reducing human infections (WHO, 2016a). These include vector control strategies, preventive therapeutic interventions, early diagnosis and prompt drug treatment. Taken together, these resulted in a reduction of malaria incidence by 40%, equalling 663 million fewer malaria cases between 2000 and 2015 (Bhatt et al., 2015). Relative contributions of anti-malaria interventions were calculated to be ~68% from insecticide-treated bed nets, ~22% from artemisinin-based combination therapy, and ~10% from indoor residual spraying of insecticides (Bhatt et al., 2015). While encouraging, the emergence and spread of resistance to insecticides and to antimalarial drugs, along with the lack of a vaccine, pose real threats to these achievements.

1.2 Vector control strategies

1.2.1 Insecticide-based vector control

Most vector control interventions rely on the use of chemical insecticides to kill adult mosquitoes. These strategies include the distribution of insecticide-treated bed nets (ITNs) and indoor spraying (IRS), but also outdoor fogging, treatments of surfaces such as curtains, window screens and eave baffles, and the used of insecticide-treated durable wall lining (WHO, 2016a; Killeen et al., 2017; Messenger & Rowland, 2017). Insecticides such as organophosphates are also use to control larval stages by treating the water in which mosquitoes breed; similarly, synthetic chemicals such as the juvenile hormone analogue pyriproxyfen (PFF) are found to be effective larvicides (WHO, 2016a).

1.2.1.1 Insecticides used in vector control

Currently four main classes of insecticides sharing two modes of actions are used for vector control. All classes can be used for indoor spraying, but only pyrethroids are approved to be used on bed nets (WHO, 2006).

Organochlorines include organic compounds containing covalently bonded atoms of chlorine. Two main groups exist with different modes of action: DDT-like compounds (e.g. DDT) (Figure 1.2) and alicyclic compounds (e.g. dieldrin) (Figure 1.2). Both organochlorine types affect nerve impulse and cause death by paralysis by interfering with the physiological function of the voltage-gated sodium channel (VGSC) (DDT) or the gamma-aminobutyric acid (GABA) receptor (dieldrin) (Coats, 1990; Anthony et al., 1993). DDT was the first synthetic insecticide introduced in public health in the 1940's. Although very effective in combatting vector-borne diseases, its environmental impact as an organic pollutant caused the Environmental Protection Agency to ban it from agriculture and restrict its use to indoor spraying campaigns according to WHO recommendations (Mellanby, 1992). The use of dieldrin was banned due to similar issues.

Organophosphates are esters of phosphoric acid that bind covalently and irreversibly to the acetylcholinesterase enzyme (AChE), which is responsible for the termination of the nerve impulse through degradation of the neurotransmitter acetylcholine. Their binding to AChE results in persistent neuronal firing and insect death by paralysis (Fukuto, 1990). They are deployed in their non-insecticidal form and need to be activated by oxidation in their toxic -oxon forms (Cohen, 1984) (Figure 1.2). Organophosphates such as temephos and fenthion have been successfully used as larvicides (WHO, 2006).

Carbamates are chemically characterised by the presence of a carbamate ester group (Figure 1.2). They share the same mode of action of organophosphate insecticides (Fukuto, 1990), although their binding to AchE is reversible.

Pyrethroid insecticides are synthetic chemicals derived from natural organic compounds produced by *Pyrethrum* flowers. They are neurotoxins that target the VGSC and share the same mechanism of action of organochlorine insecticides (Vijverberg et al., 1982). This class is the most exploited in public health due to its low mammalian toxicity and rapid knock down effect on insects, which make pyrethroids the only class allowed for treating bed nets (WHO, 2006). There are two chemically distinct forms: type I (lacking a cyanide group), such as permethrin (Figure 1.2), and type II (containing a cyanide group), such as deltamethrin (Figure 1.2).

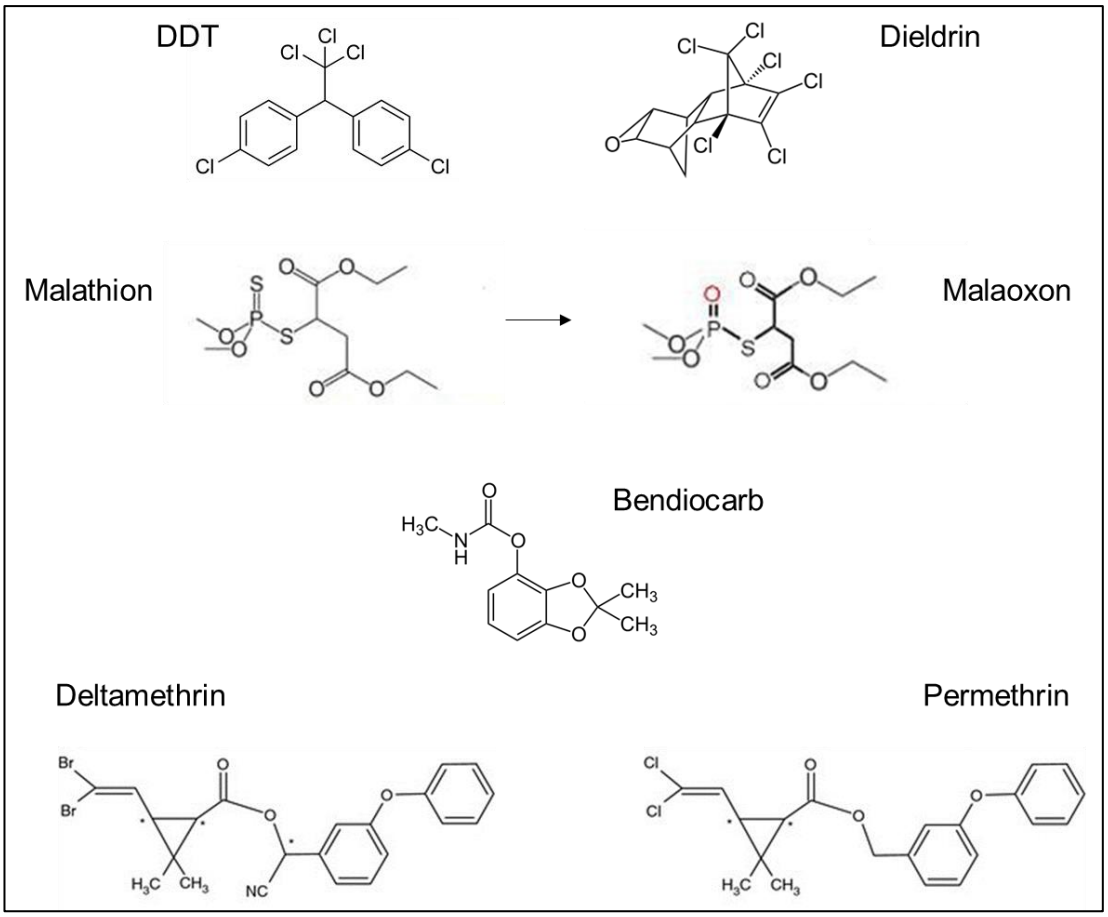

Figure 1.2 Structural representatives of the four classes of insecticides used in public health to control *Anopheles* mosquitoes.

1.2.1.2 Insecticide Treated Nets (ITNs)

Sleeping under an insecticide-treated bed net combines the protection from a physical barrier that prevents the vector from making contact with the human host, with that of a chemical barrier with killing and repellent insecticidal properties (WHO, 2006; Kawada et al., 2014). Therefore, ITNs have the dual aim of reducing human-vector contact while decreasing mosquito density by killing female indoor night biters. Pyrethroids used for ITNs include α-cypermethrin, cyfluthrin, etofenprox, λ-cyhalothrin deltamethrin and permethrin (WHO, 2006), of which the latter two were most often used in the first wave of bed nets production.

A new version of ITNs, long-lasting insecticidal nets (LLINs), has improved issues related with longevity of activity and durability (WHO, 2011). LLINs that have received full WHO approval are Olyset® (permethrin), Interceptor® (α-cypermethrin), PermaNet®2.0 and Yorkool®LN (deltamethrin) (WHO, 2012a). While nets undergoing

preliminary assessment include Olyset®Plus and PermaNet®3.0 which contain permethrin and deltamethrin respectively coupled with the synergist piperonyl butoxide (PBO) (WHO, 2015b). PBO does not have insecticidal properties but synergises the activity of pyrethroids by inhibiting the activity of P450 enzymes that are responsible for pyrethroid breakdown. Similarly, trials are ongoing for the assessment of Olyset®Duo, which contains permethrin and the juvenile hormone analogue PFF which acts as a sterilising agent in adult mosquitoes (Tiono et al., 2015).

1.2.1.3 Indoor Residual Spraying (IRS)

Vector control through IRS consists of spraying insecticides on internal household surfaces (walls, eaves, ceiling) that the malaria vector is likely to contact. Therefore, this intervention targets specifically females that rest indoors after a blood meal and thus aims to reduce lifespan and subsequently overall vector density (WHO, 2006).

Spraying is carried out by trained personnel at intervals that usually coincides with seasonal peaks of abundance of vectors in a specified geographic location (WHO, 2015a). Members from all classes of insecticides can be used for IRS, therefore the compound to be used should ideally be chosen based on the susceptibility status of the local malaria vector. IRS procedures are standardised according to guidelines from the WHO Pesticide Evaluation Scheme (WHOPES) which specifies, among others, insecticide concentrations and formulations to be used (WHO, 2009; WHO, 2015a).

1.2.2 Alternative insecticide-free vector control

Insecticide-free strategies have been developed that are safer to humans and non-target wildlife and for which resistance development is less likely (David et al., 2013). Such interventions include biological control targeted at eliminating the larval stage using bacterial toxins from *Bacillus thuringiensis israelensis*, fungal pathogens, and natural mosquito predators such as fish, nematodes, and amphibian tadpoles (Raghavendra et al., 2011). Recently, biological control of *Aedes* mosquitoes using Wolbachia has been suggested as mosquitoes carrying this bacterial symbiont showed reduced viral replication (Moreira et al., 2009) and longevity (McMeniman et al., 2009). Furthermore, cautious environmental management aimed at modifying or disrupting natural mosquito habitats and preventing the creation of artificial breeding

sites, plays a key role as part of integrated vector control strategies (Raghavendra et al., 2011). Finally, with the recent advancement in transgenic mosquito technologies, control strategies based on genetically-modified organisms and intended for suppression or replacement of wild populations open promising perspectives (Gabrieli et al., 2014). Suppression strategies are based on reducing vector populations, usually by modifying insect mating/fertility or subsequent development. The first of such strategies was the Sterile Insect Technique (SIT) (Knipling, 1955) which consists of releasing sterile males. However, this intervention has been argued to be costly, laborious, and difficult to sustain (Papathanos et al., 2009a; Alphey et al., 2010). An enhancement of the SIT technology, called RIDL (Release of Insects with Dominant Lethality), was later introduced which is based on the conditional expression of lethal genes (Thomas et al., 2000; Phuc et al., 2007). After the release of the *Ae. aegypti* OX513A RIDL strain in Brazil suppression of 95% of the local *Aedes* population was achieved over a 1-year period (Carvalho et al., 2015). In *An. gambiae*, a strategy for population suppression via sex distorsion called X shredder was designed that relies on the selective cleavage of essential genes located in the X chromosome (Windbichler et al., 2008). Population suppression can be achieved by the expression during male spermatogenesis of the homing endonuclease IPop-I or via CRISPR/Cas9 directed mutagenesis, both resulting in individuals able to produce only male offsprings (Galizi et al., 2014, 2016).

An alternative to mosquito population suppression is its replacement with genetically-modified individuals displaying reduced vectorial capacity. This is achieved by rendering mosquitoes less susceptible or refractory to parasite infection via the expression of antipathogen effectors such as antibodies (De Lara Capurro et al., 2000; Isaacs et al., 2011, 2012), antimicrobial proteins (Kim et al., 2004), synthetic peptides (Meredith et al., 2011), or by altering pathways that regulate parasite development (Luckhart et al., 2013).

In order to efficiently spread and maintain these modifications across mosquito populations, gene drive systems are being developed that induce super-Mendelian inheritance whereby a transgene can be driven at rates greater than expected as a result of a normal Mendelian cross (Sinkins & Gould, 2006). The most successful gene drives tested in *Anopheles* rely on the use of the CRISPR/Cas9 technology and achieved 91-99% efficiency in cage experiments (Gantz et al., 2015; Hammond et al., 2016).

1.3 Insecticide resistance

Insecticide-based vector control strategies continue to be the cheapest, most widely-implemented and most effective option so far (White et al., 2011; Bhatt et al., 2015) and are likely to remain the frontline malaria control interventions. Therefore, the spread of resistance is concerning, and monitoring and understanding the mechanisms of resistance developed by mosquito vectors is essential to effectively use and manage the classes of insecticides available.

Insecticide resistance in dominant African *Anopheles* vectors has been recorded to all the insecticide classes (Figure 1.3), with 60 malaria endemic countries reporting resistance to at least one class (WHO, 2016a). Furthermore, mosquito populations from West Africa, such as Tiassalé from Côte d'Ivoire and VK7 from Vallée du Kou in Burkina Faso, displayed high levels of resistance to permethrin, deltamethrin, DDT, bendiocarb, with Tiassalé also showing resistance to fenitrothion (Edi et al., 2012; Toé et al., 2014).

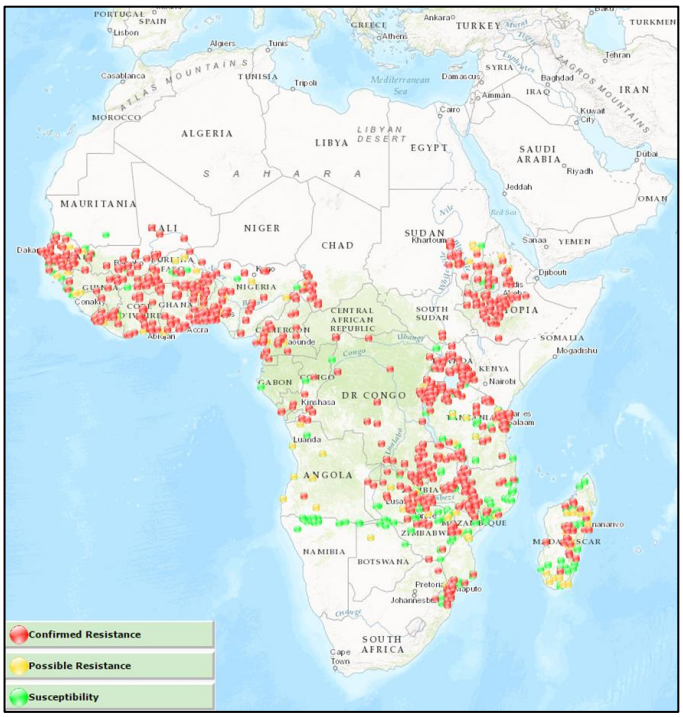

Figure 1.3 Resistance status of main malaria vector species in Africa. Data are shown for *An. arabiensis*, *An. coluzzii*, *An. funestus sensu latu* and *An. gambiae sensu latu*. They were obtained by WHO tube and CDC bottle bioassays to all insecticide classes between 2000 and 2017. Map was generated by IR Mapper (www.irmapper.com).

With the remarkable spread of insecticide resistance across Africa new strategies for operational management must be considered as outlined in the Global Plan for Insecticide Resistance Management in Malaria Vectors (GPIRM) (WHO, 2012b). These include a tighter regulation of insecticide use and dosage, insecticide rotation, and insecticide combinations. Moreover, there is an urgent need to develop new active molecules. In the effort to better design new insecticides and manage the ones that are available, it is crucial to fill the gap in our knowledge on the molecular and genetic causes of insecticide resistance, and how these can be overcome.

Extensive research over the past 60 years has led to the identification of four main mechanisms of insecticide resistance (Figure 1.4): target-site and metabolic resistance, which are the most commonly characterised, and behavioural and cuticular resistance, which are thought to be less common, or at least less investigated (Liu, 2015).

A single mode of resistance resulting in insensitivity to more than one class of insecticides is well known. This may result from the physical alteration of a target site shared by more than one insecticide, such as mutations in the voltage-gated sodium channel (*kdr*^{R}) causing resistance to DDT and pyrethroids (Williamson et al., 1993), and mutations in the *Ace-1* gene (*ace-1*^{R}) which cause resistance to organophosphates and carbamates (Ahoua Alou et al., 2010; Essandoh et al., 2013). The concomitant presence of *kdr*^{R} and *ace-1*^{R} has also been reported in West African countries including Côte d'Ivoire (Asidi et al., 2005), Burkina Faso (Dabiré et al., 2008), and Benin (Djogbénou et al., 2008). In addition, the overexpression of metabolically active enzymes with promiscuous substrate binding sites may lead to the detoxification of unrelated classes of insecticides. An example of the latter is the ability of *An. gambiae* CYP6P3 to metabolise insecticides belonging to the pyrethroid, carbamate and organophosphate classes (Yunta et al., unpublished).

Multiple resistance mechanisms may co-exist in the same organism that enhance the level or broaden the spectrum of resistance (Yewhalaw et al., 2011; Olé Sangba et al., 2017). The presence of mosquito populations showing multiple resistance (i.e. target-site and metabolic), has been reported in 50 malaria endemic countries (WHO, 2016a).

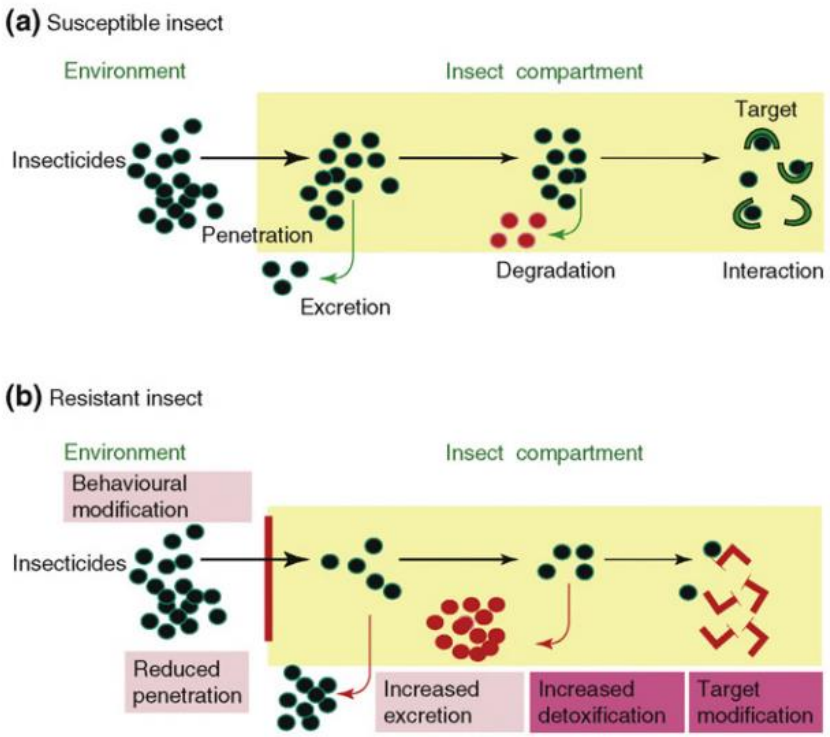

Figure 1.4 Schematic representation of the four mechanisms of resistance found in mosquitoes (taken from Lapied et al., 2009). In susceptible insects (**a**) insecticide molecules penetrate the cuticle and, although part of them are excreted and/or degraded, enough molecules are able to act on their target to exert toxicity. In resistant insects (**b**) modifications of the behaviour, reduced penetration of insecticide molecules through the cuticle, mechanisms of enhanced detoxification and excretion, and mutations in the insecticide target work alone or in combination to determine insensitivity to one or more classes of insecticides.

1.3.1 Target-site resistance

Target-site resistance results from the presence of a mutated target site that renders the binding of the insecticide less effective.

1.3.1.1 Mutations in the Voltage-Gated Sodium Channel (VGSC) (kdr^R)

Under physiological conditions, VGSCs operate between an inactive state, in which the channel is closed at resting potential and ion flux is impeded, and an active state, in which the channel is open allowing the influx of ions and therefore membrane depolarisation. The binding of insecticide molecules to specific VGSC residues prevents the inactivation of the channel, resulting in constant depolarisation and, in turn, insect paralysis and death (Davies et al., 2007).

Neuronal VGSCs are the target of pyrethroid and DDT insecticides, and mutations in these sites determine resistance and in some cases cross resistance to both classes (Williamson et al., 1993). Certain mutations in the VGSC are known as knock down resistance (*kdr*^{R}) mutations as they result in a reduction in the rapid paralytic effect that causes inability to fly or even stand on vertical surfaces (knock down) that is the typical response to pyrethroids. Kdr mutations characterised in pyrethroid-resistant *An. gambiae* and *An. coluzzii* so far include: two mutations in the transmembrane domain, L1014F in West Africa (Martinez-Torres et al., 1998) and L1014S in East Africa (Ranson et al., 2000), and a mutation in a linker domain, N1575Y, found in West and Central Africa (Jones et al., 2012) (Figure 1.5). Kdr mutations have been also identified in *Ae. aegypti*, *C. pipiens*, and *Ae. albopictus* (Hemingway et al., 2004; Nkya et al., 2013), but not in *An. funestus* (Menze et al., 2016).

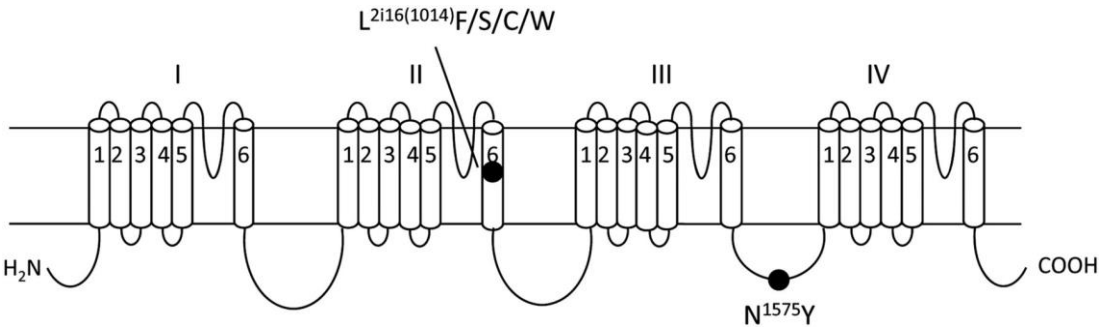

Figure 1.5 Schematic representation of VGSC and mutations associated with insecticide resistance (taken from Wang et al., 2015). The channel is formed by 4 domains (I-IV) each consisting of six transmenbran segments (S1-6). Each domain is connected via intracellular linker loops. Segments 1-4 are responsible for sensing changes in voltage, while segments 5-6 and linker loops form the channel. Mutations associated with insecticide resistance are found in pore-forming regions in position 1014 of IIS6 and in position 1575 of the loop connecting domains III and IV.

1.3.1.2 Acetylcholinesterase enzyme (AchE) mutation (ace-1^{R})

Under normal physiological conditions, AchEs catalyse the hydrolysis of the neurotransmitter acetylcholine that terminates the nerve impulse. The binding of insecticide molecules to AchE impairs its function causing constant nerve impulse and, in turn, paralysis and death. Non-synonymous mutations in the *ace-1* gene sequence can cause insensitivity to organophosphate and carbamate insecticides (Fukuto, 1990). For example, in *An. gambiae*, a G119S mutation in exon 5 of the *Ace-1* gene (Weill et al., 2004) was found implicated in resistance to organophosphates and carbamates. Resistance can also be conferred by alterations in copy number of

the mutated Ace-1 gene, as has been observed in pan-resistant Tiassalé mosquitoes (Edi et al., 2014), and in *An. arabiensis* (Dabiré et al., 2014).

1.3.1.3 Mutations in the GABA type A receptor (Rdl)

The gamma-aminobutyric acid (GABA) is an inhibitory neurotransmitter involved in restoring the membrane potential after depolarisation through chloride ions influx (Anthony et al., 1993). Mutations on the *Rdl* gene alter the channel gating properties resulting in insect paralysis and death. GABA-receptor mutations have been associated with resistance to dieldrin (Hemingway et al., 2004). Specific mutations in position 296 of the *Rdl* gene are found in dieldrin resistant mosquito species: the A296S substitution is found in *An. arabiensis* (Du et al., 2005), *An. coluzzii* (Lawniczak et al., 2010) and *An. funestus* (Wondji et al., 2011), while the A296G mutation is found in *An. gambiae* (Lawniczak et al., 2010).

1.3.2 Alteration of cuticle composition

Cuticular resistance originates from modifications in the mosquito cuticle composition that diminish or slow down insecticide penetration. While this type of resistance has been suggested in some pest species (Ahmad et al., 2006), evidence of cuticle genes overexpressed in resistant mosquitoes are recent (Gregory et al., 2011; Fossog Tene et al., 2013; Riaz et al., 2013; Ingham et al., 2014). In *An. funestus*, Wood et al. (2010) found a positive correlation between cuticle thickness and permethrin-induced knock down time in resistant mosquitoes. In *An. gambiae*, Balabanidou et al. (2016) recently found that deltamethrin resistant mosquitoes display a thicker cuticle compared to susceptible mosquitoes, which correlated with the slower internalisation of the insecticide. Further analysis also revealed a significant enrichment in cuticular hydrocarbons, thought to be produced in mosquito oenocytes, that regulate cuticle permeability (Balabanidou et al., 2016). In line with this finding, GAL4-mediated oenocyte-specific stable RNAi knockdown of *Cyp4g16* and *Cyp4g17*, both proposed to catalyse the final step of hydrocarbon synthesis, resulted in increased death by desiccation in *An. gambiae* (Lynd et al., unpublished).

1.3.3 Behavioural adaptations

Behavioural resistance results from modifications of the mosquito behaviour that allow avoidance of exposure to insecticides or reduction of the duration of exposure, most notably changes in host-seeking and feeding behaviour to circumvent ITNs and IRS (Sokhna et al., 2013).

Altered feeding patterns were found after 12 years of ITN usage in Tanzanian *An. gambiae* and *An. funestus*. Here, nocturnal biting was reduced in both species with *An. funestus* also showing reduced indoor biting (Russell et al., 2011). This was partially explained by a shift in vector dominance to more adaptable populations with *An. gambiae* being the dominant vector at the time of ITN deployment and *An. arabiensis* found the most abundant 12 years after the start of the intervention (Russell et al., 2011).

A study conducted in Senegal after LLIN deployment showed evidence for *An. funestus* diurnal biting (Sougoufara et al., 2014). Finally, in *An. gambiae* behavioural shifts from endophagy to outdoor biting, and from early evening to morning host-seeking was found in Bioko Island following IRS (Reddy et al., 2011; Meyers et al., 2016). The bases of these findings are complex to examine and remain poorly investigated. It is unclear to what extent heritable genetic traits that aid insecticide avoidance play a role compared to the selection of resistant population with more plastic feeding patterns able to fill the niche left by susceptible mosquitoes (Gatton et al., 2013).

1.3.4 Metabolic resistance

Insects showing metabolic resistance detoxify, excrete and/or sequester insecticide molecules faster than their susceptible counterparts therefore preventing the insecticide from reaching its target site. Faster metabolism can be selected for by increasing the quantity of detoxifying enzymes via transcriptional or translational up-regulation or by expression of catalytically enhanced isoforms (Hemingway et al., 2004). In some cases, both up-regulation and mutant isoforms have been found in resistant mosquito populations (Mitchell et al., 2014; Riveron et al., 2014b).

Detoxification is often a three-phase process (Xu et al., 2005). Phase I consists of the breakdown of the insecticide via oxidation or hydrolysis; such modifications generally increase the polarity of the insecticide, which reduces or eliminates toxicity, increases their aqueous solubility, and provides reactive species for phase II conjugation. Phase

II involves mechanisms that increase the hydrophilicity of phase I metabolites primarily through conjugation with endogenous molecules. Finally, phase III comprises mechanisms of excretion across cell membranes mediated by ATP-dependant transporters. In addition, or in conjunction with detoxification, insecticides can be sequestered by binding to endogenous molecules, including lipoproteins, that prevent them from reaching their targets (Shaw, 1991).

Enzymes involved in metabolic resistance include cytochrome P450 monooxygenases (P450s), glutathione S-transferases (GSTs), carboxyl/choline esterases (CCEs), and glucosyl/glucuronosyl transferases (UDPGTs). A remarkable proportion of the *An. gambiae* genome (~1.6%) is devoted to metabolism and detoxification, with 111 cytochrome P450s, 31 GSTs, 43 CCES and 26 UGTs genes annotated in the PEST genome (Holt et al., 2002; Ranson et al., 2002).

1.3.4.1 Glutathione S-transferases (GSTs)

Insect GSTs are microsomal and cytosolic enzymes, the latter being involved in resistance. At least 6 classes of cytosolic GSTs are present in *An. gambiae*, with the insect-specific subfamilies delta (δ, d) and epsilon (ε, e) being the largest (Ranson et al., 2002). They have broad substrate specificity which explains their involvement in resistance to most classes of insecticides through phase I (organochlorines) and phase II (organophosphates and pyrethroids) detoxification.

Evidence of GST-mediated DDT dehydrochlorination in mosquitoes was reported in the 1990s in both *Ae. aegypti* (Grant et al., 1991) and *An. gambiae* (Prapanthadara & Ketterman, 1993). More recently, *in vitro* degradation of DDT was shown by recombinant orthologues of *Gste2* isolated from *Ae. aegypti* (Lumjuan et al., 2005), *An. gambiae* (Ortelli et al., 2003; Mitchell et al., 2014) and *An. funestus* (Riveron et al., 2014b). In both *Anopheles* species, mutated *GSTe2* alleles were found (I114T and L119F respectively) in resistant mosquitoes that displayed increased catalytic activity compared to their susceptible counterparts. Finally, increased resistance to DDT has been observed following overexpression of the different *Anopheles Gste2* alleles in *D. melanogaster* (Daborn et al., 2012; Mitchell et al., 2014; Riveron et al., 2014b).

Phase II metabolism occurs via conjugation with reduced glutathione which results in solubilisation and more efficient excretion (Panini et al., 2016). GST-mediated secondary metabolism of organophosphates was suggested in *An. subpictus*

(Hemingway et al., 1991), and that of pyrethroids was found in *Nilaparvata lugens* (Vontas et al., 2001). In addition to phase II metabolism of pyrethroids, indications of sequestration were reported in *Tenebrio molitor* (Kostaropoulos et al., 2001).

In mosquitoes, despite increased expression of GSTs being consistently found in pyrethroid-resistant populations (Nkya et al., 2013), the molecular basis of the involvement of these enzymes in resistance to this class remain unclear. For example, RNAi interference of *Gste7* or *Gste2* in resistant *Ae. aegypti* caused an increase in deltamethrin susceptibility (Lumjuan et al., 2011). Conversely, the ubiquitous overexpression of *An. gambiae Gste2* in *D. melanogaster* did not modify resistance to permethrin (Daborn et al., 2012), while that of *An. funestus Gste2* conferred resistance to permethrin and deltamethrin (Riveron et al., 2014b).

1.3.4.2 Carboxyl/choline esterases (CCEs)

CCEs are involved in metabolic resistance through sequestration and phase I detoxification of organophosphates and carbamates (Hemingway, 1982a). Most of the work aimed at unveiling the molecular basis of CCE overexpression-mediated resistance has been conducted in organophosphate-resistant *Culex* mosquitoes (Hemingway & Karunaratne, 1998), and more recently in temephos-resistant *Aedes* mosquito larvae (Poupardin et al., 2014; Grigoraki et al., 2015, 2016).

In resistant *C. quinquefasciatus*, quantitative changes in the level of CCE expression are suggested to result in increased sequestration (coupled with slow detoxification rates) of toxic oxon forms deriving from the oxidation of organophosphates, thereby causing resistance by masking toxicity (Ketterman et al., 1992; Karunaratne et al., 1993). Sequestration of temephos-derived oxon forms by CCEs was recently suggested in *Ae. aegypti* and *Ae. albopictus* (Grigoraki et al., 2016).

Qualitative functional changes are found in CCEs overexpressed in malathion-resistant insects (Campbell et al., 1998; Claudianos et al., 2002), including *Anopheles* species (Hemingway 1982b, Hemingway & Georghiou, 1983; Herath et al., 1987). Here, the hydrolytic capacity of the enzyme is enhanced rather than the rate of sequestration, therefore these CCEs catalyse the more rapid detoxification of insecticides into their corresponding alcohol and acid metabolites which are more easily excreted. This altered activity may be the result of single amino acid substitutions as found in *Lucilia cuprina* (Newcomb et al., 1997) and *Musca domestica* (Claudianos et al., 1999), yet its molecular basis remains unclear.

Although there are reports of CCE upregulation in permethrin-resistant mosquitoes (Hemingway et al., 2004; Vontas et al., 2005), their involvement in pyrethroid metabolism has not yet been confirmed by functional analysis.

1.3.4.3 Cytochrome P450 monooxygenases (P450s)

P450s are a wide family of haem thiolate enzymes present in all organisms from bacteria (soluble) to humans (microsome and mitochondria membrane-bound). They fulfil a variety of functions catalysing over 50 different chemical reactions (Guengerich, 2001). As microsomal monooxygenases, they use two electrons provided by NADPH to reduce molecular oxygen to water and to hydroxylate a substrate:

$$RH + O_2 + NADPH + H^+ \longrightarrow R\text{-}OH + H_2O + NADP^+$$

They work as part of the so called “P450 system” where they are coupled to redox partners, most notably NADPH cytochrome P450 reductase (CPR) and cytochrome b5.

In insects, P450 functions include metabolism of juvenile hormones, ecdysteroids, fatty acids and eicosanoids, biosynthesis of hydrocarbons and pheromones (Feyereisen, 1999), and, most notably, the biotransformation of foreign compounds (xenobiotics) of both natural (i.e. plant toxins) (Gould, 1984) and artificial (insecticides) origin (Ronis & Hodgson, 1989).

P450s are encoded by genes belonging to the *Cyp* superfamily which are abundant in mosquito genomes: 111 in *An. gambiae* (Ranson et al., 2002), 160 in *Ae. aegypti* (David et al., 2005), 204 in *C. quinquefasciatus* (Yang & Liu, 2011).

In *An. gambiae*, P450s have been implicated in resistance through phase I detoxification of type I and type II pyrethroids (Müller et al., 2008b; Stevenson et al., 2011) and carbamates (Edi et al., 2014), as well as the activation of organophosphates in their toxic oxon forms (Yunta et al., unpublished).

1.3.4.4 Mechanisms of gene overexpression and increased metabolism

While the validation of role of detoxifying genes in metabolic resistance is actively being unveiled, very little is known about the transcriptional and genomic modification that lead to their overexpression.

In some insects, the presence of transposable elements within the gene promoter has been proposed to mediate overexpression. In *D. melanogaster*, resistance to DDT is associated with the presence of a 491 bp insertion within the 5' UTR of the *Cyp6g1* corresponding to the terminal repeats of a retrotransposon (Accord element) (Daborn, 2002). *Cis*-regulatory elements within the retrotransposon, including tissue-specific enhancers and xenobiotic-responsive elements, work in concert to induce overexpression in the midgut, Malpighian tubules and fat body (Chung et al., 2007, 2011). Further analysis of the *Cyp6g1* locus conducted by Schmidt et al. (2010) revealed the presence of additional transposable elements (P and HMS-Beagle) associated with resistance to DDT.

Another example of the implication of transposon elements was found in *C. quinquefasciatus* where *Cyp9m10* is upregulated in pyrethroid resistant individuals (Komagata et al., 2010) and can metabolise permethrin *in vitro* (Wilding et al., 2012). Wilding et al. (2012) found that the upregulation of this gene in a resistant strain was associated with the presence of a partial *Culex* repetitive element (CuRe1) which is absent in the susceptible strain. However, a direct role for the element was not supported by cell line luciferase assays, since its deletion had no effect on reporter expression suggesting the involvement of further regulative elements.

Copy number variation of *Cyp6g1* was found in *Drosophila spp.*, with up to four copies present, and was found associated with DDT resistance (Schmidt et al., 2010; Harrop et al., 2014). Similarly, the duplicated *D. melanogaster* gene *Cyp12d1* was involved in resistance to caffeine and other xenobiotics (Najarro et al., 2015) and, interestingly, transgenic experiments demonstrated that the overexpression of both copies is required *in vivo* to cause resistance (Daborn et al., 2007). In *An. funestus*, two genes are found duplicated, *Cyp6p4* and *Cyp6p9* (Wondji et al., 2009). Although sequence analysis suggests these duplications were not selected by pyrethroid use, the presence of multiple copies is argued to play a role in increasing the levels of resistance as both isoforms of the *Cyp6p9* gene are able to metabolise pyrethroids and confer resistance when overexpressed in *D. melanogaster* (Riveron et al., 2013, 2014a). In *An. gambiae*, recent duplication events were detected in the GSTe cluster which is implicated with DDT resistance (Ranson et al., 2001; Ding et al., 2003). Gene duplication has also been associated with target-site resistance with duplication of the Rdl locus in *D. melanogaster* (Remnant et al., 2013) and Ace-1 in *C. pipiens* (Labbé et al., 2007) and *An. gambiae* (Djogbénou et al., 2008).

Polymorphisms and allelic variation drive the creation of mutated alleles coding for detoxifying enzymes with enhanced catalytic activity which are rapidly selected in resistant populations. Such events were identified in the *Gste2* gene of *An. gambiae*, where the I114T mutation is specific for a DDT resistant allele (Mitchell et al., 2014), and *An. funestus*, where the L199F mutation is found in the pyrethroid resistant allele (Riveron et al., 2014b). In these studies, resistant *Gste2* alleles from both species were reported as metabolically more active than their susceptible counterparts *in vitro*. The precise effect of these mutations is being reassessed further in *in vitro* and *in vivo* studies (G. Lycett and H. Ismail pers. comm.).

Alterations in the transcription factor binding domains were found in *D. melanogaster* resistant to phenobarbital via *Cyp6a2* overexpression. Here, Misra et al. (2011) found that a 15 bp region located upstream of the *Cyp6a2* transcription start site is essential for inducing expression of a LacZ reporter in transgenic flies after phenobarbital exposure. This promoter region contains the binding site of the CncC/Maf-S transcription factor heterodimer which is known to regulate the expression of detoxifying genes in vertebrates. The inhibition of CncC/Maf-S via RNAi or via the overexpression of the Keap1 inhibitor results in lack of phenobarbital-mediated induction of *Cyp6a2* (Misra et al., 2011). Like in vertebrates, this pathway coordinates the induction of multiple detoxifying genes in response to phenobarbital exposure. The involvement of the Maf-S transcription factor in metabolic resistance is currently being investigated in *An. gambiae,* where it is found upregulated in pyrethroid-resistant populations across Africa. Its knockdown in the pan-resistant Tiassalé strain resulted in a decreased expression of major detoxifying genes, which, in turn, determined an increase in susceptibility (Ingham, 2016).

A new pathway regulating overexpression has been recently proposed by Liu et al., (2015) which is based on the role of G-protein coupled receptors (GPCR) that are found overexpressed in pyrethroid-resistant *C. quinquefasciatus* (Liu et al., 2007). Li et al. (2014) demonstrated that the knock-down of GPCR-related genes in two resistant strains correlated with a decrease in expression of detoxifying genes and a resulting increase in permethrin susceptibility. Further experiments demonstrated that the heterologous overexpression of a *C. quinquefasciatus* rhodopsin-like GPCR in *D. melanogaster* resulted in an increased expression of P450s genes and enhanced tolerance to permethrin (Li et al., 2015).

1.3.5 Detection of metabolic resistance

The phenotypic assessment of the resistance status of field-caught mosquitoes is traditionally performed by standard methods such as the WHO tube bioassay (WHO, 2016b). This procedure involves assessing mortality over a 24 h period following exposure of adult females to a single diagnostic dose of insecticide for a specified length of time.

To help define the contribution of single or multiple mechanisms of resistance, other molecular and phenotypical methods were developed. These include the detection of target site mutations by an optimised qPCR-based TaqMan® assay (Bass et al., 2007) and assessing the involvement of metabolic resistance via synergism studies. The latter studies are often performed with the P450-inhibitor PBO which is thought to occupy the P450 active site and inactivate the enzyme by creating a metabolism-induced inhibitor complex (Feyereisen, 2015). PBO is thought to be active against most P450s, and thus, the first step in the WHO guidelines to determine the involvement of P450-mediated detoxification is to expose resistant mosquitoes to 4% PBO prior to insecticide exposure and compare mortality rates to those obtained in the absence of PBO (WHO, 2016b). If an increase in mortality is seen when pre-exposed to PBO, then good evidence for the degree of P450 involvement is generated. However, there is evidence to suggest that PBO can inhibit other metabolic enzyme classes (Young et al., 2005; Khot et al., 2008), and so the results are not always unequivocal.

1.3.5.1 Identification of genes involved in metabolic resistance

Phenotypical assessment of metabolic resistance does not provide information on the detoxifying enzymes involved in resistance. Therefore, molecular investigations on the level of expression of specific genes are required to identify those involved in resistance. The publication of the *An. gambiae* genome (Holt et al., 2002) remarkably facilitated such studies, allowing for comprehensive investigations on the transcriptome of resistant *vs* susceptible mosquitoes.

Early transcriptome experiments were based on small-scale microarrays including probes for the detection of major detoxifying families (P450s, GSTs and CCEs). The use of these “detoxification chips” was successful in *An. gambiae* (David et al., 2005) and *Ae. aegypti* (Strode et al., 2008) in identifying candidate genes with differential expression in resistant strains within the major detoxification families tested. “Detox

chip" approaches were later substituted by the introduction of whole genome microarrays (Mitchell et al., 2012), which expanded our knowledge beyond detoxification families. Currently, transcriptome analysis is moving away from microarray-based experiments to newly-developed transcriptome profiling by RNA-Seq (Zhu et al., 2014; Bonizzoni et al., 2015). From transcriptome data on differentially expressed genes, lists of top candidate genes overexpressed in resistant mosquitoes are generated and single-gene approaches undertaken to validate overexpression by RT-qPCR and to functionally characterise them.

Single-gene validation starts with assessing the capability of candidate proteins to metabolise insecticides *in vitro*. This is classically undertaken by obtaining *E. coli*-produced recombinant proteins and assaying them for their ability to deplete specified quantities of an insecticide in a specified amount of time *in vitro*. More detailed studies will then characterise the identity and kinetics of insecticide metabolite production via HPLC analysis (Stevenson et al., 2011; Yunta et al., unpublished), which is often coupled to mass spectrometry (Hoi et al., 2014; Stevenson et al., 2012). Potential interactions with insecticide molecules can be also determined by *in silico* modelling and molecular docking simulation to explore binding modes (Riveron et al., 2014b; Ibrahim et al., 2016a, 2016b). Additional tools to identify P450s with metabolism capabilities are synthetic activity-based probes (Wright & Cravatt, 2007) that mimic insecticide structures (Ismail et al., 2013). Probes mimicking the structure of pyrethroid insecticides have been developed using 'click chemistry' (Ismail et al., 2013). These pyrethroid-mimetic probes (PyABPs) bind irreversibly to P450s that they are metabolised by and their click handle used to add a fluorescent reporter. This ultimately allows for the identification of potential pyrethroid-metabolising P450s from arrays of purified recombination proteins and can be used to define specific interacting P450s from complex *in vivo* extracts (Wright & Cravatt, 2007; Ismail et al., 2013).

Transcription analysis and data on *in vitro* metabolic activity are crucial first steps in the validation of single genes implicated in resistance, yet *in vivo* functional approaches are needed to conclusively define the role of single genes in causing resistance (Ranson et al., 2011). As mosquito genome manipulation is particularly challenging, *in vivo* analysis of insecticide metabolisers has been so far conducted via ectopic overexpression of *Anopheles* genes in *D. melanogaster* transgenics using the GAL4/UAS system (Yang et al., 2007; Daborn et al., 2012).

This multi-step approach (Figure 1.6) has been used to assay the top candidate genes involved in metabolic resistance in major African malaria vectors, which are summarised in Table 1.1.

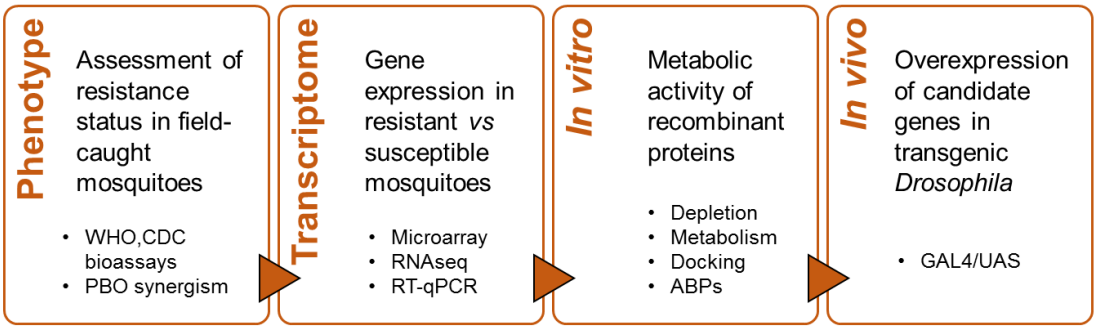

Figure 1.6 Current pipeline for metabolic resistance assessment and functional validation of single genes.

However, this approach has limitations. Whole-mosquito transcriptome approaches may underestimate the significant contribution of genes that are expressed tissue-specifically. In support of this observation, Ingham et al. (2014) found that, although many of the top candidate gene associated with resistance found by tissue-specific comparisons were also identified by whole transcriptome data, over 20 additional candidates were revealed as associated with resistance. Moreover, while *in vitro* metabolic studies have proven useful as first functional screening, they are limited to proteins with measurable enzymatic properties. In these experiments absence of metabolism does not exclude involvement in resistance via other mechanisms such as binding or secondary metabolism. Finally, limitations of the *Drosophila in vivo* model lie in its physiology. In such a model, metabolically-inactive proteins involved in resistance, such as transcription factors and sensory proteins, are difficult or impossible to test rationally. Furthermore, the insecticide dosage used to test for resistance is not directly comparable to that used in mosquitoes. To overcome these limitations and obtain representative data, an *Anopheles in vivo* validation model is needed.

Table 1.1 Functional analysis studies conducted on *Anopheles* genes.

Insecticide	Gene	*In vitro* metabolism	*Drosophila* transgenics
***An. gambiae* genes**			
Pyrethroids	*Cyp6m2*	✓ (1)	✓ (2)
	Cyp6p3	✓ (3)	✓ (2)
	Gste2 (perm)	N/A	✗ (4)
DDT	*Cyp6m2*	✗ (5)	✓ (2)
	Cyp6p3	✗ (5)	N/A
	Cyp6z1	✓ (14)	N/A
	Gste2	✓ (6, 7)	✓ (4, 7)
Bendiocarb	*Cyp6m2*	✗ (2)	✓ (2)
	Cyp6p3	✓ (2)	✓ (2)
Malathion	*Cyp6m2*	✓ (5)	N/A
	Cyp6p3	✓ (5)	N/A
***An. funestus* genes**			
Pyrethroids	*Gste2* (perm)	✓ (8)	✓ (8)
	Gste2 (delta)	✗ (8)	✓ (8)
	Cyp6m7	✓ (9)	✓ (9)
	Cyp6p9a	✓ (9)	✓ (10)
	Cyp6p9b	✓ (10)	✓ (10)
	Cyp9j11	✓ (11)	✓ (11)
	Cyp6z1	✓ (13)	N/A
DDT	*Gste2*	✓ (8)	✓ (8)
	Cyp6p9a	✗ (5)	N/A
	Cyp6p9b	✗ (10)	N/A
Bendiocarb	*Cyp6z1*	✓ (13)	N/A
***An. arabiensis* genes**			
Pyrethroids	*Cyp6p4* (perm)	✓ (12)	N/A
	Cyp6p4 (delta)	✗ (12)	N/A

Green ticks represent presence of *in vitro* depletion or that of resistance *in vivo*. Red crosses represent lack of *in vitro* depletion or that of resistance *in vivo*. (1) Stevenson et al., 2011; (2) Edi et al., 2014; (3) Müller et al., 2008b; (4) Daborn et al., 2012; (5) Yunta et al., unpublished; (6) Ortelli et al., 2003; (7) Mitchell et al., 2014; (8) Riveron et al., 2014b; (9) Riveron et al., 2014a; (10) Riveron et al., 2013; (11) Riveron et al., 2017; (12) Ibrahim et al., 2016b; (13) Ibrahim et al., 2016a (14) Chiu et al., 2008.

1.3.6 The CYP6 family

The P450 CYP6 family is found only in insects and has been widely linked to metabolic resistance in several insects. Early studies conducted in *D. melanogaster* reported the upregulation of several *Cyp6* genes in resistance to a variety of chemicals and their metabolic activity *in vitro*, including that of *Cyp6a2* (Brun et al., 1996; Saner et al., 1996; Dunkov et al., 1997; Amichot et al., 2004) and *Cyp6a8* (Helvig et al., 2004). The best characterised candidate in the fruit fly is *Cyp6g1*, whose overexpression was reported in DDT and imidacloprid resistant flies (Daborn et al., 2001). The involvement of this gene in resistance was later demonstrated by its ability to metabolise DDT and imidacloprid (Joussen et al., 2008) and via transgenic overexpression using the GAL4/UAS system in transgenic flies (Daborn et al., 2002; Chung et al., 2007). In the house fly, *M. domestica, Cyp6d1* was found overexpressed in pyrethroid-resistant flies (Tomita et al., 1995) and *Cyp6a1* in phenobarbital-resistant flies (Cariño et al., 1994) compared to a susceptible strain. Similarly, *Cyp6cm1* was found overexpressed in imidacloprid-resistant *Bemisia tabaci* strains B and Q (Karunker et al., 2008) and its heterologous overexpression in *D. melanogaster* resulted in acquisition of resistance to imidacloprid (Daborn et al., 2012). More recently, *Cyp6bq9* was found upregulated in deltamethrin-resistant *Tribolium castaneum* and its involvement in resistance also demonstrated via heterologous overexpression in *D. melanogaster* (Zhu et al., 2010).

Despite these examples of the ability of individually overexpressed *Cyp6*s to alter the resistance phenotype *in vivo*, the involvement of single *vs* multiple genes in determining resistance is actively debated (Yang et al., 2007). This is based on the observation that multiple, yet not all, P450s metabolise insecticides *in vitro* (Yunta et al., unpublished) and that P450 distribution and abundance vary in different tissues (Stevenson et al., 2011; Ingham et al., 2014). Therefore, an interplay of different P450s and other enzymes in a multistep mode of action may take place *in vivo*, similar to the separate phases of drug metabolism in mammals (Yang et al., 2007; Daborn et al., 2012).

In mosquitoes, genes encoded by the CYP6M, CYP6P and CYP6Z subfamilies have been frequently associated with resistance, with pyrethroid resistance being the most widely investigated. *Cyp6z* genes have been found upregulated in DDT (*z1* (David et al., 2005) and permethrin (*z2* (Müller et al., 2007) and *z3* (Müller et al., 2008b)) resistant *An. gambiae*; in deltamethrin resistant *Ae. aegypti* (*z6* and *z8* (Strode et al., 2008)); and in pyrethroid and carbamate resistant *An. funestus* (*z1* and *z3* (Irving et

al., 2012; Ibrahim et al., 2016a)). Similarly, upregulation of the *Cyp6p* subfamily genes was found in pyrethroid resistant *An. gambiae* (*p3* (Müller et al., 2008b) and *p4* (Edi et al., 2012)), *An. funestus* (*p9* (Amenya et al., 2008), *p4* (Wondji et al., 2009)), *An. minimus (p7* (Duangkaew et al., 2011)), and *An. arabiensis* (*p3* (Müller et al., 2008a), *p4* (Ibrahim et al., 2016b)). Finally, transcriptome data also associated *An. gambiae m2* (Djouaka et al., 2008; Müller et al., 2007), *An. funestus m7* (Riveron et al., 2014a), and *Ae. aegypti m6*, *m10* and *m1* (Marcombe et al., 2012; Poupardin et al., 2012) with resistance to pyrethroids. *An. gambiae m2* was also found upregulated in DDT resistant populations (Mitchell et al., 2012).

In vitro functional analysis on the recombinant proteins revealed the ability of *An. gambiae* CYP6Z1 to metabolise DDT (Chiu et al., 2008) and that of *An. funestus* CYP6Z1 to metabolise pyrethroids and bendiocarb (Ibrahim et al., 2016a). While a lack of pyrethroid metabolism was found for *An. gambiae* CYP6Z2 (McLaughlin et al., 2008) and its *Ae. aegypti* orthologue CYP6Z8 (Chandor-Proust et al., 2013), their involvement in resistance was instead attributed to their ability to act as phase II enzymes metabolising 3-phenoxybenzoic alcohol, a common product of CCE-mediated detoxification of pyrethroids (Chandor-Proust et al., 2013). Furthermore, to support their role in resistance, the ability of *An. gambiae* CYP6P3 and CYP6P4 and *An. funestus* CYP6P9a and CYP6P9b to metabolise permethrin and deltamethrin has been reported (Müller et al., 2008b; Riveron et al., 2013, 2014a; Yunta et al., unpublished) (Table 1.1). Surprisingly, *An. arabiensis* CYP6P4 was reported able to metabolise permethrin but not deltamethrin (Ibrahim et al., 2016b) (Table 1.1).

In vivo validation of *Anopheles* genes expressed in *D. melanogaster* is summarised in Table 1.1. This exists so far only for members of the CYP6P and CYP6M subfamilies.

1.3.6.1 Cyp6m2 and Cyp6p3: top resistance candidate genes in An. gambiae

An. gambiae Cyp6m2 and *Cyp6p3* are the best studied candidate genes associated with metabolic resistance. As mentioned above, their increased expression has been reported in mosquito populations resistant to a diverse range of insecticides across Africa and their involvement has been supported through *in vitro* and *Drosophila* studies.

Upregulation of *Cyp6m2* and *Cyp6p3* was recorded in mosquitoes resistant to permethrin in Southern Benin and Nigeria (Djouaka et al., 2008), to deltamethrin in

southern Benin (Yahouédo et al., 2016), to DDT in Benin (Djègbè et al., 2014) and they are also found upregulated in the pan resistant *An. gambiae* strain Tiassalé from Côte d'Ivoire (Edi et al., 2014). *Cyp6m2* was additionally found significantly upregulated in mosquitoes resistant to pyrethroids and DDT in Ghana (Mitchell et al., 2012; Müller et al., 2007) and Cameroon (Fossog Tene et al., 2013); while *Cyp6p3* upregulation was additionally reported in mosquitoes resistant to permethrin in Ghana (Müller et al., 2008b) and in *An. gambiae* populations collected from seven villages in Vallée du Kou in Burkina Faso that are multi-resistant to pyrethroids, DDT, dieldrin and bendiocarb (Kwiatkowska et al., 2013).

Cyp6m2 and *Cyp6p3* orthologues were also found upregulated in *An. arabiensis* mosquitoes resistant to pyrethroids in Cameroon (Müller et al., 2008a), Tanzania (Matowo et al., 2014), South Africa (Nardini et al., 2013) and Sudan (Abdalla et al., 2014). Finally, *An. funestus Cyp6p9*, the orthologue of *An. gambiae Cyp6p3,* was found upregulated in pyrethroid-resistant mosquitoes from Mozambique (Amenya et al., 2008; Riveron et al., 2013), Malawi (Riveron et al., 2013, 2015, 2014a), Zambia (Riveron et al., 2014a), Uganda and Kenya (Mulamba et al., 2014).

To further support the association of these genes with resistance, their recombinant proteins were demonstrated to metabolise a variety of insecticides *in vitro*. Specifically, CYP6M2 metabolised the pyrethroids permethrin and deltamethrin (Stevenson et al., 2011), and malathion (Yunta et al., unpublished), but not the carbamate bendiocarb (Edi et al., 2014). While in previous studies CYP6M2 was reported able to metabolise DDT (Mitchell et al., 2012), later investigations revealed that metabolism occurred only in the presence of sodium cholate as a solubilising factor and that CYP6M2 alone was not metabolically active against DDT (Yunta et al., unpublished). CYP6P3 *in vitro* metabolic activity was demonstrated for permethrin and deltamethrin (Müller et al., 2008b), malathion (Yunta et al., unpublished), and bendiocarb (Edi et al., 2014). As found for CYP6M2, no insecticide depletion was reported against DDT (Yunta et al., unpublished).

Cyp6m2 and *Cyp6p3* are amongst the limited number of genes for which *in vivo* data on the effect of their overexpression in *D. melanogaster* is available (Edi et al., 2014). These experiments confirmed the ability of CYP6M2 and CYP6P3 overexpression to confer resistance to pyrethroids, with CYP6P3 also conferring resistance to bendiocarb. Furthermore, although lacking *in vitro* activity against DDT (Yunta et al., unpublished) and bendiocarb (Edi et al., 2014), *in vivo* overexpression of CYP6M2 in *D. melanogaster* increased resistance to these insecticides (Edi et al., 2014).

Similarly, the closely related genes *Cyp6p9a/b* and *Cyp6m7* from *An. funestus* were shown to metabolise pyrethroids *in vitro* and to confer resistance to this class of insecticides when overexpressed in *D. melanogaster* (Riveron et al., 2013, 2014a).

1.3.7 Tissues involved in detoxification

Identifying the major tissue/s involved in insecticide clearance is pivotal to understanding the pathways of detoxification. This is crucial for implementing strategies for efficacious insecticide management that incorporate new insecticide chemistries and improved formulations that increase uptake, and it is also relevant for designing better diagnostic tools (Yang et al., 2007). Yet, despite the growing data on the role of specific genes in detoxification, the spatial distribution of their expression remains largely unclear. Insect tissues commonly believed to be involved in detoxification include midgut, Malpighian tubules, fat body, and brain (Wang et al., 2004; Chung et al., 2007; Yang et al., 2007; Giraudo et al., 2010; Zhu et al., 2010).

For example, the expression of *D. melanogaster Cyp6g1* is found tissue-specifically enhanced in the midgut, fat body and Malpighian tubules of resistant flies. Here, tissue-specificity is mediated by enhancers within the *Accord* retrotransposon situated upstream of the transcription start site of the resistant allele (Chung et al., 2007, 2011). In *D. melanogaster*, midgut, Malpighian tubules, fat body and brain were also suggested as detoxifying tissues by analysing the pattern of induction of *Cyp6a2* expression after phenobarbital exposure (Giraudo et al., 2010).

The involvement of the brain in detoxification was demonstrated by Zhu et al. (2010) in the red flour beetle *T. castaneum*. Here, deltamethrin-resistant beetles significantly overexpressed *Cyp6bq9*, a P450 able to metabolise deltamethrin *in vitro*, whose knockout by dsRNA injection in the resistant strain caused an increase in susceptibility to deltamethrin. Interestingly, *Cyp6bq9* was found enriched in the brain of all beetles but was specifically overexpressed in the brain of the resistant strain. Finally, heterologous overexpression of *T. castaneum Cyp6bq9* confined to the brain of *D. melanogaster* was sufficient to cause resistance to deltamethrin as efficiently as that driven by the Act5c ubiquitous driver.

Little is known about tissues specifically involved in detoxification in mosquitoes. While transcriptome data from dissected *An. gambiae* tissues are available (Marinotti et al., 2006; Dissanayake et al., 2006; Koutsos et al., 2007; Baker et al., 2011; Padrón et al., 2014; Overend et al., 2015) these are not specifically associated with

occurrence of insecticide resistance. To date, only one study assessed tissue-enrichment of resistance-associated genes and compared expression in specific tissues of susceptible *vs* resistant *An. gambiae* populations (Ingham et al., 2014). Although this study was not exhaustive in the tissues and body sections examined, it revealed a general abundance of candidate gene 'detox' transcripts in the midgut and Malpighian tubules of resistant mosquitoes, while other candidate genes had a more widespread distribution.

1.3.7.1 Midgut

The insect midgut has been associated with a role in xenobiotic metabolism as suggested by the induction of expression after exposure to various chemicals in *D. melanogaster* (Brun et al., 1996; Chung et al., 2007; Giraudo et al., 2010). In the moth *P. xylostella*, RNAi-mediated knock-down of *Cyp6bg1* in the larval midgut through dsRNA feeding resulted in an increased susceptibility to permethrin (Bautista et al., 2009). In *An. gambiae*, this is supported by the high native enrichment of *Cyp6m2* (Stevenson et al., 2011) and the P450-cofactor CPR in the midgut of susceptible mosquitoes (Lycett et al., 2006). However, *Cyp6m2* was not found specifically enhanced in the midgut of pan-resistant Tiassalé mosquitoes (Ingham et al., 2014). Conversely, transcripts from detoxification genes of the CYP6P family, including *Cyp6p3*, were found enriched in the midgut of resistant *An. gambiae* (Ingham et al., 2014). Similarly, P450 transcript enrichment was identified in in the midgut of *Ae. aegypti* larvae (Poupardin et al., 2010).

1.3.7.2 Oenocytes

Insect oenocytes have been associated with a role in detoxification for a long time but this has never been fully explored (Clark & Dahm, 1973). Oenocytes are cells of ectodermal origin located beneath the abdominal cuticle or scattered in the fat body whose function is insects has been compared to that of mammalian liver (Gutierrez et al., 2007; Martins et al., 2011). They are implicated in a variety of roles, such as cuticular hydrocarbon synthesis, regulation of haemolymph composition, lipid storage and metabolism, fatty acid metabolism, insect development, and immunity (Gutierrez et al., 2007; Martins et al., 2011; Makki et al., 2014). The role of oenocytes as site of detoxification was suggested by Lycett et al. (2006) after reporting that RNAi-mediated knock-down of the P450-cofactor CPR in this location results in enhanced

sensitivity to permethrin in *An. gambiae*. Consistent with a role in detoxification, analysis of the transcriptome of the *Ae. aegypti* pupal oenocytes revealed that P450s represented the most abundant class of transcripts (Martins et al., 2011). The candidate *Cyp4g17* is enriched in the abdomen integument of *An. gambiae* resistant mosquitoes (Ingham et al., 2014), and was found specifically localised in the oenocytes along with *Cyp6g16* (Balabanidou et al., 2016). The latter gene product was shown to catalyse cuticular hydrocarbon production and thus implication in cuticular resistance through cuticle thickening was suggested in *An. gambiae* (Balabanidou et al., 2016).

1.3.7.3 Malpighian Tubules

Malpighian tubules constitute a major component of insects' excretory system and are responsible for regulation of fluid homeostasis and excretion of products of metabolism including toxic compounds such as insecticides (Pachecho et al., 2014). In *D. melanogaster* members of the major detoxifying families P450 and GST are upregulated in the Malpighian tubules compared to the whole fly; amongst them, *Cyp6g1* transcript abundance is ~10 times higher (Wang et al., 2004). Overexpression of *Cyp6g1* using a GAL4 driver specific for the Malpighian tubule principal cells determined a decrease in sensitivity to DDT, conversely tubule-specific knockdown caused increased mortality (Yang et al., 2007). In mosquitoes, their involvement in detoxification is supported by transcriptome analysis on susceptible *An. gambiae* mosquitoes revealing enrichment of several *Cyp6* genes in the Malpighian tubules of the Cameroonian N'Gousso strain (Ingham et al., 2014) and that of *Cyp6m2* in the Kenyan Kisumu strain (Stevenson et al., 2011). Furthermore, several members of detoxifying gene families, including P450s, are found upregulated in the Malpighian tubules of pan-resistant Tiassalé mosquitoes, here transcripts from the CYP6Z family were specifically found enriched (Ingham et al., 2014). The P450-cofactor CPR was also found abundant in this organ (Lycett et al., 2006). High native expression of several *Cyp6* genes was also found in the Malpighian tubules of *Ae. aegypti* larvae (Poupardin et al., 2010).

1.4 Functional analysis in mosquitoes

With the growing abundance of transcriptomic data generated on disease vectors such as mosquitoes, tools for *in vivo* gene functional analysis are increasingly needed to examine the role of single genes in affecting a phenotype. Functional analysis of mosquito genes through loss of function (RNA interference, gene knockout) or gain of function (overexpression) has elucidated key biological pathways mostly in relation to genes relevant for parasite transmission.

Loss of function analysis

Transient RNAi via the injection of dsRNA has been employed most often to investigate *An. gambiae* mosquito immune response to pathogen invasion. Such studies assisted in defining roles for, amongst others, genes encoding antimicrobial peptides (Blandin et al., 2002), transcription factors such as REL2 (Meister et al., 2005), and the complement factors TEP1 (Blandin et al., 2004) and LRIM1 (Lombardo et al., 2013) in modulating bacterial and *Plasmodium* infection. Using transient RNAi, the list of genes acting as immunomodulators in *An. gambiae* is growing (Lombardo & Christophides, 2016).

Transient RNAi to investigate P450 genes has not been extensively reported, with few examples of successful silencing, including *Cyp307a1* shown to be involved in ecdysteroid production (Pondeville et al., 2013) and *Cyp4g16,* which could be knocked down in adults but failed to show a role in cuticular hydrocarbon production (Balabanidou et al., 2016). Attempts to knockdown *in vitro* established P450 candidates in *An. gambiae* and *An. funestus* have failed to show effects on insecticide sensitivity (G. Lycett pers. comm.). Examples of successful knockdown of other genes associated with insecticide resistance are also limited. These include knockdown of the P450 partner CPR (Lycett et al., 2006) in susceptible mosquitoes which led to increased permethrin sensitivity, the transcription factor Maf (Ingham, 2016) and the appendage protein SAP2 (V. Ingham pers. comm.), whose knock down in resistant mosquitoes was shown to increase insecticide sensitivity.

A downside of transient RNAi is that its efficiency most often does not reach 100%. Linked to this, *An. gambiae*, similarl to *Drosophila*, does not have a systemic RNAi response (Tomoyasu et al., 2008), meaning that the interference signal is not spread among tissues. In effect this means that knockdown efficiency is tissue dependant, with some tissues seemingly more efficiently targeted than others (Lycett et al., 2006).

Similarly, Boisson et al. (2006) reported that remarkably high amounts of dsRNA are required to affect salivary gland genes, compared to fat body genes. Transient RNAi studies in mosquitoes are thus both temporally (one generation) and spatially limited.

An alternative that allows for stable and inheritable silencing is transgenesis with a RNAi-cassette that carries inverted repeats of the targeted gene. Although more laborious and relying on the availability of specific promoters, this has the advantage of creating continuous lines for analysis. Stable RNAi was demonstrated in *D. melanogaster* (Kennerdell & Carthew, 2000) and proof of principle experiments were successfully performed in *An. gambiae* cell line, and *An. stephensi* larvae and adults by silencing GFP (Brown, 2003a, 2003b). In *An. gambiae*, stable GAL4-mediated RNAi driven by an oenocyte specific promoter was used successfully for the first time to demonstrate a role for the cuticular *Cyp4g* genes mentioned above that failed to show an adult phenotype with transient RNAi (Lynd et al., unpublished). In *Ae. aegypti*, stable RNAi is more common and has been used to functionally characterise immune genes (Bian et al., 2005), salivary gland proteins (Chagas et al., 2014), and sex distorter genes (Hoang et al., 2016). Nevertheless, inheritable RNAi is most often not 100% efficient, since it only targets tissues in which the promoter is active. Those untargeted tissues will produce normal quantities of protein. This can be overcome to some extent by using promoters having much broader expression profiles.

A loss of function technique that is independent of promoters, is to create null mutants, having complete gene knockout. Programmable nucleases such as TALENs, ZFs and CRISPR/Cas9 are able to target specific DNA sequences in the germline, which leads to the subsequent generation of stable knockouts (Gaj, 2014). Such technologies have recently become available for application to a wide variety of organisms, including mosquitoes (Aryan et al., 2013; DeGennaro et al., 2013; Kistler et al., 2015). Nucleases have been used in *Anopheles* (Smidler et al., 2013; DeGennaro et al., 2013; Gantz et al., 2015; Hammond et al., 2016) mainly for vector control methods but has yet to be reported for the analysis of insecticide resistance in *An. gambiae*. Stable, colonised resistant lines are an obvious target for the development of such technologies in mosquitoes, and once highly efficient systems are developed these may be applied to more experimentally limiting field populations.

Gain of function analysis

The complementary method to investigate gene function is to overexpress genes in temporal and spatial patterns derived from specific promoters controlling the effector

gene. Again, genetic analysis by gain of function or overexpression has been achieved in *Anopheles* to characterise immune genes and their role in disease transmission. These include the overexpression of the antimicrobial peptide Cecropin under the control of the midgut-specific promoter carboxypeptidase (Kim et al., 2004) and that of TEP1 in the fat body using the blood-meal inducible vitellogenin promoter (Volohonsky et al., 2017). Similarly, the transcription factor REL2 was investigated in *Ae. aegypti* transcribed by the vitellogenin promoter (Antonova et al., 2009), and in *An. stephensi* with both carboxypeptidase and vitellogenin promoters (Dong et al., 2011). Finally, in *An. stephensi*, sustained activation of the insulin signalling pathway via overexpression of Akt (Corby-Harris et al., 2010) and PTEN (Hauck et al., 2013) in the midgut was shown to limit *Plasmodium* infection intensity.

Nevertheless, as described previously, *in vivo* functional analysis of *Anopheles* P450 genes involved in resistance has only been conducted in *D. melanogaster*. A major limiting step in this development has been the availability of promoters that drive expression in tissues that relate to insecticide resistance.

1.4.1 Promoters for gene functional analysis in *Anopheles*

As indicated above, effective functional analysis via stable RNAi or overexpression depends on achieving controlled spatio-temporal patterns of transgene expression, which is largely dependent on the promoter chosen. Endogenous tissue-specific promoters available for *Anopheles spp.* transgenic analysis include: the testes-specific *β2-tubulin* promoter (Catteruccia et al., 2005); the salivary gland-specific *apyrase* and *antiplatelet protein* promoters (Lombardo et al., 2000, 2005; Yoshida & Watanabe, 2006); the germline-specific promoters *vasa*, *vitellogenin receptor,* and *nanos* (Papathanos et al., 2009b; Biedler et al., 2014); the midgut-specific *carboxypeptidase* (Moreira et al., 2000), *cecropin A* (Kim et al., 2004), *peritrophic matrix protein 1* (Abraham et al., 2005), and *G12* (Nolan et al., 2011) promoters; the blood meal inducible fat body-specific promoters *vitellogenin* (Nirmala et al., 2006; Chen et al., 2007) and *lipophorin* (Volohonsky et al., 2015, 2017); and the olfactory receptor-specific promoter *orco* (Riabinina et al., 2016). While these promoters are currently implemented for functional analysis or generating gene drive systems, promoters for other tissues important for mosquito biology research, including ovaries and Malpighian tubules, have not been characterised.

Most notable is the lack of a characterised promoter driving ubiquitous expression in *An. gambiae*. This issue was investigated by Lycett et al. (2012), who characterised

the promoter of the *An. gambiae α-tubulin-1b* gene as a possible ubiquitous candidate. *AngTubα1b* was reported to drive expression in the head, chordotonal organs, central nerve cord, and testes, while expression in other tissues varied between lines generated and thus appeared to result from positional effect. A non-endogenous promoter driving widespread expression in *An. stephensi* (Marinotti et al., 2013), as well as *D. melanogaster* (Masumoto et al., 2012) and *B. mori* (Masumoto et al., 2012) is named *hr5-ie1* (Huynh & Zieler, 1999). This naturally controls the immediate-early genes of Baculovirus and has been used in *An. gambiae* to drive the expression of transformation markers (Grossman et al., 2001; Meredith et al., 2013). Although fluorescence was detectable across the body of larvae and pupae (Meredith et al., 2013), the specific pattern of expression driven by *hr5-ie1* was not detailed in *An. gambiae* adult tissues. The lack of a fully characterised endogenous ubiquitous promoter severely limits functional analysis of genes requiring widespread multi-tissue expression.

1.4.2 Mosquito germline transformation by embryo microinjection

A pre-requisite for functional analysis via inheritable modifications is obtaining transformant individuals by embryo microinjection. Following the first *in vivo* transformation of an insect genome (Rubin & Spradling, 1982), major advancements have been made in insect transgenic technologies that expanded applications from model organisms to more demanding non-model organisms such as mosquitoes. The introduction of exogenous DNA in insect embryos by microinjection was firstly documented by Rubin & Spradling, (1982) who achieved the first successful *in vivo* germline transformation of *D. melanogaster*. Since then, several species of mosquitoes have been transformed by embryo microinjection: *Ae. aegypti* (Morris et al., 1989), *An. stephensi* (Catteruccia et al., 2000), *An. gambiae* (Grossman et al., 2001), *C. quinquefasciatus* (Allen et al., 2001), *An. albimanus* (Perera et al., 2002), *Ae. fluviatilis* (Rodrigues et al., 2006), and *Ae. albopictus* (Labbé et al., 2010).

Nevertheless, microinjection of mosquito embryos remains a remarkably challenging technique subjected to numerous variables, most notably the technical experience of the operator for egg set up, injection, and post-injection handling, the quality and development of eggs, the toxicity of injected DNA, and timing of injection.

A somewhat optimised protocol for germline transformation of mosquito embryos was reported by Lobo et al. (2006). Here, injections target the dorsal surface of the posterior pole of pre-blastoderm stage embryos (Figure 1.7), where the pole or germ

plasm is located that contains cells destined to differentiate into the germ line. In dipteran eggs, after fertilisation, a syncytial blastoderm is formed through nuclear divisions with nuclei then migrating to the periphery of the egg and forming a cellularised blastoderm (Williamson & Lehmann, 1996). Since blastoderm segmentation occurs within 3 hours from fertilisation at insectary temperatures, injections are conducted at room temperature to slow down egg development (Lobo et al., 2006).

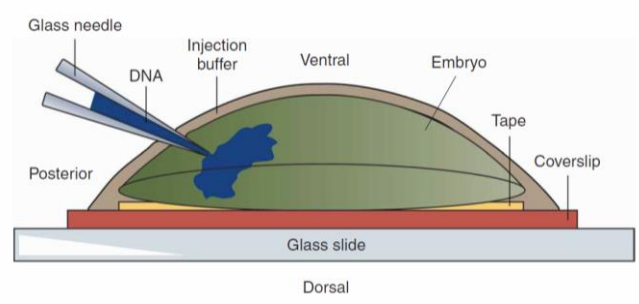

Figure 1.7 Mosquito embryo microinjections (taken from Lobo et al., 2006). Eggs are attached to a microscope slide using double sticky tape. The target of injection is the posterior end of the egg, where cells that will differentiate in the germline are located.

While protocols for injection of embryos have been optimised in *An. gambiae* (Lombardo et al., 2009; Pondeville et al., 2014), transformation efficiencies fluctuate quite extremely in separate injection experiments. From my experience, this is largely due to operator experience, however, Volohonsky et al. (2015) suggest that differences in transformation efficiency can be partly explained by the inconsistent co-delivery of the vector and the helper plasmids in the same germ cell. This was supported by the observation that when two plasmids marked with distinct fluorescent markers were co-injected, many of the cells of surviving larvae showed episomal expression of only one marker. To circumvent this issue, the transposase coding gene was instead included in the backbone of the vector plasmid. However, while reporting a dramatic improvement in transgenesis rates, co-integration of the transposase gene was recorded in 2 out of 5 experimental lines (Volohonsky et al., 2015). The issue of delivering a helper plasmid was also addressed in site-specific integration experiments by Meredith et al., (2013) who reported increased hatching rates and transformation efficiency when using a self-docking strain expressing the PhiC31 integrase gene.

1.4.3 Transposon-based transformation

Early insect transformation was entirely based on transposable elements. DNA transposons are class II mobile elements able to reposition within a genome via a cut-and-paste transposition process (Tu, 2012). Their general structure comprises a transposase gene flanked by inverted terminal repeats of variable length. The transposition process is mediated by the transposase and involves creating double-stranded staggered breaks at both recipient and donor target sites, integration of the DNA and end-repair (Tu, 2012). Target sites recognised by transposons are very short sequences, which makes the integration process essentially quasi-random (O'Brochta et al., 2014). These characteristics have been largely exploited for genome modification, as mentioned above, by using a bipartite vector-helper system in which the transposon terminal repeats which are recognised by the transposase enzyme are left intact, and the transposase gene is replaced with a DNA cassette of interest, while active transposase is supplied *in trans* encoded on a helper plasmid (Handler & O'Brochta, 2012).

Several transposable elements have been isolated from insect genomes and used for germline transformation. Among them, the *P* element was the first transposon ever isolated from an insect (*D. melanogaster*) (Kidwell et al., 1977) and the first used to transform one (Rubin and Spradling, 1982). However, *P* showed no mobility outside drosophilids which led to its limited use. Shortly after, the transposon that has probably had most widespread success in insect germline transformation, *piggyBac*, was isolated from the Lepidopteran *Trichoplusia ni* (Fraser et al., 1985) and has been used to transform non-drosophilid insects including lepidopteran, dipteran, coleopteran, hymenoptera and orthoptera (Atkinson & O'Brochta, 1999; Handler, 2002; O'Brochta et al., 2014). Following the discovery of piggyBac, members of the Tc1/mariner family (*Mariner*, *Mos1*, *Minos*) were isolated from the *Drosophila* genus (Jacobson & Hartl, 1985; Bryan et al., 1987; Franz & Savakis, 1991). While *Mariner* and *Mos1* have had a limited use due to their relatively low transposition efficiency, *Minos* has been more widely used and was the first to successfully transform an *Anopheles* mosquito, *An. stephensi,* by verified transposase mediated mobility (Catteruccia et al., 2000). Similarly, amongst the large family of hAT transposons, *Hermes*, isolated from *M. domestica* (Warren et al., 1994), has been successfully used to obtain germline transformation in coleopteran and dipteran, notably *Ae. aegypti*.

1.4.3.1 The piggyBac transposon

Transformation of insect genomes using the piggyBac transposon has revolutionised the field of insect genomic manipulation. Since its first application to transform the Mediterranean fruit fly (medfly) *Ceratitis capitata* (Handler et al., 1998), piggyBac has been implemented in germline transformation protocols of *D. melanogaster* but also of non-model organisms such as *T. castaneum* (Berghammer et al., 1999) and *B. mori* (Tamura et al., 2000). In mosquitoes, piggyBac transformation was successfully achieved in *Ae. aegypti* (Kokoza et al., 2001), *An. gambiae* (Grossman et al., 2001), *An. albimanus* (Perera et al., 2002) and *An. stephensi* (Nolan et al., 2002).

The piggyBac transposon was originally studied for its ability to transposase to the genome of baculoviruses cultured in *T. ni* cells (Fraser et al., 1985). The piggyBac element shows a symmetrical structure containing inverted repeats at each end, inverted sub-terminal repeats, and an internal gene encoding a transposase enzyme (Fraser et al., 1995) (Figure 1.8).

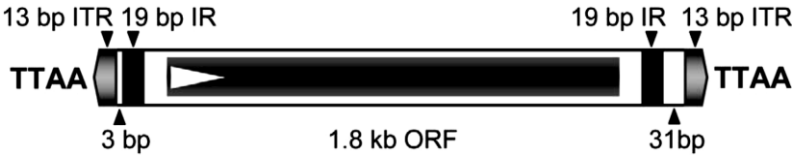

Figure 1.8 Schematic of the piggyBac element (taken from Handler, 2002). The transposon is 2476 bp long and carries two sets of 13 bp inverted repeats (one at each end), two sets of 19 bp inverted sub-terminal repeats (one at each end), and an internal 1785 bp region coding for a transposase enzyme (68 kDa). TTAA is the genomic target site and is present at each terminus.

PiggyBac-mediated transposition events occur via a non-replicative cut-and-paste mechanism that originates at TTAA target sites in the genome (Elick et al., 1996; Fraser et al., 1996; Mitra et al., 2008). Excision is initiated by a DNA double-stranded nick and mediated by the formation of a hairpin at the terminal repeats of the piggyBac transposon. DNA is then inserted and covalently joined by target site repair which restores the TTAA sites at each end (Cary et al., 1989).

The TTAA-specificity of transposition makes integration events essentially random leading to two major consequences: 1) integration may disrupt gene sequences thus inducing insertional mutations and gene knockout (lethal mutagenesis), and 2) the localisation of integration has major effects on transgene expression due to the

presence of enhancers, silencers or presence of heterochromatic structures (positional effect) (Handler & O'Brochta, 2012; O'Brochta et al., 2014). As such, generating transgenic lines using transposition is very laborious and time consuming because an evaluation of all individuals carrying unique insertions is required to select lines with minimal or no effects on fitness and active transgene expression (Fraser, 2012). Nevertheless, positional effect can be exploited in enhancer-trap systems where the presence of an enhancer nearby the site of insertion is detected by a reporter gene or GAL4 transcription factor under the control of a minimal promoter and exploited to define enhancer sequences and generate driver lines (Horn et al., 2003; O'Brochta et al., 2011).

Further limitations of the system include constrained carrying capacity (10-13 kb) (Geurts et al., 2003) and possible post-integration mobility mediated by an unintended transposase source which may lead to repositioning or loss of the transgene cassette. To overcome this, stabilisation techniques were introduced that involve the post-integration removal or rearrangement of the sequences essential for mobility such as the transposon terminal repeats (Handler, 2004).

1.4.4 Site-specific integration using the PhiC31/att system

Site-specific integration approaches were introduced to circumvent issues related with positional effect derived from random transposon-mediated transformation.

The PhiC31/att integration system is mediated by the bacteriophage PhiC31 integrase that catalyses the recombination between heterospecific attachment sites independently located in the genome of the bacteriophage PhiC31 (attP) and in that of *Streptomyces* bacteria (attB) (Figure 1.9). As recombination results in the formation of hybrid sites (attL and attR) which are no longer recognised by the integrase, integration is unidirectional, which overcomes the issue of post-integration mobilisation (Thorpe & Smith, 1998). Moreover, constructs longer than 100 kb have been reported to be successfully integrated in *D. melanogaster* overcoming carrying capacities constrains (Venken et al., 2006). Finally, analysis of phenotypes caused by different transgenes located in identical genomic locations can be performed that minimises the bias of positional effect (Bateman et al., 2006).

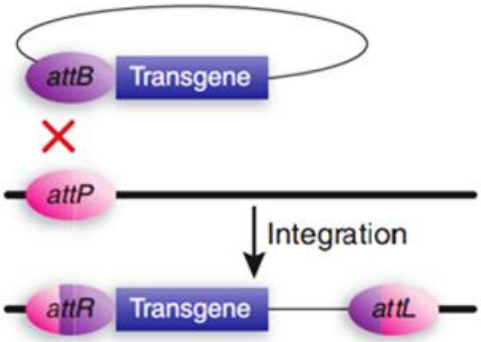

Figure 1.9 Schematic of PhiC31-mediated integration (taken from Wimmer, 2005). Plasmid DNA is integrated into the genome via recombination of the attB and attP sites resulting in the formation of hybrid sites attR and attL.

Site-specific integration can be exploited for transgenesis in a two-phase approach: transposon-mediated insertion is firstly required to create a docking line carrying attP sites in unique transcriptionally active genomic landing sites (phase I), and site-specific integration of an attB-flanked plasmid can then occur after its microinjection in the docking strain embryos (phase II) (Meredith et al., 2011). Therefore, creating docking lines still requires an initial random integration process followed by characterisation of lines with the least fitness cost and position effects. Yet, from these selected lines a great variety of new transgenic lines can be successively created by site-specific recombination.

In insects, PhiC31-mediated integration was firstly achieved in *D. melanogaster* (Groth et al., 2004) and later applied in the mosquitoes *Ae. aegypti* (Nimmo et al., 2006), *Ae. albopictus* (Labbé et al., 2010), *An. gambiae* (Meredith *et al*., 2011), and *An. stephensi* (Isaacs et al., 2012).

1.4.4.1 Recombinase-Mediated Cassette Exchange (RMCE)

A modification of the standard site-specific insertion systems, called recombinase-mediated cassette exchange (RMCE), involves the replacement of a previously integrated DNA construct with a donor DNA rather than its integration. This is achieved by flanking both donor and recipient cassettes with recombinase-specific target sites at each end, which allows for two independent crossover events resulting in cassette swop.

RMCE was achieved using the PhiC31/att system (Figure 1.10) in *D. melanogaster* (Bateman et al., 2006) and has also been applied successfully to non-model insects including the mosquitoes *An. gambiae* (Lynd et al., unpublished; Hammond et al., 2016), *Ae. aegypti* and *P. xylostella* (Haghighat-Khah et al., 2015), and *B. mori* (Long et al., 2015).

RMCE has advantages that permit new experimental designs: 1) only the DNA flanked by attB sites integrates in the specified genomic location rather than the whole donor plasmid (Bateman et al., 2006; Haghighat-Khah et al., 2015); 2) unmarked constructs can be integrated and successful integration identified by loss of fluorescent marker (Bateman et al., 2006); 3) there is an immediate gain in time and efficiency as the assessment of multiple lines to define localisation of insertion and fitness is bypassed.

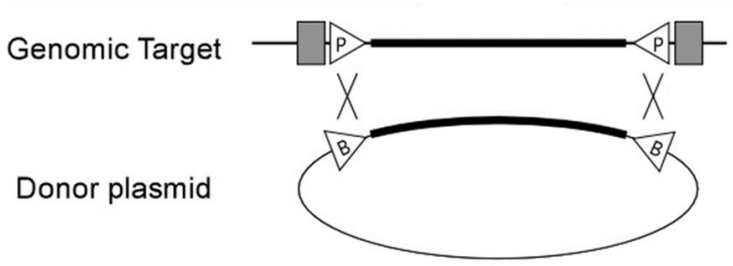

Figure 1.10 Schematic of the PhiC31-RMCE (taken from Bateman et al., 2006). The system is based on flanking the donor plasmid with attB sites (B) and the recipient cassette with attP sites (P) at each end. This results in the donor DNA flanked by attBs replacing the DNA flaked by attPs in the genomic target via two separate recombination events.

1.4.5 The GAL4/UAS system

Transgenic binary systems of expression represent a valuable tool to investigate the biological function of genes *in vivo* via localization of expression of genes linked to fluorescent reporters, gene overexpression, and gene knockouts.

Binary systems such as the GAL4/UAS, can be used for heterologous and homologous gene expression while their modular nature allows for repeated use of transgenic lines. The system was identified in the yeast *S. cerevisiae* where it is essential for the catabolism of galactose (Giniger et al., 1985). Here, gene expression is activated by the binding of 2 molecules of the transcription factor GAL4 (881 amino acids) to a 17 bp Upstream Activating Sequence (UAS) region localised upstream of the gene expressed (Laughon & Gesteland, 1982; Hong et al., 2008). GAL4/UAS was

exploited in insects to design a binary system consisting of two transgenic components independently inserted in the genome of transgenic lines, a driver or GAL4 and a reporter or UAS (Brand & Perrimon, 1993) (Figure 1.11). The driver line carries the GAL4 sequence, the expression of which is under the control of a specific promoter that defines the desired spatio-temporal pattern of expression; the responder line contains the UAS localised upstream of the sequence of the gene of interest. The system is active only in the progeny resulting from the cross between the driver and responder lines, which expresses the desired gene in the selected transcription pattern.

Figure 1.11 The GAL4/UAS bi-partite system (adapted from Lynd & Lycett, 2011). The driver construct consists of a promoter that drives the expression of the transcription activator factor GAL4. The responder construct contains the GAL4 binding site UAS (Upstream Activating Sequence) located upstream of the gene of interest. When the system is active GAL4 binds to the UAS and the genes is transcribed.

Binary systems offer several advantages compared to linear transgene expression including amplification of gene expression, repeated use of lines for comparing gene expression or promoter activity, possibility of creating lines bearing toxic genes as their expression is inactive in the parental lines, and investigation of phenotypes resulting from both gene-specific loss-of-function (silencing via RNAi) and gain-of-function (overexpression) in spatially and temporally controlled patterns. Furthermore, gene expression can be repressed by the GAL4 inhibitor GAL80, which binds to GAL4 and impairs its transactivation activity. Therefore, an additional layer of spatial or temporal control of transgene expression can be achieved by placing GAL4 and GAL80 under alternative promoters which results in the creation of mosaic organisms (Lee et al., 1999; Lai & Lee, 2006).

Since its first application in *D. melanogaster* to induce overexpression (Brand & Perrimon, 1993) or gene silencing (Piccin et al., 2001), the GAL4/UAS system has been applied to *B. mori* (Imamura et al., 2003), *T. castaneum* (Schinko et al., 2010), *Ae. aegypti* (Kokoza & Raikhel, 2011), *An. stephensi* (O'Brochta et al., 2012), and *An.*

gambiae, where the system was firstly developed in this laboratory in mosquito cell culture (Lynd & Lycett, 2011) and soon after applied to transgenic individuals to obtain gene overexpression (Lynd & Lycett, 2012) and silencing (Lynd et al., unpublished).

As mentioned previously, assessment of gene function using the GAL4/UAS system is currently limited by the availability of a restricted number of promoters and, most notably, the lack of a ubiquitous promoter. Expanding these tools available for GAL4-mediated functional analysis of resistance and other genes is one of the aims of this study.

1.5 Aims of the study

In view of the lack of functional analysis of resistance genes in *Anopheles*, this work aimed to identify the P450 genes that are physiologically involved in the emergence of metabolic resistance in *An. gambiae* mosquitoes and the tissues in which their expression is crucial for acquiring resistance.

The hypotheses to be tested included whether the upregulation of the single candidate P450 genes, *Cyp6m2* or *Cyp6p3,* is sufficient to drive the emergence of WHO-level of resistance *in vivo,* and whether resistance is dependent on expression in specific tissues (e.g. midgut, oenocytes or Malpighian tubules), or multiple tissues.

To do so we aimed to induce independent overexpression of *Cyp6m2* and *Cyp6p3* in tissue-specific and ubiquitous patterns of expression in susceptible mosquitoes using the GAL4/UAS system and to then assay for acquired resistance using WHO standard methods.

Since promoters for some of the locations we intended to investigate had not been characterised, this study also aimed to expand the flexible tools available for *An. gambiae* transgenesis by 1) identifying a promoter that drives widespread whole-body gene expression; 2) identifying a promoter that drives Malpighian tubule-specific expression; and 3) creating mosquito driver lines carrying newly identified promoters which will also serve as docking strains for PhiC31-mediated site-specific integration and cassette exchange.

Chapter 2

Characterisation of resistance phenotypes resulting from midgut or oenocyte-specific overexpression of *Cyp6m2* or *Cyp6p3*

2.1 ABSTRACT

The P450 monooxygenases CYP6M2 and CYP6P3, encoded by *Cyp6* genes, are strong candidates linked to insecticide metabolic resistance as supported by transcriptome data and *in vitro* metabolism experiments. Yet, *in vivo* analysis is needed to identify which *Cyp6* genes and tissues are responsible for the resistant phenotype to occur in the absence of other adaptations. Here, we investigated the ability of CYP6M2 and CYP6P3 to cause resistance when overexpressed in the midgut or in the oenocytes of otherwise susceptible *An. gambiae* mosquitoes. To do so, the GAL4/UAS system was used to drive overexpression of these genes in the targeted tissues of susceptible mosquitoes, which was successfully validated at RNA level for both genes and at protein level for CYP6M2. Mosquitoes overexpressing either *Cyp6m2* or *Cyp6p3* in the midgut or in the oenocytes did not show enhanced resistance to permethrin, deltamethrin, DDT, or bendiocarb compared to controls. The study provides the first *in vivo* evidence in elucidating the molecular basis of P450-mediated metabolic resistance in *An. gambiae* suggesting a potential involvement of other *Cyp6*-overexpressing tissue/s in driving resistance.

2.2 INTRODUCTION

Resistance mediated by the increased detoxification of insecticides by enzymes of the cytochrome P450 CYP6 family has been reported in a variety of mosquito species across Africa (David et al., 2013; Ranson & Lissenden, 2016). Amongst these, *An. gambiae Cyp6m2* and *Cyp6p3* are top candidate genes associated with metabolic resistance in this species as suggested by transcriptome analysis of resistant *vs* susceptible mosquitoes (Djouaka et al., 2008; Müller et al., 2008b; Mitchell et al., 2012; Fossog Tene et al., 2013; Kwiatkowska et al., 2013; Djègbè et al., 2014; Edi et al., 2014; Antonio-Nkondjio et al., 2016; Yahouédo et al., 2016), *in vitro* metabolism data (Yunta et al., unpublished) and, more recently, *in vivo* functional analysis in *D. melanogaster* (Edi et al., 2014). Taken together these data showed CYP6M2 ability to metabolise the pyrethroids permethrin and deltamethrin *in vitro* and to increase insecticide tolerance when overexpressed in *Drosophila* (Stevenson et al., 2011; Edi et al., 2014; Yunta et al., unpublished). Additionally, overexpression of CYP6M2, for which inability to metabolism DDT and bendiocarb was reported (Yunta et al, unpublished; Edi et al., 2014), caused a significant increase in LD_{50} of both insecticides in *Drosophila* (Edi et al., 2014). Similar data on CYP6P3 showed activity against pyrethroids and bendiocarb both *in vitro* and in *Drosophila* (Müller et al., 2008b; Edi et al., 2014).

Despite the growing data on the role of individual genes involved in detoxification, their physiology is overlooked with regards to the contribution of specific tissues to insecticide detoxification. The first comprehensive study of tissue-specificity of *An. gambiae* detoxifying gene families was conducted by Ingham at al. (2014), who investigated the native transcription enrichment in specific tissues compared to whole body, and compared enrichment levels in each body part in resistant *vs* susceptible mosquitoes. This revealed a general abundance of detoxifying gene transcripts in the midgut and Malpighian tubules of resistant mosquitoes, while some top candidate genes displayed a more widespread distribution of expression. Among these, *Cyp6m2* did not show tissue-specific overexpression in the locations investigated, while *Cyp6p3* was significantly overexpressed in the midgut of resistant mosquitoes in relation to the whole body. Identifying tissues where these genes are overexpressed is essential to start untangling pathways of detoxification along the mosquito body, which in turn will help understanding insecticide chemistries and the impact of routes of insecticide administration in mosquitoes. Among the tissues believed to be involved in detoxification, the midgut (Stevenson et al., 2011) and the oenocytes (Lycett et al., 2006) have been suggested in *An. gambiae* respectively via

analysis of transcript abundance and *in vivo* knockout of the P450 cofactor CPR. They constituted the first targets for analysis as driver lines specific for these tissues had already been established in the laboratory, thus effects of the overexpression in these locations was the initial focus.

2.3 AIMS AND OBJECTIVES

The study's aim was to investigate the ability of single *Cyp6* genes to drive resistance when independently overexpressed in individual mosquito tissues thought to be involved in detoxification. To do so, we used the GAL4/UAS system to overexpress candidate genes *Cyp6m2* and *Cyp6p3* in the midgut and the oenocytes of susceptible *An. gambiae* mosquitoes and tested the resulting phenotype for acquired resistance.

The study's objectives were:

- To create two transgenic responder lines for the UAS-regulated expression of *An. gambiae* genes *Cyp6m2* and *Cyp6p3*;
- To drive overexpression of *Cyp6* candidates by crossing newly created UAS responder lines to previously established GAL4 driver lines specific for expression in the midgut and the oenocytes;
- To validate *Cyp6* gene upregulation and CYP6 protein overexpression in the targeted tissues;
- To characterise the resistance phenotype obtained from midgut- and oenocyte-specific CYP6M2 and CYP6P3 overexpression using the WHO tube bioassay.

2.4 MATERIALS AND METHODS

Contributions

Dr. Amy Lynd created the driver lines for expression in the midgut and in the oenocytes and the responder plasmid in which *Cyp6* sequences were cloned.

Dr. Gareth Lycett performed the embryo microinjections.

General methods including DNA extraction, PCR, agarose gel electrophoresis, DNA purification and clean-up, restriction endonuclease digestion, ligation, *E. coli*

transformation, minipreps, midipreps, ethanol precipitation, and sequencing are described in Appendix A.

2.4.1 Plasmid preparation

2.4.1.1 The UAS-Cyp6m2 plasmid (pUASm2)

This plasmid was designed for the expression of *Cyp6m2* (AGAP008212) under the regulation of the UAS and was marked with yellow fluorescent protein (YFP). The 1500 bp coding sequence of *Cyp6m2* from the susceptible strain Kisumu was amplified from plasmid PB13:CYP6M2 (Stevenson et al., 2011) using primers M2fw and M2rv (Appendix B, Table B.1) and Phire Hot Start II DNA Polymerase (Life Technologies) following manufacturer's protocol. The *Cyp6m2* sequence was then cloned into pJET1.2/blunt vector using CloneJET PCR Cloning Kit (Thermo Scientific) and transformed into MegaX DH10B™ T1R Electrocomp™ *E. coli* cells (Invitrogen). Plasmid was purified from clonal bacterial cultures using the Merlin miniprep protocol and sequenced using primers pJETseqFW and pJETseqRV (Appendix B, Table B.1). The *Cyp6m2* sequence was finally digested out from the vector using EcoRV/XhoI and cloned into pSL*attB:Gyp:UAS14i:eYFP (Lynd et al., unpublished) to obtain the final plasmid pSL*attB:Gyp:UAS14i:Cyp6m2:eYFP (pUAS-m2) (Figure 2.1). This was harvested by miniprep and confirmed by single restriction enzyme digestions using SphI, BglII and SalI. Lastly, midiprep (Qiagen Plasmid Midi Kit) was performed following manufacturer's recommendations to isolate larger quantities of the plasmid, which was then stored at -20 °C.

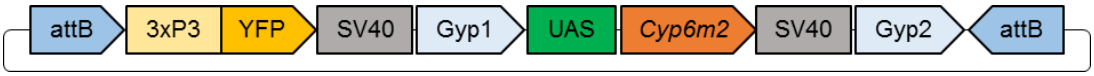

Figure 2.1 Schematic map of pUASm2. attB: PhiC31 attachment sites; 3xP3: eye-specific promoter; YFP: yellow fluorescent protein marker; SV40: Simian virus 40 PolyA transcription terminator; Gyp1 and Gyp2: Gypsy insulators; UAS: Upstream Activating Sequence, binding site of GAL4; *Cyp6m2*: coding sequence of *Cyp6m2*. Plasmid backbone is pSLfa1180fa.

2.4.1.2 The UAS-Cyp6p3 plasmid (pUASp3)

This YFP-marked plasmid was designed for the expression of *Cyp6p3* (AGAP002865) under the regulation of the UAS and was prepared as described above for *Cyp6m2*

except for the isolation of the coding sequence. The coding sequence of *Cyp6p3* was not previously cloned in its entirety as the first 24 bp were substituted by the amino-terminal sequence of the bovine steroid 17-α-hydroxilase for expression in *E. coli* (Müller et al., 2008b). Therefore, to obtain the full sequence, fusion PCR was used to join the 5' terminal sequences from cDNA to the abovementioned partial clone. A 193 bp fragment was amplified from Kisumu cDNA using primers P3fw1 and P3rv1 (Appendix B, Table B.1) and the remaining 1362 bp fragment from plasmid pCW:17α-Cyp6p3 (Müller et al., 2008b) using primers P3fw2 and P3rv2 (Appendix B, Table B.1). A third PCR was conducted to obtain the full 1555 bp sequence using primers P3EcoRIfw and P3rv2 (Appendix B, Table B.1). All PCRs were performed in a final volume of 20 µl using Phire Hot Start II DNA Polymerase (Thermo Scientific) according to manufacturer's protocol. Following amplification, cloning into the pJET1.2/blunt vector and sequencing using primers pJETseqFW and pJETseqRV (Appendix B, Table B.1), the coding sequence was cloned into pSL*attB:Gyp:UAS14i:eYFP (Lynd et al., unpublished) as described above. The map of the final plasmid pSL*attB:Gyp:UAS14i:*Cyp6p3*:eYFP (pUAS-p3) was verified by single restriction enzyme digestions using HindIII and SalI.

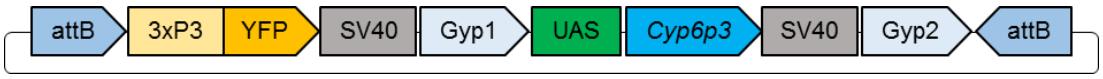

Figure 2.2 Schematic map of pUASp3. attB: PhiC31 attachment sites; 3xP3: eye-specific promoter; YFP: yellow fluorescent protein marker; SV40: Simian virus 40 PolyA transcription terminator; Gyp1 and Gyp2: Gypsy insulators; UAS: Upstream Activating Sequence, binding site of GAL4; *Cyp6p3*: coding sequence of *Cyp6p3*. Plasmid backbone is pSLfa1180fa.

2.4.2 Establishment of transgenic lines

2.4.2.1 Mosquito lines

Details of mosquito maintenance are reported in Appendix A. In this study, six mosquito lines were used:

- **G3**: wild type strain, originally isolated from The Gambia, obtained from the Malaria Research and Reference Reagent Resource Centre (MR4).
- **A11**: transgenic homozygous docking line created by piggyBac-mediated integration. The transgene cassette is inserted in 2R: 33,858,877-80 (Lynd et al.,

unpublished) and is flanked by attP sites for PhiC31-RMCE. The line is marked with 3xP3-driven cyan fluorescent protein (CFP).

- **GAL4mid**: transgenic homozygous driver line created by piggyBac-mediated integration. It expresses GAL4 under the control of the *An. gambiae* carboxypeptidase promoter (Moreira et al., 2000) which directs expression in the adult midgut. The transgene cassette lays in an imprecisely mapped site on the 3R chromosome (Lynd & Lycett, 2012) and the line is marked with 3xP3-driven *Discosoma sp.* red fluorescent protein (DsRed).
- **GAL4oeno**: transgenic homozygous driver line created by piggyBac-mediated enhancer trapping. It directs expression of GAL4 in the oenocytes of all life stages. The transgene cassette is inserted in 2R: 48,392,077-80 (Lynd et al., unpublished) and line is marked with 3xP3-driven DsRed.
- **UASm2** and **UASp3**: transgenic responder lines created by PhiC31-RMCE using the A11 docking strain. They are marked with 3xP3-driven YFP and designed for the expression of *Cyp6m2* and *Cyp6p3* respectively. Details on the creation of these lines are reported in sections 2.4.2.3 and 2.5.1.

2.4.2.2 Microinjections

Transgenic mosquitoes were produced by site-specific germline transformation (Pondeville et al., 2014) using PhiC31-RMCE.

2.4.2.2.1 DNA and needle preparation for microinjection

To prepare the pUASm2 injection mix, plasmid DNAs were harvested from bacterial cultures using Plasmid Midi Kit (Qiagen), ethanol precipitated and resuspended to obtain a solution containing 350 ng/µl of the pUASm2 responder plasmid and 150 ng/µl of the integrase helper plasmid PKC40 (Ringrose, 2009) in a total volume of 20 µl of 1x injection buffer (5 mM KCl, 0.5 mM $NaPO_4$, pH 7.2) (Lombardo et al., 2009). For pUASp3, an injection solution with a final concentration of 330 ng/µl was prepared instead at the same ratio of donor to helper plasmids. These mixes were used in two independent microinjection experiments.

Injecting needles were pulled from quartz capillaries with filament (fire polished) (Sutter Instrument Co.) with a length of 7.5 cm, 1 mm outer diameter and an inner diameter of 0.7 mm. Needles were prepared using Sutter Instrument Co. P-2000

Micropipette Puller with the following setting: HEAT = 650; FIL = 4; VEL = 25; DEL = 145; PUL = 200.

2.4.2.2.2 Embryo alignment and microinjection

Adult female mosquitoes of the A11 docking strain were allowed to lay in water for 20 minutes in the dark and embryos left to develop for further 30 minutes in insectary conditions.

Eggs were transferred in 25 mM NaCl onto a microscope slide and arranged in lines against the edge of Whatman filter paper grade 1 (Sigma). All embryos were aligned so the posterior (thinner) pole was exposed for injection and, whenever possible, so they laid on their dorsal side. After completing a line of ~50 embryos, Whatman paper was dried and removed, and eggs transferred onto a cover slip with double sticky tape. Here they were left to dry for 30 seconds before recovering them in a drop of 25 mM NaCl. Alignments were conducted using Leica MZ FLIII stereoscope at room temperature.

Microinjections were carried out in 25 mM NaCl at 200x magnification using Nikon Eclipse TE2000-U inverted microscope and Eppendorf® FemtoJet® Microinjector (Pi = 2000-3000 HPa) at room temperature (Lombardo et al., 2009). After injection, eggs were immersed in 2-3 cm of mineral water and returned to insectary conditions.

2.4.2.3 Creation of the UASm2 and UASp3 responder lines

Emerging F_0 larvae were separated by sex at pupal stage and surviving F_0 adults were pooled into sex specific founder cages and outcrossed with 3x excess of wild type G3s of the opposite sex. Five days after crossing, a first blood meal was offered and larvae of the F_1 progeny screened for YFP expression only (cassette exchange), CFP expression only (no exchange) or CFP/YFP expression (cassette integration) in the eyes and nerve cord.

For the UASm2 line, a second blood meal was offered to the founder cages and 16 individual female lays were set up to obtain F_1 isofemale lines. To do so, universal 30 ml plastic vials containing wet cotton wool and Whatman filter paper grade 3 (Sigma) were prepared and, two days after blood-meal, single females transferred inside and left laying overnight. Papers containing eggs were transferred into individual trays to

hatch. Females that did not lay were left in the vials for another night, after which they were discarded if did not lay eggs.

For the UASp3 lines, 19 isofemale lines were set up as described above from F_1 transgenic females after crossing with G3s. Orientation of insertion was then assessed in corresponding parental females and a single isofemale line established as the definitive line either by crossing transformant individuals with G3s (UASm2) or by interbreeding them with negative adults of the same batch (UASp3). Responder lines were kept as a mix of homozygous and heterozygous individuals so to obtain GAL4/+ progeny to be used as transgenic blank controls.

Minimum transformation efficiency was calculated as (*Number of independent insertions / total F_0 adult survivors) x 100.*

2.4.2.3.1 Orientation of insertion

Cassette exchange may happen in two different orientations with respect to the chromosome, designated A or B (Figure 2.3). Orientation check was performed on the parental females and on the controls G3 and A11 by PCR. Combinations of 4 primers designed to give a product only in one of the orientations were used in 4 different PCRs: piggyBacR-R2 + Red-seq4R for PCR 1, M2intFW or P3intFW + ITRL1R for PCR 2, piggyBacR-R2 + M2intFW or P3intFW for PCR3, and Red-seq4R + ITRL1R for PCR 4 (Figure 2.3). PCRs were performed using Phire Hot Start II DNA Polymerase (Life Technologies) and a 30-cycle thermal program consisting of 60°C annealing temperature and 60-second extension.
Definitive UASm2 and UASp3 isofemale lines were created from individuals showing orientation of insertion A, which was chosen consistent with previous RMCE lines created in this laboratory.

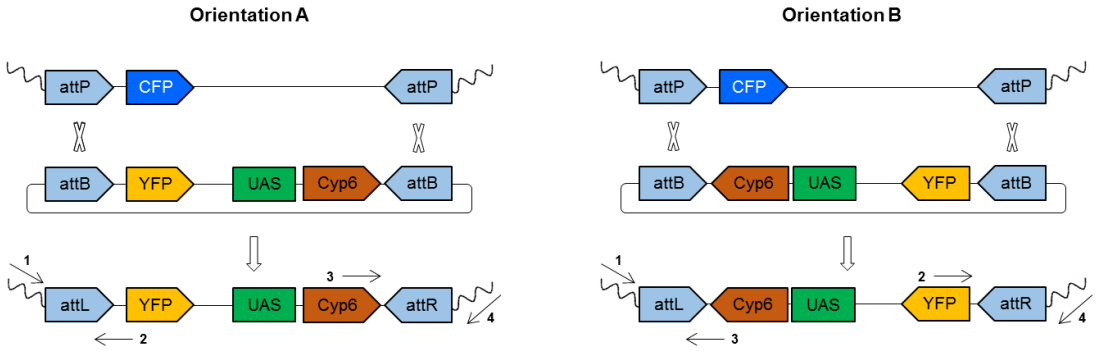

Figure 2.3 Two possible orientations of insertion, A and B, after recombination of the attP sites in the docking mosquito genome and the attB sites in the UAS-Cyp6 plasmids. attP, attB: PhiC31 recombination sites; CFP: cyan fluorescent protein; YFP: yellow fluorescent protein; UAS: upstream activating sequence; attL, attR: hybrid sites created after recombination; →: primer annealing site, 1: piggyBacR-R2; 2: Red-seq4R; 3: M2intFW or P3intFW; 4: ITRL1R (Appendix B, Table B.1).

2.4.3 GAL4 x UAS crosses

Crosses were established between the homozygous drivers specific for expression in the midgut (GAL4mid) (Lynd & Lycett, 2012) or in the oenocytes (GAL4oeno) (Lynd et al., unpublished) marked with DsRed, and opposite sex individuals of the UASm2 and UASp3 responder lines marked with YFP. A total of 4 crosses was established: GAL4mid x UASm2, GAL4mid x UASp3, GAL4oeno x UASm2 and GAL4oeno x UASp3.

The progeny of these crosses was expected to give GAL4/UAS transgenic mosquitoes expressing both YFP and DsRed and GAL4/+ mosquitoes expressing DsRed only (controls). Progeny was sorted at pupa stage according to marker colour to have DsRed/YFP-positive and DsRed-positive individuals using a Leica MZ FLIII fluorescence stereo microscope fitted with DsRed and YFP filters (Leica Microsystems).

2.4.4 Assessment of *Cyp6* gene expression in GAL4/UAS *vs* GAL4/+

2.4.4.1 Sample preparation

To quantify *Cyp6* gene expression in GAL4/UAS and GAL4/+ individuals, total RNA was harvested from pools of whole adults, pupae, larvae and their dissected body parts. For the GAL4mid crosses, RNA was isolated from whole adults, dissected midguts and remainder tissues (carcass), while for the GAL4oeno crosses collection

was carried out from whole L4 larvae, pupae, adults, dissected adult abdomens (without internal organs), and remainder adult tissues (carcass).

For adult dissections, 2-5-day-old GAL4/UAS and Ga4/+ mosquitoes were anesthetised with gaseous CO_2 and dissected in PBS supplemented with EDTA-free protease inhibitor cocktail (Roche). Dissected body parts were immediately transferred in 100 µl of TRI Reagent (Sigma) on ice and homogenised using an electrical pestle. Whole larvae, pupae and adults were directly homogenised in 100 µl of TRI Reagent. Finally, after grinding, 400 µl of TRI Reagent were added to each sample to reach a final volume of 500 µl and samples briefly spun.

Three biological replicates consisting of 5 mosquitoes (or body parts) each were collected from each mosquito population.

2.4.4.2 RNA extraction, DNase treatment and cDNA synthesis

RNA extraction was performed using the TRI Reagent® protocol (Sigma) following manufacturer's instructions. To remove genomic DNA contamination, samples were treated with DNase using a Turbo DNA-Free kit (Ambion) following manufacturer's instructions. RNA was then reverse-transcribed using the SuperScript III First-Strand Synthesis System (Life Technologies) following the oligo(dT) reaction protocol described by the manufacturer. cDNA was diluted to reach a final concentration of 50 ng/µl.

2.4.4.3 RT-qPCR

RT-qPCR reactions were set in a final volume of 20 µl using 1x Brilliant III Ultra-Fast SYBR® Green qPCR Master Mix (Agilent Technologies), 0.5 mM primers and 1 µl (50 ng/µl) of cDNA template. Amplification was conducted in Mx3005P qPCR System (Agilent Technologies) using the following conditions: 1 cycle at 95°C for 3 minutes, 40 cycles at 95°C for 10 seconds, and 60°C for 10 seconds followed by a dissociation curve protocol (95°C for 1 minute, 55°C for 30 seconds and 95°C for 30 seconds).

cDNA was tested for the expression of the targeted *Cyp6* genes using primers qM2fw and qM2rv for quantification of *Cyp6m2*, and qP3fw and qP3sub for *Cyp6p3* (Edi et al., 2014) (Appendix B, Table B.1). The qP3sub primer bears a nucleotide substitution (A11G) to conform its sequence to that of the G3 template. Two housekeeping genes, the ribosomal protein S7 (RPS7) (AGAP010592) and Ubiquitin (AGAP007927), were

also quantified using primers qS7fw, qS7rv, qUBfw and qUBrv (Jones et al., 2013) (Appendix B, Table B.1).

Efficiency of each primer pair was determined by creating standard curves from 5 serial dilutions of the plasmids carrying the cDNA template. Primer efficiency was calculated using the MxPro Mx3005P Software for SYBR Green (Agilent). Efficiency values of 95-103 % with $R^2 \geq 0.985$ were accepted.

2.4.4.4 Expression data analysis by ΔΔCt method

Transcriptional data obtained by RT-qPCR were analysed using the ΔΔCt method (Livak & Schmittgen, 2001; Schmittgen & Livak, 2008). Threshold cycle (Ct) values were corrected for primer efficiency applying the formula *Corrected Ct = Ct (Log_x / Log_2),* where *x = 2* if efficiency is >100% and *x = 1+Efficiency* if efficiency is <100%. Ct values obtained for target genes were normalised against those of the housekeeping genes RPS7 and Ubiquitin using the formula $\Delta Ct = Ct_{target} - Ct_{housekeeping}$. Mean ΔCt values of GAL4/+ mosquitoes were then compared to those of GAL4/UAS mosquitoes using the formula $\Delta\Delta Ct = \Delta Ct_{GAL4/+} - \Delta Ct_{GAL4/UAS}$. Finally, fold change (x) expression between the two populations was calculated with the formula $2^{\wedge GAL4/UAS\ \Delta\Delta Ct} / 2^{\wedge GAL4/+\ \Delta\Delta Ct}$. Native expression of *Cyp6m2* and *Cyp6p3* was evaluated in the control GAL4/+ mosquitoes compared to the expression levels of the housekeeping genes RPS7 and Ubiquitin (-ΔCt) and plotted with the difference in expression levels between transgenic GAL4/UAS mosquitoes and GAL4/+ controls (ΔΔCt). Statistical differences between expression (ΔΔCt values) in GAL4/UAS *vs* GAL4/+ were determined using Welch's t-test (two-tails, unequal variance). Names of files containing all raw data and analysis are reported in Appendix B.

2.4.5 Assessment of CYP6 protein expression in GAL4/UAS *vs* GAL4/+

2.4.5.1 Sample preparation

To detect CYP6 protein expression in GAL4/UAS and GAL4/+ individuals, total protein extracts were obtained from whole 2-5-day-old female adults, L4 larvae, pupae, and their dissected body parts.

For the GAL4mid crosses, protein extracts were obtained from a single whole adult, a single carcass (whole body minus the midgut) and two midguts.

For the GAL4oeno crosses, total protein content was obtained from a single larva (without the midgut), a female pupa, a female adult, a single pupa without the head-thorax, a single adult dissected abdomen cuticle (without internal organs) and a single adult carcass (whole adult without abdomen cuticle). In all samples except pupae the midgut was removed to minimise the action of proteinases.

For adult dissections, mosquitoes were anesthetised with gaseous CO_2 and dissected in ice-cold PBS supplemented with EDTA-free protease inhibitor cocktail (Roche). Dissected body parts were immediately transferred in a solution of PBS and 2x Laemmli Sample Buffer (Bio-Rad) supplemented with 2.5% 2-Mercaptoethanol. Samples were then homogenised using an electrical pestle, incubated at 95°C for 10 minutes and briefly spun before being stored at -20°C.

2.4.5.2 SDS-PAGE

10 ml of 10% resolving gel solution was prepared using 4.1 ml of double-distilled water, 3.3 ml Acrylamide/Bis-acrylamide (Sigma), 2.5 ml resolving buffer (1.5 M Tris-HCl, pH 8.8), 100 µl 10% SDS, 75 µl ammonium persulphate (APS), 7 µl TEMED (Sigma) in a 0.75 mm cast. After 1 h of polymerisation, 2.4 ml of 3% stacking gel was prepared using 2.05 ml of double-distilled water, 450 µl Acryl-Bis, 850 µl of stacking buffer (0.5 M Tris-HCl, pH 6.8), 35 µl 10% SDS, 25 µl APS and 5 µl TEMED, poured on the resolving gel and left to polymerase for 30-60 minutes with a 0.75 mm comb inserted.

20 µl of single mosquito preparations, equivalent to 1/3 of a mosquito or its body part, were analysed by SDS-PAGE. The only exception was the midgut samples, for which 20 µl contained 2 whole midguts. The higher amount of midgut sample was required to visualise signal of the α-tubulin loading control.

Electrophoresis was carried out at 80 V through the stacking gel and at 150 V through the resolving gel in 1x running buffer (2.5 mM Tris, 19.2 mM Glycine, 0.01% SDS, pH 8.3).

2.4.5.3 Western blot

Gels were blotted into nitrocellulose membrane (Amersham Hybond-ECL, GE Healthcare) using a transfer buffer (10% 25 mM Tris, 192 mM Glycine, 0.1% SDS, 20% methanol) at 300 mA for 1 h. All washing steps were performed 3 times for 10

minutes using TBST (50 mM Tris, 150 mM NaCl, 0.1% Tween 20, pH 7.6) as washing buffer. Membranes were blocked using 5% skimmed-milk in TBST usually overnight at 4°C, occasionally for 1 h at room temperature.

For probing CYP6, membranes were firstly incubated with affinity-purified polyclonal peptide antibodies produced in rabbit against CYP6M2 or CYP6P3 (gifts from M. Paine) diluted 1:200 in TBST 5% milk for 1 h and, following washing, with horseradish peroxidase (HRP)-tagged goat anti-rabbit IgG antibodies (Bethyl Laboratories) diluted 1:10,000 in TBST 3% milk for 1 h.

After detection of the CYP6 signal, membranes were re-probed with anti-housekeeping antibodies to account for quantity of protein loaded. For this purpose, membrane was incubated in Restore™ PLUS Western Blot Stripping Buffer (Life Technologies) for 15 minutes, washed and blocked as described above, and probed with anti-αtubulin antibodies (Sigma or Fisher Scientific) diluted 1:2,000 in TBST 3% milk for 1 h followed by washing and incubation with HRP-conjugated goat anti-mouse IgG antibodies (Abcam) diluted 1:20,000 in TBST 3% milk for 1 h.

Signal detection was carried out using SuperSignal™ West Dura Extended Duration Substrate (Life Technologies) and Amersham Hyperfilm ECL (GE Healthcare).

2.4.6 Assessment of mosquito susceptibility to insecticides by WHO bioassay

Mosquito susceptibility to insecticides was assessed using the WHO tube bioassay (WHO, 2016b). Pools of ~20 GAL4/UAS and GAL4/+ adult female mosquitoes 2-5 day-old were exposed to filter papers impregnated with standard discriminating doses of insecticide – 0.75% permethrin, 0.05% deltamethrin, 0.1% bendiocarb, 4% DDT – for 1 h in insectary conditions. After exposure, mosquitoes were returned to the holding tube and a 24 h recovery period was allowed with 10% sugar solution provided *ad libitum* in insectary conditions (Figure 2.4). At the end of the 24 h, mortality rates were calculated as: (*Total number of dead mosquitoes / Total sample size) × 100.* When ≥5%-<20% mortality was recorded in unexposed control tubes, the Abbott's formula was used to correct the data: *(% observed mortality – % control mortality) / (100 – % control mortality) x 100.*

Mortality rates were interpreted as follows:

- ≥98%: susceptibility
- <98% – ≥90%: potential resistance
- <90%: resistance

Following WHO guidelines, that mitigate against variability in quality control of insecticide papers, only assays showing 95-100% mortality in the sensitive control population (GAL4/+) were included in the results.

A modified version of the WHO bioassay was also performed reducing the exposure time to 20 minutes (Lycett et al., 2006).

Each experiment included mosquitoes from independent batches deriving from independent crosses or from subsequent gonotrophic cycles of the same cross, therefore they were considered as biological replicates. 1-4 experiments were performed for each insecticide tested. Generally, two technical replicate tubes were tested for each population in each experiment. Number of bioassay experiments conducted are reported in Table 2.1.

Welch's t-test (two-tails, unequal variance) was performed to determine statistical significant differences between mortality rates in GAL4/UAS and GAL4/+ mosquitoes with P values (p) interpreted as follows:

- $p > 0.05$: not significant
- $p \leq 0.05$: significant (*)
- $p \leq 0.01$: significant (**)
- $p \leq 0.001$: significant (***)
- $p \leq 0.0001$: significant (****)

File names with raw data and analysis are listed in Appendix B.

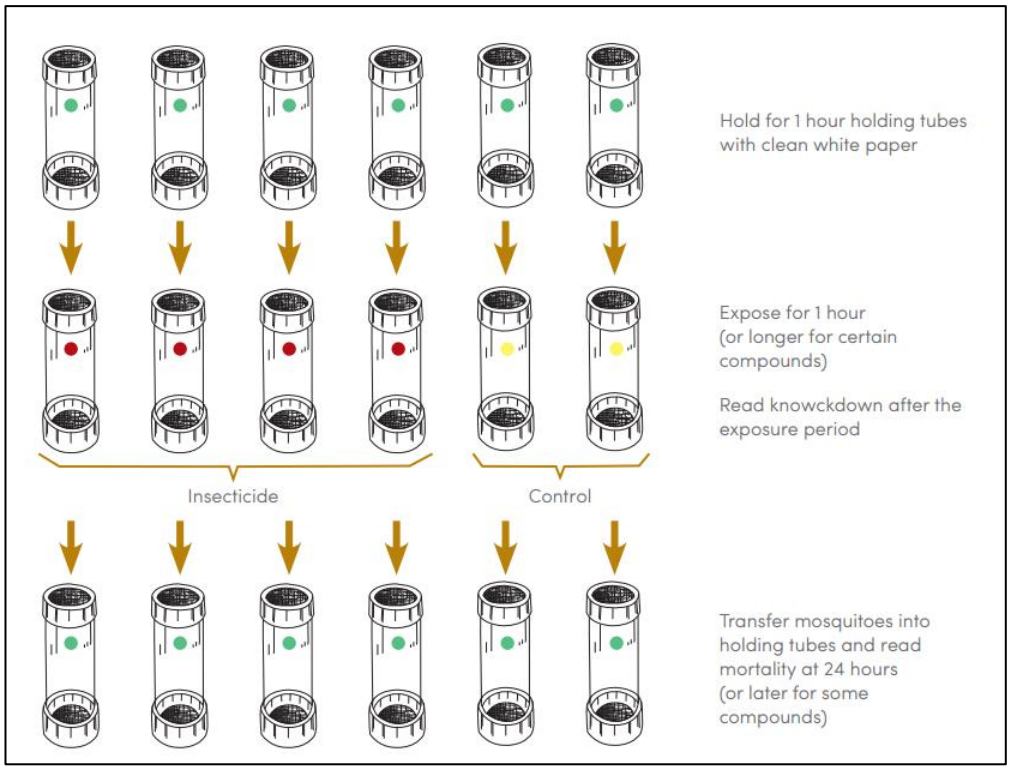

Figure 2.4 Set up and protocol of the WHO tube bioassay for assessing resistance to standard discriminating insecticide doses (taken from WHO,2016b).

Table 2.1 Bioassay experiments performed.

Cross	Insecticide	1 h exposure		20 min exposure	
		Experiment (Biol. reps)	Tot. tech. reps	Experiment (Biol. reps)	Tot. tech. reps
GAL4mid x UASm2	Permethrin 0.75%	2	3	3	6
	Deltamethrin 0.05%	1	2	1	2
	DDT 4%	2	3	1	2
	Bendiocarb 0.1%	1	2	1	2
GAL4mid x UASp3	Permethrin 0.75%	1	2	3	6
	Deltamethrin 0.05%	1	2	1	2
	DDT 4%	1	2	1	2
	Bendiocarb 0.1%	1	2	1	2
GAL4oeno x UASm2	Permethrin 0.75%	1	2	4	8
	Deltamethrin 0.05%	1	2	2	4
	DDT 4%	1 (4)	2 (8)	1	2
	Bendiocarb 0.1%	1	2	1	2
GAL4oeno x UASp3	Permethrin 0.75%	2	3	3	6
	Deltamethrin 0.05%	1	2	1	2
	DDT 4%	1 (2)	2 (4)	2	3
	Bendiocarb 0.1%	1	2	1	2

Numbers reported represent the experiments and replicates that were included in the analysis as mortality in the controls reached at least 95%, while those in brackets show the total number of experiments and replicates performed.

2.5 RESULTS

2.5.1 Mosquito lines for UAS-regulated expression of *Cyp6* genes

2.5.1.1 UASm2 mosquito line

The *Cyp6m2* coding sequence (1500 bp) showed 100% nucleotide identity with the plasmid template upon sequencing (Appendix B, Figure B.1) and was successfully cloned into pSL*attB:Gyp:UAS:14i:eYFP to give the pUASm2 plasmid (8999 bp) (Figure 2.1).

Of the 347 A11 embryos injected with pUASm2, 81 larvae (23%) hatched. From these 49 (60%) adults (F_0) emerged, 24 females and 25 males, which were separated by sex in two cages. A summary of the screening and crossing strategy used to establish the UASm2 transgenic line is reported in Table 2.2. After offering a first blood meal to

F_0 adults, no transformant larvae were recovered from the male cage, while progeny from the female cage included 13 transgenic larvae: 3 YFP-positive and 10 expressing both YFP and CFP likely resulting from cassette integration, which were discarded. Of the 3 YFP-positive larvae a single adult male survived that did not give progeny. After offering a second blood meal to the F_0 female cage, 16 isofemale lines (A-P) were set up of which 11 laid eggs. Two single-laying females gave F_1 transgenic progeny: isofemale J yielded 4 (10%) transgenic YFP-positive larvae, and isofemale G gave 2 (2.9%) YFP/CFP expressing larvae (discarded). From isofemale J, 2 males reached adulthood (J1 and J2), which displayed orientation of insertion A (specific fragment sizes reported in Table 2.3, Figure 2.5). To create the definitive line, these were crossed with wild type G3 females and a total of 80 (54%) F_2 YFP transformant larvae was obtained.

At least two transformation events (one cassette exchange and one integration) occurred independently, with a minimum overall transformation efficiency of 4% (2 events/49 F_0) and efficiency of cassette-exchange of 2% (1 event/49 F_0).

Table 2.2 Screening and crossing strategy to establish the UASm2 transgenic line.

F_0 pool	F_0 No. and sex	F_1 + progeny 1st blood meal	F_1 + progeny 2nd blood meal	F_2
1	24 F	3 YFP+ 10 YFP/CFP+	Isofemale J: 2M YFP+ Isofemale G: 2 larvae YFP/CFP+	From J males: 54% (80/148)
2	25 M	0	0	N/A

F: female, M: male. N/A: not applicable

Table 2.3 Expected fragment sizes derived from the integrated UASm2 cassette following 4 specific PCRs performed on parental males J1 and J2 to check for two alternative orientations of insertion.

PCR	Primers*	Orientation	J1 – J2	G3	A11
PCR 1	piggyBacRR2 RedSeq4R	A	838 bp	--	902 bp
PCR 2	M2intFW ITRL1R		2662 bp	--	--
PCR 3	piggyBacRR2 M2intFW	B	2349 bp	--	--
PCR 4	RedSeq4R ITRL1R		1606 bp	--	--

* All primer sequences are reported in Appendix B, Table B.1. Primer combinations include one primer that binds to one of the piggyBac arms present on the original docking cassette inserted in A11, and one annealing within the sequence of the newly inserted cassette.

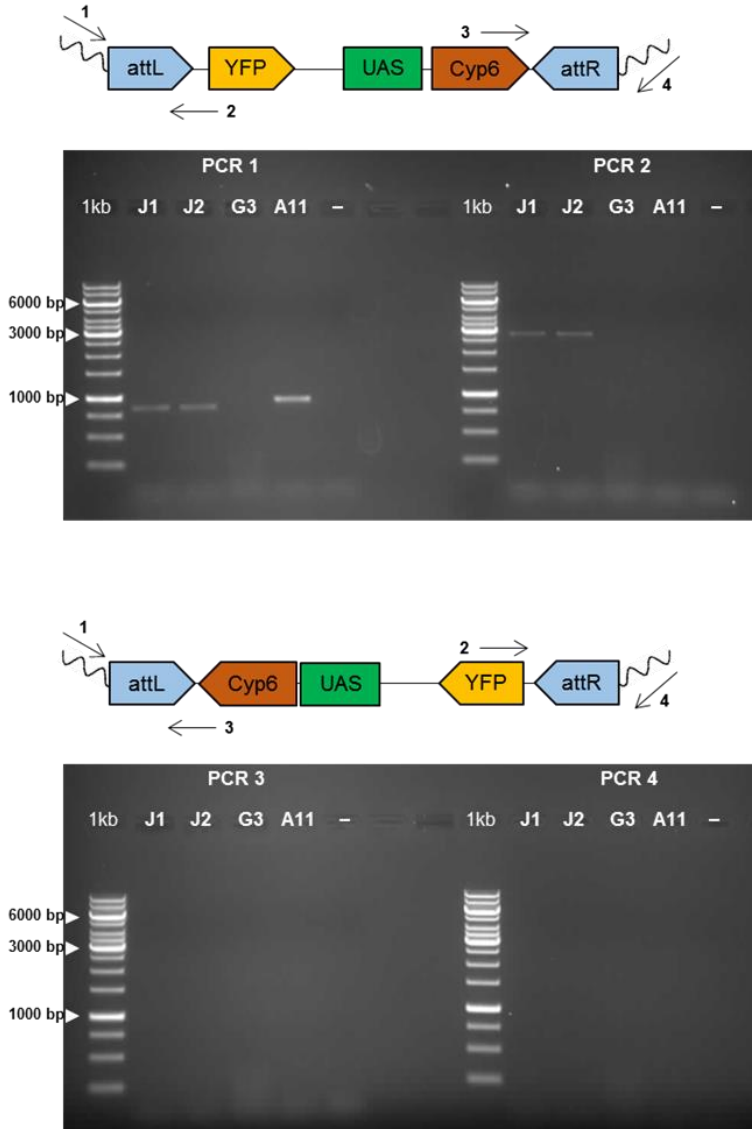

Figure 2.5 Orientation of insertion in UASm2 transgenic males obtained from isofemale J (J1 and J2). G3: wild type (control); A11: docking line (control); –: negative control (PCR mix without DNA). Ladder is GeneRuler 1 kb (Thermo Scientific). Each PCR gives a distinct amplification fragment that is diagnostic for the orientation of the insertion (Table 2.3).

2.5.1.2 UASp3 mosquito line

The *Cyp6p3* sequence (1530 bp) showed 100% nucleotide identity to the respective annotated PEST sequence and plasmid templates upon sequencing (Appendix B, Figure B.2). The sequence was successfully cloned into pSL*attB:Gyp:UAS:14i:eYFP to give the pUASp3 plasmid (9007 bp) (Figure 2.2).

460 embryos of the A11 docking line were injected with UASp3. Of these 204 (44%) larvae hatched and 124 (60.8%) individuals reached adulthood, 68 females and 56

males. F_0 adults were separated by sex in 4 cages, 3 female cages (1-3) and 1 male cage (4), and outcrossed with G3s. A summary of the screening and crossing strategy used to establish the UASm2 transgenic line is reported in Table 2.4. F_1 transgenic individuals were detected in the progeny of cages 1, 2 and 4, which overall produced 74 YFP-positive and 7 YFP/CFP-positive transformant individuals (discarded). Of the 74 YFP-positive larvae, 44 reached adulthood, 25 males and 19 females. F_1 transgenic males were discarded, while females were crossed with G3s and 19 isofemale lines (A-S) set up. From these, 9 gave at least 1 F_2 transgenic progeny of which 4 (B, D, H, M) showed orientation A and 5 (A, C, I, O, P) orientation B. Specific fragment sizes expected for both orientations are reported in Table 2.5 and Figure 2.6. Progeny from isofemale M was kept for establishing the definitive colony by interbreeding transgenics with negative adults of the same batch.

Data suggest that at least 9 separate transgenic events (3 cassette exchanges, in both orientation A and B, and 3 cassette integrations) occurred independently, with a minimum overall transformation efficiency of 7% (9 events/124 F_0) and cassette-exchange efficiency of 4.8% (6 events/124 F_0).

Table 2.4 Screening and crossing strategy to establish the UASp3 transgenic line.

F_0 pool	**F_0 No. and sex**	**F_1 + progeny**		**F_2 + progeny**	
		YFP+	**YFP/CFP+**	**Isofemale**	**Orientation**
1	28 F	11 (7F, 4M)	1	A B C D E	B A B A B
2	27 F	10 (2F, 8M)	2	H I	A B
3	13 F	0		N/A	
4	56 M	23 (10F, 13M)	4	M O P	A B B

F: female, M: male. N/A: not applicable

Table 2.5 Expected fragment sizes derived from the integrated UASp3 cassette following 4 specific PCRs performed on parental females M, O and P to check for two alternative orientations of insertion.

PCR	Primers	Orientation	p3 (M-O-P)	G3	A11
PCR 1	piggyBacRR2 RedSeq4R	A	838 bp	--	902 bp
PCR 2	P3intFW ITRL1R		2662 bp	--	--
PCR 3	piggyBacRR2 +P3intFW	B	1789 bp	--	--
PCR 4	RedSeq4R ITRL1R		1551 bp	--	--

* All primer sequences are reported in Appendix B, Table B.1. Primer combinations include one primer that binds to one of the piggyBac arms present on the original docking cassette inserted in A11, and one annealing within the sequence of the newly inserted cassette.

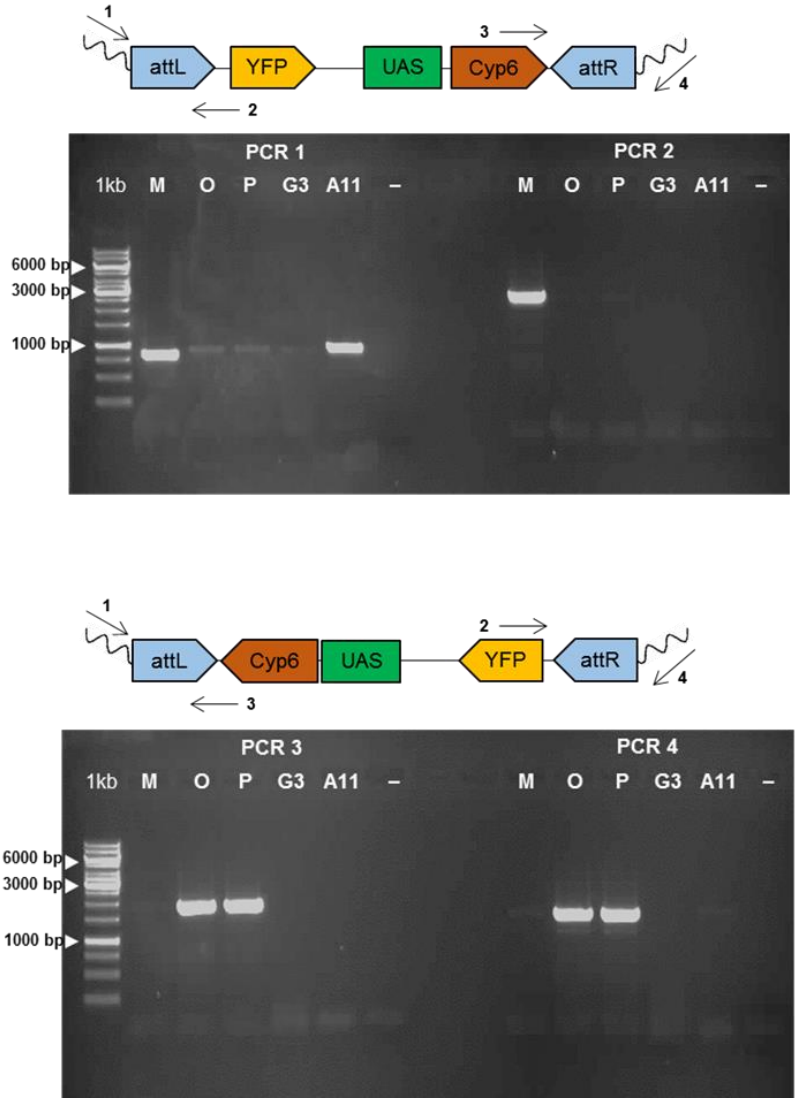

Figure 2.6 Orientation of insertion in UASp3 transgenic single-laying females M, O, and P. G3: wild type (control); A11: docking line (control); –: negative control (PCR mix without DNA). Ladder is GeneRuler 1 kb (Thermo Scientific). Each PCR gives a distinct amplification fragment that is diagnostic for the orientation of the insertion (Table 2.5).

2.5.2 *Cyp6* transcription in midgut- and oenocyte-specific crosses

2.5.2.1 Cyp6 transcription levels in GAL4mid crosses

RT-qPCR analysis in the progeny of GAL4mid crosses revealed that *Cyp6m2* was 889x overexpressed in whole GAL4mid/UASm2 compared to native expression in GAL4mid/+ adult females (ΔΔCt = 9.8, p = 9.36E-07) (Figure 2.7A), with highly enriched (2731x) localisation of over-transcription in the dissected midgut (ΔΔCt = 11.4, p = 2.03E-06) (Figure 2.7A). A lower 77x overexpression was detected in the carcass of transgenic mosquitoes of the same cross compared to controls (ΔΔCt = 6.1, p = 0.0023) (Figure 2.7A).

In the progeny of GAL4mid crosses, *Cyp6p3* was found 135x overexpressed in whole GAL4mid/UASp3 adult females compared to GAL4mid/+ controls (ΔΔCt = 7.08, p = 0.0002) (Figure 2.7B), with a 659x over-transcription specifically localised in the dissected midgut (ΔΔCt = 9.6, p = 0.001) (Figure 2.7B). A 7x overexpression was also detected in the carcass of transgenic mosquitoes of the same cross compared to control carcasses (ΔΔCt = 2.6, p = 0.035) (Figure 2.7B).

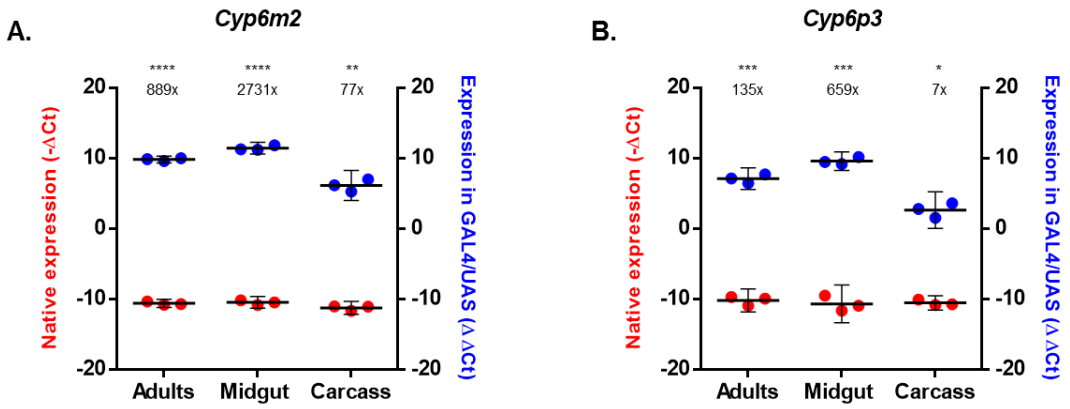

Figure 2.7 Transcription of *Cyp6* genes in GAL4mid crosses. Native expression in GAL4/+ mosquitoes (red circles) is expressed as -ΔCt ($Ct_{Housekeepings}$ – Ct_{Cyp6}). Expression in GAL4/UAS mosquitoes compared to GAL4/+ controls (blue circles) is reported as ΔΔCt ($\Delta Ct_{GAL4/+}$ – $\Delta Ct_{GAL4/UAS}$). Transcription of *Cyp6m2* (**A)** and *Cyp6p3* **(B)** in adult females and their dissected body parts. Carcass is whole body without the midgut. Numbers above show the fold change (x) expression in GAL4/UAS compared to GAL4/+ mosquitoes. Vertical lines represent 95% confidence intervals and middle lines the mean from three replicates. Statistical significance was calculated using Welch's test. * $p < 0.05$, ** $p \leq 0.01$, *** $p \leq 0.001$, **** $p \leq 0.0001$. File names with raw data and analysis are listed in Appendix B.

2.5.2.2 Cyp6 transcription levels in GAL4oeno crosses

RT-qPCR analysis on different life stages of individuals from the GAL4oeno cross revealed that *Cyp6m2* was 12x upregulated in GAL4/UAS adults compared to GAL4oeno/+ controls (ΔΔCt = 3.8, p = 0.007) (Figure 2.8A). Upregulation was higher (66x) in transgenic dissected abdomens compared to blank abdomens (ΔΔCt = 6.1, p = 0.0006) (Figure 2.8B). A 26x upregulation was also found in the carcass of GAL4/UAS adults (ΔΔCt = 4.7, p = 0.0012) (Figure 2.8B).

In individuals of the GAL4oeno/UASp3 cross, *Cyp6p3* was 18x upregulated in whole adults (ΔΔCt = 4.2, p = 0.0004) (Figure 2.8C) and 153x in dissected abdomens (ΔΔCt = 7.5, p = 0.007) (Figure 2.8D). A 2x upregulation was also detected in the carcass of GAL4/UAS compared to control carcass (ΔΔCt = 0.99, p = 0.0002) (Figure 2.8D).

Pupae showed the highest levels of upregulation of both *Cyp6m2* (102x, ΔΔCt = 6.6, p = 0.0002) (Figure 2.8A) and *Cyp6p3* (836x, ΔΔCt = 9.7, p = 0.0001) (Figure 2.8C). While no significant upregulation was detected at larval stage for either *Cyp6m2* (Figure 2.8A) or *Cyp6p3* (Figure 2.8C).

Cyp6m2 and *Cyp6p3* displayed a similar pattern of native expression (Figure 2.8A,C). They shared a higher native transcription at the larval stage, a trough of expression levels at pupal stage, and an increase in adults, although not reaching larval values.

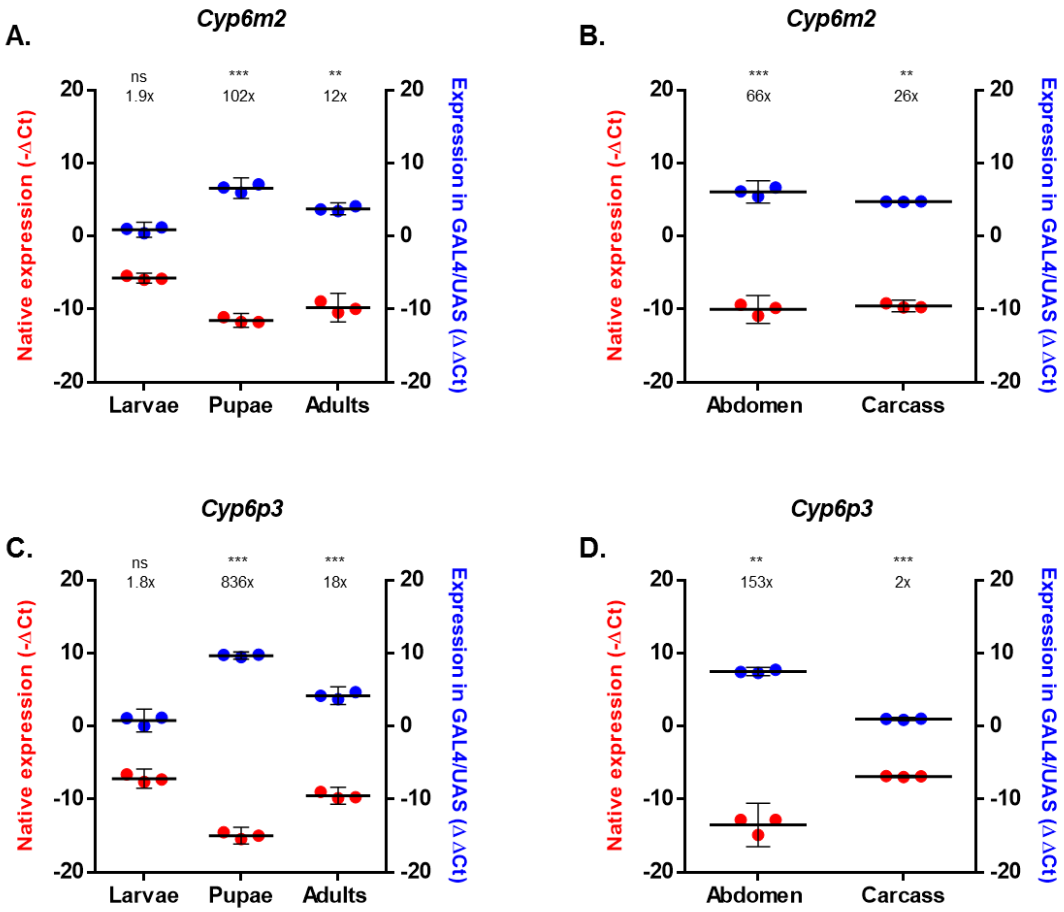

Figure 2.8 Transcription of *Cyp6* genes in GAL4oeno crosses. Native expression in GAL4/+ mosquitoes (red circles) is expressed as -ΔCt ($Ct_{Housekeepings}$ – Ct_{Cyp6}). Expression in GAL4/UAS mosquitoes compared to GAL4/+ controls (blue circles) is reported as ΔΔCt ($\Delta Ct_{GAL4/+}$ – $\Delta Ct_{GAL4/UAS}$). **A)** Transcription of *Cyp6m2* in adults, pupae and larvae. **B)** Transcription of *Cyp6m2* in dissected body parts of adult females. **C)** Transcription of *Cyp6p3* in larvae, pupae and adults. **D)** Transcription of *Cyp6p3* in dissected body parts of adult females. Carcass is whole body without the abdomen cuticle. Numbers above show the fold change (x) expression in GAL4/UAS compared to GAL4/+ mosquitoes. Vertical lines represent 95% confidence intervals and middle lines the mean from three replicates. Statistical significance was calculated using Welch's test. * $p < 0.05$, ** $p \leq 0.01$, *** $p \leq 0.001$, **** $p \leq 0.0001$. File names with raw data and analysis are listed in Appendix B.

2.5.3 CYP6 protein expression in GAL4mid and GAL4oeno crosses

In western blot analysis of GAL4mid crosses (Figure 2.9), CYP6M2 was detected at ~58 KDa in whole GAL4/UAS adult female extracts and in dissected midgut, but was not detectable in the carcass. Native CYP6M2 expression was also not at a detectable level in whole or dissected body part extracts of GAL4mid/+ samples.

Signal from the α-tubulin loading control was detected at ~55 KDa in all samples (Figure 2.9). While, CYP6M2 signal was robust when loading 1/3 of a midgut, to detect α-tubulin in midgut extracts the amount loaded was increased to 2 whole midguts. Due to protein size similarity, detection of the α-tubulin signal in GAL4/UAS midguts appeared to be partially masked by that of CYP6M2 due to blot stripping limiting detection of proteins of similar size on subsequent exposures.

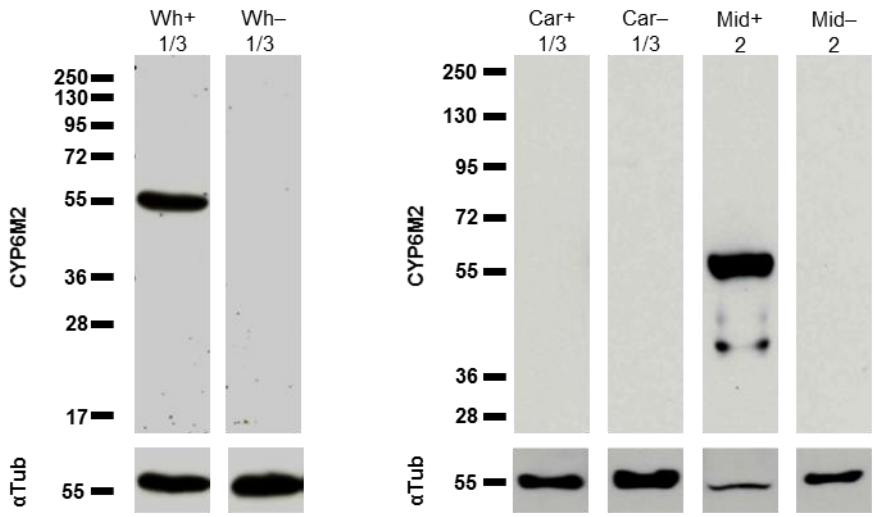

Figure 2.9 Western blots on 2-5-day-old adult females from the GAL4mid x UASm2 cross to determine expression of CYP6M2 (top) and α-tubulin (bottom). Wh: whole adult; Car: carcass (whole body without midgut); Mid: midgut. +: GAL4mid/UASm2; –: GAL4mid/+ controls. Whole and carcass lanes contain the protein extract from 1/3 of a single whole mosquito, while midgut lanes contain protein extract from 2 midguts. CYP6M2 signal was obtained after 30-second (whole) and 3-second (carcass and midgut) exposure; α-tubulin was detected after 1-minute (whole) and 30-second (carcass and midgut) exposure.

In GAL4oeno crosses, CYP6M2 signal was detected in whole GAL4oeno/UASm2 adult female extracts and in dissected abdomens, but not in the remaining carcass extracts (Figure 2.10). A similar pattern of expression was observed at the pupal stage, with CYP6M2 only detectable in whole GAL4oeno/UASm2 female pupae and

their dissected abdomens, but not in the carcass (Figure 2.10). Again, no native signal was detected in GAL4mid/+ whole body or dissected extracts.

CYP6M2 was also detected GAL4oeno/UASm2 larvae at ~58 KDa along with a second band of smaller size (<55 KDa) and variable intensity among samples, while in GAL4/+ larvae controls just the variable <55 KDa band appeared (Figure 2.10).

Furthermore, a minor band at ~100 KDa is also detected in pupa and adults, and as a major band in occasional late 4th instar larvae (Figure 2.10).

Signal from α-tubulin was detected at ~55 KDa for all the examined samples (Figure 2.10) suggesting an equal loading of crude protein extract in GAL4/UAS and GAL4/+ samples.

Although attempts were made to detect CYP6P3 with previously untested antiserum, these were unsuccessful in both GAL4mid or GAL4oeno crosses. Antibody titration failed to detect specific signals in any tissues in transgenic lines or controls (not shown).

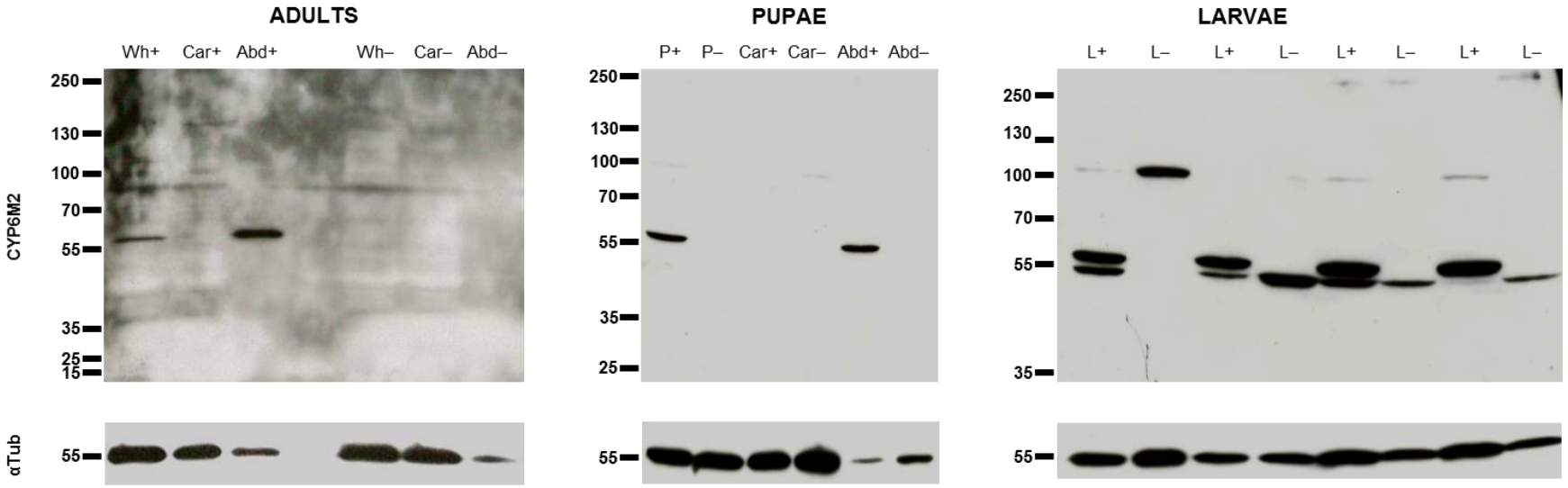

Figure 2.10 Western blot on 2-5-day-old adults, pupae and L4 larvae from the GAL4oeno x UASm2 cross to determine expression of CYP6M2 (top) and α-tubulin (bottom). Wh: whole adult female; Car: carcass (whole body without abdomen cuticle); Abd: abdomen cuticle. P: female pupa; L: L4 larva. +: GAL4oeno/UASm2; –: GAL4oeno/+ controls. Each lane contains the protein extract from 1/3 of a single mosquito or 1/3 of its body part. CYP6M2 signal was obtained after 3-minute (adults), 30-second (pupae), and 2-minute (larvae) exposure; α-tubulin was detected after a 30-second exposure in all films.

2.5.4 WHO tube bioassays

2.5.4.1 Resistance phenotypes in mosquitoes overexpressing Cyp6m2 or Cyp6p3 in the midgut

Analysis of WHO-defined sensitivity to permethrin 0.75%, deltamethrin 0.05%, DDT 4%, or bendiocarb 0.1% in adult females showed that GAL4/UAS and GAL4/+ populations were ~100% susceptible to all insecticides tested after 1 h exposure, with no significant difference between mortality rates in mosquitoes overexpressing *Cyp6m2* or *Cyp6p3* in the midgut and controls (Figure 2.11A).

In order to identify subtle differences in susceptibility between GAL4/UAS and GAL4/+ mosquitoes, the assays were repeated reducing the exposure time. Again no significant differences were found in the mortality rates of mosquitoes overexpressing *Cyp6m2* or *Cyp6p3* in the midgut and their respective controls when exposed for 20 minutes to the same diagnostic doses of the four insecticides (Figure 2.11B).

2.5.4.2 Resistance phenotypes in mosquitoes overexpressing Cyp6m2 or Cyp6p3 in the oenocytes

WHO-tube bioassay analysis showed that female mosquitoes overexpressing *Cyp6m2* or *Cyp6p3* in the oenocytes were susceptible to 0.75% permethrin, 0.05% deltamethrin, 4% DDT, and 0.1% bendiocarb according to WHO definitions and no difference was detected in the mortality rates of GAL4/UAS mosquitoes compared to GAL4/+ controls (Figure 2.12A).

When the same assay was performed with a 20-minute exposure to the same diagnostic doses of the four insecticides, again no significant differences were found between GAL4/UAS mosquitoes overexpressing *Cyp6m2* or *Cyp6p3* in the oenocytes and their respective controls (Figure 2.12B).

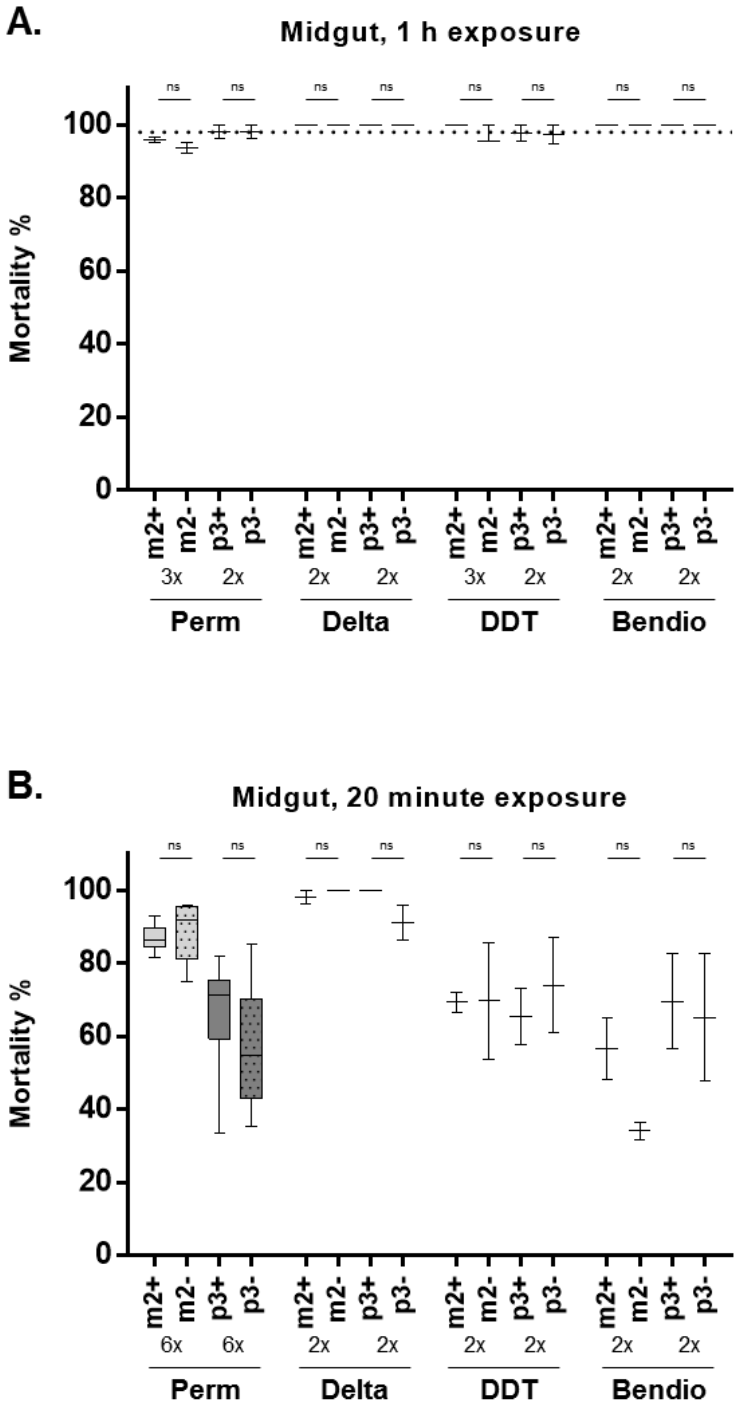

Figure 2.11 Sensitivity to insecticides of 2-5-day-old adult females overexpressing *Cyp6m2* or *Cyp6p3* in the midgut compared to GAL4/+ controls. Perm: 0.75% permethrin; Delta: 0.05% deltamethrin; DDT: 4% DDT; Bendio: 0.1% bendiocarb. **A)** Standard WHO tube bioassay representing mortality rates after 1 h of exposure and 24 h recovery. Dotted line represents 98% mortality which is the threshold for resistance indicated by the WHO. **B)** Modified WHO tube bioassay representing mortality rates after 20 minutes of exposure and 24 h recovery. m2+: GAL4mid/UASm2; m2-: GAL4mid/+ controls from m2 cross; p3+: GAL4mid/UASp3; p3-: GAL4mid/+ controls from p3 cross. When <4 replicates are examined, no box is drawn, whiskers represent minimum and maximum values, and line in the middle represents the median (mean). When >4 replicates are examined, a box is drawn the bottom and the top of which represent the first and third quartile respectively. Line inside the box is the second quartile (median). Whiskers represent minimum and maximum values. ns: not significant. Number of technical replicates (x) for each population is indicated. File names with raw data and analysis are listed in Appendix B.

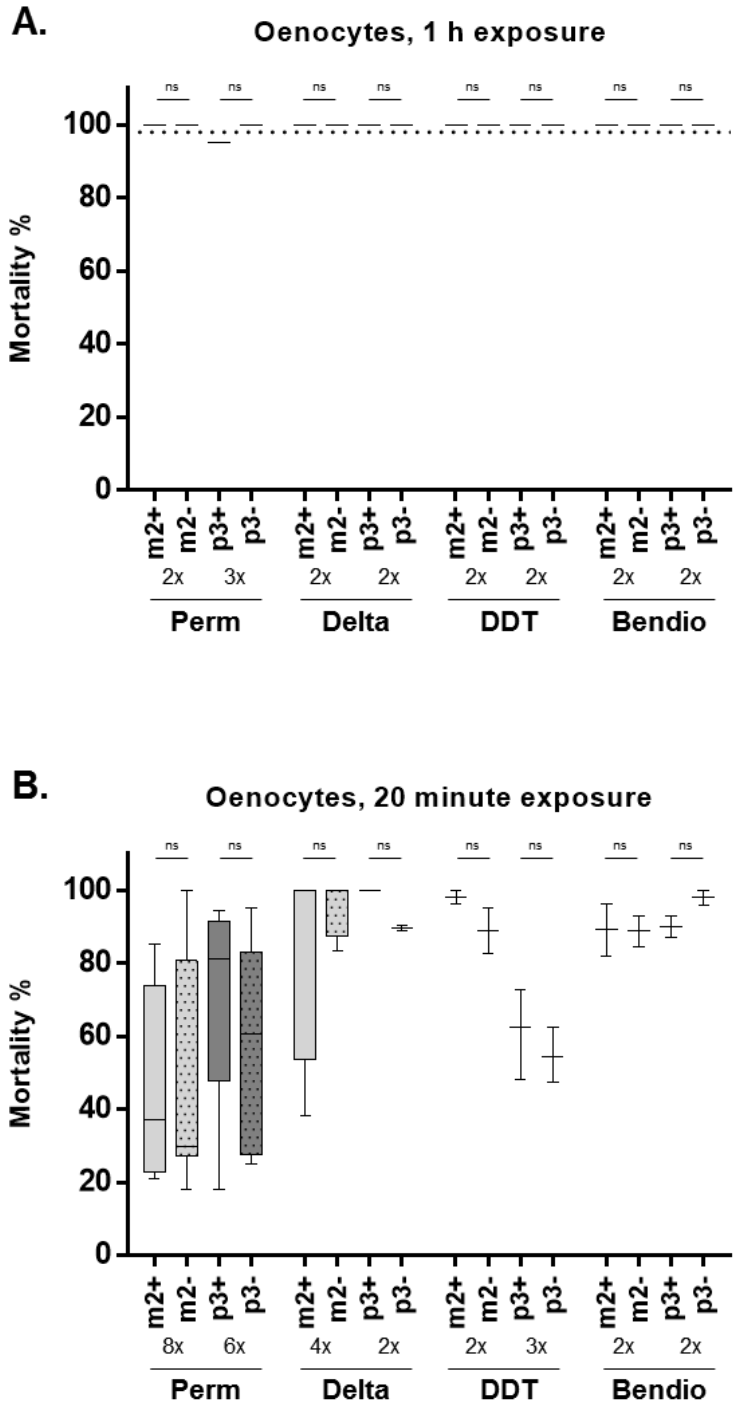

Figure 2.12 Sensitivity to insecticides of 2-5-day-old adult females overexpressing *Cyp6m2* or *Cyp6p3* in the oenocytes compared to GAL4/+ controls. Perm: 0.75% permethrin; Delta: 0.05% deltamethrin; DDT: 4% DDT; Bendio: 0.1% bendiocarb. **A)** Standard WHO tube bioassay representing mortality rates after 1 h of exposure and 24 h recovery. Dotted line represents 98% mortality which is the threshold for resistance indicated by the WHO. **B)** Modified WHO tube bioassay representing mortality rates after 20 minutes of exposure and 24 h recovery. m2+: GAL4mid/UASm2; m2-: GAL4mid/+ controls from m2 cross; p3+: GAL4mid/UASp3; p3-: GAL4mid/+ controls from p3 cross. When <4 replicates are examined, no box is drawn, whiskers represent minimum and maximum values, and line in the middle represents the median (mean). When >4 replicates are examined, a box is drawn the bottom and the top of which represent the first and third quartile respectively. Line inside the box is the second quartile (median). Whiskers represent minimum and maximum values. ns: not significant. Number of technical replicates (x) for each population is indicated. File names with raw data and analysis are listed in Appendix B.

2.6 DISCUSSION

2.6.1 Efficiency of PhiC31-RMCE

PhiC31-RMCE was successfully used to create transgenic *An. gambiae* responder lines for the UAS-mediated overexpression of candidate resistance genes *Cyp6m2* (UASm2) and *Cyp6p3* (UASp3). In doing so, good hatching rates were achieved (23-44%) which are either comparable or higher than that reported elsewhere using PhiC31 (~9-58%) (Meredith et al., 2013; Pondeville et al., 2014; Haghighat-Khah et al., 2015; Hammond et al., 2016). Furthermore, PhiC31-RMCE demonstrated to be a reliable method for site-specific transformation. Minimum transformation efficiencies of 2-5% were obtained, which are consistent with other recent reports of PhiC31-RMCE in *Ae. aegypti* (~4.5%) (Haghighat-Khah et al., 2015) and *An. gambiae* (2-7%) (Hammond et al., 2016).

2.6.2 *Cyp6* gene and CYP6 protein overexpression

Overexpression of *Cyp6m2* and *Cyp6p3* was achieved by crossing *An. gambiae* responder lines UASm2 and UASp3 with previously established GAL4mid and GAL4oeno drivers. In doing so, *Cyp6m2* and *Cyp6p3* transcript upregulation was achieved in the midgut and abdomen respectively, and we were also able to detect CYP6M2, but not CYP6P3, protein overexpression in the targeted body parts.

Although the data from western and qRT-PCR analysis are mostly in agreement for overexpression of the *Cyp6* genes in the target tissues, there is some conflict in the extent of off-target expression. Western analysis of CYP6M2 expression indicates very strong signals in extracts from the expected tissues or body sections, and an absence of signal from the remaining carcasses. The antibody could not detect native expression of the protein in control samples with the quantity of extracts used in these assays. In fact, to readily detect native CYP6M2, microsomal extracts need to be purified from several hundred mosquitoes (M. Paine pers. comm.). The protein data thus support the tissue distribution pattern from fluorescence analysis of live and dissected mosquitoes using the GAL4oeno and GAL4mid driver lines (Lynd & Lycett, 2012, Lynd et al., unpublished), validating their ability to drive CYP6M2 expression in the targeted locations. Without a suitable antiserum for CYP6P3 it was not possible to verify CYP6P3 overexpression.

At the RNA level, the expected tissue-specific upregulation of both genes was also clear. However, *Cyp6* transcript upregulation in GAL4/UAS mosquitoes was also observed in the carcass left after removal of the targeted tissue or body section in all crosses. As mentioned above, tissue-specificity of the midgut driver (GALmid) had been previously investigated by Lynd & Lycett (2012) in adults after crossing with a dual responder line expressing UAS:nuclearYFP and luciferase. This revealed that in GAL4/UAS individuals YFP fluorescence was specific to the midgut, in which luciferase expression was ~50,000x higher than in GAL4 controls. Nevertheless, the luciferase assay showed low levels (2x) of relative activity above background in the carcass. This may be due to contamination from overexpressing body parts as a consequence of imperfect imperfections or off-target leakiness in the expression of the GAL4. Expression induced by the GAL4oeno driver was found to be specific to the abdomen of 4th instar larvae via fluorescent assessment and luciferase assay. The latter analysis also showed luciferase expression in adult head and thorax (Lynd et al., unpublished), which might explain the significant transcript differences found between the carcasses. Taken altogether, it would appear that the transcript upregulation found in the carcasses of all crosses is mostly due to the higher sensitivity of the RT-qPCR technique which is dependent on the exponential amplification of signal against a background of relatively low levels of native expression and thus the presence of even small amounts of contamination from other sources, including target tissues or leaky expression, is amplified. Such contamination could not be picked up in the Western analysis. Potential leakiness from the UAS construct was not assessed. This was due primarily to time constraints and workload. Indeed, the tissue-specific driver lines used were homozygous, so no UAS/+ individuals could be obtained after crossing with UAS lines. Therefore, the rearing of additional mosquitoes would have been required, which was not manageable. Additionally, assessing mosquitoes deriving from the same cross and separated at pupal stage assures identical condition of rearing, which is essential to accurately assess gene expression. Finally, the focus of the study was on levels of overexpression compared to individuals equivalent to wild types in terms of P450 expression (i.e. GAL4/+ carrying a single copy of the P450 gene examined).

Whilst optimising western blot analysis of CYP6M2 abundance several issues were overcome. In initial experiments, when protein extracts from a 1/3 of a mosquito were analysed, CYP6M2 appeared more abundant in the whole adult compared to the midgut sample, which was unexpected for the midgut-specific driver and was not in agreement with the qRT-PCR data. In addition, the α-tubulin signal was not detectable

in midgut extracts from any of the mosquitoes analysed. This was likely due to protein degradation caused by the high content of midgut proteases, and indeed was largely circumvented by performing faster dissections on ice. In the final confirmation experiments to improve the α-tubulin signal, 2 midgut equivalents were loaded for comparison, which still showed a degree of degradation of CYP6M2 as indicated by a number of smaller bands detected on the western.

In GAL4oeno crosses, the expected relative difference in CYP6M2 abundance between adult body sections was detected and was in line with qPCR data. Additionally, since the GAL4oeno driver is active throughout the mosquito life cycle, CYP6M2 protein overexpression was detected at all life stages, while significant transcript upregulation was detected in adults and pupae, but not larvae. Here, although a 2-fold upregulation of *Cyp6m2* and *Cyp6p3* was found in GAL4/UAS individuals, it was not significantly higher than in controls. Transcripts levels are not always directly comparable to protein abundance due to reasons including post-transcriptional modifications, variability in *in vivo* protein half-lives, mRNA stability, and assay sensitivity (Greenbaum et al., 2003), but the western analysis does cast doubt on the accuracy of the larval RT-qPCR data.

It should be emphasised that the differences observed in the level of upregulation of the two transgenes expressed using the same driver should not be misinterpreted. Such differences are not strictly comparable because the magnitude of expression is relative to native expression of the individual *Cyp6* rather than absolute transcription. The idea that native levels of *Cyp6* transcription are generally low was confirmed by RT-qPCR data. Analysis of the relative native transcription of *Cyp6m2* and *Cyp6p3* throughout the mosquito life cycle in GAL4oeno crosses could be achieved by comparison with expression of housekeeping genes (ΔCt). This revealed that both genes share a high native expression at larval stage which drops at pupal stage and raises again at adult stage. In the light of a detoxification role, we could speculate that high amounts of xenobiotic-metabolising enzymes are needed in the early aquatic stages when larvae actively feed and are therefore potentially more exposed to external challenges. In the pupal stage, which does not ingest food, this may be less needed, while expression in adults may again increase to face their active feeding behaviour and different environmental exposures. However, this remains a speculation as detoxification is not the only potential role of these P450s and also this analysis does not take into consideration tissue-specific expression enrichment in different life stage (Scott, 2008).

In relation to the larval expression of CYP6M2 it is also interesting to note that in the western analysis of the GAL4oeno x UASm2 cross, as well as the ~58 KDa band seen in all stages and expected body sections of the overexpressing progeny, an additional band of <55 KDa was also detected in most larvae. The origin of this signal is unknown, but most likely it is the result of a larval-specific (or microbial contaminant) protein that binds the polyclonal peptide antibodies used for detecting CYP6M2. It is also possible, but unlikely, that the band detected at <55 KDa is the native CYP6M2 and the band detected at ~58 KDa and in all the other western analysis corresponds to the transgenically expressed CYP6M2 that has undergone modification. P450s can undergo modifications such as phosphorylation, glycosylation, nitration and ubiquitination at transcriptional, translational and post-translational levels as a means to modulate enzymatic activity and to tag the protein for transport to specific cellular compartments or for degradation (Aguiar et al., 2005). Such modifications may result in protein size increase. Nevertheless, the variability in the abundance of this additional band in different larval samples strongly suggests its non-specific nature. This is further supported by the presence of an additional unspecific band of variable intensity at ~100 KDa.

2.6.2.1 GAL4/UAS-driven vs natural overexpression levels

Levels of *Cyp6* overexpression found in resistant *An. gambiae* populations are generally lower than those generated in this study through the GAL4/UAS system and quantified by RT-qPCR. Here the midgut driver induced 889x and 135x overexpression of *Cyp6m2* and *Cyp6p3* respectively in the whole mosquitoes and 2731x and 659x in the midgut; while the oenocyte-specific driver induced 12x and 18x overexpression of *Cyp6m2* and *Cyp6p3* respectively in whole mosquitoes and 66x and 153x in dissected abdomens.

In *An. gambiae* across Africa, *Cyp6m2* is found 1-10x upregulated in resistant mosquitoes (Djouaka et al., 2008; Mitchell et al., 2012; Fossog Tene et al., 2013; Djègbè et al., 2014; Edi et al., 2014), with a notable exception of 44x upregulation found in deltamethrin-resistant mosquitoes from Benin (Yahouédo et al., 2016); while *Cyp6p3* is reported to be 1-12x overexpressed (Djouaka et al., 2008; Kwiatkowska et al., 2013; Djègbè et al., 2014; Edi et al., 2014; Yahouédo et al., 2016).

However, our data on overexpression levels found in the midgut and in the abdomen cannot be easily related to field data as very little is known about levels of *Cyp6* upregulation in specific tissues and their contribution to resistance in the whole

mosquito. This is because data on gene upregulation in resistant populations has been generated from whole mosquitoes with a consequent overall dilution of the specific overexpression in single tissues. This means that relatively lower levels of upregulation found in natural population when comparing whole mosquitoes may hide much higher levels of upregulation when comparing single tissue transcriptomes (Ingham et al., 2014). This topic is discussed in greater details in Chapter 5.

2.6.3 Effects on resistance of tissue-specific overexpression of single P450s

Despite the high levels of overexpression of *Cyp6m2* or *Cyp6p3* restricted to the midgut or the oenocytes, this did not affect resistance according to WHO definitions (i.e. at least 98% mortality 24 h after 1 h exposure) (WHO, 2016b). Of note is that, despite working with susceptible populations, we often recorded mortality rates below the WHO threshold when exposing mosquitoes to 0.75% permethrin and 4% DDT. Several factors related to the mosquitoes or the papers used may have contributed to this reduced mortality which will be discussed in more details in Chapter 4.

The use of WHO standard discriminating doses, set to assess resistance in field populations, limits the detection of subtler phenotypic differences. Therefore, to detect possible fine differences in mortality between GAL4/UAS and GAL4/+ mosquitoes, the exposure time was reduced to 20 minutes. This did not result in significant differences in mortality rates between the two transgenic populations and produced greater variability among biological and technical replicates. Further work may define any differences by examining LC_{50} curves following exposure to a gradation of doses either through CDC bottle assays (Brogdon & McAllister, 1998) or custom impregnated papers.

Although UAS/+ mosquitoes were not included in the analysis, the lack of resistance in GAL4/UAS individuals would suggest that, even if leaky expression may occur, this would not be sufficient to visibly affect WHO resistance.

While the transgene sequences used are known to encode functional proteins able to actively metabolise insecticides *in vitro* (Müller et al., 2008a, Stevenson et al., 2011; Edi et al., 2014; Yunta et al., unpublished), it may be that there are limiting amounts of CPR co-factor present in the targeted tissues that are unable to functionally sustain CYP6 activity relative to its overexpression. However, co-upregulation of CPR not has been reported in resistant *An. gambiae* (Ingham, 2016) or in *An. funestus* (J. Riveron

pers. comm.). Immune-fluorescence experiments also showed that CPR is natively highly expressed in both oenocytes and midgut (Lycett et al., 2006), furthermore, *in vivo* evidence from *D. melanogaster* supports the production of a resistant phenotype in the absence of CPR overexpression (Edi et al., 2014; Riveron et al., 2013, 2014a/b, 2017). Taken together, these findings suggest that the amount of CPR would not be limiting in these tissues.

Overall, our data suggest that tissue-specific location of overexpression is a limiting factor for the occurrence of resistance as phenotype is not affected when overexpression of *Cyp6m2* or *Cyp6p3* is confined to the midgut or the oenocytes. Nevertheless, overexpression of these genes in other single tissues may confer resistance. In *Drosophila,* most detoxifying genes show tissue-specific distribution which may imply the importance of local *vs* global defence mechanisms against xenobiotics. For example, Yang et al. (2007) demonstrated that *D. melanogaster* susceptibility to DDT was decreased by the overexpression of *Cyp6g1* specifically localised in the Malpighian tubules, but not in the brain or fat body. More recently, brain-specific overexpression of *T. castaneum Cyp6bq9* was demonstrated to be sufficient to confer resistance to deltamethrin in transgenic beetles (Zhu et al., 2010). Alternatively, a multi-tissue pattern of overexpression may be essential to affect the phenotype. Indeed, Riveron et al. (2013) reported that the overexpression of *An. funestus Cyp6p9a/b* in transgenic *D. melanogaster* affects resistance to pyrethroids when it is driven by the ubiquitous driver Actin5-GAL4 but not by 6g1HR-GAL4 targeting midgut, Malpighian tubules and fat body (Chung et al., 2007).

2.6.4 Conclusions

The GAL4/UAS system developed in this laboratory for *An. gambiae* was successfully employed to independently drive overexpression of *Cyp6m2* and *Cyp6p3* in the midgut of adult mosquitoes and in the abdominal oenocytes of all mosquito life stages. While upregulation of *Cyp6m2* and *Cyp6p3* was validated at the RNA level and CYP6M2 overexpression at protein level, relative mosquito susceptibility to insecticides was not affected in transgenic compared to control mosquitoes after 1-hour or 20-minute exposure to single WHO discriminating doses of permethrin, deltamethrin, DDT, and bendiocarb. This suggests that overexpression of *Cyp6m2* and *Cyp6p3* confined in the midgut or in the oenocytes is not sufficient to alter the resistance phenotype according to WHO definitions, and other specific tissues or a combination of them may be physiologically important in driving resistance. To

explore these scenarios, the next chapter describes work aimed at the identification of a Malpighian tubule-specific promoter and a ubiquitous promoter and the creation of corresponding driver lines for assessing mosquito phenotypes following expression in different tissues.

Chapter 3

Driver lines for ubiquitous and Malpighian tubule-specific expression

3.1 ABSTRACT

Location of overexpression of P450 genes appears critical to generate resistance, as transgenic mosquitoes overexpressing *Cyp6m2* or *Cyp6p3* in the midgut and in the oenocytes fail to alter resistance phenotypes. Thus, other locations of overexpression, namely the Malpighian tubules and multi-tissue expression were investigated. As promoters that regulate expression in these locations were yet to be identified in *An. gambiae*, this work aimed initially to isolate regulatory regions of candidate genes displaying the tissue-specific expression of interest, and then to create corresponding driver lines for transgenic analysis. To do so, the *An. gambiae* expression database MozAtlas was queried and regulatory regions from ubiquitous expressed candidates cloned and analysed by mosquito cell transfection, before creating transgenic driver lines using the piggyBac transposon. For Malpighian tubule-candidates, driver lines were directly established using PhiC31-RMCE. Patterns of expression driven by these new GAL4 lines were assessed by fluorescence analysis after crossing with a UAS-mCherry line. We found multiple promoters that were active in the *An. gambiae* cell line. Moreover, the polyubiquitin-c gene promoter had the highest activity in cells and drives widespread expression in all life stages of transgenic mosquitoes. The two driver lines created, A8 and A10, express at different levels in a similar multiple tissue pattern. Furthermore, these lines may act as PhiC31-RMCE docking lines as they carry attP recombination sites at single, unique chromosomal integration loci. A second ubiquitous candidate, the phosphoglucose isomerase promoter, did not drive detectable reporter gene expression in transgenic mosquitoes despite being active in cells. Finally, we did not identify regulatory regions capable of driving observable GAL4-driven expression in the Malpighian tubules. Overall, this work greatly advances the tools available for *An. gambiae* functional analysis allowing for the investigation of phenotypes resulting from widespread multi-tissue expression.

3.2 INTRODUCTION

In light of results described in the previous chapter, here we aim to create GAL4 driver lines directing expression in the Malpighian tubules and ubiquitously. This would allow us to test whether overexpression of *Cyp6m2* or *Cyp6p3* in the Malpighian tubules is sufficient to drive resistance, or whether simultaneous expression in more than one tissue is necessary for the resistant phenotype to manifest.

An endogenous promoter able to express ubiquitously in *An. gambiae* has not been identified, which greatly limits our understanding of phenotypes resulting from genes expressed in a multi-tissue manner. In an effort to obtain multi-tissue expression, promoters of ubiquitin genes have been investigated in different insects. These encode proteins involved in a wide range of biological processes mediated by protein conjugation and are evolutionary remarkably conserved thus representing promising candidates. Amongst these, the *D. melanogaster* polyubiquitin (PUB) promoter was reported to drive widespread expression in transgenic *D. melanogaster* (Handler & Harrell, 1999), *Anastrepha suspensa* (Handler & Harrell, 2001), *L. cuprina* (Heinrich et al., 2002), and *An. albimanus* (Perera et al., 2002). A similar phenotype was also described for the regulatory region of the PUB gene of *T. castaneum* in transgenic beetles (Lorenzen et al., 2002). Finally, the promoter of the *Aedes aegypti* PUB gene was shown to drive widespread expression across all developmental stages of transgenic *Ae. aegypti* (Anderson et al., 2010).

When expression targeting certain specific tissues is required, tools are more numerous (these are described in section 1.5.1). Nevertheless, we lack promoters acting in most tissues, including ovaries and Malpighian tubules, which makes it difficult to investigate phenotypes emerging from modulation of expression in these tissues.

The role of Malpighian tubules in xenobiotic detoxification has been shown in *D. melanogaster* through transcriptomic (Wang et al., 2004; Yang et al., 2007) and *in vivo* functional analysis in transgenic flies (Yang et al., 2007). In *An. gambiae*, a similar role is suggested by the enrichment of several P450 families in this tissue in susceptible (Baker et al., 2011; Ingham et al., 2014; Stevenson et al., 2011) and resistant mosquitoes (Ingham et al., 2014). Thus, Malpighian tubules are thought to be a main site for insecticide clearance and the characterisation of a promoter specific for this tissue would allow us to functionally define its contribution to resistance in *An. gambiae*.

Identification of tissue-specific transcription factor binding sites is challenging due to their short length (6-12 bp) and their typical location within intergenic genomic regions (Dissanayake et al., 2006; Sieglaff et al., 2009). One method to identify sequences that will produce specific expression patterns is to investigate the 5' regions of genes that display the required pattern of expression. This promoter identification is facilitated by the availability of online databases integrating collections of *An. gambiae* gene expression data, which allows analysis of gene transcript enrichment in specific tissues, life stages or conditions of interest (Sieglaff et al., 2009; Koutsos et al., 2007). Resources such as VectorBase (Giraldo-Calderón et al., 2015) (www.vectorbase.org/) and angaGEDUCI (Dissanayake et al., 2006) (www.angaged.bio.uci.edu) incorporate gene expression data, mostly generated by microarray analysis (Marinotti et al., 2006; Baker et al., 2011) with more recent RNAseq data, as well as gene expression maps (MacCallum et al., 2011). Amongst others, the MozAtlas database (Baker et al., 2011) (http://mozatlas.gen.cam.ac.uk/mozatlas/) hosts a collection of the transcriptional profiles of *An. gambiae* genes across somatic (head, salivary glands, midgut, Malpighian tubules, ovaries, carcass) and reproductive tissues (ovaries and testis) of adult male and female mosquitoes. For building the database, microarray analysis was conducted in a population of mosquitoes originated from a single strain reared in standardised conditions. As such, it provides a promising tool to retrieve comparative gene expression data from several female adult tissues. Candidate promoter sequences can then be used to drive expression of reporter genes in transgenic lines to observe the subsequent patter of expression (Lycett et al., 2012).

Achieving the desired expression pattern of transgenes, however, does not solely depend on identifying the promoter region that will produce the intrinsic spatio-temporal pattern required, but is affected by the precise genomic environment into which it is inserted. Positional effect is a consequence of the essentially random integration mediated by transposons and results in the laborious process of creation of multiple lines and their assessment for gene expression and fitness (Handler & O'Brochta, 2012; O'Brochta et al., 2014). To overcome the repeated creation of transgenic lines using transposons, docking lines can be established that bear a reusable transcriptionally active docking site. In general, defining a universally permissive expression site is challenging as the properties of any DNA sequence are likely to be affected by its relocation in the genome. Nevertheless, the isolation of active sites that permit multi-tissue expression is desirable as they would represent an established context for future comparative experiments. From docking lines

bearing insertions in permissive areas of the genome it is then possible to create a great variety of other lines by integrating the target DNA alongside the existing construct or by replacing the existing cassette with a donor cargo via RMCE (Bateman et al., 2006). PhiC31-RMCE has been applied to *An. gambiae* (Lynd et al., unpublished; Hammond et al., 2016) but a very limited number of docking strains has been created so far.

3.3 AIMS AND OBJECTIVES

This work aimed to identify candidate promoters for ubiquitous and Malpighian tubule-specific expression and to investigate their ability to drive expression *in vivo* using the GAL4/UAS system in cell line and transgenic mosquitoes. In doing so, we also aimed to create GAL4 driver lines bearing docking sites for PhiC31 site-specific integration or RMCE in single, unique transcriptionally active regions of the genome.

Specific objectives of the study were:

- To retrieve data on gene expression in adult female tissues from the MozAtlas database, isolate 5' regulatory regions of candidate ubiquitous and Malpighian tubule-specific genes and clone them into GAL4 driver plasmids.
- To assess relative promoter strength of candidate ubiquitous promoters in *An. gambiae* SUA5.1 cell line after co-transfection with a UAS plasmid driving luciferase expression.
- To create docking driver lines carrying single copies of the ubiquitous candidate promoters PUBc (AGAP001971) and PGI (AGAP012167), and the Malpighian tubule candidate promoter VATG (AGAP001823).
- To characterise the fluorescent pattern of expression driven by GAL4 lines bearing a single copy of the transgenic cassette after crossing with a UAS-mCherry line.
- To identify and isolate transcriptionally active genomic locations sustaining ubiquitous expression to be exploited for site-specific integration or cassette exchange using the PhiC31 attP sites present in the integrated construct.

3.4 MATERIALS AND METHODS

Contributions

Dr. Gareth Lycett performed the embryo microinjections of the PUBc_GAL4 plasmid. Amalia Anthousi dissected and prepared mosquito tissues for fluorescence analysis.

General methods including DNA extraction, PCR, agarose gel electrophoresis, DNA purification and clean-up, restriction endonuclease digestion, ligation, *E. coli* transformation, minipreps, midipreps, ethanol precipitation, and sequencing are described in Appendix A.

3.4.1 Selection of promoter candidates

To find candidate promoters, the MozAtlas database (Baker et al., 2011) was used to search for genes showing either widespread expression across *An. gambiae* adult female tissues or expression confined to the Malpighian tubules. To do so, raw gene expression data (log_2 fluorescence values derived from microarray analysis) from the carcass, head, Malpighian tubules, midgut, ovaries and salivary glands were extracted to Excel for analysis.

For ubiquitous candidates, data for all tissues were classified into three expression level categories: “low” (100 – 1000 log_2 fluorescence), “medium” (1000 – 4000 log_2 fluorescence), and “high” (2000 – > 10 000 log_2 fluorescence). This was to test different promoter strengths and to account for potential toxicity that different levels of GAL4 expression may have *in vivo.* Gene IDs showing the highest and most consistent expression within each category were searched in VectorBase (Giraldo-Calderón et al., 2015) to assess the quality of gene maps from associated transcriptome (RNAseq) data. The top two or three candidates from each category were taken forward for cloning based on quality of transcript distribution along the genome (i.e. transcripts that map to annotated exonic regions of the genome). The promoter of the polyubiquitin-c gene (AGAP001971) was added to the list of candidates as its orthologue was reported to drive ubiquitous expression *Ae. aegypti* (AAEL003877) (Anderson et al., 2010).

For Malpighian tubule-specific candidates, gene IDs were sorted in descending order according to raw fluorescence values in the Malpighian tubules. Transcript enrichment in the tubules was calculated as fold change (x) from the average expression in other tissues (carcass, head, midgut, ovaries and salivary glands). Three expression categories were defined: “low” (2 – 50 x), “medium” (51 – 400 x), and “high” (401 – 1500 x). Two top candidates from each category were taken forward for cloning.

3.4.2 Plasmid preparation

3.4.2.1 pPUBc_GAL4

The plasmid was designed to carry: piggyBac inverted repeats for random insertion, attP sites for site-specific integration through RMCE, a CFP marker under the control of the 3xP3 eye-specific promoter, Gypsy insulators, and the GAL4 sequence under the control of the 5’ and 3’ regulatory regions of the *An. gambiae* polyubiquitin-c (PUBc) gene (AGAP001971). As annotated in the PEST genome, the cloned 5’ sequence consisted of 2005 bp upstream of the ATG translation start site in the second exon and included the first exon, the intron, and the intergenic space that separates PUBc from the preceding gene (PUBb, AGAP001970) (Figure 3.1). The selected 3’ sequence included 407 bp downstream of the second exon covering the intergenic space between the gene stop codon and the succeeding gene (TSR4 protein, AGAP001972) (Figure 3.1). The GAL4 coding sequence was used to replace that of the coding exon.

Figure 3.1 Schematic of the *An. gambiae* polyubiquitin-c gene and its regulatory sequences (not to scale). Orange fragments represent the cloned 5’ (PUB5) and the 3’ regulatory region (PUB3). PUB5 includes 2005 bp upstream of the predicted start codon of exon 2 (E2) until the preceding gene. PUB3 comprises 407 bp downstream of the predicted stop codon of E2 up to the following gene. In the transgenic construct, the GAL4 coding sequence seamlessly replaces that of E2.

The cloning strategy consisted of using a CFP-marked piggyBac plasmid carrying an attP-left site (attPl) as backbone to create the final plasmid PUBc_GAL4 by adding the six following components in order: Gypsy1 (Gyp1), PUBc 5' region (PUB5), GAL4, PUBc 3' region (PUB3), Gypsy2 (Gyp2), and attP-right site (attPr). To do so, the cloning strategy combined Gibson Assembly (Gibson et al., 2009, 2010) and restriction enzyme-based cloning and included the following steps:

1) Using Gibson assembly to create two intermediate plasmids each containing three fragments: pSL*Gyp1:PUB5:GAL4 and pSL*PUB3:Gyp2:attPr (Figure 3.2A).
   Single fragments were amplified using primers carrying overlapping regions using Phusion High-Fidelity DNA Polymerase (Thermo Scientific) as detailed in Table 3.1, and the backbone plasmid pSLfa1180fa digested with BamHI/NsiI. Gibson assembly reactions were set up in a total volume of 20 µL using 100 ng of digested backbone plasmid pSLfa1180fa, 0.02-0.1 pmol/µL of each fragment and 10µL of 2x Gibson Assembly® Master Mix (New England Biolabs) and incubated at 50°C for 1 h. Diagnostic restriction digestions were carried out using BglII/NheI and HindIII/NcoI before sequencing. pSL*Gyp1:PUB5:GAL4 sequence was verified using primers attB3-seqR, seq5'UTR-RV, seqINTRON-FW, pUB5-GAL4-FW, 1971-int-fw, GAL4-seq-2F, GAL4-pSL-RV, and PSL1180-1; while pSL*PUB3:Gyp2:attPr was sequenced using attB3-seqR and PSL1180-1 (Appendix C, Table C.1).

Table 3.1 Amplification of single components for creating two intermediate plasmids, pSL*Gyp1:PUB5:GAL4 and pSL*PUB3:Gyp2:attPr (Figure 3.2A), by Gibson cloning.

Fragment	Template	Primers*	RES Tag	Size (bp)	T_m (°C)	Ext. time	No. cycles
Gyp1	attB:UAS: Cyp6m2	pSL-Gypsy1-FW Gypsy1-pUB5-RV	-- NheI	126	65	5 sec	35
PUB5	Kisumu gDNA	Gypsy1-pUB5-FW pUB5-GAL4-RV	NheI --	2005	62	30 sec	35
GAL4	attB:GAL4: DsRed	pUB5-GAL4-FW GAL4-pSL-RV	-- BglII	2646	70	30 sec	35
PUB3	Kisumu gDNA	pSL-pUB3-FW pUB3-Gypsy2-RV	BglII NdeI	407	65	5 sec	35
Gyp2	attB:UAS: Cyp6m2	pUB3-Gypsy2-FW Gypsy2-attP-RV	NdeI SacI	126	70	5 sec	35
attPr	pBACl:attP :CFP	Gypsy2-attP-FW attP-pSL-RV	SacI --	204	72	5 sec	35

*All primer sequences are reported in Appendix C, Table C.1.

2) Restriction enzyme-based cloning was used to perform the final cloning steps. The PUB3:Gyp2:attPr fragment was cut out from pSL*PUB3:Gyp2:attPr and inserted into the BglII/NotI sites of pSL*Gyp1:PUB5:GAL4 to generate pSL*Gyp1:PUB5:GAL4:PUB3:Gyp2:attPr (Figure 3.2B). Gyp1:PUB5:GAL4:PUB3:Gyp2:attPr was then excised from the shuttle plasmid and cloned into the AscI sites of pBACl:attPl:CFP:pBACr to obtain the final plasmid pBACl:attPl:CFP:Gyp1:PUB5:GAL4:PUB3:Gyp2:attPr:pBACr (Figure 3.2C). Plasmid map was verified by SphI/NheI and BglII/EcoRI double enzymatic restriction.

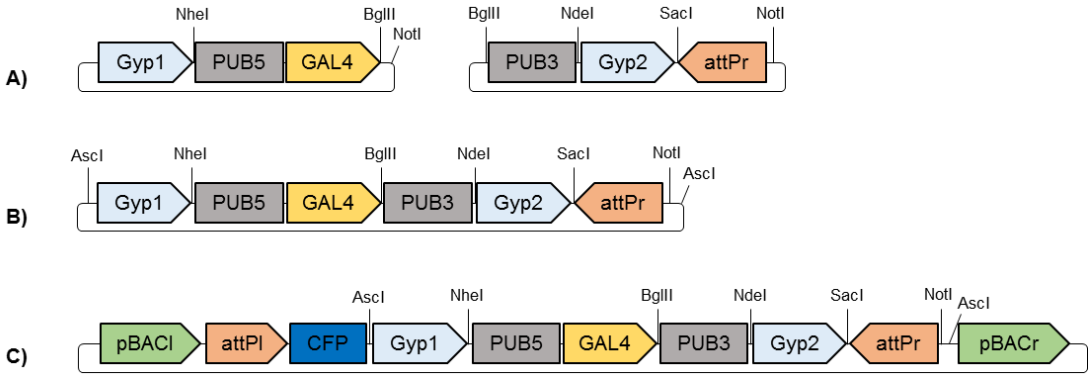

Figure 3.2 Schematic of cloning steps used to create the PUBc_GAL4 plasmid (13 839 bp) (not to scale). **A**) Two intermediate plasmids, pSL*Gyp1:PUB5:GAL4 and pSL*PUB3:Gyp2:attPr, were created by Gibson assembly. **B**) pSL*Gyp1:PUB5:GAL4:PUB3:Gyp2:attPr was obtained by cloning PUB3:Gyp2:attPr into the BglII/NotI sites of pSL*Gyp1:PUB5:GAL4. **C**) Final plasmid PUBc_GAL4 was obtained using AscI to clone the Gyp1:PUB5:GAL4:PUB3:Gyp2:attPr fragment into a pBACl:attPl:CFP:pBACr plasmid. This construct was used for both cell transfection and G3 embryo injection. Gyp1 and Gyp2: Gypsy insulators; PUB5: 5' regulatory region upstream of PUBc; PUB3: 3' regulatory region downstream of PUBc; attPl and attPr: PhiC31 attachment sites left and right respectively; pBACl and pBACr: piggyBac arms left and right respectively; CFP: cyan fluorescent protein used as 3xP3-driven eye maker.

3.4.2.2 GAL4 plasmids carrying MozAtlas ubiquitous promoter candidates

The 5' regions of eight putative ubiquitous genes selected from MozAtlas - AGAP006459, AGAP006782, AGAP003864, AGAP004654, AGAP012167, AGAP010572, AGAP011050 - were cloned upstream of the GAL4 sequence in a plasmid marked with 3xP3-driven DsRed (Figure 3.3). Putative promoters were amplified from Kisumu genomic DNA using Phusion High-Fidelity DNA Polymerase or Phire Hot Start II DNA Polymerase (Thermo Scientific) and primers tagged with SpeI and EcoRV as reported in Table 3.2. After SpeI/EcoRV double digestion and purification, PCR products were independently cloned into pSL*attB:HSP:GAL4:DsRed:attB replacing the HSP promoter originally contained in

the plasmid. Plasmid maps were verified by restriction digestion with NheI/EcoRV or HindIII and sequencing of the newly cloned fragments. Primers used for sequencing were: M13fw, RT-GAL4-2R and SpeI-6459-EcoRV-fw for AGAP006459; M13fw, RT-GAL4-2R and SpeI-6782-EcoRV-fw for AGAP006782; M13fw and RT-GAL4-2R for AGAP003864; M13fw, RT-GAL4-2R and SpeI-4654-EcoRV-fw for AGAP004654; M13fw, RT-GAL4-2R and SpeI-12167-EcoRV-fw for AGAP012167; M13fw, RT-GAL4-2R and SpeI-10572-EcoRV-fw for AGAP010572; and M13fw, RT-GAL4-2R and SpeI-11050-EcoRV-fw for AGAP011050 (Appendix C, Table C.1).

Figure 3.3 Schematic map of pSL*attB:Promoter:GAL4:DsRed:attB (not to scale). Eight independent reactions using SpeI and EcoRV were performed to replace the original promoter with each of the 5' regulatory regions of putative ubiquitous genes. This construct was used for both cell transfection and docking line embryo injection. attB: PhiC31 attachment sites; SV40: transcription terminator; DsRed: red fluorescent protein used as 3xP3-driven eye maker.

Table 3.2 Amplification of 5' regions upstream of ubiquitous gene candidates.

Gene ID	Primers*	RES Tag	Region amplified	T_m (℃)	Ext. time	No. cycles
AGAP006459	SpeI-6459-EcoRV-fw SpeI-6459-EcoRV-rv	SpeI EcoRV	2000 bp	56	50 sec	35
AGAP002182	SpeI-2182-EcoRV-fw SpeI-2182-EcoRV-rv	SpeI EcoRV	1331 bp	58	30 sec	35
AGAP006782	SpeI-6782-EcoRV-fw SpeI-6782-EcoRV-rv	SpeI EcoRV	1842 bp	60	50 sec	35
AGAP003864	SpeI-3864-EcoRV-fw SpeI-3864-EcoRV-rv	SpeI EcoRV	605 bp	60	20 sec	35
AGAP004654	SpeI-4654-EcoRV-fw SpeI-4654-EcoRV-rv	SpeI EcoRV	996 bp	60	35 sec	35
AGAP012167	SpeI-12167-EcoRV-fw SpeI-12167-EcoRV-rv	SpeI EcoRV	2000 bp	60	35 sec	35
AGAP010572	SpeI-10572-EcoRV-fw SpeI-10572-EcoRV-rv	SpeI EcoRV	1172 bp	53	35 sec	35
AGAP011050	SpeI-11050-EcoRV-fw SpeI-11050-EcoRV-rv	SpeI EcoRV	1757 bp	60	35 sec	35

*All primer sequences are reported in Appendix C, Table C.1.

3.4.2.3 pPGI_GAL4

The driver plasmid PGI_GAL4 was designed to carry the following components: piggyBac sites, attP sites, CFP marker under the control of the 3xP3 eye-specific promoter, Gypsy insulators, and the 2 kb 5' regulatory region of the phosphoglucose isomerase gene (PGI) (AGAP012167) upstream of the GAL4 sequence (Figure 3.4B). The cloning strategy adopted consisted of replacing the PUB5:GAL4:PUB3 component of the pSL*Gyp1:PUB5:GAL4:PUB3:Gyp2:attPr plasmid (Figure 3.2B) with PGI:GAL4:SV40 and then to clone the resulting Gyp1:PGI:GAL4:SV40:Gyp2:attPr fragment into the AscI sites of the pBACI:attPI:CFP:pBACr plasmid. To do so, the cloning strategy combined Gibson Assembly (Gibson et al., 2009, 2010) and restriction enzyme-based cloning including the following steps:

1) Gibson assembly was used to clone PGI, GAL4 and SV40 into pSL*Gyp1:PUB5:GAL4:PUB3:Gyp2:attPr to give pSL*Gyp1:PGI:GAL4:SV40:Gyp2:attPr (Figure 3.4A). The 2 Kb 5' region upstream the PGI gene was amplified from pSL*attB:PGI:GAL4:DsRed:attB (Figure 3.3), and GAL4 and SV40 sequences from plasmid templates using Phusion High-Fidelity DNA Polymerase (Thermo Scientific) and primers carrying overlapping regions as reported in Table 3.3. Plasmid pSL*Gyp1:PUB5:GAL4:PUB3:Gyp2:attPr was digested with NheI/NdeI. After gel purification, Gibson Assembly reactions were set up in a total volume of 25.4 µL using 90 ng of digested backbone plasmid pSL*Gyp1:PUB5:GAL4:PUB3:Gyp2:attPr, 0.099 pmols of each fragment and 12.7 µL of 2x Gibson Assembly® Master Mix and were incubated at 50°C for 1 h. Plasmid pSL*Gyp1:PGI:GAL4:SV40:Gyp2:attPr sequence was verified by EcoRV/HindIII digestion and sequenced using primers AttB3-seqR, p9_pSL_fw, p9_GAL4_rv, GAL4_p9_fw, GAL4_sequ_2F, GAL4_SV40_rv, SV40_GAL4_fw, SV40_pSL_rv and pSL1180-1 (Appendix C, Table C.1).

Table 3.3 Amplification of PGI_GAL4 components for Gibson cloning.

Fragment	Template	Primers*	RES Tag	Region amplified	T_m (℃)	Ext. time	No. cycles
PGI	attB:PGI:GAL4:DsRed	p9_pSL fw p9_GAL4 rv	NheI EcoRV	2000 bp	60	50 sec	35 X
GAL4	attB:GAL4:DsRed	GAL4_p9 fw GAL4_SV40 rv	EcoRV --	2646 bp	60	50 sec	35 X
SV40	attB:GAL4:DsRed	SV40_GAL4 fw SV40_pSL rv	-- NdeI	693 bp	60	50 sec	35 X

*All primer sequences are reported in Appendix C, Table C.1.

2) Restriction enzyme-based cloning was used to obtain the final plasmid PGI_GAL4. The Gyp1:PUB5:GAL4:PUB3:Gyp2:attPr fragment was excised from pSL*Gyp1:PGI:GAL4:SV40:Gyp2:attPr and cloned into the AscI sites of pBACl:attPl:CFP:pBACr to obtain the final plasmid pBACl:attPl:CFP:Gyp1:PGI:GAL4:SV40:Gyp2:attPr:pBACr (Figure 3.4B). Plasmid map was verified by enzymatic restriction using NcoI/NotI and HindIII.

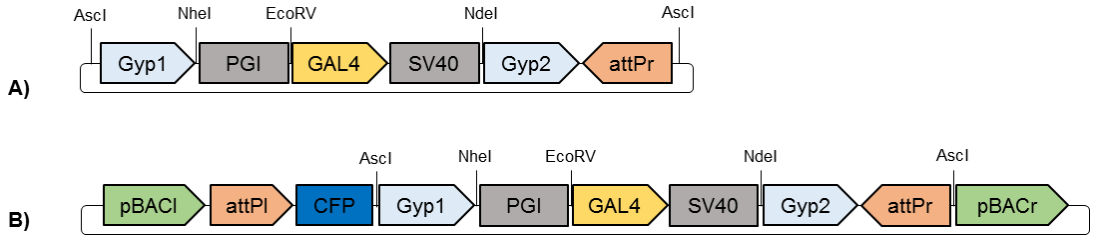

Figure 3.4 Schematic of cloning steps used to create the PGI_GAL4 plasmid (14 039 bp) (not to scale). **A**) Creation of pSL*Gyp1:PGI:GAL4:SV40:Gyp2:attPr by Gibson assembly. **B**) Final plasmid PGI_GAL4 was obtained using AscI to clone the Gyp1:PGI:GAL4:SV40:Gyp2:attPr fragment into a pBACl:attPl:CFP:pBACr plasmid. This construct was used for G3 embryo injection only; experiments on cells were conducted using pSL*attB:PGI:GAL4:DsRed:attB. Gyp1 and Gyp2: Gypsy insulators; PGI: 5' regulatory region upstream of the PGI gene; SV40: transcription terminator; attPl and attPr: PhiC31 attachment sites left and right respectively; pBACl and pBACr: piggyBac arms left and right respectively; CFP: cyan fluorescent protein used as 3xP3-driven eye maker.

3.4.2.4 GAL4 plasmids carrying MozAtlas Malpighian-specific promoter candidates

The 5' regions of six genes selected from MozAtlas showing enriched expression in the Malpighian tubules - AGAP002587, AGAP001823, AGAP011426, AGAP002629, AGAP010364, AGAP010975 - were cloned upstream of the GAL4 sequence in pSL*attB:Promoter:GAL4:DsRed:attB (Figure 3.3). Putative promoters were amplified from Kisumu genomic DNA using Phusion High-Fidelity DNA Polymerase or Phire Hot Start II DNA Polymerase (Thermo Scientific) and primers tagged with AflII/EcoRV or SpeI/EcoRV as reported in Table 3.4. After AflII/EcoRV or SpeI/EcoRV double digestion and purification, PCR products were independently cloned into pSL*attB:Promoter:GAL4:DsRed:attB replacing the original HSP promoter. Restriction digestion with NheI/EcoRV and HindIII and sequencing with M13F and RT-GAL4-2R (Appendix C, Table C.1) were performed to confirm plasmid maps.

Table 3.4 Amplification of 5' regions upstream of six Malpighian tubule-specific gene candidates.

Gene ID	Primers*	RES Tag	Region amplified	T_m (˚C)	Ext. time	No. cycles
AGAP002587	AflII-2587-EcoRV-fw AflII-2587-EcoRV-rv	AflII EcoRV	2000 bp	60	50 sec	35
AGAP001823	NheI-1823-EcoRV-fw AflII-1823-EcoRV-rv	NheI EcoRV	2000 bp	60	50 sec	35
AGAP011426	AflII-11426-EcoRV-fw AflII-11426-EcoRV-rv	AflII EcoRV	1140 bp	60	25 sec	35
AGAP002629	SpeI-2629-EcoRV-fw SpeI-2629-EcoRV-rv	SpeI EcoRV	2000 bp	60	35 sec	35
AGAP010364	SpeI-10364-EcoRV-fw SpeI-10364-EcoRV-rv	SpeI EcoRV	2000 bp	58	35 sec	35
AGAP010975	SpeI-10975-EcoRV-fw SpeI-10975-EcoRV-rv	SpeI EcoRV	2000 bp	58	35 sec	35

*All primer sequences are reported in Appendix C, Table C.1.

3.4.3 *An. gambiae* mosquito cell transfection and luciferase assay

3.4.3.1 An. gambiae cell line

The haemocyte-like *An. gambiae* cell line Sua5.1 (Müller et al., 1995) was maintained at 28˚C in Schneider's medium (Invitrogen) supplemented with 7-10% foetal bovine serum (PAA) and 100 U/ml Ampicillin + 100 U/ml Streptomycin (Invitrogen). Cells were kept in 25 cm^2 15 ml flasks and sub-cultured every 7-10 days.

3.4.3.2 Cell transfection and luciferase assay

Cells were split 24 h before transfection in 16-well plates and then transfected using EffecteneTransfection Reagent (Qiagen) following manufacturer's instructions. Briefly, 202 ng of total DNA, 1.6 µl enhancer, 5 µl Effectene, 60 µl Buffer EC and 350 µl medium were applied dropwise to each well. DNA samples contained 100 ng of GAL4 driver plasmid, 100 ng of a responder plasmid driving the expression of firefly luciferase (UAS-Luc) (Lynd & Lycett, 2011), and 2 ng of Actin Renilla plasmid to normalise for efficiency of transfection (Table 3.5). The pPUBc-GFP plasmid (Lycett, unpublished), which expresses cytoplasmic GFP under the control of a similar PUBc promoter sequence than the one used in this study, was used to visually assay transfection efficiency and measure background activity (blank) in the absence of a GAL4 driver. The activity of each GAL4/UAS combination was tested in 3-6 technical replicates. After 48 h incubation, cell extracts were tested for luciferase expression using a Dual-Luciferase® Reporter Assay System (Promega). Cells were lysed in 100

µl/well of Passive Lysis Buffer, 8 µl of cell extract was added to 100 µl of LAR II and Firefly activity measured. Renilla luciferase activity was then measured after adding 100 µl of Stop&Glo®. All measurements were carried out using a Lumat LB 9507 tube luminometer (EG&G Berthold) programmed to perform a 2-second premeasurement delay followed by a 10-second measurement. Relative light units (RLU) measurements obtained for each well were normalised by Renilla activity (RLU_{Luc} / RLU_{Ren}) and adjusted for the activity of the blank (RLU_{sample} – RLU_{blank}).

One-way ANOVA with multiple comparison analysis was performed to determine statistical significant differences ($p < 0.05$) between each GAL4/UAS combination. The Dunnett's test was used to perform pairwise comparisons between each GAL4/UAS combination and the control, while the Tukey's test was used for pairwise comparisons between GAL4/UAS combinations.

Table 3.5 Experimental set up of luciferase reporter assay in SUA5.1 cells to test relative promoter-GAL4 activity.

Promoter-GAL4 plasmid	UAS-Luciferase plasmid	Renilla plasmid	No. replicates
pBPnucl	pUAS-Luc	Actin Renilla	6
pPGl	pUAS-Luc	Actin Renilla	6
pLTV1	pUAS-Luc	Actin Renilla	6
pALDred	pUAS-Luc	Actin Renilla	6
pAGAP003864	pUAS-Luc	Actin Renilla	3
pSUI1	pUAS-Luc	Actin Renilla	3
pATPcar	pUAS-Luc	Actin Renilla	3
pPUBc	pUAS-Luc	Actin Renilla	5
--	pUAS-Luc	Actin Renilla	6
pPUBc-GFP	--	Actin Renilla	6

3.4.4 Creation and characterisation of *An. gambiae* transgenic lines

3.4.4.1 Mosquito lines

Details of mosquito maintenance are reported in Appendix A.

Three mosquito lines were used in this study including the wild type colony **G3**, the docking line **A11** (described in Chapter 2), and the **UAS-mCherry** line. This is a transgenic homozygous responder line for UAS-mediated expression of mCherry fluorescent protein targeted to cell membranes. Line carries 3xP3-driven CFP and YFP eye-specific markers created by PhiC31-mediated modification of line E

(Meredith et al., 2011) with a attB:UAS-mCherry expression cassette (gift of E. Pondeville).

3.4.4.2 Embryo microinjections

Transgenic mosquitoes for ubiquitous expression were produced by piggyBac-mediated germline transformation as previously described (Lycett et al., 2012; Lynd & Lycett, 2012). The line for Malpighian tubule-specific expression was created by site-specific germline transformation (Pondeville et al., 2014).

Plasmid DNA was purified using Plasmid Midi Kit (Qiagen) and ethanol precipitation was carried out to obtain a solution containing 350 ng/µL of GAL4 driver plasmid and 150 ng/µL of the helper plasmid (transposase plasmid phsp-pBac (Handler & Harrell, 1999) for piggyBac and integrase plasmid PKC40 (Ringrose, 2009) for RMCE) in a total volume of 25 µL of 1X injection buffer (5 mM KCl, 0.5 mM $NaPO_4$, pH 7.2) to give a final concentration of 500 ng/µL (Lombardo et al., 2009).

Microinjections were carried out as described in Chapter 2.

3.4.4.3 Establishment of transgenic lines

3.4.4.3.1 Lines created by piggyBac-mediated germline transformation

3.4.4.3.1.1 Screening and husbandry

F_0 L1 larvae were screened for transient (episomal) CFP expression in the anal papillae to have an indication of successful DNA uptake, and positive larvae were reared separately. Adults emerged in sex-specific cages and backcrossed with 3-5-fold excess of opposite sex wild type G3. F_1 L2-L3 larvae were assessed for stable expression of the eye marker and negative larvae discarded. F_1 transformant adult females were backcrossed with wild type G3 individuals. Isofemale lines were obtained from single laying females and scored for inheritance of the CFP marker. In most cases, lines yielding a percentage of transformants not compatible with a single insertion (i.e. >50% fluorescent progeny) were discarded. Individuals from isofemale lines showing ~50% of transgenic progeny were interbred to create stable lines.

3.4.4.3.1.2 Inverse-PCR

Inverse PCR was conducted as described by Lycett et al., 2012. Genomic DNA was extracted from pools of 20 F_2 transgenic adults from selected isofemale lines that showed ~50% of transgenic progeny using Qiagen Genomic tips (Qiagen). 1 µg of gDNA was then digested with BfuCI (NEB), self-ligated using T4 ligase (NEB) at a final concentration of 5 ng/µl for 14-18 h at 16 ˚C, and PCR was performed to amplify DNA regions flanking the piggyBac arms at the site of insertion (primers ITRL1F and ITRL1R for left arm, ITRR1F and ITRR1R for right arm, Appendix C, Table C.1). Amplification reactions were performed using 2.5 µl of ligation product in a total volume of 50 µl using Phire Hot Start II DNA Polymerase (Thermo Scientific) and annealing temperatures of 65 ˚C for the piggyBac left arm, 58 ˚C for the right arm. PCR products were sequenced and genomic location of insertions identified using the BLAST tool integrated in VectorBase (Giraldo-Calderón et al., 2015). In case of ambiguity in the location of integration due to short sequence or lack of PCR product from one of the piggyBac arms, genomic DNA was digested at 65 ˚C using TaqαI (NEB) and the protocol repeated.

For the A8 and A10 lines, location of insertion was additionally confirmed by amplification of the regions flanking each piggyBac arm using ITRL1F and A10_insert_rv for A10 left arm, ITRR1F and A10_R_check_rv for A10 right arm, ITRL1F and A8_L_check_rv for A8 left arm, and A8_R_check_fw2 and ITRR1F for A8 right arm (Appendix C, Table C.1). PCRs were performed using DreamTaq DNA polymerase (Thermo Scientific), 55°C annealing temperature, a 30-second extension and 35 cycles.

3.4.4.3.2 Lines created by PhiC31 site-specific germline transformation

3.4.4.3.2.1 Screening and husbandry

F_0 L1 larvae were screened for transient (episomal) expression of DsRed in the anal papillae to have an indication of DNA uptake and to confirm the presence of the CFP marker of the A11 docking strain. Adults emerged in sex-specific cages and were backcrossed with 3-5-fold excess of opposite sex wild type G3. F_1 L2-L3 larvae were assessed for stable expression of the red eye marker and positive adults backcrossed with wild type individuals. Six single-laying female lines were set up and, after laying eggs, their DNA was extracted to check the orientation of insertion.

3.4.4.3.2.2 Orientation of insertion

Orientation check was performed on the parental females and on the controls G3 and A11 by PCR. Four combinations of 4 primers designed to give a product just in one of the orientations were used in 4 different PCRs: piggyBacR-R2 + Red-seq4R for PCR 1, P6_int_rv + ITRL1R for PCR 2, piggyBacR-R2 + P6_int_rv for PCR3, and Red-seq4R + ITRL1R for PCR 4 (Appendix C, Table C.1). PCRs were performed using DreamTaq DNA polymerase (Thermo Scientific) and thermal program involving 54°C annealing temperature, a 3-minute extension and 30 cycles.
F_2 progeny from a single female that showed orientation of insertion A was kept and a definitive line created by interbreeding.

3.4.4.3.3 Transformation efficiency calculations

Minimum transformation efficiency was calculated as (*Number of independent founder families yielding transgenics / total F_0 adult survivors) x 100.* When molecular characterisation of insertion location was conducted, transformation efficiency was calculated as *(Number of independent single insertions / total F_0 adult survivors) x 100.*

3.4.4.4 GAL4 x UAS crosses for assessing promoter activity

Crosses were established between GAL4 driver lines marked with CFP (A10, A8 and PGI) or DsRed (VATG), and opposite sex individuals of the UAS-mCherry line, which is marked with CFP and YFP. Progeny of these crosses was sorted at pupa stage according to marker colour:

- A10, A8, PGI: CFP and YFP for GAL4/UAS and CFP only for GAL4/+ mosquitoes (controls);
- VATG: DsRed, CFP and YFP for GAL4/UAS and DsRed only for GAL4/+ controls.

3.4.4.5 Dissections

2-5-day-old GAL4/UAS and GAL4/+ mosquitoes were anesthetised with gaseous CO_2 and dissected in PBS supplemented with EDTA-free protease inhibitor cocktail (Roche). Body parts were incubated in fixing solution (4% paraformaldehyde, 1x PBS pH 7.4, 2 mM $MgSO_4$, 1 mM EGTA) for 30-45 minutes at room temperature, washed in PBS, mounted on a microscope slide using Vectashield mounting medium (Vector

Laboratories), and stored in the dark at 4 ˚C. For preparation of abdomens, after removing internal organs, they were cut and flatten open to reveal the fat body attached to the cuticle and incubated for 2 minutes in methanol before fixing using the same conditions described above.

3.4.4.6 Imaging

All mosquitoes were observed with Leica MZ FLIII fluorescence stereo microscope fitted with CFP, DsRed and YFP filters (Leica Microsystems).
Fluorescence photos were taken using the LAS X Microscope Software integrated within a Leica M165 FC fluorescent stereo microscope (Leica Microsystems).

3.5 RESULTS

3.5.1 Candidate ubiquitous genes and cloning of their 5' regulatory regions

Nine candidate genes showing widespread expression across all tissues were selected from MozAtlas: AGAP004654, AGAP012167, AGAP010572 for low expression; AGAP002182, AGAP003864, AGAP011050 for medium expression; and AGAP006459, AGAP006782, AGAP001971 for high expression. Details on selected genes and their cloning are listed in Table 3.6 and raw gene expression levels reported in Appendix C, Figure C.1A.
Cloning of the 5' regions located upstream of the predicted start codon into the pSL*attB:Promoter:GAL4:DsRed:attB RMCE plasmid (Figure 3.5A) was successful for all candidates except AGAP002182 which did not amplify from genomic DNA. PUBc was cloned directly into a piggyBAC vector and carried its native 3' region downstream of the GAL4 (Figure 3.5B), while the RMCE-based plasmids carried the SV40 terminator (Figure 3.5A).

Table 3.6 List of selected ubiquitous candidate genes.

Gene ID	Protein	Promoter name	Chr.	Cloned 5' region (bp)	Plasmid size (bp)
AGAP004654	3'(2'), 5'-bisphosphate nucleotidase	BPnucl	2R	990	9763
AGAP012167	glucose-6-phosphate isomerase	PGI	3L	2003	10776
AGAP010572	protein LTV1	LTV1	3L	1168	9941
AGAP002182	ATP-binding cassette transporter	ATPtra	2R	N/A	N/A
AGAP011050	aldehyde reductase	ALDred	3L	1752	10525
AGAP003864	unknown	UKW	2R	606	9379
AGAP006459	protein translation factor SUI1	SUI1	2L	2473	11246
AGAP006782	ADP,ATP carrier protein 1	ATPcar	2L	1772	10545
AGAP001971	Polyubiquitin-c	PUBc	2R	2005	13839

N/A: not applicable

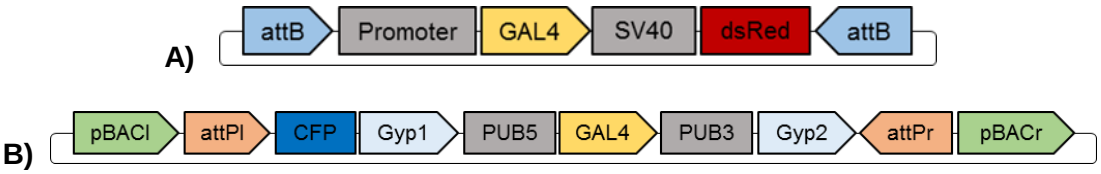

Figure 3.5 Schematic maps of driver plasmids carrying ubiquitous candidate promoters (not to scale). **A)** pSL*attB:Promoter:GAL4:DsRed:attB. Seven 5' regulatory regions were independently cloned upstream of the GAL4. attB: PhiC31 attachment sites; SV40: transcription terminator; DsRed: red fluorescent protein used as 3xP3-driven eye maker. **B)** PUBc_GAL4. Gyp1 and Gyp2: Gypsy insulators; PUB5: 5' regulatory region upstream of PUBc start codon; PUB3: 3' regulatory region downstream of PUBc stop codon; attPl and attPr: PhiC31 left and right attachment sites; pBACl and pBACr: piggyBac left and right arms; CFP: cyan fluorescent protein used as 3xP3-driven eye maker.

3.5.2 Candidate Malpighian tubule-specific genes and cloning of their 5' regulatory regions

Malpighian tubule-specific candidates selected from MozAtlas were AGAP001823 and AGAP002629 for low expression, AGAP010364 and AGAP010975 for medium expressions, AGAP002587 and AGAP011426 for high expression. Details on selected genes and their cloning are listed in Table 3.7 and raw gene expression levels reported in Appendix C, Figure C.1B.

All candidate 5' region cloning into pSL*attB:Promoter:GAL4:DsRed:attB was successful except AGAP011426 and AGAP010364. Plasmids carrying AGAP001823, AGAP002629, AGAP010975 contained two attB sites (Figure 3.6A), while that carrying AGAP002587 had only one attB site (Figure 3.6B). This was due to the unavailability of a suitable restriction site to digest out the original promoter without altering the attB site located upstream of it, which resulted in its loss.

Table 3.7 List of Malpighian tubule-specific candidate genes

Gene ID	Protein encoded	Promoter name	Chr.	Cloned 5' region (bp)	Plasmid size (bp)
AGAP002587	unknown	P5	2R	2000	10438
AGAP001823	V-type ATPase subunit G	VATG (P6)	2R	1937	10710
AGAP011426	Solute carrier family 17	P7	3L	N/A	N/A
AGAP002629	unknown	P14	2R	2001	10774
AGAP010364	unknown	P15	3L	N/A	N/A
AGAP010975	unknown	P16	3L	1998	10771

N/A: no amplification product

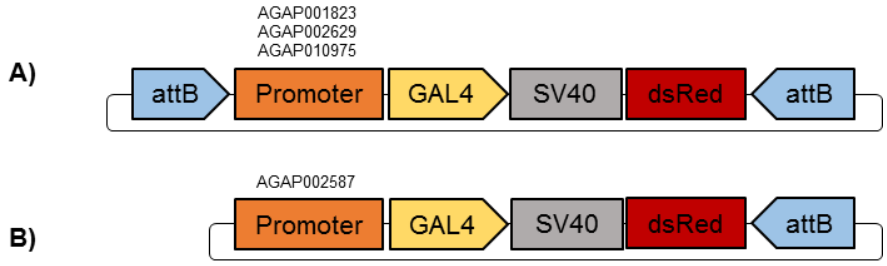

Figure 3.6 Schematic maps of driver plasmids carrying Malpighian tubule-specific candidate promoters (not to scale). **A)** pSL*attB:Promoter:GAL4:DsRed:attB. Three promoters were independently cloned upstream of the GAL4. **B)** pSL*Promoter:GAL4:DsRed:attB. One promoter was cloned upstream of the GAL4. attB: PhiC31 attachment sites; SV40: transcription terminator; DsRed: red fluorescent protein used as 3xP3-driven eye maker.

3.5.3 *In vivo* assessment of putative ubiquitous promoters in *An. gambiae* cells

The GAL4-mediated activity of the putative ubiquitous promoters BPnucl, PGI, LTV1, AGAP003864, ALDred, SUI1, ATPcar and PUBc was investigated by luciferase assay after co-transfection with the responder plasmid pUAS-Luc in *An. gambiae* SUA5.1 cells.

pPUBc and pPGI were active in cells showing significantly higher activity than control transfections with the responder plasmid only (~4220x, p = < 0.0001; ~950x, p = 0.0417 respectively) (Figure 3.7). In addition, background activity from a GAL4-less (blank) plasmid was not significantly different to the pUAS-Luc control (P = 0.16) (not shown), indicating limited leakiness in UAS regulated expression. The other six promoters tested had observable activity in these cells (Figure 3.7), but did not show a statistically significant difference from control transfections using one-way ANOVA with multiple comparison analysis (Appendix C, Table C.2).

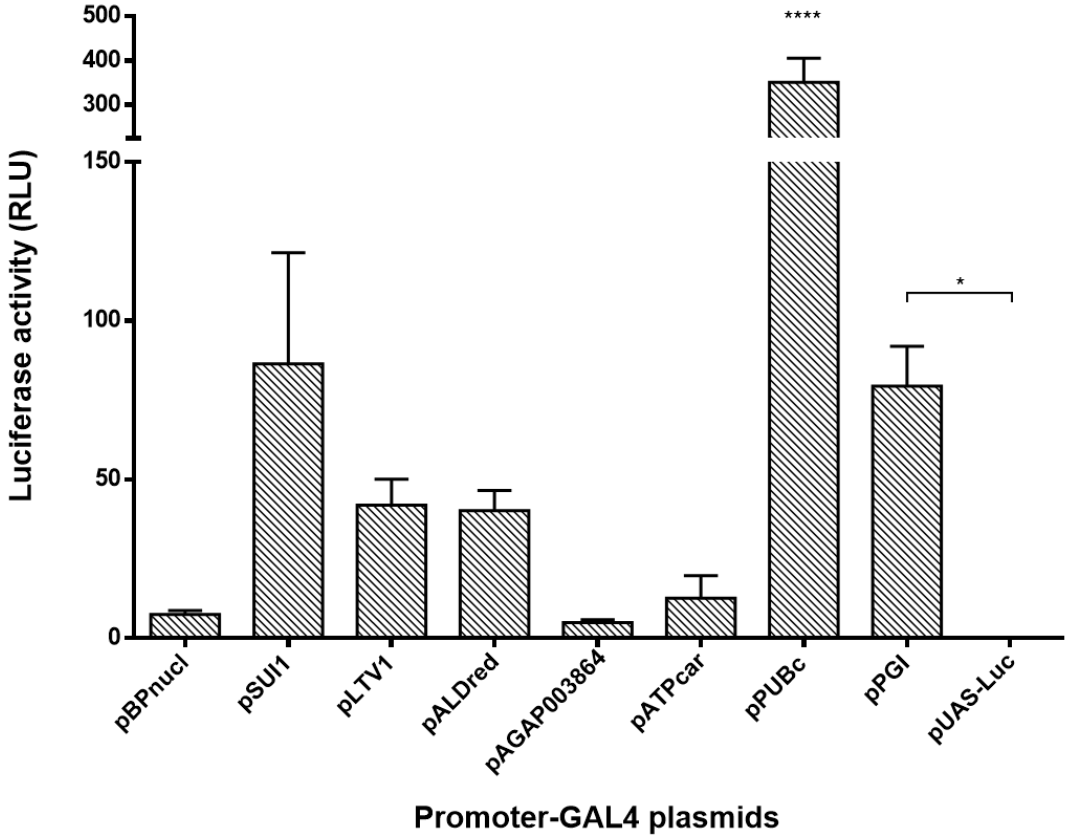

Figure 3.7 Relative GAL4-mediated activity of putative promoters in *An. gambiae* SUA5.1 cells. Promoter activity is shown as luciferase expression after co-transfection of driver plasmids containing putative promoters with the pUAS-Luc responder. Luciferase expression (Relative Lights Units – RLU) is standardised for Renilla expression and shown as average from three (pSUI1, pATPcar, pAGAP003864), five (pPUBc), or six (pBPnucl, pPGI, pLTV1, pALDred, pUAS-Luc) technical replicates. Top bars represent standard error from mean. Significant differences were calculated using One-way ANOVA with multiple comparison analysis. * $p < 0.05$, **** $p \leq 0.0001$.

3.5.4 Generation of mosquito driver lines and assessment of promoter activity

3.5.4.1 PUBc_GAL4 driver lines for ubiquitous expression

3.5.4.1.1 Establishment of transgenic lines

To assess the ability of PUBc-GAL4 to express *in vivo* in transgenic mosquitoes, we used the piggyBac transposon to create a series of driver lines carrying the cassette in single, unique genomic locations.

A total of 180 *An. gambiae* G3 strain embryos were injected with pPUBc_GAL4 (Figure 3.5B); of these 113 (63%) larvae hatched and 77 (68%) showed CFP transient expression in the anal papillae. The mating and screening strategy used to isolate transgenic isofemale lines is summarised in Table 3.8. 97 adults (54% of eggs injected) were obtained and pooled into 6 sex-specific F_0 founder cages (A-F). Transgenic F_1 progeny (45) were recovered from each of the 4 F_0 cages established from founders showing transient expression (A-D), while no transformants were recovered from negative F_0 founders (cages E,F). F_1 transgenic females derived from A, C and D founder cages and males from B (no transgenic F_1 females recovered) were backcrossed with wild-type individuals and F_2 progeny from individual females assessed for inheritance of the eye-marker to estimate transgene copy number. We identified 14 isofemale lines showing 47-53% transgene inheritance (A2, A3, A6, A7, A8, A10, A11, A12, A15, B3, B8, C1, C2, D2), consistent with single copy insertions. 4 lines yielding ≥58% transgenic progeny (A5, B1, B2, B7), which may be caused by multiple integrations some of which may be in close linkage, were discarded.

Table 3.8 Selection strategy to isolate stable transgenic driver lines carrying a single insertion of the PUBc_GAL4 cassette.

F_0 pool	**F_0 adults No. and sex**	**Transient CFP expression**	**No. +F_1 (sex)**	**% +F_2 larvae (No. +larvae/total)**
A	13 F	+	34 (17 F, 17 M)	A 2 – 49% (84/173) A 3 – 48% (74/154) A 5 – 62% (5/8) A 6 – 42% (80/190) A 7 – 50% (52/103) A 8 – 49% (67/136) A 10 – 47% (65/139) A 11 – 52% (63/121) A 12 – 53% (102/193) A 15 – 51% (93/181)
B	14 M	+	3 (3 M)	B 1 – 73% (8/11) B 2 – 58% (18/31) B 3 – 44% (31/71) B 7 – 59% (69/116) B 8 – 53% (62/116)
C	18 F	+	5 (2 F, 3 M)	C 1 – 47% (28/59) C 2 – 47% (73/155)
D	20 M	+	3 (2 F, 1 M)	D 2 – 46% (53/115)
E	23 M	–	0	N/A
F	9 F	–	0	N/A

F: female, M: male. NS: not screened. N/A: not applicable.
Other isofemales: A1: dead (mosquito died without laying eggs). A4, B9: not mated (eggs did not hatch). A9, A13, A14, B4, B5, B6, B10, D1: sterile (mosquito did not lay eggs).

Isofemale lines A2, A3, A6, A7, A8, A10, A11, A12, A15, B3, C1, D2 were characterised to verify number and location of integration sites by inverse-PCR and sequencing. In several instances, identical integration sites were found in distinct isofemale lines from the same founder cage (A8=A15, A10=A12, A3=A6=A7=A11) (Figure 3.8). Replicate lines were discarded thus overall the final analysis was consistent with the isolation of 7 isofemale lines carrying separate single integration sites (Table 3.9). Four lines (A8, A10, B3, C1), carried intergenic insertions, one line (A3) carried an insertion within the open reading frame of *Cyp6m4* (AGAP008214), and two (A2, D2) carried insertions within highly repetitive regions that precluded their exact localisation in the genome (Table 3.9). Inverse-PCR failed to amplify the region flanking the piggyBac right arm of lines A8 and A10 so, using the information derived from the left arm, location in these lines was confirmed with primers designed on the genomic DNA flanking the insertion (Appendix C, Figure C.2). All sites of integration characterised occurred at TTAA genomic sequences that are canonical for piggyBac-mediated insertion (Table 3.9).

Overall, we achieved a minimum transformation efficiency of 7% (% of independent insertions). All 7 lines were interbred and underwent preliminary assessment of *in vivo* promoter activity in larvae.

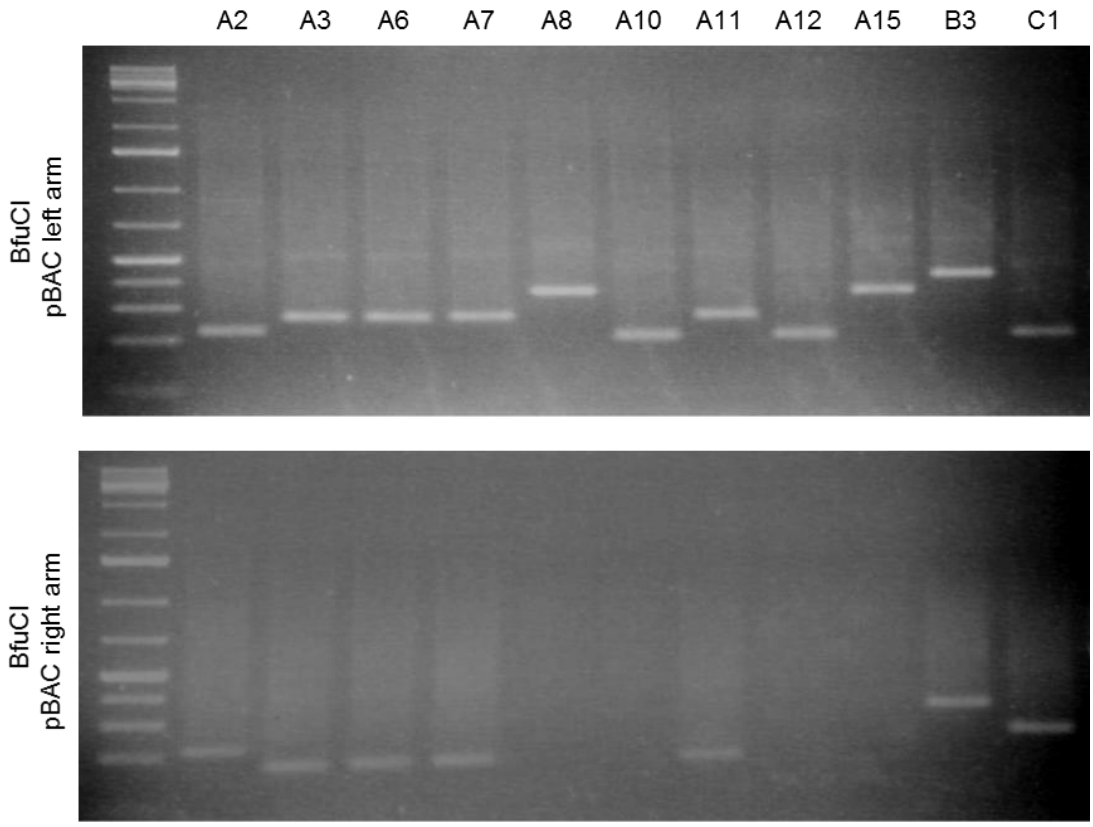

Figure 3.8 Agarose gel electrophoresis showing results for inverse-PCR on regions flanking the piggyBac arms after BfuCI digestion and self-ligation of genomic DNA isolated from isofemale lines. Among the isofemales derived from cage A, those sharing the same PCR product size derive from the same F_0 founder individual and thus bear an insertion in the same genomic location. Six different single insertions are shown: 1) A2; 2) A3 = A6 = A7 = A11; 3) A8 = A15; 4) A10 = A12, 5) B3; 6) C1. Results for Taq1α digestions of A2, A8, A10, C1 and D2 are shown in Appendix C, Figure C.3. Ladder is GeneRuler 1 kb Plus (Thermo Scientific).

Table 3.9 Molecular characterisation of transgenic lines carrying single insertions by inverse-PCR.

Line	pBAC arm	Enzyme	Sequence	Query length	Alignment length	Identity %	PEST Chromosome	Position	
A2	Left	TaqαI	TTAAATGGATAGCGGTAGCT	795	653-6	95-96	Multiple hits	N/A	
	Right	BfuCI	CCGGTGAGTGCGTAGCTTAA	79	79	100			
A3	Left	BfuCI	TTAAACTGTTTGCCGGCCGC	75	75	96	3 R	6,934,418	Intragenic
	Right	BfuCI	GTCCTCCAGGTAGTCTTTAA	33	31	100		6,934,415	AGAP008214
A8	Left	TaqαI	TTAATCTCGGTTCTCGGTAT	323	323	100	2 R	32,162,290	Intergenic
	Right*	--	ATATTTACGCAGATTCTTAA	53	42	90.5		32,162,293	
A10	Left	TaqαI	TTAAAGAACTGATCAATACA	404	329**	99.1	2 R	5,816,202	Intergenic
	Right*	--	CAAACGCACAGTACCATTAA	368	353	98.9		5,816,199	
B3	Left	BfuCI	TTAAAGCTCGTTCATACTCT	221	221	98.2	3 R	32,092,431	Intergenic
	Right	BfuCI	GAAGCTGTAAAAAGCTTTAA	192	191	95.8		32,092,428	
C1	Left	TaqαI	TTAAAAGAGATCCCGCGAGG	652	648	99.2	X	21,936,498	Intergenic
	Right	BfuCI	TAGGTCGATGAACTCCTTAA	102	102	100		21,936,501	
D2	Left	TaqαI	TTAAAGTGCTTTCAACGTTA	700	700	98.6-99.4	Multiple hits	N/A	

*the genomic position flanking this arm was obtained by amplification of genomic DNA using primer sequences deducted by the position of the left arm.
**there is an insertion in the PEST sequence that is not present in A10, Pimperena, or *An. coluzzii*.

3.5.4.1.2 In vivo assessment of PUBc promoter activity in transgenic mosquitoes

To investigate the patterns of expression driven by PUBc and identify multiple insertion sites able to sustain ubiquitous expression, profiles generated by selected transgenic PUBc_GAL4 isofemales lines (A2, A3, A8, A10, B3, C1 and D2) and male pools were assessed and compared after crossing with a responder line carrying UAS-regulated mCherry.

The expression profiles driven by individual isofemale lines differed in terms of signal intensity and distribution with the following phenotypes detected in larvae (Appendix C, Figure C.4): intensely bright and widespread mCherry signal detected throughout the whole body (A10 and D2), symmetrically patterned mCherry signal distributed along the abdomen with intense signal in the head and mouthparts (A8), asymmetrical mCherry signal along the abdomen, in the head and mouthparts (A3 and C1), asymmetrical mCherry signal limited to the terminal part of the abdomen (A2), and intense signal in the brain and mouthparts (B3).

No fluorescent phenotypes from male pool progeny (Appendix C, Figure C.4) were observed that differed from those derived from the single isofemales lines, suggesting that the male pool members examined originated from the same F_0 individuals as their female counterparts, or that they carried insertions in similarly permissive sites. Therefore, progeny from males was discarded. Due to the large number of lines produced, we restricted our in-depth analysis to the isofemale lines A10 and A8 which showed the most widespread signal and were representative of two distinct levels of expression, higher and lower respectively.

From the dorsal side of both A10/ch and A8/ch larvae, mCherry fluorescence was evident in the mouthparts, brain, fat body, and muscles surrounding the aorta and the heart (Figure 3.9 A,C). On the ventral side, strong mCherry expression was detectable in the developing thoracic imaginal discs and the central nerve cord (Figure 3.9 E,G). Fluorescent signal in A10/ch larvae was more intense compared to A8/ch larvae, with the only exception of the mouthparts (Figure 3.9 A,C,E,G). Furthermore, in A8/ch larvae a distinct symmetrical expression pattern was detected dorsally and ventrally in each abdominal segment (Figure 3.9 C,G), while A10/ch individuals displayed a very bright and dispersed signal throughout the larval body (Figure 3.9 A,E).

In pupae, the difference in signal intensity and the distinct abdominal pattern of expression was maintained, and strong fluorescence was detected in the developing appendages in both A10/ch and A18/ch female pupae (Figure 3.10).

At adult stage, mCherry expression was widespread in females and males of both A10 and A8 crosses with A10/ch displaying a brighter signal than A8/ch mosquitoes. In both crosses, fluorescence was detected in all the appendages including legs, veins of the wings, antennae, palps, and proboscis/labium (Figure 3.11). Here, fluorescence appeared strongly at the tip of palps and proboscis as well as at the junction of leg segments, which can be explained by the lack of cuticle sclerotization in these areas (Figure 3.11). Expression was also robust at the base of the antennae in the pedicel, which hosts the Johnston's organ, and in the brain (Figure 3.11). A10/ch mosquitoes showed bright mCherry expression in a variable proportion of the ommatidia, while in A8/ch individuals this generally occurred in fewer ommatidia (Figure 3.11). Finally, fluorescence was widely detected in the thorax and along the abdomen both dorsally and ventrally with bright signal visible through the non-sclerotized areas of the cuticle (Figure 3.11).

To identify internal organs and tissues where the PUBc promoter is active, we performed dissections on A10/ch and A8/ch adult female mosquitoes. In dissected abdomens expression was readily detectable in the cuticle, fat body, lateral muscles and nerve cord (Figure 3.12 A,C). Besides displaying a lower signal intensity, A8/ch abdomens showed a mosaic pattern of expression in muscular tissues (Figure 3.12 C). The PUBc promoter was active in the salivary glands of A10/ch, with mCherry fluorescence detected in all lobes, while the signal was weak in A8/ch salivary glands (Figure 3.12 M,O). Along the digestive tract, a comparable level of fluorescence was detected in A10/ch and A8/ch mosquitoes in the trachea surrounding the foregut, midgut, hindgut and Malpighian tubules of unfed females; no expression was detectable in the midgut epithelium (Figure 3.12 I,K). 24-48 h after blood meal the stretched muscles and nerves surrounding the midgut were clearly visible (not shown). Ovaries of sugar-fed A10/ch females showed bright oviducts and follicles (Figure 3.12 E,G), and fluorescence was also strongly detected 24-48 h after blood meal in the developing oocytes (not shown); while fluorescence in these tissues in A8/ch mosquitoes was weaker (Figure 3.12 E,G). In the males from A10 or A8 lines mCherry signal was barely discernible in the testes (not shown). In the haemolymph of mosquitoes from both lines, different classes of haemocytes were found expressing mCherry (not shown). The fat body of both lines also appeared diffusely fluorescent (not shown).

Overall, fluorescence driven by A10 and A8 lines was widespread and maintained from new-born larvae to adults of both sexes and was detected in a variety of tissues and body parts with levels of fluorescence generally lower in A8/ch compared to A10/ch individuals.

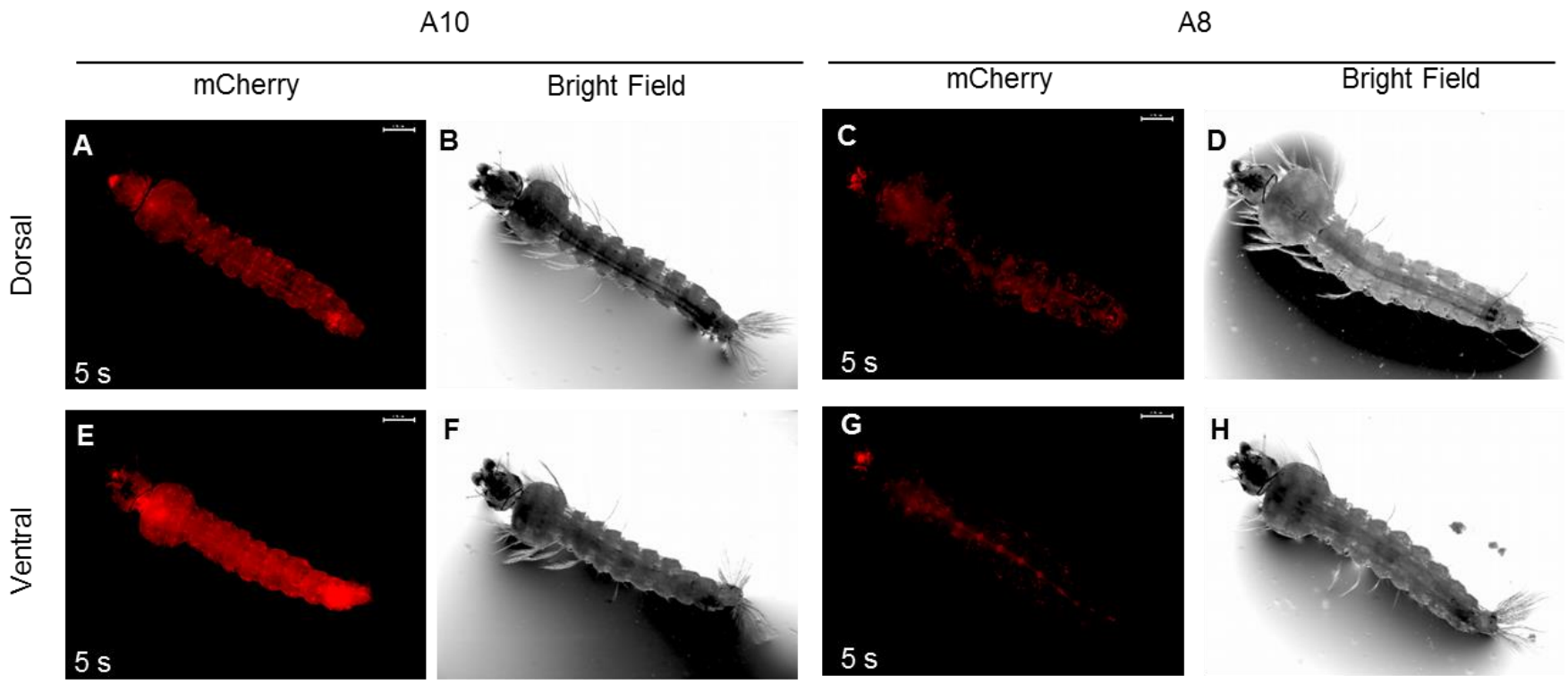

Figure 3.9 Expression profiles driven by the PUBc promoter in A10/ch (left) and A8/ch (right) L3-L4 larvae. A-D are dorsal views, E-H ventral views. A,C,E,G represent mCherry signal at 650 nm; numbers show seconds (s) of exposure. B,D,F,H are the corresponding bright fields. Bar = 0.5 mm.

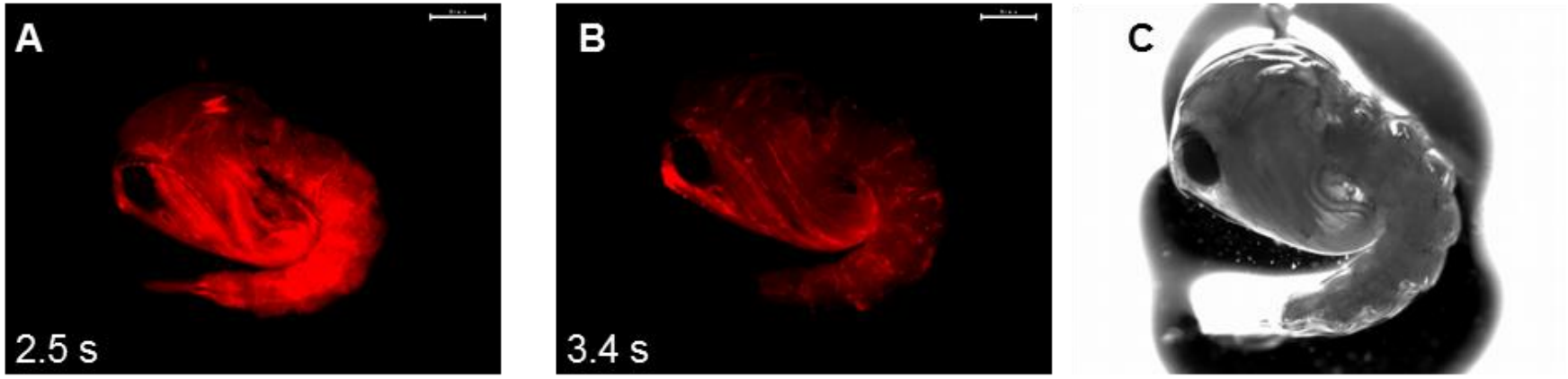

Figure 3.10 Expression profiles driven by the PUBc promoter in A10/ch (left) and A8/ch female pupae (centre and right). A and B represent mCherry signal at 650 nm; numbers show seconds (s) of exposure. C is the bright field image of B. Bar = 0.5 mm.

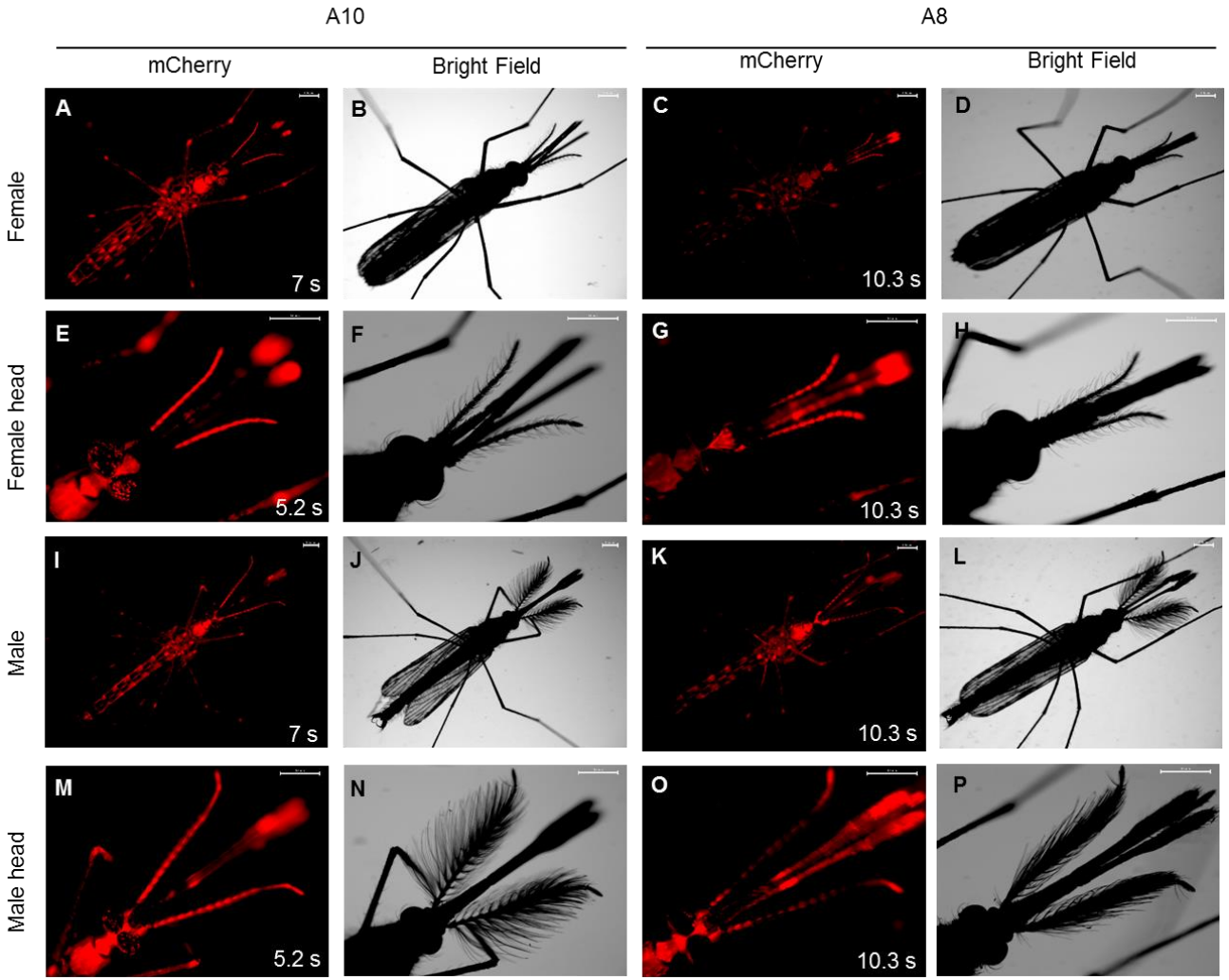

Figure 3.11 Expression profile driven by the PUBc promoter in A10/ch (left) and A8/ch (right) adult mosquitoes. All images are ventral views. A,C,E,G,I,K,M,O represent mCherry signal at 650 nm; numbers show seconds (s) of exposure. B,D,F,H,J,L,N,P are the corresponding bright fields. Bar = 0.5 mm.

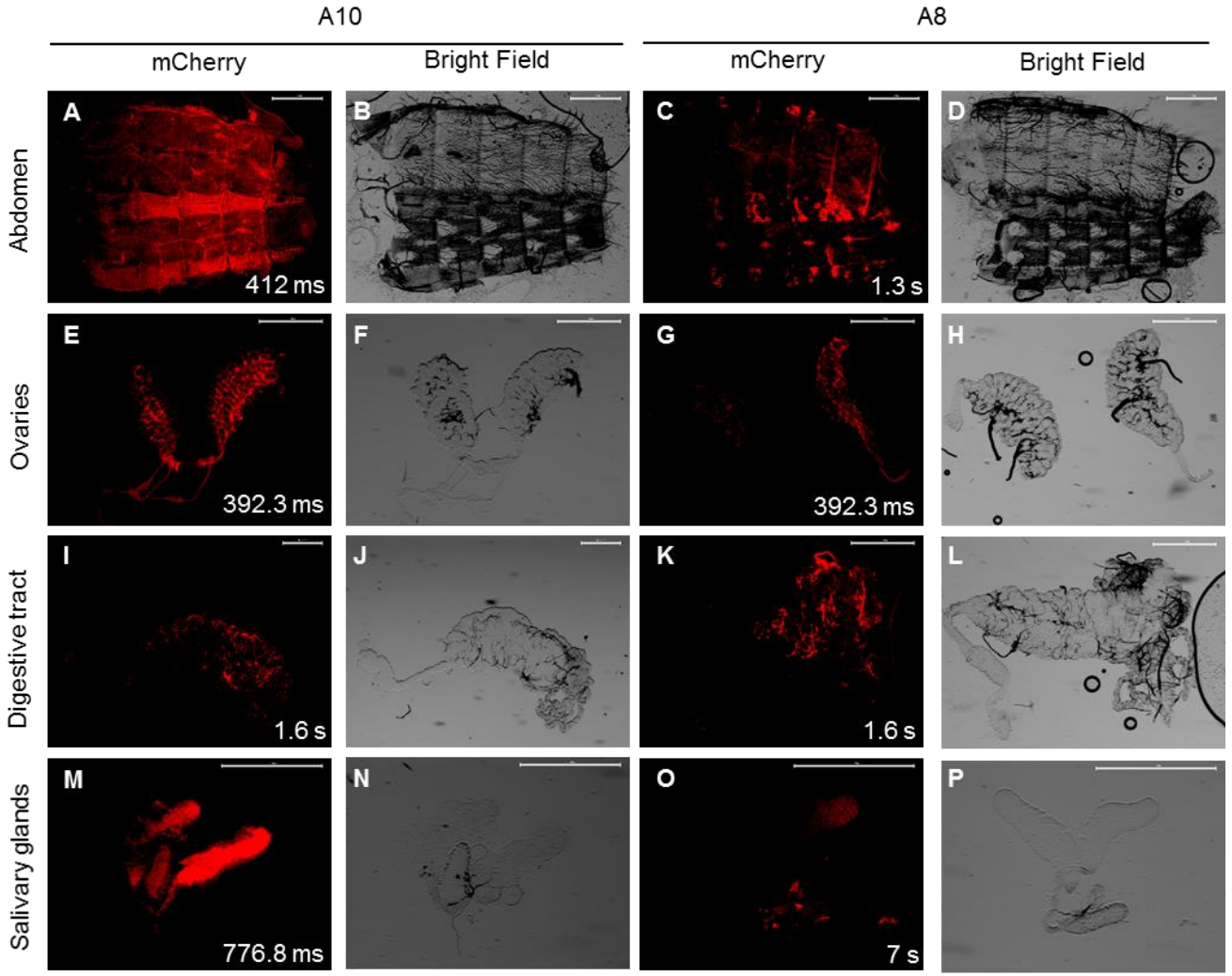

Figure 3.12 Expression profile driven by the PUBc promoter in A10/ch (left) and A8/ch (right) adult dissected and fixed tissues. A,C,E,G,I,K,M,O represent mCherry signal at 650 nm; numbers show milliseconds (ms) or seconds (s) of exposure. B,D,F,H,J,L,N,P are the corresponding bright fields. Bar = 0.5 mm.

3.5.4.2 PGI_GAL4 driver lines for ubiquitous expression

PGI_GAL4 driver lines were created using piggyBac-mediated germline transformation. 193 embryos of the G3 strain were injected with pPGI_GAL4 (Figure 3.4B) and 24 (14.5%) larvae hatched, of which 10 (42%) showed transient CFP expression. Eighteen (9.3%) F_0 adults, 8 positives and 10 negatives, survived and were pooled into 4 F_0 founder sex-specific families (G-J) (Table 3.10). After backcross with G3s, 17 F_1 transgenic larvae were recovered from family G only, which included mosquitoes showing transient expression of CFP at early larval stage (Table 3.10). Mosquitoes that did not show CFP transient expression (I, J) did not produce transgenic progeny (Table 3.10). F_1 transgenic females from cage G were crossed with G3s and 7 isofemale lines set up (G 1-7) to determine the percentage of transgenics obtained in the F_2. All lines yielded 100% inheritance of the eye-marker, suggesting a large number of insertions of the transposon or another unusual transformation event had occurred in one or multiple founders. Therefore, these lines were not molecularly characterised for integration site.

Overall, we report a minimum transformation efficiency, i.e. % of F_0 survivors producing fluorescent offspring, of 5.5%.

Table 3.10 Selection strategy to isolate stable transgenic GAL4 lines carrying a single insertion of the PGI promoter.

F_0 pool	**F_0 adults No. and sex**	**Transient CFP expression**	**No. +F_1 (sex)**	**% +F_2 larvae (No. +larvae/total)**
G	4 F	+	17 (8 F, 9 M)	G1 – 100% (74/74) G2 – 100% (10/10) G3 – 100% (183/183) G4 – 100% (85/85) G5 – 100% (144/144) G6 – 100% (2/2) G7 – 100% (59/59)
H	4 M	+	0	N/A
I	4 F	–	0	N/A
J	6 M	–	0	N/A

F: female, M: male. N/A: not applicable

Despite the likely presence of multiple integrated copies, the ability of the PGI promoter to drive expression was tested by crossing individuals of the G5 line with UAS-mCherry mosquitoes. No mCherry signal was detected in the progeny of this cross at any life stage.

The G5 line was outcrossed with wild types for two generations attempting to reduce the number of integrated copies, but 100% fluorescent progeny was recovered each time and colony eventually discarded.

3.5.4.3 VATG_GAL4 driver lines for Malpighian tubule-specific expression

Owing to their predicted tissue specific activity, Malpighian-specific putative promoters were not tested by transfection in the haemocyte-like mosquito cell cultures available. Instead, we used RMCE to integrate the VATG_GAL4 cassette site-specifically and created a driver line to test the ability of the 5' sequence upstream of V-type ATPase subunit G gene (AGAP001823) to drive Malpighian tubule-specific expression in transgenic mosquitoes.

349 eggs of the A11 docking line were injected with VATG_GAL4 (Figure 3.6A), 86 larvae (25%) hatched of which 39 (45%) showed transient expression of the DsRed marker in the anal papillae. 57 (66%) F_0 adults emerged, 31 females and 26 males, which were separated into 6 sex-specific cages (A-F) and backcrossed with G3 individuals (Table 3.11). Transgenic F_1 progeny was recovered from founder cage F only, which produced 68 DsRed-positive (cassette exchange events) and 8 DsRed/CFP-positive (integration events) larvae. Isofemale lines were set up from 6 randomly-chosen cassette-exchange females, 5 of which displayed orientation A (F_A-F_E) and 1 (F_F) orientation B (Table 3.11). The F_A line was kept for *in vivo* analysis while other lines were discarded. The minimum transformation efficiency achieved was 3.5% (2 events/57 F_0).

To test the ability of the VATG promoter to drive expression, individuals of the F_A line were crossed with UAS-mCherry mosquitoes. Progeny of this cross did not display mCherry signal in the Malpighian tubules or in any other tissue in any life stage.

Table 3.11 Selection strategy to isolate a stable transgenic GAL4 lines carrying the VATG_GAL4 cassette

F_0 pool	**F_0 adults No. and sex**	**Transient DsRed expression**	**No. +F_1 adults (sex)**	**F_2 isofemale lines**
A	7 M	–	0	N/A
B	15 F	–	0	N/A
C	6 M	–	0	N/A
D	4 F	–	0	N/A
E	13 M	+	0	N/A
F	12 F	+	60 (27 F, 33 M)	F_A – orientation A F_B – orientation A F_C – orientation A F_D – orientation A F_E – orientation A F_F – orientation B

F: female, M: male. N/A: not applicable

3.6 DISCUSSION

3.6.1 Candidate promoter selection for *in vivo* analysis

The availability of publicly accessible gene expression catalogues, such as the MozAtlas database (Baker et al., 2011), should facilitate promoter search allowing for direct comparison of relative gene expression in a diverse range of mosquito tissues. Further transcriptome studies, particularly with RNAseq technology will also improve the depth of coverage available (Padrón et al., 2014; Matthews et al., 2016).

In this study one in eight of the putative ubiquitous regulatory regions selected *in silico*, PGI, showed statistically significant promoter activity in cell transfections compared to controls. This may be explained by the lack of critical regulatory elements that may be located further upstream of the region cloned in some cases. However, it is clear that the analysis was not done in sufficient depth to obtain rigorous statistical power. Further biological and technical repeats would be required to provide more confidence in the relative activity of the different promoters in this haemocyte-like cell line.

Although promoter activity in a single mosquito cell line does not provide much information on the *in vivo* specificity or on the location of expression in transgenic organisms, cell screening was a preliminary tool to check plasmid constructs before embarking in transgenic experiments. One could hypothesise that a truly ubiquitous promoter would have activity in all cell lineages.

In interpreting relative driver strength, is of note that the activity observed in the SUA5.1 cell line may be haemocyte-specific and gives no indication on the extension or strength of expression in transgenic individuals. For example, the *An. gambiae* LRIM promoter is active in this cell line (Lynd & Lycett, 2011; Lombardo et al., 2013) but its activity in transgenic mosquitoes is confined to the haemocytes (Volohonsky et al., 2017).

The other promoter active in SUA5.1 cells was PUBc, which was chosen via comparative analysis with *Ae. aegypti* and was not identified by MozAtlas search. Of note is that the PUBc regulatory region used included the 3' sequence downstream of the gene instead of the SV40 terminator present in all the other plasmids. This may have had a role in enhancing the intrinsic characteristic of the promoter.

Malpighian tubule-specific candidate promoters were excluded from analysis by cell transfection due to their predicted tissue specificity. To screen the selected

candidates, it was initially intended to perform transient expression experiments by injecting putative Malpighian drivers into the embryos of a UAS-YFP line (Lynd & Lycett, 2012) and screening for larval Malpighian-specific fluorescence. However, due to time limits, a single promoter was selected for direct transgenic analysis based on previous experiments conducted in our laboratory that had shown transient activity driven by an alternative version of this promoter in larvae derived from UAS-YFP injected embryos (Lynd et al., unpublished).

The other cloned candidate promoters could be examined by transgenic analysis, however the search for Malpighian-specific candidates would benefited from cross analysis with the more recent MozTubules database (Overend et al., 2015) (www.moztubules.org/search2016.cgi), which contains data on the *An. gambiae* Malpighian tubule transcriptome in males and females at different life stages and diet conditions. Furthermore, screening for common Malpighian tubule transcription factor binding domains would narrow our analysis to fewer specific candidates sharing common features in their upstream regions.

The MozAtlas database was built using microarray data obtained with a variable number of probes per gene with some non-consistent results identified amongst probes used to quantify expression of the same gene. In this respect, more stringent criteria and search parameters should have been used to perform the selection including gene IDs showing consistent results across multiple probes and excluding those with high variability amongst probes.

Overall, with the availability of the sequences of all major species of mosquito vectors, genome-wide *in silico* comparative approaches can be used to identify *cis*-regulatory elements (CREs) and transcription factor binding sites within them (Sieglaff et al., 2009). Recently, a methodology for high-throughput discovery of CREs based on the sequencing of nucleosome-free strands of chromatin (FAIRE – formaldehyde-assisted isolation of regulatory elements) was proven useful to identify CREs in *Ae. aegypti* (Behura et al., 2016) and may be used to support CRE identification in *An. gambiae*.

3.6.2 Embryo microinjections

Microinjection of *An. gambiae* embryos is a challenging technique that requires practice.

In initial experiments, very low hatching rates were recorded (Appendix C, Tables C.3 and C.4). Factors affecting post-injection egg survival include: purity, concentration and toxicity of injected DNA solution, quality of eggs and pre-injection handling, and needle-induced mechanical damage. Also, the size and number of plasmids injected negatively affect the transformation efficiency with single small plasmids transforming more successfully than multiple larger ones (Venken et al., 2006; Volohonsky et al., 2015).

To investigate the cause of high post-injection mortality, controls were introduced including un-injected egg lines to monitor egg quality and pre-injection handling procedures, and injections with buffer to control for DNA toxicity. In doing so, high hatching rates in un-injected controls and high mortality were observed when injecting buffer only, suggesting that neither the quality of eggs nor the toxicity of the DNA injected was the cause of low post-injection survival.

In order to exclude technical issues other than the practical challenge of performing microinjections, all buffers and solutions were freshly prepared which, along with technical skills improved by practice, determined an increase in survival. Despite that, low transient expression rates and no transformants were obtained (Appendix C, Tables C.3 and C.4). For inheritable transgenesis, injections must precisely target the egg posterior pole so to modify the germ cells (Lobo et al., 2006). Therefore, while transient expression of the fluorescent marker gives an indication of DNA uptake, it does not assure stable transformation which is successful in a small proportion of individuals.

The concentration of the DNA injected plays a crucial role in transformation experiments. In general, concentration affects the viscosity of a solution decreasing the ease of injection and thus increasing the likelihood of egg damage (Lobo et al., 2006), but it also increases the amount of DNA delivered into the embryo and, in turn, the likelihood of transformation. Therefore, while in intermediate experiments the concentration of the solution injected was decreased to 250-300 ng/µl to aid survival, in latter experiments it was increased to 500 ng/µl, which is the recommended concentration (Lombardo et al., 2009). Accordingly, in these last experiments survival declined but higher transient expression rates were obtained and transgenic individuals recovered.

Overall, the combination of improved technical skills, which were practised over a seven-month period, freshly prepared buffers, and the increased concentration of DNA injected combined to achieve higher hatching rates and successful germline

transformation. In these experiments, hatching rates of 14.5% (PGI) and 40% (PUBc) were achieved which are comparable or higher compared to survival rates reported in *An. gambiae* elsewhere for piggyBac 11-23% (Grossman et al., 2001; Kim et al., 2004; Lombardo et al., 2009; Meredith et al., 2013). Minimum transformation efficiencies were 4% (PGI) and 5.5% (PUBc), which are similar to the most efficient rates reported elsewhere using piggyBac (0.6-5%) (Grossman et al., 2001; Kim et al., 2004; Lobo et al., 2006; Lombardo et al., 2009; Lycett et al., 2012; Meredith et al., 2013).

Interestingly, transgenic progeny was yielded only from F_0 mosquitoes showing transient episomal expression of the transformation marker in the anal papillae at early larval stage. This has been previously reported by Pondeville et al., (2014) indicating that, when high survival rates are achieved, screening workload could be reduced by breeding only from subsets of F_0 mosquitoes that show marker gene fluorescence.

3.6.3 Strategy for phenotypical and molecular assessment of driver docking lines for ubiquitous expression

PiggyBac-mediated integration occurs in an essentially random manner in TTAA genomic sites and can therefore lead to the insertion of multiple copies of the transgenic cassette. The selection strategy used here aimed at maximising the identification of single reusable intergenic genomic sites, desirable for docking lines, and looking for variation in expression profiles, whilst also maintaining a manageable workload. To do so, of all the lines carrying the PUBc cassette, we molecularly and phenotypically characterised those derived from F_1 transgenic females only as they are easier to breed from. F_1 males were crossed in pools to UAS-mCherry to assess phenotypes generated as a backup in case other interesting phenotypes (and thus likely to be alternative insertions) were observed solely through the male lines. Lines derived from males were eventually discarded as corresponding mCherry phenotypes were recovered in female lines too.

Phenotypic assessment by crossing all drivers carrying single insertions with the mCherry responder line revealed a variety of phenotypes that reflected positional effect both in terms of intensity and localisation of expression of the mCherry signal. Although differences in the expression of the 3xP3-CFP marker were detected in different lines, these were minor and did not correlate with the variegation observed in the mCherry signal. This may suggest that genomic sites from which good levels of

neuronal expression are obtained are not all capable to sustain ubiquitous expression. This is supported by findings in *Ae. aegypti*, where 3xP3 was an unreliable marker for inferring efficiency of transgene expression at specific genomic locations (Franz et al., 2011).

The variety of position variegation in the expression of mCherry also suggests that the presence of gypsy insulators flanking the GAL4 cassette was not effective in mitigating the influence of nearby effectors and/or chromatin status on transgene expression. Gypsy insulators (Roseman et al., 1993) have been previously reported to determine an increase of gene expression by repressing the action of nearby suppressors when flanking a 3xP3-eye marker cassette in *D. melanogaster* and *An. stephensi* (Sarkar et al., 2006; Carballar-Lejarazú et al., 2013). Yet, no quantitative study has been conducted in *Anopheles spp*. using the GAL4/UAS system. When insulating a UAS-Luciferase cassette in *D. melanogaster*, gypsy insulators were proven useful to equalise expression in various attP landing sites, with efficiency of insulation depending on genomic locus (Markstein et al., 2008). In *An. gambiae*, when gypsy sequences flanked a UAS-Luciferase cassette, the carboxypeptidase-GAL4 cassette drove midgut-specific expression in all transgenic lines generated using piggyBac regardless of position of insertion (Lynd & Lycett 2012). Nevertheless, consistent tissue-specific detection across lines may also be attributed to the GAL4-induced signal amplification which may lead to saturation. Indeed, when the *Ae. aegypti* carboxypeptidase promoter was inserted in a non-insulated GFP-fusion reporter cassette, tissue-specific expression was detected only in 2/9 lines (Franz et al., 2011). In addition, there may be differences in the insulation capacity of the gypsy sequences when flanking UAS compared to GAL4 constructs.

3.6.4 Polyubiquitin-c (PUBc) promoter

Here, we isolated and characterised for the first time the regulatory regions of the *An. gambiae* PUBc gene (AGAP001971) and demonstrated their ability to drive widespread multi-tissue expression *in vivo*.

As described previously, regulatory regions of polyubiquitin genes were identified in *D. melanogaster* (Handler & Harrell, 1999) and *Ae. aegypti* (Anderson et al., 2010) and their ability to drive ubiquitous expression reported in several dipteran species including mosquitoes (Handler & Harrell, 2001; Heinrich et al., 2002; Perera et al., 2002; Anderson et al., 2010). In *An. gambiae* three PUB genes (AGAP001969, AGAP001970, and AGAP001971) cluster in chromosome 2R:12 and share the same

structure consisting of two exons, one of which is non-coding. Transcriptome studies indicate that *An. gambiae* PUBc (3368 bp) is strongly expressed in larvae, pupae and adults (Marinotti et al., 2006) and it shares 100% protein identity with the *Ae. aegypti* PUB gene AAEL003877, the promoter of which was shown to drive multi-tissue expression in transgenic *Ae. aegypti* (Anderson et al., 2010).

In this study, *An. gambiae* PUBc was demonstrated to drive luciferase expression via the GAL4 transactivator in haemocyte-like cells, in which it showed the highest activity compared to other 7 candidate promoters examined. Furthermore, visual assessment of progeny derived from selected PUBc driver lines (A10 and A8) crosses with UAS-mCherry individuals, revealed that the regulatory regions identified for PUBc are active in a variety of tissues and organs in all mosquito life stages examined and presumably in embryonic stages too, as neonate larvae are intensely fluorescent. In adults, these tissues include: eyes, brain, and ventral nerve cord; muscles of the aorta and heart; trachea, nerves and muscles surrounding the digestive tract and the Malpighian tubules; salivary glands; sugar-fed and blood-fed ovaries and developing oocytes; fat body; appendages (legs, palps, antennae, proboscis); and haemocytes. Tissues where expression was not readily detectable include the epithelium of the digestive tract and Malpighian tubules. We cannot exclude that expression occurs in these tissues at a level that is not detectable by fluorescence. It is also possible that the expression of mCherry as a membrane protein is not as efficient in these tissues as it is in others, although progeny from the cross with the midgut-specific driver line show observable gut epithelium fluorescence (not shown).

The expression pattern reported here largely overlaps those described for promoter fragments derived from other insect PUB genes (Handler & Harrell, 2001; Heinrich et al., 2002; Perera et al., 2002) and, more specifically, with that of the *Ae. aegypti* PUB promoter (Anderson et al., 2010). In *Ae. aegypti* a combination of fluorescence and transcription data was used to show that PUB-driven expression was robust and widespread throughout the mosquito body from larvae to adults (Anderson et al., 2010). Two major differences were noted between expression pattern described in *Ae. aegypti*. We found that the A10 line drives strong fluorescence in the salivary glands, while in *Ae. aegypti* these tissues displayed little fluorescence and lacked mRNA signal. Conversely, strong fluorescence was seen in *Ae. aegypti* midguts, whilst it was observed only in the trachea and nerves surrounding the gut but not the midgut epithelium in *An. gambiae*. These differences may be due to innate variation in promoter activity from the region selected in the two species or they may be the result of positional effect.

To date, the profile described here represents the most widespread expression driven by an endogenous promoter in *An. gambiae.* Of note, however, is that expression also appears very low or absent in the Malpighian tubules.

3.6.5 Phosphoglucose isomerase (PGI) promoter

The *An. gambiae* PGI promoter was the most active in cells after PUBc. Yet, when corresponding driver lines were created, no activity was detected in transgenic mosquitoes after crossing with the UAS-mCherry line.

All the isofemale lines obtained for this cassette when outcrossed to wild type showed 100% inheritance of the transformation marker suggesting the presence of multiple integrated copies. Although the molecular basis of this finding was not explored to discover how many transposon copies were integrated or their genomic locations, it can be argued that the likely presence of multiple copies is involved in the lack of functionality of the driver construct and, in turn, the absence of the UAS-driven mCherry signal.

It is of note that low transformation efficiency was achieved for this construct with transgenic progeny likely to have originated from a single founder individual, which may suggest toxicity. If multiple cassette integration is lethal, then the transgenic individuals isolated represent an exception in which the expression of the GAL4 was silenced while that of the fluorescent marker remained functional allowing the identification of transegnics. The presence of high copy number can trigger transposon silencing mechanisms put in place as a defensive mechanism by the host genome. In *Drosophila*, these silencing mechanisms are usually based on small RNAs interfering with the expression of mobile genetic elements via DNA methylation or degradation of their transcripts (Rozhkov et al., 2010). It is possible that such silencing involved only a portion of the cassette, leaving the fluorescent marker unaffected.

In a different scenario, it is possible that the high number of copies was caused by the integration of the transposase gene, supplied via the helper plasmid at the time of injection, as well as the transposon resulting in persistent repositioning of the PGI cassette as a self-driving element. This would be supported by the observation that multiple successive outcrosses failed to reduce the percentage of fluorescent progeny.

3.6.6 VATG promoter for Malpighian tubule-specific expression

VATG genes code for the subunit G of the vacuolar-type H^+-transporting ATPase (V-ATPase). Insect V-ATPases are large proton pumps found in epithelia (Dow et al., 1997) where they energise transport across membranes (Pullikuth et al., 2003). These enzymes are found enriched in the highly active epithelium of the Malpighian tubules of *D. melanogaster* (Wang et al., 2004) and *An. gambiae* (Overend et al., 2015) as demonstrated by tissue-specific microarray-based transcriptome analysis. Nevertheless, despite the past evidence of transient expression, the promoter analysis conducted here using a stable VATG_GAL4 driver line showed no expression in the Malpighian tubules or elsewhere. The promoter sequence used here was ~700 bp shorter than that used in past transient experiments, thus it possibly lacked crucial regulatory elements. Another explanation may be linked to the fact that V-ATPases consist of at least 13 subunits, which in *D. melanogaster* are encoded by 31 genes (Dow et al., 1999); the expression of each subunit might be subjected to tight stoichiometric regulation by *cis*-acting elements working in concert and located elsewhere in the genome.

3.6.7 Conclusions

This work greatly contributes to the expansion of the toolkit for *An. gambiae* transgenesis and *in vivo* functional analysis through the characterisation of a ubiquitous endogenous promoter and two driver docking lines.

We found that PUBc_GAL4 drives robust luciferase expression in SUA5.1 cells and widespread multi-tissue expression in all life stages in transgenic mosquitoes. This widespread expression pattern is unprecedented for an *An. gambiae* driver line carrying an endogenous promoter. As part of the promoter analysis, we characterised two novel driver lines, A10 and A8, bearing a single copy of the PUBc_GAL4 cassette in genomic locations that sustain widespread gene expression at high or low levels respectively and are designed for PhiC31-RMCE. Since these genomic sites allow for robust widespread expression, they are likely to be suitable locations for the expression of other transgenic cassettes.

Future work should include demonstrating docking with these lines and performing an assessment of fitness cost inflicted by GAL4 expression in homozygous individuals compared with other transgenes inserted in these sites.

For the purpose of this thesis, the ability to express transgenes in a whole-body manner enabled the examination of resistance phenotypes generated by the ubiquitous overexpression of the CYP6 P450s, which is the aim of the following chapter.

Chapter 4

Characterisation of resistance phenotypes resulting from multi-tissue overexpression of *Cyp6m2* or *Cyp6p3*

4.1 ABSTRACT

Characterisation of genes and their physiological patterns of overexpression that confer insecticide resistance is crucial for effective vector control. As previously demonstrated, the overexpression of *An. gambiae* candidate genes *Cyp6m2* and *Cyp6p3* confined in the midgut or in the oenocytes is not sufficient to induce resistance, therefore here we investigated whether more widespread expression can drive resistance, exploiting the newly-established driver lines. To do so, crosses were performed to generate mosquitoes overexpressing *Cyp6m2* and *Cyp6p3* under the control of the ubiquitous *An. gambiae* polyubiquitin promoter. Our results show that, under these conditions, *Cyp6m2* confers resistance to WHO-defined diagnostic doses of the pyrethroids permethrin and deltamethrin, whilst *Cyp6p3* also confers diagnostic resistance to bendiocarb. Resistance to DDT was not conferred by overexpressing either gene. Additionally, increased susceptibility to malathion was recorded when either *Cyp6m2* or *Cyp6p3* were overexpressed. The study provides the first evidence of the ability of *Cyp6m2* and *Cyp6p3* overexpression and resulting insecticide metabolism to drive WHO-levels of insecticide resistance to a diverse range of insecticides.

4.2 INTRODUCTION

The physiological spatio-temporal pattern of P450 overexpression has crucial implications in insecticide management, yet it has been somewhat neglected. Results presented as part of this thesis showed that the midgut and oenocytes do not play a crucial role in driving resistance when *Cyp6m2* and *Cyp6p3* are overexpressed. Therefore, two driver lines for multi-tissue overexpression were established that exploit the ubiquitous properties of the *An. gambiae* polyubiquitin promoter and express at two different levels, higher (A10) and lower (A8) (Chapter 3). These lines allow for testing the effects of widespread expression of *Cyp6m2* and *Cyp6p3* on insecticide resistance.

To date, the involvement of *Anopheles* resistance genes (*Cyp6p9a/b* (Riveron et al., 2013), *Cyp6m7* (Riveron et al., 2014a) and *Cyp9j11* (Riveron et al., 2017) from *An. funestus*, and *Cyp6m2*, *Cyp6p3* (Edi et al., 2014) and *Gste2* (Daborn et al., 2012; Mitchell et al., 2014) from *An. gambiae*) in determining resistance *in vivo* has been only investigated in transgenic *D. melanogaster.* This was achieved using either the ubiquitous promoters Actin5 and TubulinP or the 6g1HR promoter which expresses in midgut, Malpighian tubules and fat body. In these studies, methods to determine resistance varied from assessing mortality after 24h exposure to a range of insecticide doses (Daborn et al., 2012; Edi et al., 2014) to measuring mortality at different time points during the 24 h exposure to a single insecticide dose chosen after dose-response curve analysis (Riveron et al., 2013, 2014a/b). These methodologies and the insecticide concentrations used in *D. melanogaster* are not equivalent to the standard procedures used for testing mosquitoes, such as the WHO tube bioassay or the CDC bottle assay, therefore results are not directly comparable to those obtained in mosquitoes and thus not operationally relevant.

P450-mediated metabolism of pyrethroids and carbamates derives from the oxidation of these insecticides into non-neurotoxic metabolites that are then cleared from the system (Guengerich, 2001). In contrast, metabolites resulting from the oxidation of organophosphate insecticides, such as the malathion metabolite malaoxon, are more toxic than their precursors (Cohen, 1984; Berkman et al., 1993). Therefore, overexpression of specific P450s may be expected to increase susceptibility to organophosphate pro-insecticides, making them suitable to specifically target mosquitoes that are resistant to pyrethroids through enhanced expression of the same P450. As such, organophosphate-based synergistic formulations are promising tools for vector control and synergistic combinations of pyrethroids and

organophosphates have been successfully used for controlling agricultural pests (Martin et al., 2003).

4.3 AIMS AND OBJECTIVES

The aim of the work described in this chapter was to investigate the ability of single *Cyp6* genes to drive resistance when overexpressed in multiple tissues. To do so, the GAL4/UAS system was employed to induce overexpression of candidate genes *Cyp6m2* and *Cyp6p3* ubiquitously in susceptible *An. gambiae* mosquitoes and the resulting phenotype was tested for acquired resistance by WHO tube bioassay.

The study's objectives were:

- To drive overexpression of *Cyp6* candidates by crossing UASm2 and UASp3 responder lines to GAL4 driver lines A10 and A8, which carry a PUBc_GAL4 construct in single, unique genomic locations;
- To validate gene and protein overexpression in progeny of these crosses;
- To characterise resistance to the insecticides permethrin, deltamethrin, DDT and bendiocarb using the WHO tube bioassay;
- To characterise susceptibility to the pro-insecticide malathion resulting from the overexpression of *Cyp6m2* and *Cyp6p3* in the midgut, oenocytes or ubiquitously.

4.4 MATERIALS AND METHODS

4.4.1 Mosquito lines and GAL4 x UAS crosses

Details of mosquito maintenance are reported in Appendix A. Mosquito lines used in this study were:

- **A10** and **A8**: driver lines for ubiquitous expression carrying the PUBc_GAL4 at single unique integration sites. Lines consist of a mixture of heterozygous and homozygous individuals and are marked with 3xP3-driven CFP. Details on the creation of these lines are described in Chapter 3.
- **UASm2** and **UASp3**: responder lines for the UAS-regulated expression of *Cyp6m2* and *Cyp6p3*. Lines consist of a mixture of heterozygous and homozygous individuals and are marked with 3xP3-driven YFP. The creation of these lines is described in Chapter 2.

- **GAL4mid** and **GAL4oeno**: driver lines for expression in the midgut and in the oenocytes respectively. Lines are homozygous and are marked with 3xP3-driven DsRed. Details on these lines are reported in Chapter 2.

To obtain ubiquitous expression crosses were established between CFP-marked A10 and A8 drivers and opposite sex individuals of the UASm2 and UASp3 responder lines marked with YFP. A total of 4 crosses was established: A10 x UASm2, A10 x UASp3, A8 x UASm2 and A8 x UASp3. For tissue-specific expression crosses were established between DsRed-marked driver lines GAL4mid and GAL4oeno and YFP-marked responder lines UASm2 and UASp3.

Progeny was sorted at pupa stage based on eye marker colour using a Leica MZ FLIII fluorescence stereo microscope fitted with CFP, DsRed and YFP filters (Leica Microsystems). CFP/YFP-positive and CFP-positive individuals were isolated for the ubiquitous crosses, and DsRed/YFP-positive and DsRed-positive for tissue-specific crosses.

4.4.2 Assessment of *Cyp6* gene expression in GAL4/UAS *vs* GAL4/+

To quantify *Cyp6* gene expression in GAL4/UAS and GAL4/+ individuals, total RNA was harvested from pools of 2-5-day-old adult females. RNA extraction, DNase treatment, cDNA synthesis, RT-qPCR were performed as described in Chapter 2. Three biological replicates consisting of 5 adult mosquitoes each were collected from each mosquito population.

Data analysis was performed as described in Chapter 2 with the exception that, to compare *Cyp6* expression driven by A10 and A8, mean ΔCt values were obtained by pooling data from A10/+ and A8/+ mosquitoes. Statistical differences between expression (ΔΔCt values) in GAL4/UAS *vs* GAL4/+ were determined using Welch's t-test (two-tails, unequal variance). File names reporting raw data are reported in Appendix D.

4.4.3 Assessment of CYP6 protein expression in GAL4/UAS *vs* GAL4/+

To detect CYP6 protein expression in GAL4/UAS and GAL4/+ individuals, total protein extracts were obtained from single 2-5-day-old adult females. Extracts were prepared in a total volume of 60 µL (30 µl PBS supplemented with EDTA-free protease inhibitor

cocktail (Roche) and 30 µl 2x Laemmli Sample Buffer (Bio-Rad) supplemented with 2.5% 2-Mercaptoethanol as described in Chapter 2.

SDS-PAGE and Western blot were conducted as described in Chapter 2, except in this case, because of interference between the similarly sized abundant CYP6M2 and α-tubulin proteins, two gels were run simultaneously, one for detection of CYP6M2 and one for assessing α-tubulin. 6 µL of each extract (equivalent of 1/10 of a single female mosquito) were loaded onto each gel. Detection of the CYP6M2 signal was performed using 1:500 anti-CYP6M2 or anti-CYP6P3 peptide antibodies produced in rabbit (gifts from M. Paine) and 1:10,000 anti-rabbit-HRP IgG antibodies (Bethyl Laboratories); while detection of the α-tubulin control was carried out using 1:2,000 anti-αtubulin (Sigma) and 1: 20,000 anti-mouse-HRP IgG antibodies (Abcam).

4.4.4 Assessment of mosquito susceptibility to insecticides by WHO bioassay

Mosquito susceptibility to insecticides was assessed using the WHO tube bioassay (WHO, 2016b) as described in Chapter 2. 2-5 day-old females were exposed to 0.75% permethrin, 0.05% deltamethrin, 0.1% bendiocarb, 4% DDT, for 1 h. A modified version of the WHO bioassay was performed for testing 5% malathion by reducing the exposure time to 25 minutes.

1-3 experiments (biological replicates) were performed for each insecticide tested. 4-6 technical replicate tubes were tested for each population. Number of bioassay experiments conducted are reported in Table 4.1. Following WHO guidelines, that mitigate against variability in quality control of insecticide papers, only assays showing 95-100% mortality in the sensitive control population (GAL4/+) were included in the results. File names with raw data and analysis is reported in Appendix D.

Table 4.1 Bioassay experiments performed.

Cross	Insecticide	Experiments (biol reps)	Tot tech reps
A10 x UASm2	Permethrin 0.75%	2 (3)	5 (7)
	Deltamethrin 0.05%	2	4
	Bendiocarb 0.1%	1 (2)	4 (5)
	DDT 4%	1 (2)	4 (5)
	Malathion 5%	2	4
A10 x UASp3	Permethrin 0.75%	3 (5)	5 (9)
	Deltamethrin 0.05%	1	4
	Bendiocarb 0.1%	2	6
	DDT 4%	2 (4)	6 (9)
	Malathion 5%	2	4
A8 x UASm2	Permethrin 0.75%	2 (3)	5 (7)
	Deltamethrin 0.05%	2	4
	Bendiocarb 0.1%	3	4
	DDT 4%	2	4
	Malathion 5%	2	5
A8 x UASp3	Permethrin 0.75%	3 (5)	5 (9)
	Deltamethrin 0.05%	2	4
	Bendiocarb 0.1%	2 (4)	4 (8)
	DDT 4%	3	6
	Malathion 5%	3	4
GAL4mid x UASm2	Malathion 5%	2	4
GAL4mid x UASp3	Malathion 5%	3	5
GAL4oeno x UASm2	Malathion 5%	3	6
GAL4oeno x UASp3	Malathion 5%	3	5

Numbers represent the experiments and replicates that were included in the analysis as mortality in the controls reached at least 95%, while those in brackets show the total number of experiments and replicates performed.

4.5 RESULTS

4.5.1 *Cyp6* transcription levels obtained by the A10 and A8 drivers

RT-qPCR analysis in the progeny of A10 crosses revealed that *Cyp6m2* was 2447x overexpressed in A10/m2 compared to native expression in adult female A10/+ controls ($\Delta\Delta Ct = 11.2$, $p = 0.0007$) (Figure 4.1A). *Cyp6p3* was also found significantly overexpressed (513x), in A10/p3 ($\Delta\Delta Ct = 8.99$, $p = 0.0002$), yet to a lesser extent (Figure 4.1B).

The relative *Cyp6* transcription levels in progeny of the A8 crosses were significantly lower than the respective A10 crosses. *Cyp6m2* was 420x overexpressed in A8/m2 compared to native expression in adult females (ΔΔCt = 8.7, p = 0.0004) (Figure 4.1A). Whereas *Cyp6p3* was 73x overexpressed in A8/p3 mosquitoes (ΔΔCt = 6.12, p = 0.002) (Figure 4.1B).

When comparing driver strength, A10 drove 5.5x (p = 0.0038) (Figure 4.1A) and 7.5x (p = 0.0042) (Figure 4.1B) higher transcription compared to the A8 driver when quantifying *Cyp6m2* and *Cyp6p3* respectively.

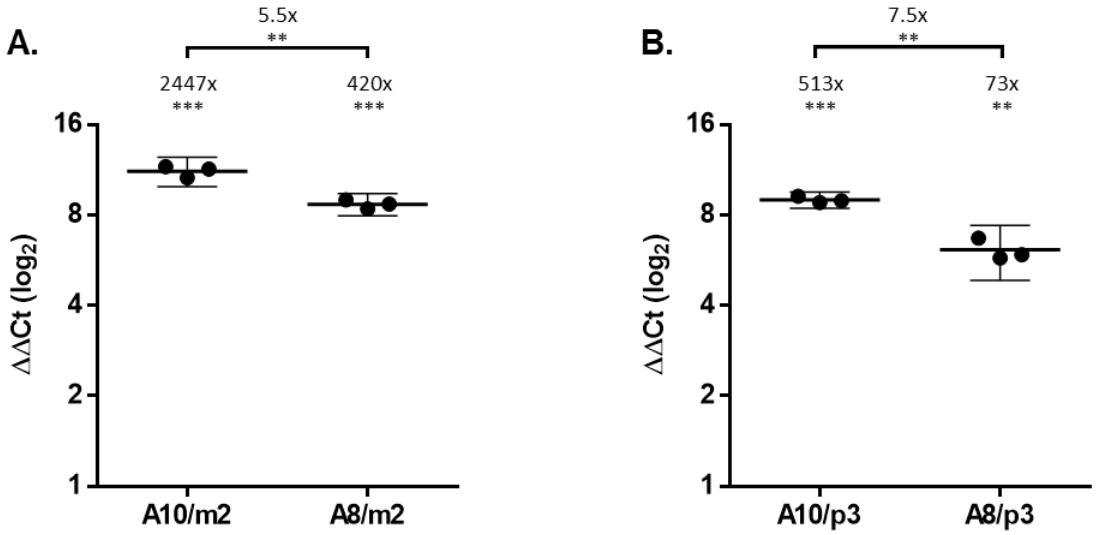

Figure 4.1 Quantification of *Cyp6* gene expression driven by A10 and A8. Expression in GAL4/UAS mosquitoes compared to GAL4/+ controls is reported as ΔΔCt ($\Delta Ct_{GAL4/+} - \Delta Ct_{GAL4/UAS}$) on a log_2 scale. **A)** Transcription of *Cyp6m2* in adult females of the A10 x UASm2 and A8 x UASm2 crosses. **B)** Transcription of *Cyp6p3* in adult females of the A10 x UASp3 and A8 x UASp3 crosses. Mean values with 95% confidence intervals are shown. Numbers on the top represent the fold change (x) expression. Statistical differences between ΔΔCt values from three biological replicates were calculated using Welch's test. * $p < 0.05$, ** $p \leq 0.01$, *** $p \leq 0.001$, **** $p \leq 0.0001$. File names reporting raw data are in Appendix D.

4.5.2 CYP6 protein expression driven by the A10 and A8 lines

Western blot was carried out to monitor CYP6M2 expression in protein extracts from adult female mosquitoes overexpressing *Cyp6m2* under the control of the A10 and A8 drivers and respective GAL4/+ and +/ UASm2 individuals.

A single clear band of the correct size (~58 kDa) for CYP6M2 was detected in extracts from A10/m2 and A8/m2 mosquitoes, but not in GAL4/+ or +/UASm2 controls (Figure 4.2), providing clear evidence for overexpression of CYP6M2 in the A10/m2 and

A8/m2 mosquitoes. The signal from CYP6M2 appeared more abundant in A10/m2 compared to A8/m2 adults (Figure 4.2) when also taking into account the α-tubulin loading controls, which were of similar abundance in all samples (Figure 4.2), suggesting that similar loading of crude protein extracts was achieved.

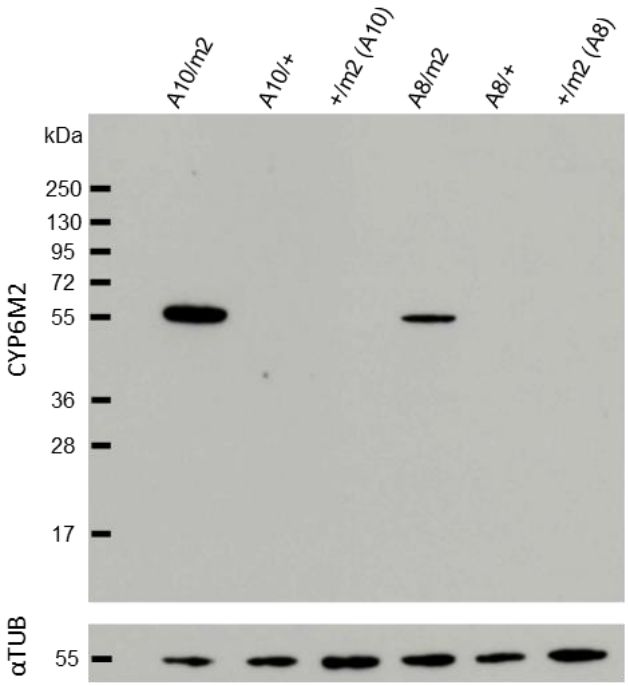

Figure 4.2 Two parallel western blots on 2-5-day-old adult females from the A10 x UASm2 and A8 x UASm2 crosses to determine expression of CYP6M2 (top) and α-tubulin (bottom). Protein extract from the equivalent of 1/10 of a whole mosquito was loaded in each lane. 2-minute exposure.

The CYP6P3 antiserum again failed to detect specific signals in Western analysis (data not shown) of A10xP3 and A8xP3 crosses and controls.

4.5.3 WHO tube bioassays

4.5.3.1 Resistance phenotypes resulting from A10-driven overexpression of Cyp6m2 or Cyp6p3

WHO bioassay analysis revealed that the A10-driven multi-tissue overexpression of *Cyp6m2* or *Cyp6p3* is sufficient to cause WHO-defined resistance to standard doses

of the pyrethroid insecticides permethrin and deltamethrin. Significantly different mortality rates were found between GAL4/UAS and GAL4/+ mosquitoes when tested against 0.75% permethrin (p = 0.0007 for *Cyp6m2*; p = 1.811E-05 for *Cyp6p3*) and 0.05% deltamethrin (p = 0.04 for *Cyp6m2*; p = 0.003 for *Cyp6p3*) (Figure 4.3). The magnitude of reduction in mortality was comparable in *Cyp6m2*- and *Cyp6p3*-overexpressing mosquitoes after exposure to permethrin, while individuals overexpressing *Cyp6p3* showed a greater decrease in mortality when exposed to deltamethrin compared to mosquitoes overexpressing *Cyp6m2* (p = 0.003) (Figure 4.3).

Mosquitoes overexpressing *Cyp6m2* under the control of the A10 driver did not show resistance to 4% DDT or 0.1% bendiocarb as 100% mortality was recorded in both GAL4/UAS and GAL4/+ mosquitoes (Figure 4.3A). Similarly, individuals overexpressing *Cyp6p3* did not show resistance to 4% DDT (Figure 4.3B). Instead, a significant decrease in mortality was recorded in A10/p3 mosquitoes compared to controls after exposure to 0.1% bendiocarb (p = 0.00015) (Figure 4.3B).

4.5.3.2 Resistance phenotypes resulting from A8-driven overexpression of Cyp6m2 or Cyp6p3

WHO bioassay analysis on females overexpressing *Cyp6m2* under the control of the A8 driver revealed that the lower *Cyp6m2* overexpression is sufficient to drive resistance to 0.75% permethrin as a significant difference in mortality was recorded in A8/m2 mosquitoes compared to A8/+ controls (p = 0.027) (Figure 4.4A). No significant differences in mortality rates were recorded in A8/m2 mosquitoes compared to controls after exposure to WHO diagnostic doses of 0.05% deltamethrin, 4% DDT, or 0.1% bendiocarb (Figure 4.4A).

Mosquitoes overexpressing *Cyp6p3* under the control of the A8 driver line showed no significant resistance to all the insecticides tested (Figure 4.4B). Nevertheless, trends of reduced mortality were found in A8/p3 compared to A8/+ after exposure to permethrin and bendiocarb (Figure 4.4B).

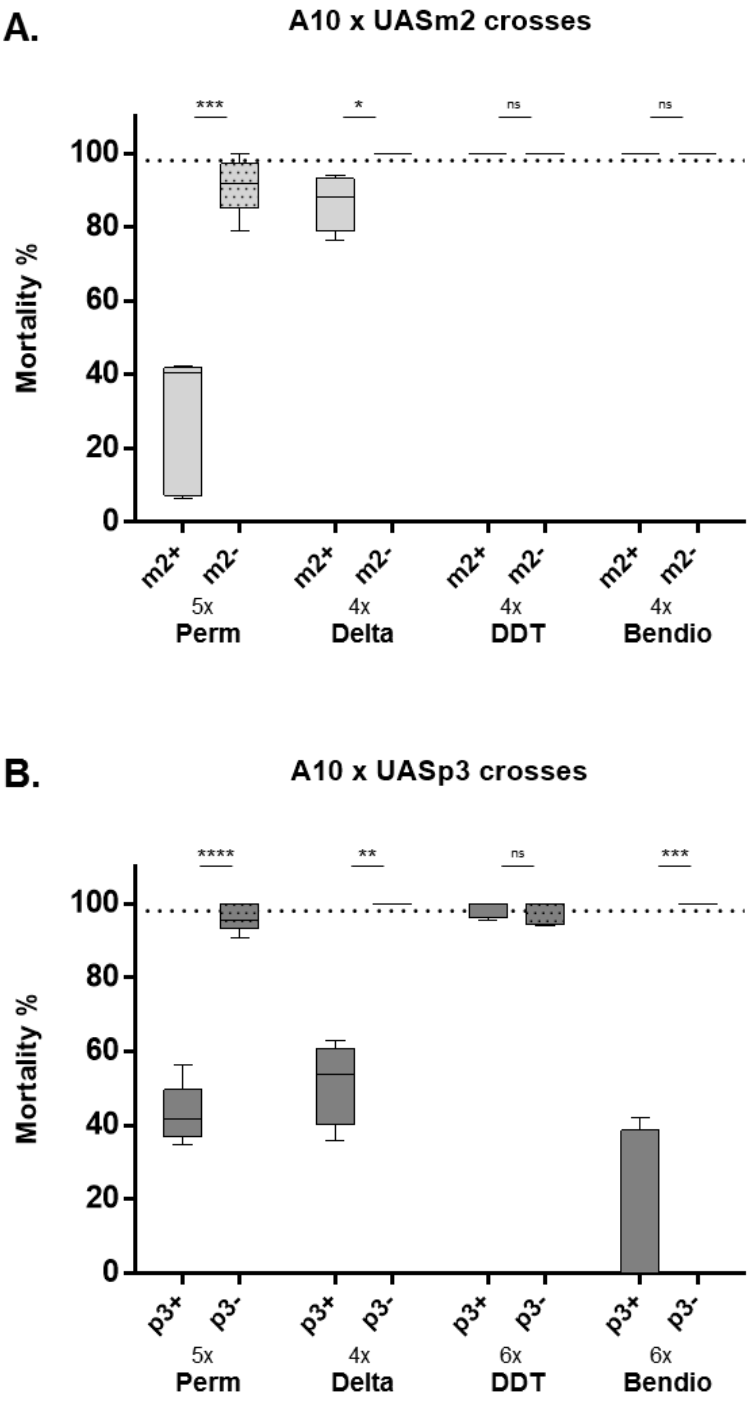

Figure 4.3 Sensitivity to insecticides of 2-5-day-old adult females overexpressing *Cyp6m2* or *Cyp6p3* ubiquitously under the control of the A10 driver. **A)** Sensitivity of the progeny from A10 x UASm2 crosses. **B)** Sensitivity of the progeny from A10 x UASp3 crosses. Mortality rates were obtained by WHO tube bioassay after 1 h exposure to insecticides and 24 h recovery. Dotted line represents 98% mortality which is the threshold for resistance indicated by the WHO. Perm: 0.75% permethrin; Delta: 0.05% deltamethrin; DDT: 4% DDT; Bendio: 0.1% bendiocarb. m2+: A10/UASm2 females; m2-: A10/+ controls from m2 cross; p3+: A10/UASp3 females; p3-: A10/+ controls from p3 cross. Statistical significance was calculated using Welch's test. ns: not significant, * $p < 0.05$, ** $p \leq 0.01$, *** $p \leq 0.001$, **** $p \leq 0.0001$. The bottom and the top of each box represent the first and third quartile respectively, line inside the box is the second quartile (median), and whiskers represent minimum and maximum values. Number of technical replicates (x) for each population is indicated. File names with raw data and analysis is reported in Appendix D.

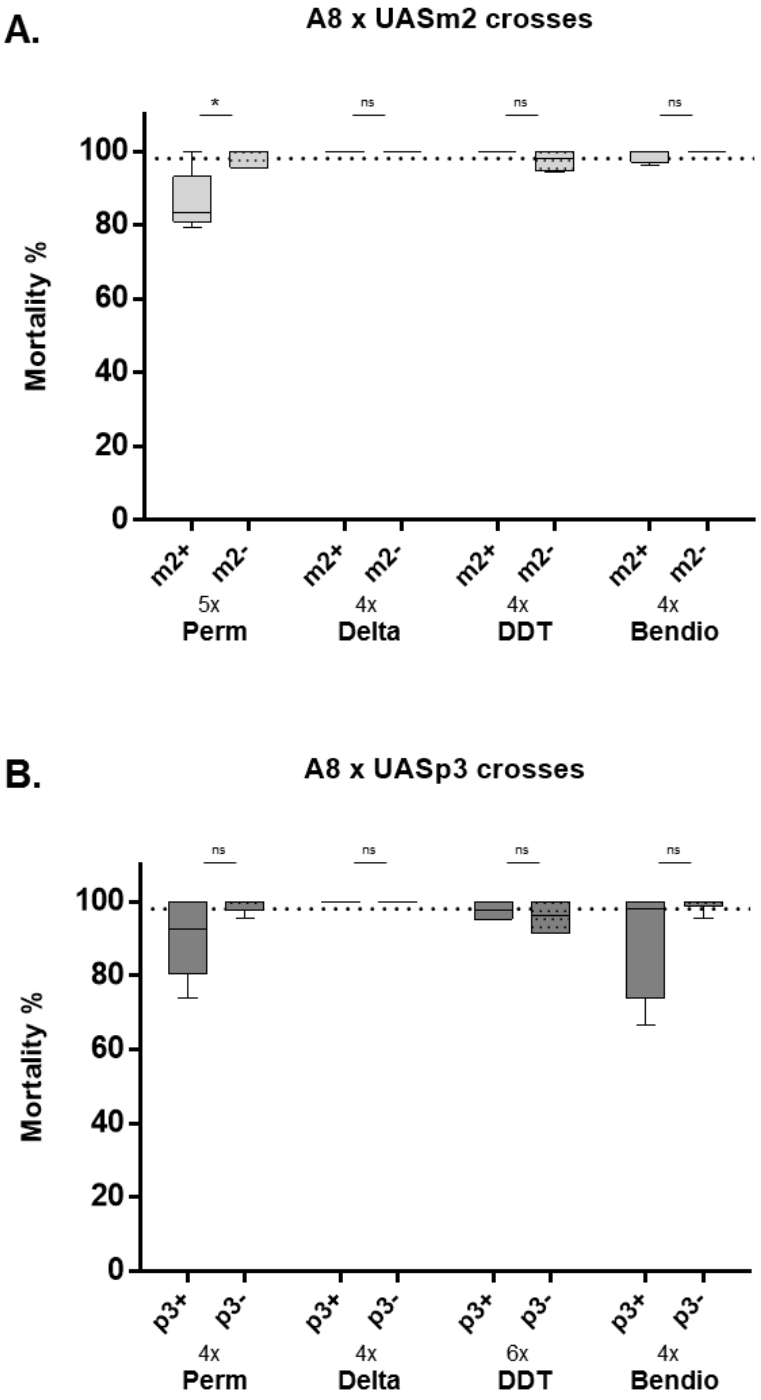

Figure 4.4 Sensitivity to insecticides of 2-5-day-old adult females overexpressing *Cyp6m2* or *Cyp6p3* ubiquitously under the control of the A8 driver. **A)** Sensitivity of the progeny from A8 x UASm2 crosses. **B)** Sensitivity of the progeny from A8 x UASp3 crosses. Mortality rates were obtained by WHO tube bioassay after 1 h exposure to insecticides and 24 h recovery. Dotted line represents 98% mortality which is the threshold for resistance indicated by the WHO. Perm: 0.75% permethrin; Delta: 0.05% deltamethrin; DDT: 4% DDT; Bendio: 0.1% bendiocarb. m2+: A8/UASm2 females; m2-: A8/+ controls from m2 cross; p3+: A8/UASp3 females; p3-: A8/+ controls from p3 cross. Statistical significance was calculated using Welch's test. ns: not significant, * $p < 0.05$. The bottom and the top of each box represent the first and third quartile respectively, line inside the box is the second quartile (median), and whiskers represent minimum and maximum values. Number of technical replicates (x) for each population is indicated. File names with raw data and analysis are reported in Appendix D.

4.5.3.3 Susceptibility to Malathion in mosquitoes overexpressing Cyp6m2 or Cyp6p3 tissue-specifically or ubiquitously

Susceptibility to the pro-insecticide malathion was assessed by a modified WHO bioassay exposing mosquitoes overexpressing *Cyp6m2* or *Cyp6p3* either tissue-specifically (midgut or oenocytes) or ubiquitously (A10 or A8 drivers) for 25 minutes rather than 1 hour.

Mosquitoes overexpressing *Cyp6m2* under the control of the A10 driver showed significantly higher mortality rates compared to controls (p = 8.06345E-05) (Figure 4.5A). Similarly, but to a significantly lesser extent compared to A10/m2 (p = 0.002), A10/p3 mosquitoes also showed a significant increase in mortality compared to A10/+ controls (p = 0.048) (Figure 4.5B).

The A8-driven multi-tissue overexpression of *Cyp6m2* or *Cyp6p3* resulted in a significant increase in mortality rates in GAL4/UAS mosquitoes compared to controls (p = 0.0015 for *Cyp6m2*; p = 0.0009 for *Cyp6p3*) (Figure 4.5). No significant differences were found between the two genes (p = 0.19).

Both A10- and A8-driven expression was correlated with 80-100% mortality in mosquitoes overexpressing *Cyp6m2.* A significantly greater degree of mortality (p = 0.008) was found in A10/p3 compared to A8/p3 mosquitoes.

No significant difference was found in the susceptibility of mosquitoes overexpressing *Cyp6m2* or *Cyp6p3* in the midgut or in the oenocytes compared to controls, although a trend of increased mortality in GAL4/UAS mosquitoes is seen (Figure 4.5).

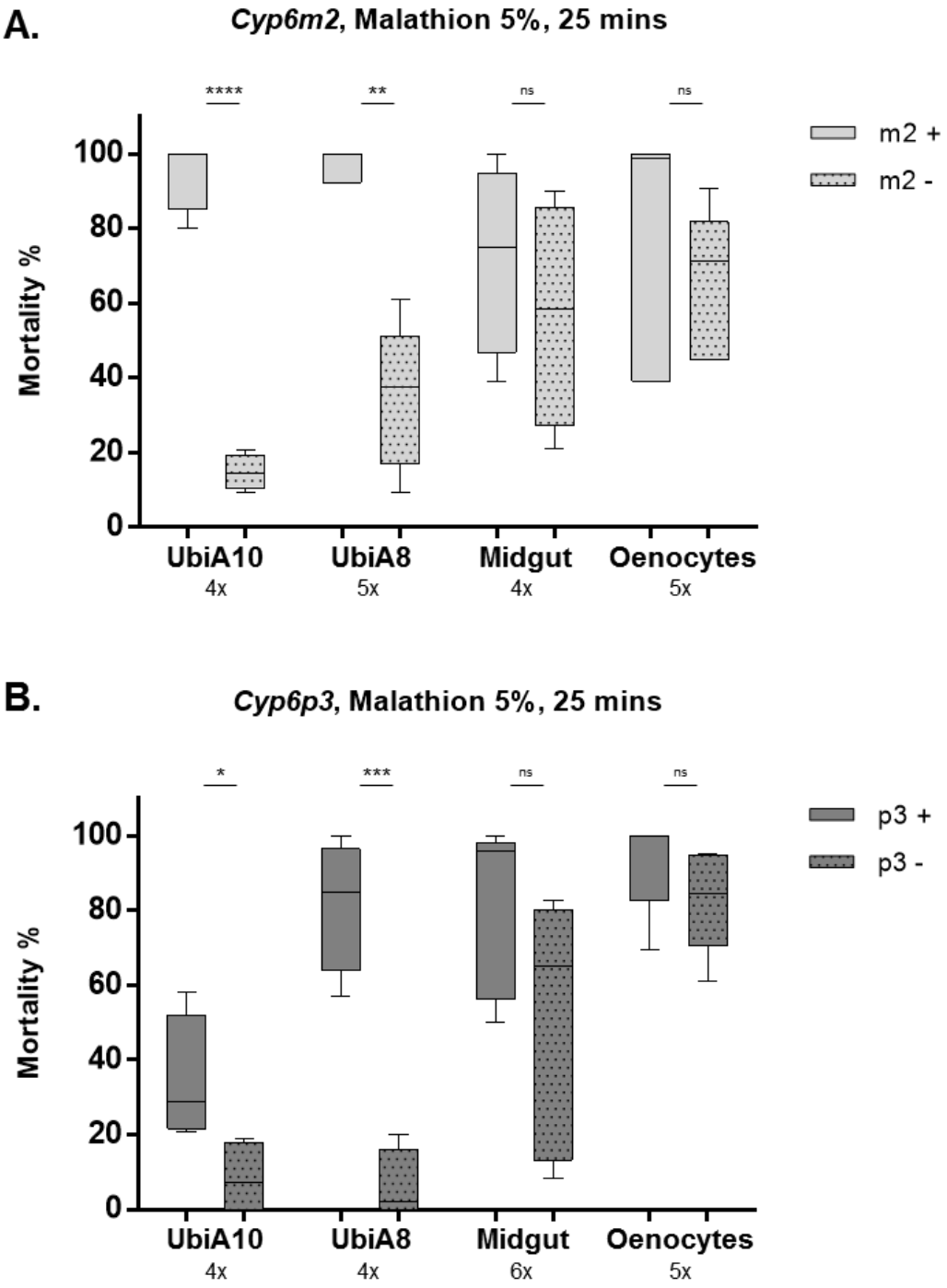

Figure 4.5 Sensitivity to 5% malathion of 2-5-day-old adult females overexpressing *Cyp6m2* or *Cyp6p3* ubiquitously or tissue-specifically under the control of the A10 (UbiA10), A8 (UbiA8), GAL4mid (Midgut) or GAL4oeno (Oenocytes) drivers. **A)** Sensitivity of the progeny deriving from the overexpression of *Cyp6m2*. m2+: mosquitoes overexpressing *Cyp6m2*; m2-: blank controls from the UASm2 cross. **B)** Sensitivity of the progeny deriving from the overexpression of *Cyp6p3*. p3+: mosquitoes overexpressing *Cyp6p3*; p3-: blank controls from the UASp3 cross. Mortality rates were obtained by modified WHO tube bioassay after 25-minute exposure and 24 h recovery. Whiskers represent minimum and maximum values, line in the middle is the median. Statistical significance was calculated using Welch's test. ns: not significant, * $p < 0.05$, ** $p \leq 0.01$, *** $p \leq 0.001$, **** $p \leq 0.0001$. The bottom and the top of each box represent the first and third quartile respectively, line inside the box is the second quartile (median), and whiskers represent minimum and maximum values. Number of technical replicates (x) for each population is indicated. File names with raw data and analysis are reported in Appendix D.

4.6 DISCUSSION

4.6.1 *Cyp6* gene and CYP6 protein overexpression

We achieved the overexpression of *Cyp6* candidate genes by independently crossing responder lines created for *Cyp6m2* (UASm2) and *Cyp6p3* (UASp3) overexpression with driver lines promoting multi-tissue overexpression at higher (A10) and lower (A8) levels. Widespread pattern of transcription driven by A10 and A8 was previously demonstrated assessing the expression of the fluorescent reporter mCherry and assumed to be representative for that of P450s.

To compare data on relative driver strength, RT-qPCR results obtained from A10/+ and A8/+ controls on the native expression levels of each gene were pooled and compared to overexpressing mosquitoes. This revealed that the A10 driver induces higher levels of transgene transcription compared to the A8 driver. This finding is in line with the relative intensities observed during fluorescence analysis in progenies from crosses to the UAS-mCherry line (Chapter 3) and by the western analysis of relative CYP6M2 abundance.

Although quantification of protein levels was not performed, Western blot analysis indicated abundant CYP6M2 protein when driven both by A10 and A8 lines. It is impossible to absolutely compare with native expression from this data, since CYP6M2 was never detected in GAL4/+ controls when extracts from 1/3 or 1/10 of a single mosquito were analysed to get a reasonable signal from the overexpressing lines. In previous experiments assessing tissue-specific expression, 1/3 of an adult mosquito or its body parts was sufficient for CYP6M2 and α-tubulin detection, with the exception of midgut samples. However, when the same amount was used to assess expression driven by ubiquitous drivers, the intense signal obtained from CYP6M2 impeded the detection of α-tubulin due to size similarity. We encountered a similar issue with size and intensity of CYP6M2 signal covering that of α-tubulin when loading protein content from 2 whole midguts. Nevertheless, even when the amount of protein extract loaded was reduced to the equivalent of 1/10 of a single mosquito expressing ubiquitously, α-tubulin was still not detectable due to CYP6M2 abundance. Thus, in the latter experiments, two identically loaded parallel gels were run and detection of the two proteins performed independently.

4.6.2 GAL4/UAS-driven *vs* natural overexpression levels

Our current knowledge on magnitude of P450 overexpression in natural mosquito populations mostly derives from comparative microarray followed by validation of top candidate hits by RT-qPCR. In this study, GAL4/UAS induction with the A10 driver generates 2447x and 513x overexpression of *Cyp6m2* and *Cyp6p3* respectively, while the A8 line drives 430x and 73x respectively. In *An. gambiae* natural populations levels of transcription of *Cyp6* genes, including the ones investigated here, are generally lower. For example, in DDT-resistant *An. gambiae* populations collected in Ghana and Cameroon *Cyp6m2* transcript abundance was respectively 4x and 3-10x higher than in susceptible populations from Cameroon and Benin (Mitchell et al., 2012; Fossog Tene et al., 2013); while in DDT-resistant mosquitoes from Benin *Cyp6m2* was found 1.2-4.6x upregulated and *Cyp6p3* 3.8-2.5x (Djègbè et al., 2014). Increased levels of expression of both *Cyp6m2* (~2.6x) and *Cyp6p3* (2.8-12.4x) were also recorded in permethrin-resistant *An. gambiae* from Benin and Nigeria compared to a susceptible Nigerian strain (Djouaka et al., 2008); while *Cyp6p3* was 1.6x upregulated in permethrin-resistant samples from Ghana (Müller et al., 2008b). *Cyp6m2* was recently reported to be 44x upregulated in deltamethrin-resistant *An. gambiae* populations from Benin, while an upregulation of 4.8x was found for *Cyp6p3* (Yahouédo et al., 2016). Finally, in pan-resistant *An. gambiae* Tiassalé mosquitoes from Côte d'Ivoire fold changes of ~8x and ~6x were recorded for *Cyp6m2* and *Cyp6p3* respectively compared to susceptible laboratory and field populations (Edi et al., 2014). Similar levels of *Cyp6p3* upregulation (7-10x) were found in pan-resistant samples from Burkina Faso (Kwiatkowska et al., 2013).

However, in respect of the magnitude of transcription a few observations must be made. In most of these studies, mosquitoes used as susceptible controls are not, in sympatry with the resistant population tested or are laboratory established populations. As such, relative quantifications are made irrespective of the native transcription levels of those genes, which may naturally vary in geographically separated populations without affecting the phenotype.

Furthermore, multiple mechanisms of resistance occur simultaneously in the field. Therefore, most data are collected from mosquitoes bearing target-site mutations (kdr^R or $ace\text{-}1^R$) alongside P450 upregulation. It is not clear how multiple mechanisms of resistance affect the levels of P450 overexpression but we can speculate that the presence of target-site resistance could lower the level of P450 upregulation needed.

This is supported by the levels of *Cyp6* upregulation found in natural *An. funestus* mosquitoes in which target-site resistance has not been described (Menze et al., 2016). Mosquitoes of this species from Mozambique and Malawi were found to upregulate *Cyp6p9a* and *Cyp6p9b* ~40-75x and ~27-88x respectively compared to the FANG susceptible strain (Riveron et al., 2013, 2014a, 2015). *Cyp6m7* was also found ~38x overexpressed in *An. funestus* mosquitoes from Zambia (Riveron et al., 2014a). Similarly, multiple resistance candidates are usually overexpressed in natural populations which may reduce upregulation levels of single genes. This was for example suggested in Zambian *An. funestus* populations where *Cyp6p9a* and *Cyp6p9b* were found 2-7x less upregulated compared to Malawian and Mozambican samples which was partly attributed to the concomitant ~38x overexpression of *Cyp6m7* in mosquitoes from this area (Riveron et al., 2014a).

As mentioned, our data on magnitude of overexpression are, to some extent, comparable to those found in the field for *An. funestus* mosquitoes, where *Cyp6* genes are found upregulated up to 88 times compared to susceptible strains (Riveron et al., 2013, 2014a, 2015). This is similar to the 75x upregulation of *Cyp6p3* obtained with the A8 driver which did not affect resistance. This may suggest that levels of upregulation required for the resistant phenotype to manifest are gene specific and dependant on levels of basal expression and actual amount of active protein produced. In addition, differently from mosquitoes generated here, the overexpression seen in *An. funestus* may occur only in key detoxifying tissues that affect the phenotype.

4.6.3 Effects on resistance to insecticides of ubiquitous overexpression of *Cyp6m2* and *Cyp6p3*

In vivo overexpression of *Cyp6m2* or *Cyp6p3* in the multi-tissue pattern promoted by the A10 driver was correlated with WHO-defined levels of resistance to diagnostic doses of the pyrethroids insecticides permethrin and deltamethrin. This data build on the evidence of these single genes to alter LD_{50} to pyrethroids in transgenic *D. melanogaster* (Edi et al., 2014). It also supports *in vitro* data on the ability of CYP6M2 and CYP6P3 recombinant proteins to metabolise pyrethroids *in vitro* (Müller et al., 2008b; Stevenson et al., 2011). A10-driven *Cyp6m2* and *Cyp6p3* overexpression caused a comparable decrease in mortality after exposure to permethrin, while resistance to deltamethrin was significantly more evident in A10/p3 compared to A10/m2 mosquitoes. This is in line with data showing ~98% of deltamethrin depletion

when incubated with recombinant CYP6P3 compared to ~55% seen with CYP6M2 (Yunta et al., unpublished). In general, CYP6P3 is found to have a more promiscuous substrate specificity compared to CYP6M2 during *in vitro* depletion experiments (Yunta et al., unpublished).

Resistance to DDT was not affected by the ubiquitous overexpression of *Cyp6m2* or *Cyp6p3* driven by either A10 or A8. This result is in accordance with *in vitro* data showing lack of substrate depletion when recombinant CYP6M2 or CYP6P3 are incubated with DDT (Yunta et al., unpublished). DDT is not depleted in the presence of several other candidates of the *Anopheles* CYP6 and CYP9 families (Yunta et al., unpublished). Although the expression of *Cyp6* genes in tissues not targeted with A10 and A8 may confer resistance to DDT, the results would support the idea that DDT resistance could mainly rely on the presence of kdr^R and upregulation of GSTs (Mitchell et al., 2014). Indeed, *An. gambiae* recombinant GSTE2 metabolises DDT *in vitro* (Ortelli et al.,2003; Mitchell et al., 2014) and its overexpression in transgenic *D. melanogaster* determines acquisition of resistance to DDT (Daborn et al., 2012; Mitchell et al., 2014). However, further *in vivo* evidence in *D. melanogaster* showed a significant difference in the DDT LD_{50} in flies overexpressing CYP6M2 ubiquitously (Edi et al., 2014). Such discrepancies between results obtained in *Anopheles* and *Drosophila* transgenics will be discussed in Chapter 5.

Resistance to bendiocarb is affected only in mosquitoes overexpressing *Cyp6p3* under the control of the A10 driver. Once again, this is in accordance with *in vitro* metabolism data showing the ability of recombinant CYP6P3, but not CYP6M2, to metabolise bendiocarb (Edi et al., 2014). Remarkably, CYP6P3 was the only enzyme able to deplete bendiocarb *in vitro* among nine CYP6 (including CYP6M2) and CYP9 enzymes tested elsewhere (Yunta et al., unpublished). In comparison, *in vivo D. melanogaster* data showed that both CYP6M2 and CYP6P3 confer resistance to 0.1 µg bendiocarb when ubiquitously overexpressed (Edi et al., 2014).

Overall, despite the high level of overexpression driven by A10, the resultant enzyme activity is able to be sustained sufficiently by the native levels of CPR in relevant tissues to impart resistance. Although it would be interesting to assess whether there is an upregulation of CPR in these crosses in response to transgenic P450 expression.

When *Cyp6* overexpression is induced by the A8 driver, WHO levels of resistance to insecticides are not observed, with the exception of A8/m2 mosquitoes showing low, but significant, resistance to permethrin. In these mosquitoes, reduction in mortality is

less marked than in A10/m2. Also, a trend of decrease in mortality, although not significant, is found in A8/p3 mosquitoes exposed to permethrin or bendiocarb. In these instances, since resistance is suspected, additional replicate experiments are required to define resistance status according to WHO guidelines (WHO, 2016b); increasing the number of repeats increases the power of statistical analysis and may show defined significant differences. The levels of resistance observed from the A8 crosses thus support the data on driver strength obtained by fluorescence (Chapter 3) and analysis of transcript and protein abundance. It would suggest that the amount of CYP6 produced in A8 lines is not saturating relative to A10, and that higher enzyme quantities in A10 provide greater resistance even at these levels of ubiquitous overexpression. Clearly, it may be that expression is required in only a few key detoxifying tissues to confer resistance, and in these tissues the A10 lines produce more enzyme than the A8 lines.

Overall the data suggest that, besides location of overexpression, levels of overexpression are crucial for the resistance phenotype to manifest.

4.6.4 Effects on resistance to the pro-insecticide malathion of ubiquitous *vs* tissue-specific overexpression of *Cyp6m2* and *Cyp6p3*

This work reports on the first *in vivo* evidence of the involvement of *Cyp6m2* and *Cyp6p3* in the sensitivity to malathion in *An. gambiae* mosquitoes. When exposed to the WHO diagnostic dose of malathion for 25 minutes, both *Cyp6m2* and *Cyp6p3* determined an increase in susceptibility when overexpressed ubiquitously but not tissue-specifically in the midgut or in the oenocytes. This negative cross resistance can be explained by the bioactivation of malathion in its toxic metabolite malaoxon via P450-mediated oxidation (Cohen et al, 1984; Berkman et al., 1993). The ability of both the P450s tested to deplete malathion *in vitro* has been recently demonstrated (Yunta et al., unpublished), which correlates with the increased toxicity seen in P450-overexpressing mosquitoes compared to controls.

Although all mosquitoes were susceptible to malathion after 1 h of exposure, during this exposure time GAL4/UAS mosquitoes were knocked-down much faster than controls suggesting involvement of P450 metabolism (not shown). This observation led us to reduce the exposure time to 25 minutes to observe differences between GAL4/UAS and GAL4/+ mosquitoes.

Cyp6m2 caused a range of 80-100% mortality when it was driven by either the A10 or A8 drivers, suggesting the toxic oxidation of malathion into malaoxon is sustained even by lower levels of P450 overexpression. Conversely, differences in mortality induced by the overexpression of *Cyp6p3* were found between the A10 and A8 drivers. Here, levels of overexpression driven by the weaker driver A8 induced significantly higher mortality compared to that induced by the stronger driver A10. This may be explained considering that P450-induced metabolism of malathion is likely to be a two-step process involving 1) oxidation-mediated activation of malathion into its highly toxic metabolite malaoxon (Matolcsy, 1988), and 2) oxidative degradation of malaoxon. It can be speculated that in A8/p3 mosquitoes the lower level of CYP6P3 favours oxidation of malathion into malaoxon with resultant high toxicity, while in A10/p3 mosquitoes, where higher quantity of enzyme is present, oxidation of malathion is accompanied by detoxification of malaoxon. Nevertheless, the kinetics of this two-step oxidation is unclear. Overall, mortality rates induced by A10-driven *Cyp6m2* overexpression were higher than those found in *Cyp6p3*-overexpressing mosquitoes suggesting that CYP6M2 may show higher catalytic activity for malathion compared to malaoxon and therefore the bioactivation step is favoured.

In mosquitoes overexpressing *Cyp6* in the midgut or in the oenocytes, despite a trend of increased mortality being observed, this was not significantly different from mortality in control mosquitoes. This suggests that tissue location of malathion turn-over is critical and is not sufficient to significantly affect the susceptibility when it is confined to the midgut or the oenocytes.

While resistance to pyrethroids is widespread in Africa (Ranson & Lissenden, 2016), resistance to organophosphates is much less so due to the decreased use of this class of insecticides as adulticides since the advent of pyrethroids. Therefore, the enhanced susceptibility to malathion after 25 minutes of exposure and the faster knock-down observed after 1 h of exposure in mosquitoes overexpressing P450s ubiquitously is promising for control strategies based on exploiting the combined effect of insecticides with different modes of action. One such strategy involves combining the use of pyrethroid-based LLINs with malathion-based IRS. This would combine the additive effect of the two classes of insecticides on susceptible mosquitoes, while specifically targeting pyrethroid-resistant mosquitoes overexpressing P450 enzymes. In these mosquitoes, malathion could also synergise the toxicity of pyrethroids by acting as a competitive substrate for P450s (Martin et al., 2003). The binding of malathion to P450s would result in the production of the toxic malaoxon form while rendering the P450 active site unavailable for pyrethroid binding,

thus preventing detoxification. Furthermore, the use of two different classes of insecticides would reduce the currently high selective pressure imposed by pyrethroids on the mosquito population (WHO, 2012b). The synergetic action of organophosphates on the efficacy of pyrethroids was demonstrated in the cotton pest *Helicoverpa armigera* (Martin et al., 2003). To my knowledge, the combination of organophosphate-based IRS with pyrethroid-impregnated LLINs has not yet been investigated in field trials.

4.6.5 Considerations on the WHO tube bioassay

In this study resistance was assessed by WHO tube bioassay whose guidelines define the threshold of resistance at 98% when performing 1-hour exposure to single doses of insecticides that are defined as twice the concentration that kills 99.9% of a susceptible population ($LD_{99.9}$) (WHO, 2016b).

When performing WHO test, there are several variables that may affect mortality rates contributing to variable results, including factors related with mosquito rearing such as age and fitness, and quality control issues with the papers such as uneven impregnation, usage and inappropriate conditions of storage affecting insecticide stability.

In this study, despite working with susceptible laboratory colonies, in some instances we recorded mortality below 98% after 1 h of exposure to diagnostic doses of permethrin, DDT and bendiocarb. Therefore, in compliance with WHO guidelines, only experiments in which GAL4/+ controls showed 95-100% mortality were included in the analysis. Experimental mosquitoes are reared at near optimal conditions of temperature, humidity, density, and availability of food which results in a generally bigger size and increased fitness compared to field populations. This may partly explain the issue with reduced mortality at WHO diagnostic doses. Furthermore, the efficacy of papers is known to decline over time, especially when pyrethroids are tested (WHO, 2016b). Thus, although according to WHO guidelines papers can be reused up to 6 times (equivalent of the exposure of 150 mosquitoes) (WHO, 2016b), in our experiments fresh papers were used which were stored for a maximum of three days. Despite alleviating the problem, even fresh permethrin papers showed decreased performance which leads us to suggest that diagnostic dose for this insecticide (0.75%) may need to be revised. Similarly, issues with some of the bendiocarb- and DDT-impregnated papers showing a decreased efficacy against susceptible populations, could be explained by technical issues during paper

manufacturing at the Universiti Sains Malaysia, reference centre for paper production (WHO, 2016b).

Besides possible issues with quality of papers, factors such as size, age, fitness or behaviour of the mosquitoes tested may cause variability in the results when using the WHO bioassay. In our experiments, mosquitoes overexpressing P450s and blank controls were reared together and selected as pupa on the same days. No obvious differences in size or fitness were noticed between the two populations, although we did not specifically assay this. In terms of optimal age for testing, even within the WHO recommended range of age, 3-5-day-old, field resistant mosquitoes show remarkably different mortality rates when exposed to deltamethrin, permethrin and propoxur, with 2-3 day-old mosquitoes displaying similarly high levels of resistance that are consistently higher than 5-day-old mosquitoes (Chouaibou et al., 2012). In this study, we tested 2-5 day-old females, but often this range of age was reduced to 2-3, 3-4 or 4-5 day-old since, in the condition of rearing used, mosquitoes pupated synchronously over two days. This may have contributed to the variability within replicates and experiments. Furthermore, "the uptake of [a discriminating concentration] depends on the time of actual tarsal contact" with the insecticide (WHO, 2016b). The WHO tube setup does not ensure continuous contact with the insecticide-impregnated paper as this adheres to the tube wall leaving the top and bottom uncovered where mosquitoes can rest without being exposed. Thus, the length of time spent in these areas is expected to affect results due to altered exposure. Here, this is particularly relevant in experiments where exposure time was reduced to 20-25 minutes, which may explain the higher variability found in these experiments. Moreover, reducing the time of exposure to 20-25 minutes amplifies the effect of excito-repellency (Kawada et al., 2014) that some of the compounds (e.g. pyrethroids) induce which leads mosquitoes to fly frantically instead of resting on the paper further reducing the total exposure.

4.6.6 Conclusions and Future Directions

This study provides the first *in vivo* evidence of the ability of single *Cyp6* genes, *Cyp6m2* and *Cyp6p3*, to cause resistance to a diverse range of insecticides in *An. gambiae*. Also, for the first time in *in vivo* transgenic experiments, levels of resistance identified here are those defined by the WHO, so data are directly comparable to those obtained from field mosquitoes using the WHO tube bioassay.

Upcoming work will include investigating the effect that pre-exposure to the synergist PBO has on the resistance phenotype. PBO in known to inhibit P450-mediated

metabolism enhancing insecticide potency and is used as preliminary screening to ascertain the involvement of metabolic resistance in the field-caught resistant mosquitoes (Feyereisen, 2015). Such experiments would indicate whether CYP6M2 and CYP6P3 are affected similarly by PBO when metabolising different insecticide classes and to what extent. It would also show whether the WHO-recommended PBO concentration (4%) (WHO, 2016b) is sufficient to increase mortality in the resistant populations created in this study that display remarkably high levels of P450 overexpression.

While fluorescence assessment of drivers' activity showed expression of at all life stages, CYP6 overexpression and its effect on resistance has only been assessed in adults. Therefore, future work should include validating overexpression in other life stages and testing resistance to larvicides in aquatic stages.

In addition, genetically stable resistant mosquitoes were created that can be implemented in the pipeline for assessing new active compounds, such as insecticides, pro-insecticides, synergists and sterilising agents, in a solely metabolic resistance background. The implementation of these lines in such pipeline is discussed in Chapter 5.

Chapter 5

General Discussion

5.1 Effect of tissue-specific *vs* ubiquitous *Cyp6* overexpression

Identifying the tissues involved in insecticide metabolism is key to defining physiological insecticide detoxification pathways, which, in turn, greatly assists the quest to discover new active compounds and formulations with chemistries that evade detoxification. The work presented here demonstrates that location of overexpression of top resistance candidates *Cyp6m2* and *Cyp6p3* is critical in causing WHO levels of resistance, as this has only been obtained when single P450s are overexpressed ubiquitously but not tissue-specifically in the midgut or oenocytes. Overexpression confined to these tissues was initially targeted because of their proposed role in detoxification and the immediate availability of corresponding GAL4 drivers; while achieving ubiquitous overexpression required the characterisation and validation of a novel endogenous promoter driving expression in multiple tissues.

Knowledge on tissue-specific distribution of P450 overexpression is very limited in mosquitoes, therefore it is difficult to predict what body parts may be specifically linked to *Cyp6m2*- and *Cyp6p3*-mediated detoxification. To date, only one study investigated the expression of resistance-associated genes in dissected body parts (Malpighian tubules, midgut, abdomen integument, and carcass) of resistant *An. gambiae* populations (Ingham et al., 2014). In this study, *Cyp6m2* overexpression did not show tissue-specificity, while *Cyp6p3* was significantly overexpressed in the midgut of resistant mosquitoes in relation to the whole body.

A limited number of studies in other insects have implicated different tissues in metabolism-mediated resistance which include the midgut, Malpighian tubules and oenocytes. In *An. gambiae*, the involvement of the oenocytes in resistance was supported by the natural enrichment of the P450 cofactor CPR (Lycett et al., 2006) as well as that of resistance-associated P450 genes such as *Cyp4g16* and *Cyp4g17* (Ingham et al., 2014; Balabanidou et al., 2016). Consistent with a role in detoxification, oenocyte-specific CPR knockdown, which affects the function of all P450s, caused increased sensitivity to permethrin in susceptible *An. gambiae* (Lycett et al., 2006).

Nevertheless, our data show that overexpression of candidate resistance P450 genes in this tissue does not alter resistance to the four classes of insecticides under the conditions tested. Recently, Balabanidou et al. (2016) found that *Cyp4g16* and *Cyp4g17* are specifically localised in *An. gambiae* oenocytes, and the former is essential for cuticular hydrocarbon production. In line with this finding, stable oenocyte-specific knockdown of either gene via transgenic RNAi imposed a remarkable fitness cost and drastically increased susceptibility to desiccation in *An. gambiae* (Lynd et al., unpublished). In related work, Balabanidou et al. (2016) also demonstrated that the rate of insecticide penetration was greater in susceptible mosquitoes, which correlated with resistant *An. gambiae* displaying a thicker cuticle compared to susceptible mosquitoes. In light of these recent findings, the phenotype observed by Lycett et al. (2006) as a result of CPR knockdown may be in fact due to fitness costs associated with defective cuticle which determines an increase in insecticide internalisation or increased desiccation sensitivity. Similar conclusions were recently reached by Yu et al. (2016) after the RNAi-mediated knock down of *Cyp4g102* in *Locusta migratoria*.

The P450-cofactor CPR is also highly expressed in the mosquito midgut (Lycett et al., 2006), and together with the high native expression of *Cyp6m2* and *Cyp6p3* (Stevenson et al., 2011; Baker et al., 2011) supports an involvement of this tissue in conferring resistance. Furthermore, transcripts from other genes of the CYP6P family, including *Cyp6p3*, were found enriched in the midgut of resistant strains (Ingham et al., 2014). Despite this, we found that overexpression of *Cyp6m2* or *Cyp6p3* confined to this tissue does not affect resistance to all insecticides under the conditions tested. Consistent with this, fluorescence assessment of the activity of the A10 and A8 drivers used to obtain widespread expression, revealed absence of expression in the midgut. The emergence of resistance derived from overexpression induced by these ubiquitous drivers thus supports the notion that the midgut does not play a major detoxification role, at least via overexpression of these specific P450s tested and in the absence of other factors.

Finally, the involvement of Malpighian tubules in detoxification has also been suggested by P450 gene enrichment in this organ in *An. gambiae* (Baker et al., 2011; Ingham et al., 2014). Furthermore, the P450-cofactor CPR was also found abundantly in the mosquito Malpighian tubules (Lycett et al., 2006). However, as described above for the midgut, the absence of expression driven by the A10 and A8 lines in Malpighian tubules, with corresponding resistance observed to different classes of insecticides in *Cyp6*-overexpressing mosquitoes, would also suggest a non-essential role in P450-

mediated detoxification for this tissue. At least for the insecticides tested, taken together, this evidence suggests that the midgut and oenocytes are not essential for *Cyp6m2*- or *Cyp6p3*-mediated detoxification, while the role of the Malpighian tubules remains not fully explored. Nevertheless, these tissues may still be relevant for other P450s that are specifically enriched in these locations, or play synergistic roles with other resistance mechanisms. Perhaps significantly, Yang et al. (2007) found that transgenic overexpression of endogenous *Cyp6g1* specifically induced in the Malpighian tubules, but not in the brain or in the fat body, caused resistance to DDT in *D. melanogaster*. In the future, an *Anopheles* Malpighian-specific driver would be invaluable to further investigate the potential role of these excretory organs.

Functional analysis in *D. melanogaster* has also shown tissue-specific roles in insecticide detoxification when *Anopheles* genes are heterologously expressed. For example, Daborn et al. (2012) found no difference in the DDT resistance phenotype emerging from the overexpression of *An. gambiae Gste2* when driven by a ubiquitous driver or a driver specific for the midgut, Malpighian tubules and fat body. Implicating roles for the latter tissues in resistance mediated by GSTs. However, when investigating the effect of overexpression of *An. funestus Cyp6p9a*/*b* genes, Riveron et al. (2013) found that resistance to pyrethroids emerged only when overexpression was driven ubiquitously but not by the midgut, Malpighian and fat body driver. This suggests the presence of gene-specific responses that are dependent on location of expression. If individual enzymes are specifically associated with certain tissues to produce a resistance phenotype, it is possible that the minimum pattern of overexpression required for *Cyp6m2* or *Cyp6p3* to cause resistance may differ or may not require all the tissues where the PUBc_GAL4 driver is active. Similarly, different insecticides may be detoxified in different tissues that require different enzymes or enzyme classes. Tissue specialisation in insecticide metabolism may derive from unequal exposure to xenobiotics. The fate of insecticides after uptake by the mosquito and the detoxification pathways they undergo are not well defined and they are likely to depend on the administration route, with ingested insecticides encountering different tissues compared to those that are topically acquired (Yang et al., 2007). In this scenario, lack of resistance observed in our studies when *Cyp6s* are overexpressed in the midgut may be due to the mode of exposure to the insecticide (contact), and this tissue may be relevant when xenobiotics are instead ingested. An example of this would be the increased susceptibility to permethrin observed in *P. xylostella* after droplet-feeding larvae *Cyp6bg1* dsRNA droplets (Bautista et al., 2009).

Owing to their generally lipophilic nature, insecticides may be transported around the mosquito tightly bound to lipoproteins (Shaw, 1991) and therefore not access all tissues equally, which would result in their compartmentalisation in the mosquito body. If this is the case, it is expected that certain tissues may have specific detoxification roles compared to others.

Examples of tissue specialisation in insecticide metabolism demonstrated by gene functional analysis include the brain and the Malpighian tubules. Central nervous system-specific overexpression of *T. castaneum Cyp6bq9* gene in *D. melanogaster* transgenics determined acquisition of resistance to deltamethrin (Zhu et al., 2010). Since the nervous system is the target of most insecticides, it would be interesting to explore the phenotype resulting from overexpression in this location. Another single tissue that have not been investigated in this study and may play a significant role in insecticide metabolism is the fat body. Promoters targeting these locations are available in *An. gambiae,* thus experiments similar to those conducted here could be performed to investigate the contribution of these tissues.

This study suggests that not only location of overexpression is relevant but also levels of overexpression are critical for resistance, with high levels of *Cyp6m2 or Cyp6p3* overexpression required in more than one tissue for the mosquito to acquire WHO-levels of resistance to insecticides. However, as mentioned, the data on overexpression in the whole mosquitoes does not implicate specific tissues.

5.2 Detection of insecticide resistance in adult mosquitoes

This study provides the first *in vivo* evidence that WHO-levels of resistance in *An. gambiae* can be produced by the overexpression of single P450 genes. The WHO tube bioassay is the recommended surveillance tool to detect resistance in mosquito populations (WHO, 2016b). As such, data produced in this work were obtained under standardised conditions that are directly comparable to those obtained by other laboratories and/or in the field.

WHO-defined resistance refers to the percentage mortality recorded 24 h after 1 h of exposure to papers impregnated with diagnostic single doses of insecticides (WHO, 2016b). The discriminating concentrations used to impregnate papers correspond to two-times the dose that kills 99.9% of a susceptible population ($LD_{99.9}$) (WHO, 2016b). As such, detection of resistance at discriminating doses does not necessarily correlate with insecticide failure in the field and assessment of “intensity” of resistance

is now considered necessary to determine operational implications (Bagi et al., 2015; WHO, 2016b). Therefore, in the revised version of the WHO guidelines, testing 5x and 10x concentrations is suggested to assess strength of resistance, with the assumption that identification of resistance at 5x, and particularly at 10x concentration, predicts operational failure (WHO, 2016b).

An alternative method to determine intensity of resistance is the CDC bottle bioassay (CDC, 2012), which is based on incubating mosquitoes in glass bottles coated with ascending insecticide concentrations. However, when we attempted to build dose-response curves in susceptible GAL4/+ populations using this technique, data were highly inconsistent among doses and replicates. We believe this was due to difficulties in obtaining a uniform coating of the bottles. Eventually the test was discarded as the coating and washing protocols were too laborious, and results variable. For simplicity and consistency, we attempted to assess whether the oenocytes and midgut driven expression caused an observable resistance phenotype at lower insecticide exposures than the standard WHO assay. This modified WHO tube test involved decreasing the exposure time to yield a lower dose. As discussed in Chapter 4, although trends were observed, no significant difference was detected in the tissue specific lines, but again the high variability in results may mask small differences in resistance that would require many more repeats to yield a small significant difference.

With more time, it would be informative to assess the intensity of resistance by building dose-response curves LD_{50} for all the GAL4/UAS mosquitoes. This could be achieved using custom papers with grading insecticide doses or using a newly designed tarsal assay, where mosquitoes are exposed to custom doses of insecticides in disposable Petri dishes. This last method would have been of choice because it uses a lower number of mosquitoes per test allowing more technical and biological replicates for the same mosquito numbers (i.e. 10 females per replicate compared to 25 needed for the WHO tube bioassay).

5.3 Comparison of *in vitro* metabolism with *in vivo* phenotype assays in transgenic *Anopheles* and *Drosophila.*

As discussed extensively in this thesis*, in vivo* gene functional analysis is critical to determine causative links between the overexpression of a candidate gene associated with resistance and the occurrence of the resistance phenotype. This work reports on the first functional analysis of mosquito resistance genes conducted in transgenic *An. gambiae*. Additionally, while the involvement of *Cyp6m2* and *Cyp6p3* in conferring resistance to permethrin, deltamethrin, DDT and bendiocarb was previously investigated in *D. melanogaster* transgenics (Edi et al., 2014), this work shows for the first time the endogenous role of these genes in altering sensitivity to malathion via P450-mediated activation.

Table 5.1 summarises the phenotypic data obtained in this study in comparison with *in vitro* assays with recombinant *An. gambiae* CYP6M2 and CYP6P3 and *in vivo* data from previous reports from *D. melanogaster* transgenic analysis with *Cyp6m2* and *Cyp6p3*.

Table 5.1 Summary of functional validation experiments of *Anopheles* resistance candidate genes *Cyp6m2* and *Cyp6p3*. Table reports main findings from *in vitro* depletion experiments with recombinant CYP6s and *in vivo* studies performed in *An. gambiae* and *D. melanogaster* models using GAL4/UAS-mediated overexpression.

Gene	Insecticide	***In vitro* metabolism*** (Yunta et al., unpub.)	***Anopheles* transgenics** (this study)	***Drosophila* transgenics*** (Edi et al., 2014)
Cyp6m2	Permethrin	58.5 ± 2.2 ✓	✓	✓
	Deltamethrin	55.4 ± 1.4 ✓	✓	✓
	DDT	2.9 ± 2.1 ✗	✗	✓
	Bendiocarb	0 ± 11.2 ✗	✗	✓
	Malathion	26.8 ± 8.8 ✓	✓	N/A
Cyp6p3	Permethrin	100.0 ± 0.0 ✓	✓	✓
	Deltamethrin	98.2 ± 0.2 ✓	✓	✓
	DDT	4.1 ± 5.6 ✗	✗	N/A
	Bendiocarb	35.0 ± 2.5 ✓	✓	✓
	Malathion	68.8 ± 8.4 ✓	✓	N/A

Green ticks represent presence of *in vitro* depletion or that of resistance *in vivo*. Red crosses represent lack of *in vitro* depletion or that of resistance *in vivo*.
* Values represent mean % of insecticide depletion ± SD assessed by HPLC analysis. 20% was set as cut-off for activity.
** Results based on LD_{50} curve analysis for all insecticides except bendiocarb, which was tested at a single dose of 0.1 µg.

Generation of resistance in *An. gambiae* is in all cases consistent with the ability of the specific P450 tested to metabolise the corresponding insecticide *in vitro*, i.e. a WHO level resistant phenotype in *An. gambiae* was only recovered when the P450 tested had been shown to deplete the specific insecticide tested *in vitro*. These results give confidence to *in vitro* metabolic assays as a primary screen of candidate genes. Nevertheless, further genes need to be screened *in vivo* to strengthen the data. Moreover, absence of *in vitro* metabolism does not necessarily mean lack of involvement in resistance, since other P450 interactions may occur (binding or secondary metabolism) that are relevant for developing resistance. As such, *in vivo* testing will be an important element for candidate validation in *Anopheles*.

When comparing *in vivo* data obtained in the *Drosophila* and *Anopheles* models discrepancies do emerge. *Drosophila* overexpression of CYP6M2 was reported as increasing resistance to DDT and bendiocarb (Edi et al., 2014), which are not metabolised *in vitro* by this enzyme (Yunta et al., unpublished; Edi et al., 2014). In

contrast, this study demonstrates that overexpression of CYP6M2 does not cause WHO levels of resistance to DDT or bendiocarb in *An. gambiae*, suggesting that this P450 does not significantly interact with these insecticides in *Anopheles*. However, it is noteworthy that *in vivo* results obtained in the two systems are not directly comparable as the method used to assess resistance differs in the two insects. While data reported here for *An. gambiae* was obtained by WHO tube bioassay, resistance data on *D. melanogaster* was mostly reported as LD_{50} values obtained from exposing flies to different concentrations of insecticides for 24 h. Concentrations used for testing flies are typically lower compared to those used for testing mosquitoes using the WHO test, and thus may pick up small differences in resistance phenotype. Whether these small differences in resistance in *Drosophila* give useful information for operational field control of mosquitoes may be debatable.

Incongruity between *in vitro* insecticide depletion and *in vivo* data obtained in *Drosophila* was also found when characterising the *An. funestus Gste2* gene, which was shown not to metabolise deltamethrin *in vitro* yet resistance emerged in flies overexpressing the gene (Riveron et al., 2014b). It would be informative to test this gene in *Anopheles* in comparison since interactions not involving metabolism may occur, such as sequestration.

Overall, using *Anopheles* transgenics appears to be a more suitable alternative to investigate endogenous gene function *in vivo* compared to the *Drosophila* model. The *Anopheles* model clearly allows more physiologically relevant and representative results by overexpressing endogenous genes. In doing so, it also allows the assay of candidate genes difficult or impossible to test *in vitro* or in *Drosophila*, such as evolutionary diverged cuticle genes, transcription factors regulating genetic pathways, or sensory proteins. As examples, recent RNAi investigations revealed the involvement of a Maf transcription factor in regulating overexpression of a resistance gene pathway (Ingham, 2016) and a putative odorant-binding protein that modifies a resistance phenotype (V. Ingham pers. comm.). Owing to their lack of enzymatic activity these candidates cannot be readily screened for *in vitro* activity and their assessment in *Drosophila* may not be physiologically representative, due to lack of interacting partners.

5.4 Applications of insecticide resistant lines

The work flow for assessing the efficacy of new active compounds before commercialisation includes testing the effect of new chemistries on field-caught resistant populations. Naturally resistant *An. gambiae* populations display multiple mechanisms of resistance, usually target-site resistance and up-regulation of multiple detoxifying genes. While representative of natural populations, the presence of multiple resistance mechanisms along with the natural genetic diversity existing in these populations complicates pinpointing the precise molecular basis of resistance to new chemistries. Further complications when using recently colonised field populations include maintaining their resistance status, which often requires periodical selection and generating sufficient numbers to create a stable population.

Mosquitoes created as part of this work are resistant to permethrin, deltamethrin, and bendiocarb in a solely metabolic background, whose resistance is readily obtained upon crossing of parental lines that gives large numbers of genetically nearly-identical individuals. The genetic markers are fluorescent labels which are easy to score and monitor for contamination. They are therefore useful to be implemented in the pipeline for discovery of new active compounds, including insecticides, pro-insecticide as well as for testing synergists such as PBO or sterilising agents such as pyriproxyfen. Indeed, pyriproxyfen metabolism mediated by CYP6M2 and CYP6P3 has been recently demonstrated *in vitro* (Yunta et al., 2016). Furthermore, as P450 overexpression occurs in all life stages, these resistant lines are also suitable for larvicides testing. These resistant mosquitoes are thus currently being used to test a series of new and repurposed compounds for the product development consortium IVCC to select those compounds that are least liable to CYP6M2- and CYP6P3-mediated metabolism.

Owing to their stable, common genetic background, and consistent resistance phenotype, these lines are highly suited to directly compare the different techniques used to assess resistance in *An. gambiae*, such as WHO tube, CDC bottle, cone, and topical tarsal assays. This would, for example, include investigating relationships between defined resistance and diagnostic doses. In particular, testing these lines with the cone bioassay, a more realistic assay in which mosquitoes are exposed to LLINs or insecticide-sprayed surfaces (to mimic IRS interventions), would be very informative in comparison with the resistance phenotypes observed with the current universal WHO field test.

5.5 New tools for *Anopheles* transgenesis and *in vivo* gene functional analysis

This work provides important new tools for transgenesis and gene expression manipulation in *An. gambiae* including a novel endogenous promoter driving widespread expression and new docking driver lines.

Owing to its widespread expression, the PUBc promoter can be used whenever a multi-tissue patter of expression is required. This may include its use as an alternative marker for efficient screening of large numbers of transgenic individuals or for the use of automated screening systems (Marois et al., 2012; Volohonsky et al., 2015) as it allows performing mass screening at low magnification. Currently, screening of transformant mosquitoes relies on the activity of the 3xP3 promoter which drives neuronal expression. In transgenic *D. melanogaster*, expression in the nervous system was found robust in several genomic landing sites (Markstein et al., 2008). However, the promoter is still susceptible to position effect as demonstrated by fluorescence detection either in the eyes, brain, anal plates, nerve cord, or in all the mentioned locations, depending on genomic locus, which may limit transformant detection. Due to its broader activity, PUBc may be a more reliable screening marker.

The A10 and A8 PUBc driver lines, both carrying a single insertion in intergenic regions of chromosome 2R, were selected as exemplification of a common PUBc pattern of widespread expression at different intensities, higher and lower respectively. These drivers represent valuable and versatile tools for gene functional analysis in *An. gambiae* using the GAL4/UAS system as they can be used to obtain widespread gain- or loss-of-function of any gene or RNAi template located in suitable UAS lines. GAL4-mediated gene silencing experiments can now be performed in a widespread fashion, which will for example broaden the efficiency of RNAi-mediated knock-down experiments, particularly those for which no tissue specific promoter is available. In this context, PUBc driver lines can be also combined with the CRISPR/Cas9 system for inducing a more efficient mutagenesis-mediated gene silencing by crossing PUBc_GAL4 with previously established UAS:Cas9/gRNA transgenic individuals (Xue et al., 2014).

Using the A10 and A8 drivers, gene expression manipulation can be achieved in a similar spatial and temporal manner at two different levels. This is advantageous for overexpression of target genes that are toxic, for which a lower level of expression is desirable or, vice versa, for genes that are endogenously lowly expressed, for which

signal amplification is needed. Similarly, they potentially allow for manipulation of knockdown levels.

As an alternative use, the efficiency of the A10 line for recombinant protein production within the mosquito can be investigated. Currently, mosquito-derived recombinant proteins are produced in bacterial or viral systems such as *E. coli* and Baculovirus. A mosquito system would produce less protein, but this should be correctly modified and folded, and thus potentially more active and representative. Tagging would also be possible to facilitate purification.

Importantly, A10 and A8 carry two attP sites for RMCE or site-specific integration. Indeed, when injecting embryos of a docking line carrying two attP sites, occasional cassette integration occurs alongside with cassette exchange as a result of single crossover events. Progeny can then be selected by screening for the presence of a double or single marker. Integration may be desirable, for example, to insert a UAS construct flanking the GAL4 cassette to create stable GAL4/UAS individuals without the need of crossing and maintaining two separate lines. On the other hand, the ability of replacing the present cassette with any other DNA cargo containing attB sites would allow for comparison of direct gene expression at an identical genomic location limiting the confounding factor of positional effect (Bateman et al., 2006; Meredith et al., 2013). For example, the activity of other promoters could be assessed and directly compared to that of PUBc, including the other candidate ubiquitous promoters developed in this study; similarly, expression of transgenes from different UAS cassettes could be compared when induced by the same driver.

Taken together, this work provides an integrated system to validate genes in *An. gambiae*. Advantages of the system include the ability to 1) express or silence genes in *An. gambiae* in alternative patterns of expression, including tissue-specifically or ubiquitously, at two different levels and in all life stages; 2) express genes that cannot be tested *in vitro* or in *D. melanogaster*; 3) compare expression data in individuals with a nearly-identical genetic background; 4) generate lines relatively rapidly via RMCE which allows comparative assessment of gene function by swopping cassettes in the same genomic locus.

5.6 Future perspectives for investigating resistance

The overall aim to this work was to investigate which P450 genes and tissues are physiologically relevant for the emergence of insecticide resistance. While, the

overexpression of *Cyp6m2* and *Cyp6p3* have been found directly correlated with resistance and location and levels of their expression found to be critical, the key tissues involved in detoxification remain a point of ambiguity. Our analysis of expression driven by the A10 and A8 lines using a fluorescent reporter revealed that the main difference between the two lines is intensity of expression. Nevertheless, a detailed analysis of expression using more sensitive techniques such as qPCR or Northern blot analysis in dissected tissues may reveal more substantial differences in location of expression that could help to pinpoint tissues relevant to detoxification. These locations could be then further investigated to validate their involvement in resisatnce.

More broadly, next generation tools for geneme manipulation, such as CRISPR/Cas9, are set to facilitate investigations on insecticide resistance. The CRISPR/Cas9 system is revolutionising the field of genome editing in insects due to its versatility and efficiency. It allows for stable gene knock-outs, through non-homologous end joining (NHEJ) of cleaved sites, or gene knock-ins and specific mutations via homology directed repair (HDR) if a template flanked by homologous regions is provided. In recent years, the CRISPR/Cas9 technology has been successfully applied to mosquitoes such as *Ae. aegypti* (Dong et al., 2015; Kistler et al., 2015), *An. stephensi* (Gantz et al., 2015), *An. gambiae* (Hammond et al., 2016), and *C. quinquefasciatus* (Itokawa et al., 2016), with first examples of its application in insecticide resistance research emerged very recently. However, CRISPR/Cas9 has not been reported for the analysis of insecticide resistance in *An. gambiae*. In the context of this study, if multiple, defined mechanisms of resistance are to be examined, resistant mosquitoes created as part of this work can be modified to bear specific target-site mutations (kdr^R and/or $ace\text{-}1^R$). This would allow examination of the contributions of single or multiple mechanisms of insecticide insensitivity to the overall resistance phenotype.

In *D. melanogaster*, a point mutation was induced in the AchE receptor using CRISPR/Cas9 and found to be sufficient to confer resistance to spinosad (Zimmer et al., 2016). With the abundance of genomic data being generated for *An. gambiae*, similar experiments could be conducted to validate the role of novel polymorphisms associated with resistance and/or the cumulative effect of multiple point mutations.

Recently, Itokawa et al. (2016) demonstrated that the CRISPR/Cas9-mediated disruption of the P450 gene *Cyp9m10* in pyrethroid-resistant *C. quinquefasciatus* larvae results in an increased sensitivity to permethrin. Similar experiments may be conducted to assess the effects of the knockout of single P450 genes, including

Cyp6m2 and *Cyp6p3*, or entire subfamilies in resistant field caught populations. Similarly, the effects of gene duplications and multiple copies of P450 genes could be assessed.

CRISPR/Cas9 will also facilitate studies aimed at unveiling the regulation of the overexpression of P450 genes in *Anopheles*. Such experiments may include investigating the promoter regions of these genes by inducing point mutations at sites critical for gene regulation. Additonally, CRISPR/Cas9 will also greatly ease investigations of the genomic context in which P450s are expressed and allow to exploit patterns of expression of interest by repositioning their sequences along the genome. This could for example involve placing P450 sequences under the control of non native promoters driving patterns of expression of interest or substituting genes dispalying a desired pattern of expression with the targeted P450 gene.

There is no doubt in the near future the CRISPR/Cas9 technology will be largely employed to design inventive experiments to further explore the molecular bases of insecticide resistance in *An. gambiae* and other disease vectors.

Appendix A

General Methods

DNA extraction

Single female mosquitoes were ground with an electrical pestle and genomic DNA extracted using DNeasy Blood & Tissue Kit (Qiagen) following manufacturer's protocol. Final elution was performed in 100 µl of dH_2O.

Polymerase Chain Reaction (PCR)

PCR reaction were set up using 2.5 mM dNTPs mix (Sigma), 10 µM primers (Integrated DNA Technologies) working solutions, and either DreamTaq DNA polymerase (Thermo Scientific), Phire Hot Start II DNA Polymerase (Thermo Scientific) or Phusion High-Fidelity DNA Polymerase (Thermo Scientific) according to manufacturer's guidelines using a Biorad T100 thermal cycler.

Agarose gel electrophoresis

DNA was visualised on 0.8-2% agarose (Bioline) gels prepared in TAE buffer (Severn Biotech) and stained with Ethidium Bromide (Sigma) or Midori Green (Gene Flow). Samples were loaded using 6x gel loading dye (Thermo Scientific) and bands sized using 100 bp, 1 kb or 1 kb plus DNA Ladders (Thermo Scientific). Images were taken in a G-Box transilluminator (SynGene) using GeneSnap image acquisition software (SynGene).

DNA purification and clean-up

PCR products were mixed with 600 µl of buffer P4 (66.9 g of Guanidine hydrochloride in 33.3 ml of P3, pH 5, volume adjusted at 100 ml with dH_2O, 0.22 µm filter sterilised, 1.5 g diatomaceous earth), passed through a spin column (Wizard MiniColumns, Promega) and washed twice with buffer P5 (200 mM NaCl, 20 mM Tris, 5 mM EDTA, 1 volume ethanol) before being re-suspended in 30 µl of dH_2O.

For purifying DNA from agarose gels the band of interest was cut out the gel and incubated in 0.8-1 ml of buffer QG (Sigma) supplemented with 1.5 mg/ml diatomaceous earth (Sigma) at 50 ˚C until completely dissolved. Sample was then

passed through a spin column, washed twice with buffer P5, and re-suspended in 30 µl of dH_2O.

Ethanol precipitation of DNA

$1/10^{th}$ volume of 3M sodium acetate was added to the solution of DNA to precipitate followed by 2.5 volumes of ice cold ethanol. Solution was then stored at -20 ˚C for 1h or overnight to allow for precipitation. DNA pellet was collected after 20-minute centrifugation at 4 ˚C, resuspended in 1 ml of 70% ice cold ethanol, and spun for 2 minutes at 4 ˚C. Supernatant ethanol was removed, pellet air dried and finally resuspended in a desired amount of dH_2O.

Restriction endonuclease digestion

All restriction enzyme digestions were carried out using restriction enzymes from New England Biolabs according to manufacturer's instructions.

Ligation of DNA

To ligate DNA fragments into a plasmid vector 3:1 insert-to-vector molar ratio was calculated and 50-100 ng of digested vector used. Ligations were carried out using T4 DNA ligase (Thermo Scientific) in a final volume of 10 µl and incubated at 16 ˚C overnight or for 1 h at room temperature.

E. coli transformation

1 µl of the ligation mix was diluted 1:20 and 3 µl of cells added, placed into pre-chilled electroporation cuvettes (Sigma) and transformed by electroporation (1.8 KV, 200 Ω, 25 µF) into MegaX DH10B™ T1R Electrocomp™ *Escherichia coli* cells (Invitrogen). After electroporation, cells were recovered in 1 ml LB-Miller broth (Fisher Scientific) and incubated at 37 ˚C for 1 h at 200rpm. 20-100 µl of bacterial culture were then plated out in LB-Miller agar plates supplemented with 100 µg/ml ampicillin (Sigma) and incubated overnight at 37 ˚C.

To set up clonal cultures from plasmid extraction, a single colony was collected from the plate and transferred into 5 ml (for miniprep) or 100 ml (for midiprep) of LB-Miller broth supplemented with 100 µg/ml ampicillin and incubated for 16 h at 37 ˚C with 200rpm.

Gibson Assembly®

To carry out Gibson cloning (Gibson et al., 2009, 2010) DNA sequences of interest were amplified using Phusion High-Fidelity DNA Polymerase (Life Technologies) following to manufacturer's guidelines and vector backbones obtained by restriction digestion. All single components were purified before being added to the Gibson master mix. Ligations were set up in a total volume of 20-25 µl using 50-100 ng of digested backbone plasmid, 0.02-0.1 pmol/µl of each fragment and 2X Gibson Assembly® Master Mix (New England Biolabs) and incubated at 50°C for 1 h. Ligations were then treated as described above.

Plasmid Minipreps

Plasmids were purified from 5 ml overnight clonal *E. coli* cultures using the Merlin Miniprep protocol based on diatomaceous earth (Sigma) purification. Bacteria pellet was prepared by centrifuging 3 ml of bacterial culture and re-suspended in buffer P1 (50 mM Tris Base, 10 mM EDTA, pH 8.0). Samples are then lysed with buffer P2 (0.2 M NaOH, 1% SDS) and P3 (1.25 M Potassium Acetate, pH 5.5), then mixed to buffer P4 (66.9 g of Guanidine hydrochloride in 33.3 ml of P3, pH 5, volume adjusted at 100 ml with dH_2O, 0.22 µm filter sterilised, 1.5 g diatomaceous earth) and passed through a spin column before being washed twice with buffer P5 (200 mM NaCl, 20 mM Tris, 5 mM EDTA, 1 volume ethanol) and re-suspended in 30 µl of dH_2O.

Plasmid Midipreps

Plasmids for microinjection were purified from 100 ml overnight clonal *E. coli* cultures using Plasmid Midi Kit (Qiagen) following manufacturer's instructions. After final elution, samples were ethanol precipitated using $1/10^{th}$ volume of 3M Sodium Acetate pH 5.2 and 2.5 volumes of ice cold 100% ethanol, washed in 70% ethanol and re-suspended in 150 µl of dH_2O.

Sequencing

Sequencing of plasmids and PCR products was performed using Sanger sequencing by Source Bioscience. Sequences were manually analysed using BioEdit Sequence Alignment Editor (Ibis Biosciences).

Mosquito rearing

Mosquitoes were maintained in insectary conditions (27±2°C, 70±10% humidity) with a photoperiod of 12h light:12h dark and 30 minutes of dawn and dusk. Sugar solution and water were provided *ad libitum* and blood meal offered to 10-12-day-old adults using human blood through Hemotek membrane feeding system. Eggs were collected on Whatman filter paper grade 3 (Sigma) 48 h after blood-feeding. Larval stages were reared in 23x23 cm plastic trays using distilled water supplemented with tonic salt (Blagdon) and were fed on ground TetraMin© fish food.

Screening of fluorescent mosquitoes

All mosquitoes were observed with Leica MZ FLIII fluorescence stereo microscope fitted with CFP, DsRed and YFP filters (Leica Microsystems).

Fluorescence pictures were taken using the LAS X Microscope Software integrated within a Leica M165 FC fluorescent stereo microscope (Leica Microsystems).

Appendix B

List of primers

Table B.1 List of primer sequences used in Chapter 2.

Primer	Sequence 5'-3'
M2fw	TTCTGATATCAAAAATGTTTAGCTTGTTGGATTTCA
M2rv	TTCTCTCGAGCTAAATCTTATCCACCTTCAACCAC
pJETseqFW	CGACTCACTATAGGGAGAGCGGC
pJETseqRV	AAGAACATCGATTTTCCATGGCAG
P3fw1	TTCTAGATCTAACGATGGAGCTAATTAACGCGGTGCTGG
P3rv1	GGTACAGCTCCTGATGGATGTCGGC
P3EcoRIfw	TTCTGAATTCAACGATGGAGCTAATTAACGCGGTCGTGG
P3rv2	TTCTCTCGAGCTACAACTTTTCCACCTTCAAG
piggyBacR-R2	TTTGCCTTTCGCCTTATTTTAGA
Red-seq4R	CGAGGGTTCGAAATCGATAA
M2intFW	CGTATAGGGCTGGCGTATCT
P3intFW	GCTGAGAAAGTTCCGCTTCT
ITRL1R	TGACGAGCTTGTTGGTGAGGATTCT
qM2fw	TACGATGACAACAAGGGCAAG
qM2rv	GCGATCGTGGAAGTACTGG
qP3fw	TGTGATTGACGAAACCCTTCGGAAG
qP3sub	ATAGTCCACAGATGGTACGCGGG
qS7fw	AGAACCAGCAGACCACCATC
qS7rv	GCTGCAAACTTCGGCTATTC
qUBfw	CGACTCCGTGGTGGTATCAT
qUBrv	GCACTTGCGGCAAATCATCT

Cyp6m2 sequence alignment

Figure B.1 *Cyp6m2* coding sequence alignment. M2 is the consensus sequence obtained from sequencing with pJETseqFW and pJETseqRV primers and present in pUASm2. PB13:CYP6M2 is the template plasmid from which the sequence was amplified.

```
M2              ATGTTTAGCTTGTTGGATTTCACATTTCTGGTGGCGGCACTGGCCGCCGGCTTGTACTAC
PB13:CYP6M2     ATGTTTAGCTTGTTGGATTTCACATTTCTGGTGGCGGCACTGGCCGCCGGCTTGTACTAC
                ************************************************************

M2              TATCTCGATCGGAAGCGCTCCTACTGGCAGGATCGTGGTGTGCCCGGTCCGAAGGGTGAG
PB13:CYP6M2     TATCTCGATCGGAAGCGCTCCTACTGGCAGGATCGTGGTGTGCCCGGTCCGAAGGGTGAG
                ************************************************************

M2              CTGCTGTTCGGGAACTTTGGCTCGATCGGCACGAAGGAACACATTACCGTGCCGTTTAAG
PB13:CYP6M2     CTGCTGTTCGGGAACTTTGGCTCGATCGGCACGAAGGAACACATTACCGTGCCGTTTAAG
                ************************************************************

M2              AGGATCTACGATGACAACAAGGGCAAGCATCCGTTCGCGGGCATGTATCAGTTCGTGAAG
PB13:CYP6M2     AGGATCTACGATGACAACAAGGGCAAGCATCCGTTCGCGGGCATGTATCAGTTCGTGAAG
                ************************************************************

M2              CCGGTGGCACTGATTACCGATCTGGAGCTGCTGAAGTGTGTGTTTGTGAAGGATTTCCAG
PB13:CYP6M2     CCGGTGGCACTGATTACCGATCTGGAGCTGCTGAAGTGTGTGTTTGTGAAGGATTTCCAG
                ************************************************************
```

```
M2              TACTTCCACGATCGCGGTACGTTCTACAATGAGCGGGATGATCCACTGTCGGCGCATCTG
PB13:CYP6M2     TACTTCCACGATCGCGGTACGTTCTACAATGAGCGGGATGATCCACTGTCGGCGCATCTG
                ************************************************************

M2              TTCAATCTGGAGGGTCAGAAGTGGCGCTCGCTGCGCAACAAACTCTCGCCCACGTTCACG
PB13:CYP6M2     TTCAATCTGGAGGGTCAGAAGTGGCGCTCGCTGCGCAACAAACTCTCGCCCACGTTCACG
                ************************************************************

M2              TCCGGCAAGATGAAGATGATGTTCCCCACGATCGTGACTGCCGGCAAACAGTTTAAGGAC
PB13:CYP6M2     TCCGGCAAGATGAAGATGATGTTCCCCACGATCGTGACTGCCGGCAAACAGTTTAAGGAC
                ************************************************************

M2              TTTATGGAGGAAACGGTGCTGCGTGAGAACGAGTTCGAGCTGAAGGATCTGCTGGCACGG
PB13:CYP6M2     TTTATGGAGGAAACGGTGCTGCGTGAGAACGAGTTCGAGCTGAAGGATCTGCTGGCACGG
                ************************************************************

M2              TTCACGACGGACGTGATCGGGATGTGTGCGTTCGGCATTGAGTGTAACAGTATGCGCAAT
PB13:CYP6M2     TTCACGACGGACGTGATCGGGATGTGTGCGTTCGGCATTGAGTGTAACAGTATGCGCAAT
                ************************************************************

M2              CCGGATGCGGAGTTCCGTGCGATGGGTCGCAAGATCTTTGAGATCTCGCCCGGTACGTTC
PB13:CYP6M2     CCGGATGCGGAGTTCCGTGCGATGGGTCGCAAGATCTTTGAGATCTCGCCCGGTACGTTC
                ************************************************************

M2              AAGACGATGATGATGAATGGAATGCCCGAGTTGGCAAAGATGCTGCGCATGACACAAACC
PB13:CYP6M2     AAGACGATGATGATGAATGGAATGCCCGAGTTGGCAAAGATGCTGCGCATGACACAAACC
                ************************************************************

M2              GACAAGGATGTGTCGGACTTTTTCATGAACGCGGTGCGGGACACGATCAACTATCGCGTG
PB13:CYP6M2     GACAAGGATGTGTCGGACTTTTTCATGAACGCGGTGCGGGACACGATCAACTATCGCGTG
                ************************************************************

M2              AAGAACAACGTGCAGCGGAATGATTTCGTCGATCTGCTGATCAAGATGATGAGCAAAGAC
PB13:CYP6M2     AAGAACAACGTGCAGCGGAATGATTTCGTCGATCTGCTGATCAAGATGATGAGCAAAGAC
                ************************************************************

M2              GGAGAGAAGTCGGACGAGGATTCGCTAACGTTCAACGAAATTGCTGCACAGGCGTTTGTG
PB13:CYP6M2     GGAGAGAAGTCGGACGAGGATTCGCTAACGTTCAACGAAATTGCTGCACAGGCGTTTGTG
                ************************************************************

M2              TTTTTCCTGGCCGGGTTTGAGACTTCGTCGACTCTCCTCACATGGACGCTGTACGAGCTG
PB13:CYP6M2     TTTTTCCTGGCCGGGTTTGAGACTTCGTCGACTCTCCTCACATGGACGCTGTACGAGCTG
                ************************************************************

M2              GCGCTGAATCCAGAGGTACAGGAGAAAGGTCGTGAGTGTGTGAGAGAAATCCTGCAAAAG
PB13:CYP6M2     GCGCTGAATCCAGAGGTACAGGAGAAAGGTCGTGAGTGTGTGAGAGAAATCCTGCAAAAG
                ************************************************************

M2              CACAACGGAGAGATGTCGTACGATGCGGTCGTGGAAATGAAGTATCTTGATCAAATTCTT
PB13:CYP6M2     CACAACGGAGAGATGTCGTACGATGCGGTCGTGGAAATGAAGTATCTTGATCAAATTCTT
                ************************************************************

M2              AATGAATCACTGCGCAAATATCCACCAGTCCCGGTACATTTCCGTGTGGCTTCGAAAGAC
PB13:CYP6M2     AATGAATCACTGCGCAAATATCCACCAGTCCCGGTACATTTCCGTGTGGCTTCGAAAGAC
                ************************************************************

M2              TACCACGTCCCCGGTACGAAATCCGTCCTGGAGGCCGGTACAGCCGTCATGATCCCAGTG
PB13:CYP6M2     TACCACGTCCCCGGTACGAAATCCGTCCTGGAGGCCGGTACAGCCGTCATGATCCCAGTG
                ************************************************************

M2              CATGCCATCCATCACGATCCGGAAGTGTTCCCCAACCCCGAACAGTTCGATCCGGAGCGT
PB13:CYP6M2     CATGCCATCCATCACGATCCGGAAGTGTTCCCCAACCCCGAACAGTTCGATCCGGAGCGT
                ************************************************************

M2              TTCAGTCCGGAGCAGGAGGCAAAGCGTCACCCGTACGCTTGGACACCGTTCGGAGAGGGT
PB13:CYP6M2     TTCAGTCCGGAGCAGGAGGCAAAGCGTCACCCGTACGCTTGGACACCGTTCGGAGAGGGT
                ************************************************************
```

```
M2              CCGAGGATATGTGTTGGGCTGCGATTCGGTATGATGCAGGCCCGTATAGGGCTGGCGTAT
PB13:CYP6M2     CCGAGGATATGTGTTGGGCTGCGATTCGGTATGATGCAGGCCCGTATAGGGCTGGCGTAT
                ************************************************************

M2              CTGCTGGATGGGTTCCGGTTTGCACCAAGCTCGAAAACCGTCATCCCGATGGAACTCTCT
PB13:CYP6M2     CTGCTGGATGGGTTCCGGTTTGCACCAAGCTCGAAAACCGTCATCCCGATGGAACTCTCT
                ************************************************************

M2              AAGGAAAGTTTCATTATGGCACCGAAGGGTGGGCTGTGGTTGAAGGTGGATAAGATTTAG
PB13:CYP6M2     AAGGAAAGTTTCATTATGGCACCGAAGGGTGGGCTGTGGTTGAAGGTGGATAAGATTTAG
                ************************************************************
```

Cyp6p3 sequence alignment

Figure B.2 *Cyp6p3* coding sequence alignment. P3 is the consensus sequence obtained from sequencing with pJETseqFW and pJETseqRV primers and present in pUASp3. pCW:17α-Cyp6p3 is the template plasmid from which the sequence was amplified which lacks the first 24 bp from the native sequence (shown in small letters). Grey shaded sequence was amplified from Kisumu cDNA and fused with the rest of the sequence amplified from the plasmid template.

```
P3              atggagctaattaacgcggtgctgGCCGCGTTCATCTTCGCAGTGTCGATCGTGTATCTG
pCW:17α-Cyp6p3                          GCCGCGTTCATCTTCGCAGTGTCGATCGTGTATCTG
                                        **********************************

P3              TTCATACGCAATAAGCATAACTATTGGAAGGACAATGGGTTTCCGTACGCGCCGAATCCA
pCW:17α-Cyp6p3  TTCATACGCAATAAGCATAACTATTGGAAGGACAATGGGTTTCCGTACGCGCCGAATCCA
                ************************************************************

P3              CACTTTCTGTTCGGGCATGCGAAGGGCCAGGCCCAGACGCGGCACGGCGCCGACATCCAT
pCW:17α-Cyp6p3  CACTTTCTGTTCGGGCATGCGAAGGGCCAGGCCCAGACGCGGCACGGCGCCGACATCCAT
                ************************************************************

P3              CAGGAGCTGTACCGATACTTCAAGCAGCGGGGCGAACGGTACGGCGGCATTAGCCAGTTT
pCW:17α-Cyp6p3  CAGGAGCTGTACCGATACTTCAAGCAGCGGGGCGAACGGTACGGCGGCATTAGCCAGTTT
                ************************************************************

P3              ATCGTGCCCTCGGTGCTGGTGATCGACCCGGAGCTGGCGAAGACGATCCTGGTGAAGGAT
pCW:17α-Cyp6p3  ATCGTGCCCTCGGTGCTGGTGATCGACCCGGAGCTGGCGAAGACGATCCTGGTGAAGGAT
                ************************************************************

P3              TTTAACGTGTTTCACGATCACGGCGTGTTTACCAATGCAAAGGACGACCCGCTCACGGGA
pCW:17α-Cyp6p3  TTTAACGTGTTTCACGATCACGGCGTGTTTACCAATGCAAAGGACGACCCGCTCACGGGA
                ************************************************************

P3              CATCTGTTCGCACTGGAGGGTCAACCGTGGCGGTTGATGCGCCAGAAGCTTACGCCGACG
pCW:17α-Cyp6p3  CATCTGTTCGCACTGGAGGGTCAACCGTGGCGGTTGATGCGCCAGAAGCTTACGCCGACG
                ************************************************************

P3              TTCACCTCGGGCCGGATGAAGCAAATGTTCGGCACAATATGGGATGTGGGGCTTGAGCTG
pCW:17α-Cyp6p3  TTCACCTCGGGCCGGATGAAGCAAATGTTCGGCACAATATGGGATGTGGGGCTTGAGCTG
                ************************************************************

P3              GAAAAGTGTATGGAGCAAAGCTACAACCAACCGGAGGTTGAGATGAAGGATATCCTGGGC
pCW:17α-Cyp6p3  GAAAAGTGTATGGAGCAAAGCTACAACCAACCGGAGGTTGAGATGAAGGATATCCTGGGC
                ************************************************************

P3              CGTTTTACGACGGACGTGATTGGGACGTGCGCGTTCGGCATCGAGTGCAATACACTTAAG
pCW:17α-Cyp6p3  CGTTTTACGACGGACGTGATTGGGACGTGCGCGTTCGGCATCGAGTGCAATACACTTAAG
                ************************************************************
```

```
P3              ACGACAGACTCGGAGTTCCGCAAGTACGGCAACAAGGCGTTCGAGTTGAATACGATGATC
pCW:17α-Cyp6p3  ACGACAGACTCGGAGTTCCGCAAGTACGGCAACAAGGCGTTCGAGTTGAATACGATGATC
                ************************************************************

P3              ATGATGAAGACTTTCCTCGCGTCGTCCTACCCGACGCTGGTGCGCAATCTGCACATGAAG
pCW:17α-Cyp6p3  ATGATGAAGACTTTCCTCGCGTCGTCCTACCCGACGCTGGTGCGCAATCTGCACATGAAG
                ************************************************************

P3              ATCACGTACAACGATGTGGAGCGATTCTTCCTGGACATCGTGAAGGAAACGGTCGACTAC
pCW:17α-Cyp6p3  ATCACGTACAACGATGTGGAGCGATTCTTCCTGGACATCGTGAAGGAAACGGTCGACTAC
                ************************************************************

P3              CGGGAGGCGAACAACGTGAAGCGGAACGACTTCATGAACCTGATGCTGCAGATCAAGAAC
pCW:17α-Cyp6p3  CGGGAGGCGAACAACGTGAAGCGGAACGACTTCATGAACCTGATGCTGCAGATCAAGAAC
                ************************************************************

P3              AAGGGCAAGCTGGACGATAGTGATGACGGTAGTGTGGGCAAGGGAGAGGTCGGCATGACA
pCW:17α-Cyp6p3  AAGGGCAAGCTGGACGATAGTGATGACGGTAGTGTGGGCAAGGGAGAGGTCGGCATGACA
                ************************************************************

P3              CAGAACGAGCTAGCGGCCCAGGCGTTTGTGTTTTTCCTGGCGGGTTTTGAGACGTCGTCC
pCW:17α-Cyp6p3  CAGAACGAGCTAGCGGCCCAGGCGTTTGTGTTTTTCCTGGCGGGTTTTGAGACGTCGTCC
                ************************************************************

P3              ACCACACAAAGCTTCTGTCTGTACGAGCTGGCAAAGAACCCGGACATCCAGGAGCGGCTG
pCW:17α-Cyp6p3  ACCACACAAAGCTTCTGTCTGTACGAGCTGGCAAAGAACCCGGACATCCAGGAGCGGCTG
                ************************************************************

P3              AGAGAGGAAATTAATCGAGCTATTGCAGAGAACGGTGGAGAGGTGACGTACGACGTGGTC
pCW:17α-Cyp6p3  AGAGAGGAAATTAATCGAGCTATTGCAGAGAACGGTGGAGAGGTGACGTACGACGTGGTC
                ************************************************************

P3              ATGAACATAAAGTATTTGGACAATGTGATTGACGAAACCCTTCGGAAGTACCCACCGGTG
pCW:17α-Cyp6p3  ATGAACATAAAGTATTTGGACAATGTGATTGACGAAACCCTTCGGAAGTACCCACCGGTG
                ************************************************************

P3              GAATCGTTAACCCGCGTACCATCTGTGGACTATCTCATCCCCGGCACAAAGCATGTGATC
pCW:17α-Cyp6p3  GAATCGTTAACCCGCGTACCATCTGTGGACTATCTCATCCCCGGCACAAAGCATGTGATC
                ************************************************************

P3              CCGAAGCGAACACTGGTGCAAATTCCAGCCTACGCGATTCAACGCGATCCGGACCACTAT
pCW:17α-Cyp6p3  CCGAAGCGAACACTGGTGCAAATTCCAGCCTACGCGATTCAACGCGATCCGGACCACTAT
                ************************************************************

P3              CCCGACCCGGAACGGTTCAATCCTGATCGATTCCTACCGGAGGAAGTGAAAAAACGACAC
pCW:17α-Cyp6p3  CCCGACCCGGAACGGTTCAATCCTGATCGATTCCTACCGGAGGAAGTGAAAAAACGACAC
                ************************************************************

P3              CCGTTCACGTTCATCCCATTCGGCGAGGGACCACGCATCTGCATTGGGCTGCGGTTTGGC
pCW:17α-Cyp6p3  CCGTTCACGTTCATCCCATTCGGCGAGGGACCACGCATCTGCATTGGGCTGCGGTTTGGC
                ************************************************************

P3              TTGATGCAAACCAAGGTGGGATTGATTACGCTGCTGAGAAAGTTCCGCTTCTCGCCGTCC
pCW:17α-Cyp6p3  TTGATGCAAACCAAGGTGGGATTGATTACGCTGCTGAGAAAGTTCCGCTTCTCGCCGTCC
                ************************************************************

P3              GCGCGTACGCCCGAACGGGTAGAATACGATCCGAAAATGATAACCATAGCGCCGAAAGCG
pCW:17α-Cyp6p3  GCGCGTACGCCCGAACGGGTAGAATACGATCCGAAAATGATAACCATAGCGCCGAAAGCG
                ************************************************************

P3              GGCAACTACTTGAAGGTGGAAAAGTTGTAG
pCW:17α-Cyp6p3  GGCAACTACTTGAAGGTGGAAAAGTTGTAG
                *****************************
```

qPCR files

qPCR raw data and data analysis are reported in files named: GAL4mid-M2 adult whole.xlsx; GAL4mid-M2 adult carcasses.xlsx; GAL4mid-M2 adult midguts.xlsx; GAL4mid-P3 adult whole.xlsx; GAL4mid-P3 adult carcasses.xlsx; GAL4mid-P3 adult midguts.xlsx; GAL4oeno-M2 adult whole.xlsx; GAL4oeno-M2 pupae whole.xlsx; GAL4oeno-M2 L4 larvae whole.xlsx; GAL4oeno-M2 adult carcasses.xlsx; GAL4oeno-M2 adult abdomens.xlsx; GAL4oeno-P3 adult whole.xlsx; GAL4oeno-P3 pupae whole.xlsx; GAL4oeno-P3 L4 larvae whole.xlsx; GAL4oeno-P3 adult carcasses.xlsx; GAL4oeno-P3 adult abdomens.xlsx

Bioassay files

Bioassay raw data and analysis are reported in files named: GAL4midxM2.xlsx; GAL4midxP3; GAL4oenoxM2; GAL4oenoxP3.

Appendix C

List of primers

Table C.1 Primer sequences used in Chapter 3.

Primer name	Sequence 5'-3'
seq5'UTR-rv	TGCACCACAGTCACAGCTCACTGC
seqINTRON-fw	GAATTCGCGGAAGCAGACCGAGCC
seqINTRON-rv	ACATCAAAAATGTGTTTAACAAGAAC
1971-int-rv	ATCCAATTAAACCTACGTCAATCAA
AttB3-seqR	CTTTATGCTTCCGGCTCGTA
pUB5-GAL4-FW	GTTTTCGTTTATATTTACAGATAAAATATGAAGCTACTGTCTTCTATCGAACAAGCATG
1971-int-fw	TTGATTGACGTAGGTTTAATTGGAT
GAL4-seq-2F	AGATCCACAACATCCCGTTT
GAL4-pSL-RV	CAGCTGCAGGCGGCCGCCATATGCAAGATCTTTACTCTTTTTTTGGGTTTGGTGGG
pSL1180-1	GTGCTGCAAGGCGATTAAGT
M13fw	CGTTGTAAAACGACGGCCAGT
RT-GAL4-2R	GTCAGATGTGCCCTAGTCAGC
p9_pSL_fw	ACGTGAGTAGTTAAGATACATTGGGCTAGCATGGTATTGCCAGCCTCAGACGCGAGAGAG
p9_GAL4_rv	TAGAAGACAGTAGCTTCATGATATCTTTCGCTGCACCTTTCACTTTCCACGGG
GAL4_p9_fw	AGTGAAAGGTGCAGCGAAAGATATCATGAAGCTACTGTCTTCTATCGAACAAGC
GAL4_sequ_2F	AGATCCACAACATCCCGTTT
GAL4_SV40_rv	GAAGTAAGGTTCCTTCACAAAGATCTTACTCTTTTTTTGGGTTTGGTGGGGTATC
SV40_GAL4_fw	CCACCAAACCCAAAAAAAGAGTAAGATCTTTGTGAAGGAACCTTACTTCTGTGG
SV40_pSL_rv	CATTTAGCCGATCAATTCTAGTCACATATGAGACATGATAAGATACATTGATGAGTTTGG
pSL-Gypsy1-FW	GAGGTAATTATAACCCGGGCCCTATATATGACTAGAATTGATCGGCTAAATGGTATGGCA
Gypsy1-pUB5-RV	GAAATATTTTTTTATTCGCTAGCCAATGTATCTTAACTACTCACGTAATAAGTGTGCG
Gypsy1-pUB5-FW	GAGTAGTTAAGATACATTGGCTAGCGAATAAAAAAATATTTCTTAATAATATTCTAAC
pUB5-GAL4-RV	GAAGACAGTAGCTTCATATTTTATCTGTAAATATAAACGAAAACAAC
pUB5-GAL4-FW	GTTTTCGTTTATATTTACAGATAAAATATGAAGCTACTGTCTTCTATCGAACAAGCATG
GAL4-pSL-RV	CAGCTGCAGGCGGCCGCCATATGCAAGATCTTTACTCTTTTTTTGGGTTTGGTGGG
pSL-pUB3-FW	TAATTATAACCCGGGCCCTATATATGAGATCTTTCGTTGAATAAAGCATATTGAAGCTTC
pUB3-Gypsy2-RV	AGCCGATCAATTCTAGTCATATGCCGTCGAAATTGTTTTACAATGACAATTTT
pUB3-Gypsy2-FW	GTAAAACAATTTCGACGGCATATGACTAGAATTGATCGGCTAAATGGTATGGCA
Gypsy2-attP-RV	GTCAGTCGCGCGAGCGCGCCGCGGCAATGTATCTTAACTACTCACGTAATAAGTGTGCG
Gypsy2-attP-FW	AGTAGTTAAGATACATTGCCGCGGCGCGCTCGCGCGACTGACGGTCGTAAGCAC
attP-pSL-RV	AGCTGCAGGCGGCCGCCATATGCACGAAGCCCCGGCGGCAACCCTCAGCG
SpeI-6459-EcoRV-fw	TTCTACTAGTTCCGTTTAGGTAGAGAACTT
SpeI-6459-EcoRV-rv	TTCTGATATCACGATAAACAAAATAGACAC
SpeI-2182-EcoRV-fw	TTCTACTAGTAAGACAAATCGGCCCGTGCT
SpeI-2182-EcoRV-rv	TTCTGATATCTTTCTACAATAGAAAGTGGG
SpeI-6782-EcoRV-fw	TTCTACTAGTGGCTATTCCGATGCCTTTTT
SpeI-6782-EcoRV-rv	TTCTGATATCTTTTGATGGATCTGGTCTGG
SpeI-3864-EcoRV-fw	TTCTACTAGTTCTAGCGAGGCATGGCAGGA
SpeI-3864-EcoRV-rv	TTCTGATATCTGTTGCGTTCCGGTGGAAAA
SpeI-4654-EcoRV-fw	TTCTACTAGTATAGAATGTCGGTGCCCA
SpeI-4654-EcoRV-rv	TTCTGATATCTGCAATATTATCCCTGTT
SpeI-12167-EcoRV-fw	TTCTACTAGTATGGTATTGCCAGCCTCA
SpeI-12167-EcoRV-rv	TTCTGATATCTTTCGCTGCACCTTTCAC
SpeI-10572-EcoRV-fw	TTCTACTAGTTCTGTACGATCGATGCTA
SpeI-10572-EcoRV-rv	TTCTGATATCTGGTTAGGTATGACGGCC
SpeI-11050-EcoRV-fw	TTCTACTAGTTTGTTCGTGTGATCGATC
SpeI-11050-EcoRV-rv	TTCTGATATCGATTAGTGCGGTAGGACG
AflII-2587-EcoRV-fw	TTCTCTTAAG TTAACATCTGCTGGATATTA
AflII-2587-EcoRV-rv	TTCTGATATC CGTTTCCGGGTTTCCGTTCC
NheI-1823-EcoRV-fw	TTCTGCTAGCTCGGTTTAAATAAAAACATT
AflII-1823-EcoRV-rv	TTCTGATATCCGTCAAAAGTCCACGGGCAC
AflII-11426-EcoRV-fw	TTCTCTTAAGGCAAAAAGAATCAAATAGTA
AflII-11426-EcoRV-rv	TTCTGATATCTCTGCCAACTTGAGCAGCGC
SpeI-2629-EcoRV-fw	TTCTACTAGTCGTTCGAAACCGCCCAAC
SpeI-2629-EcoRV-rv	TTCTGATATCTCTGCACGCGGTCGTTGT
SpeI-10364-EcoRV-fw	TTCTACTAGTACATTTACCCTATTCTCA
SpeI-10364-EcoRV-rv	TTCTGATATCTTTGCAACGGACTGAACG

SpeI-10975-EcoRV-fw	TTCTACTAGTAAAAACACACATAGTTGG
SpeI-10975-EcoRV-rv	TTCTGATATCCTCACGTGCCGACACTCG
ITRL1F	ATCAGTGACACTTACCGCATTGACA
ITRR1F	TACGCATGATTATCTTTAACGTA
A10_insert_rv	ACATGTTTTCGCATTGAATCTG
A10_R_check_rv	AACCTTCCAGCAATCCACAC
A8_L_check_rv	ATGGTTCGCTGTGTTGTTCA
A8_R_check_fw2	CATCACGCTTTCATGCATGC
piggyBacR-R2	TTTGCCTTTCGCCTTATTTTAGA
Red-seq4R	CGAGGGTTCGAAATCGATAA
P6_int_rv	TCTGATCATACGGTTCACGTTC
ITRL1R	TGACGAGCTTGTTGGTGAGGATTCT

Sequencing files

The full sequence of plasmid pPUBc_GAL4 (p155) is reported in a file named p155sequence.docx. This includes sequences of the following fragments: Gypsy1 (Gyp1), PUBc 5' region (PUB5), GAL4, SV40, PUBc 3' region (PUB3), Gypsy2 (Gyp2), and attP-right (attPr).

Sequences of candidate ubiquitous genes are reported in files named: AGAP004654.docx; AGAP012167.docx; AGAP010572.docx; AGAP011050.docx; AGAP003864.docx; AGAP006459.docx; AGAP006782.docx.

Sequences of candidate Malpighian tubule-specific genes are reported in files named: AGAP002587.docx; AGAP001823.docx; AGAP002629.docx; AGAP010975.docx

Expression of candidate genes from MozAtlas

Figure C.1 Expression levels of candidate ubiquitous (**A**) and Malpighian tubule-specific (**B**) genes in the carcass, head, Malpighian tubules, midgut, ovaries and salivary glands of adult female An. gambiae mosquitoes. Data was retrieved from the MozAtlas database where it is expressed as log_2 fluorescence values obtained from microarray experiments (Baker et al., 2011).

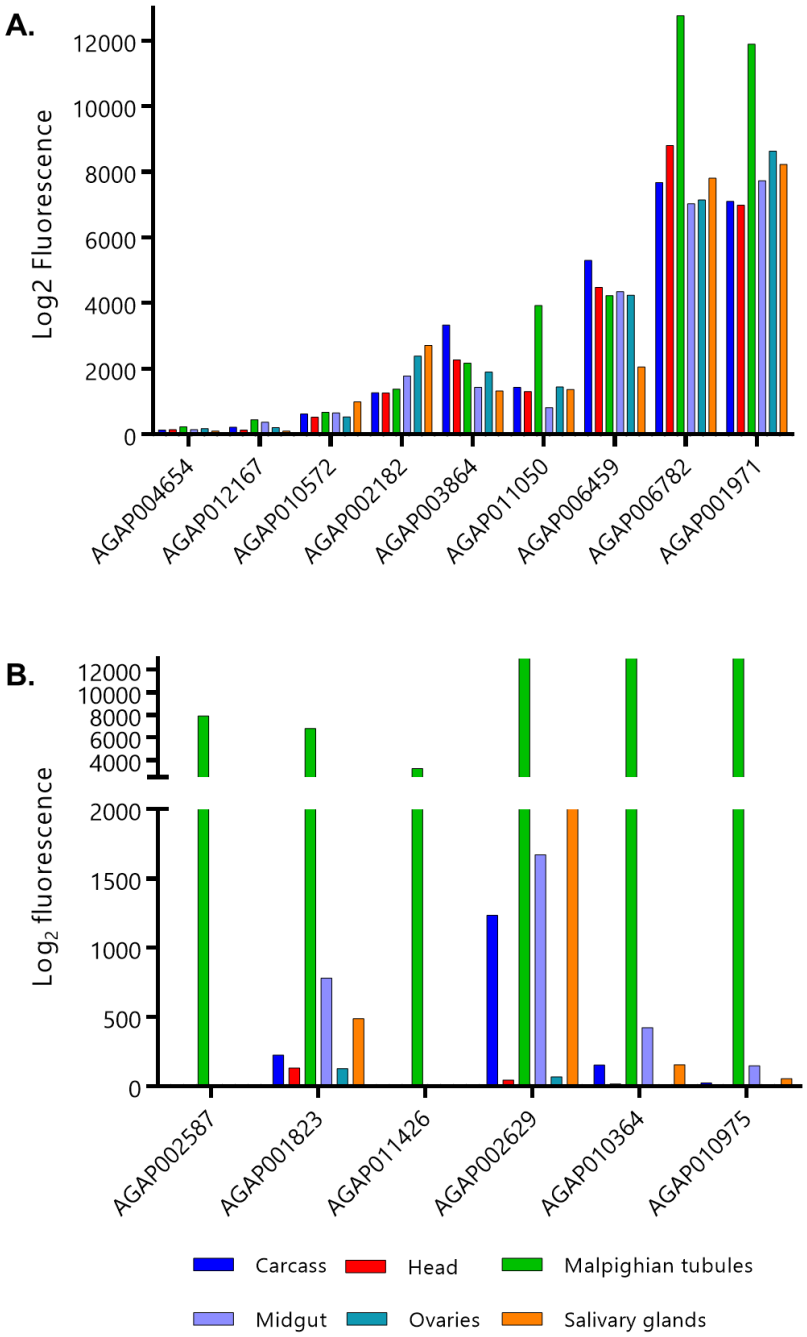

Table C.2 Results of the One-way ANOVA with multiple pairwise comparison analysis to assess statistical differences between relative activity of putative ubiquitous promoters.

Dunnett's multiple comparisons test	**95% CI of diff.**	**Significance**
pUAS-Luc vs. pBPnucl	-81.88 to 67.14	ns
pUAS-Luc vs. pPGI	-153.8 to -4.827	*
pUAS-Luc vs. pLTV1	-116.4 to 32.66	ns
pUAS-Luc vs. pALDred	-114.6 to 34.38	ns
pUAS-Luc vs. pAGAP003864	-96.05 to 86.47	ns
pUAS-Luc vs. pSUI1	-177.6 to 4.943	ns
pUAS-Luc vs. pATPcar	-103.7 to 78.77	ns
pUAS-Luc vs. pPUBc	-429.1 to -272.8	****

Tukey's multiple comparisons test	**95% CI of diff.**	**Significance**
pBPnucl vs. pPGI	-160.1 to 16.16	ns
pBPnucl vs. pLTV1	-122.6 to 53.65	ns
pBPnucl vs. pALDred	-120.9 to 55.37	ns
pBPnucl vs. pAGAP003864	-105.4 to 110.5	ns
pBPnucl vs. pSUI1	-186.9 to 28.99	ns
pBPnucl vs. pATPcar	-113.1 to 102.8	ns
pBPnucl vs. pPUBc	-436.0 to -251.2	****
pBPnucl vs. pUAS-Luc	-80.76 to 95.50	ns
pPGI vs. pLTV1	-50.64 to 125.6	ns
pPGI vs. pALDred	-48.92 to 127.3	ns
pPGI vs. pAGAP003864	-33.39 to 182.5	ns
pPGI vs. pSUI1	-114.9 to 101.0	ns
pPGI vs. pATPcar	-41.09 to 174.8	ns
pPGI vs. pPUBc	-364.1 to -179.2	****
pPGI vs. pUAS-Luc	-8.793 to 167.5	ns
pLTV1 vs. pALDred	-86.41 to 89.85	ns
pLTV1 vs. pAGAP003864	-70.88 to 145.0	ns
pLTV1 vs. pSUI1	-152.4 to 63.47	ns
pLTV1 vs. pATPcar	-78.57 to 137.3	ns
pLTV1 vs. pPUBc	-401.6 to -216.7	****
pLTV1 vs. pUAS-Luc	-46.28 to 130.0	ns
pALDred vs. pAGAP003864	-72.60 to 143.3	ns
pALDred vs. pSUI1	-154.1 to 61.76	ns
pALDred vs. pATPcar	-80.29 to 135.6	ns
pALDred vs. pPUBc	-403.3 to -218.4	****
pALDred vs. pUAS-Luc	-48.00 to 128.3	ns
pAGAP003864 vs. pSUI1	-206.2 to 43.11	ns
pAGAP003864 vs. pATPcar	-132.3 to 116.9	ns
pAGAP003864 vs. pPUBc	-457.7 to -234.7	****
pAGAP003864 vs. pUAS-Luc	-103.1 to 112.7	ns
pSUI1 vs. pATPcar	-50.81 to 198.5	ns
pSUI1 vs. pPUBc	-376.1 to -153.2	****
pSUI1 vs. pUAS-Luc	-21.62 to 194.3	ns
pATPcar vs. pPUBc	-450.0 to -227.0	****
pATPcar vs. pUAS-Luc	-95.45 to 120.4	ns
pPUBc vs. pUAS-Luc	258.5 to 443.4	****

Figure C.2 Agarose gel electrophoresis showing insertion sites in A8 and A10 line confirmed by PCR using a primer binding in the predicted genomic location and the other annealing to the transgenic construct. A10: genomic regions external to the left (L) and right (R) piggyBac arms at the insertion site in the A10 line. A8: genomic regions external to the left (L) and right (R) piggyBac arms at the insertion site in the A8 line. Ladder is GeneRuler 100 bp (Thermo Scientific). Expected product sizes are: 516 bp for A10L, 447 for A10R, 358 bp for A8L, and 132 bp for A8R. Sequence obtained for A8L was ~150 bp shorter than expected due to miss-annealing of the primer onto the left arm of the piggyBac.

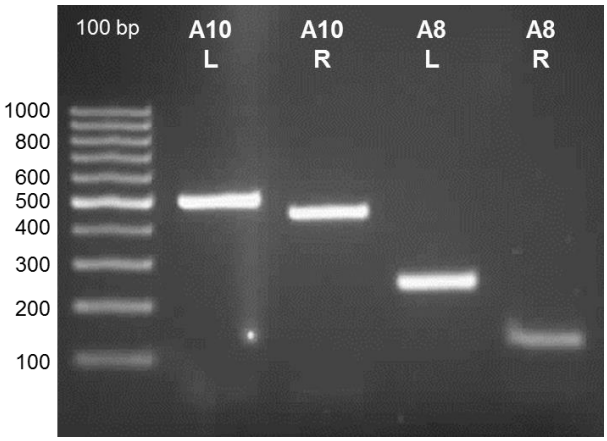

Figure C.3 Agarose gel electrophoresis showing results for inverse-PCR on regions flanking the piggyBac left arm after TaqαI digestion and self-ligation of genomic DNA isolated from isofemale lines. Ladder is GeneRuler 1 kb Plus (Thermo Scientific).

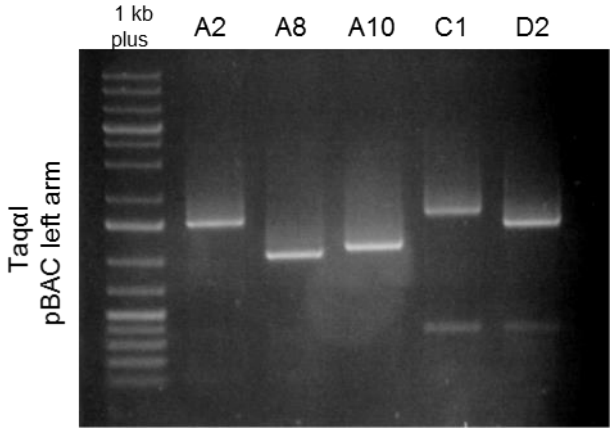

Figure C.4 Example of phenotype variegation in the PUBc_GAL4 lines. mCherry phenotypes in L2-3 larvae derived from PUBc_GAL4 F_1 transformant males. These are also representative of the phenotypes observed in the progeny of single laying females.

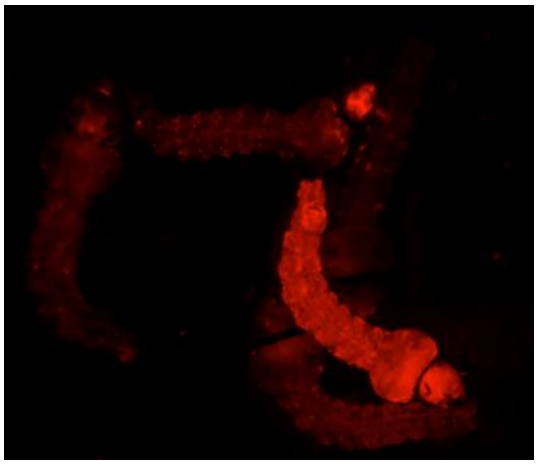

Microinjection experiments that did not yield transgenics

Table C.3 List of microinjections of ubiquitous candidate promoters into G3 wild type embryos.

Experiment date	Plasmid Injected	Concentration injected DNA (ng/µl)	No. eggs	No. larvae hatched (%)	Transient CFP expression (%)	No. F_0 adults
20/11/15	PUBc_GAL4	250	332	14 (4%)	NS	13
25-27/11/15	PUBc_GAL4	250	308	21 (7%)	0 (0%)	17
	Un-injected	N/A	106	97 (91.5%)	N/A	N/A
	Inj. buffer	N/A	194	2 (1%)	N/A	N/A
	Other operator	250	157	7 (5%)	3 (43%)	4
16-17/12/15	PUBc_GAL4	250	686	166 (24%)	NS	118
	Un-injected	N/A	58	48 (83%)	N/A	N/A
	Inj. buffer	N/A	116	60 (52%)	N/A	N/A
18-19/01/16	PUBc_GAL4	300	784	185 (24%)	10 (5%)	127
	Inj. buffer	N/A	56	4 (7%)	N/A	N/A
04-05/02/16	PGI_GAL4	300	935	380 (41%)	NS	262

N/A: not applicable; NS: not screened.

Table C.4 List of microinjections of Malpighian-specific candidate promoters into the A11 docking lines.

Experiment date	Plasmid Injected	Concentration injected DNA (ng/µl)	No. eggs	No. larvae hatched (%)	Transient CFP expression (%)	No. F_0 adults
01-02/10/15	P14	250	508	N/A	NS	20
15/10/15	P14	300	429	31 (7%)	NS	17
16/10/15	P16	300	454	34 (7.5%)	NS	18
23/10/15	P16	300	155	6 (3%)	NS	N/A
10/11/15	P16	300	118	9 (8%)	4	3
17-18/11/15	VATG (P6)	300	611	31 (5%)	NS	22
23-24/11/15	VATG (P6)	300	571	18 (3%)	NS	10
07-08/12/15	VATG (P6)	265	677	120 (18%)	9	88
17-18/02/16	P14	350	763	223 (29%)	NS	143

N/A: not applicable; NS: not screened.

Appendix D

qPCR files

qPCR raw data and data analysis are reported in files named: A10xM2adults.xlsx; A10xP3adults.xlsx; A8xM2adults.xlsx; A8xP3adults.xlsx.

Bioassay files

Bioassay raw data and analysis are reported in files named: A10xM2.xlsx; A10xP3.xlsx; A8xM2.xlsx; A8xP3.xlsx; Malathion all crosses

References

Abdalla, H., Wilding, C.S., Nardini, L., Pignatelli, P., Koekemoer, L.L., Ranson, H. & Coetzee, M. (2014). Insecticide resistance in Anopheles arabiensis in Sudan: temporal trends and underlying mechanisms. Parasites & Vectors. 7 (1). p.p. 213.

Abraham, E.G., Donnelly-Doman, M., Fujioka, H., Ghosh, A., Moreira, L. & Jacobs-Lorena, M. (2005). Driving midgut-specific expression and secretion of a foreign protein in transgenic mosquitoes with AgAper1 regulatory elements. Insect Molecular Biology. 14 (3). p.pp. 271–279.

Aguiar, M., Masse, R. & Gibbs, B.F. (2005). Regulation of Cytochrome P450 by Posttranslational Modification. Drug Metabolism Reviews. 37 (2). p.pp. 379–404.

Ahmad, M., Denholm, I. & Bromilow, R.H. (2006). Delayed cuticular penetration and enhanced metabolism of deltamethrin in pyrethroid-resistant strains of Helicoverpa armigera from China and Pakistan. Pest Management Science. 62 (9). p.pp. 805–810.

Ahoua Alou, L.P., Koffi, A.A., Adja, M.A., Tia, E., Kouassi, P.K., Koné, M. & Chandre, F. (2010). Distribution of ace-1R and resistance to carbamates and organophosphates in Anopheles gambiae s.s. populations from Côte d'Ivoire. Malaria Journal. 9 (1). p.p. 167.

Allen, M.L., O'Brochta, D.A., Atkinson, P.W. & Levesque, C.S. (2001). Stable, Germ-Line Transformation of Culex quinquefasciatus (Diptera: Culicidae). Journal of Medical Entomology. 38 (5). p.pp. 701–710.

Alphey, L., Benedict, M., Bellini, R., Clark, G.G., Dame, D.A., Service, M.W. & Dobson, S.L. (2010). Sterile-Insect Methods for Control of Mosquito-Borne Diseases: An Analysis. Vector-Borne and Zoonotic Diseases. 10 (3). p.pp. 295–311.

Amenya, D.A., Naguran, R., Lo, T.-C.M., Ranson, H., Spillings, B.L., Wood, O.R., Brooke, B.D., Coetzee, M. & Koekemoer, L.L. (2008). Over expression of a cytochrome P450 (CYP6P9) in a major African malaria vector, Anopheles Funestus, resistant to pyrethroids. Insect molecular biology. 17 (1). p.pp. 19–25.

Amichot, M., Tarés, S., Brun-Barale, A., Arthaud, L., Bride, J.M. & Bergé, J.B. (2004). Point mutations associated with insecticide resistance in the Drosophila cytochrome P450 Cyp6a2 enable DDT metabolism. European Journal of Biochemistry. 271 (7). p.pp. 1250–1257.

Anderson, M.A.E., Gross, T.L., Myles, K.M. & Adelman, Z.N. (2010). Validation of novel promoter sequences derived from two endogenous ubiquitin genes in transgenic Aedes aegypti. Insect Molecular Biology. 19 (4). p.pp. 441–449.

Anthony, N.M., Harrison, J.B. & Sattelle, D.B. (1993). GABA receptor molecules of insects. Exs. 63 (614). p.pp. 172–209.

Antonio-Nkondjio, C., Poupardin, R., Tene, B.F., Kopya, E., Costantini, C., Awono-Ambene, P. & Wondji, C.S. (2016). Investigation of mechanisms of bendiocarb resistance in Anopheles gambiae populations from the city of Yaoundé, Cameroon. Malaria Journal. 15 (1). p.p. 424.

Antonova, Y., Alvarez, K.S., Kim, Y.J., Kokoza, V. & Raikhel, A.S. (2009). The role of NF-kappaB factor REL2 in the Aedes aegypti immune response. Insect Biochem Mol Biol. 39 (4). p.pp. 303–314.

Aryan, A., Anderson, M.A.E., Myles, K.M. & Adelman, Z.N. (2013). TALEN-Based Gene Disruption in the Dengue Vector Aedes aegypti. PLoS ONE. 8 (3).

Asidi, A.N., N'Guessan, R., Koffi, A.A., Curtis, C.F., Hougard, J.-M., Chandre, F., Corbel, V., Darriet, F., Zaim, M. & Rowland, M.W. (2005). Experimental hut evaluation of bednets treated with an organophosphate (chlorpyrifos-methyl) or a pyrethroid (lambdacyhalothrin) alone and in combination against insecticide-resistant Anopheles gambiae and Culex quinquefasciatus mosquitoes. Malaria Journal. 4 (1). p.p. 25

Atkinson, P.W. & O'Brochta, D.A. (1999). Genetic transformation of non-drosophilid insects by transposable elements. Annals of the Entomological Society of America. 92 (6). p.pp. 930–936.

Bagi, J., Grisales, N., Corkill, R., Morgan, J.C., N'Falé, S., Brogdon, W.G. & Ranson, H. (2015). When a discriminating dose assay is not enough: measuring the intensity of insecticide resistance in malaria vectors. Malaria Journal. 14 (1). p.p. 210.

Baker, D.A., Nolan, T., Fischer, B., Pinder, A., Crisanti, A. & Russell, S. (2011). A comprehensive gene expression atlas of sex- and tissue-specificity in the malaria vector, Anopheles gambiae. BMC Genomics. 12 (1). p.p. 296.

Balabanidou, V., Kampouraki, A., MacLean, M., Blomquist, G.J., Tittiger, C., Juárez, M.P., Mijailovsky, S.J., Chalepakis, G., Anthousi, A., Lynd, A., Antoine, S., Hemingway, J., Ranson, H., Lycett, G.J. & Vontas, J. (2016). Cytochrome P450 associated with insecticide resistance catalyzes cuticular hydrocarbon production in Anopheles gambiae. Proceedings of the National Academy of Sciences. 113 (33). p.pp. 9268–9273.

Barrangou, R., Fremaux, C., Deveau, H., Richards, M., Boyaval, P., Moineau, S., Romero, D.A. & Horvath, P. (2007). CRISPR Provides Acquired Resistance Against Viruses in Prokaryotes. Science. 315 (5819). p.pp. 1709–1712.

Bass, C., Williamson, M.S., Wilding, C.S., Donnelly, M.J. & Field, L.M. (2007). Identification of the main malaria vectors in the Anopheles gambiae species complex using a TaqMan real-time PCR assay. Malar J. 6. p.p. 155.

Bateman, J.R., Lee, A.M. & Wu, C.T. (2006). Site-specific transformation of Drosophila via PhiC31 integrase-mediated cassette exchange. Genetics. 173 (2). p.pp. 769–777.

Bautista, M.A.M., Miyata, T., Miura, K. & Tanaka, T. (2009). RNA interference-mediated knockdown of a cytochrome P450, CYP6BG1, from the diamondback moth, Plutella xylostella, reduces larval resistance to permethrin. Insect Biochemistry and Molecular Biology. 39 (1). p.pp. 38–46.

Behura, S.K., Sarro, J., Li, P., Mysore, K., Severson, D.W., Emrich, S.J. & Duman-Scheel, M. (2016). High-throughput cis-regulatory element discovery in the vector mosquito Aedes aegypti. BMC Genomics. 17 (1). p.p. 341.

Berghammer, A., Bucher, G., Maderspacher, F. & Klingler, M. (1999). A system to efficiently maintain embryonic lethal mutations in the flour beetle Tribolium castaneum. Development Genes and Evolution. 209 (6). p.pp. 382–388.

Berkman, C.E., Quinn, D. a & Thompson, C.M. (1993). Interaction of acetylcholinesterase with the enantiomers of malaoxon and isomalathion. Chemical research in toxicology. 6 (5). p.pp. 724–30.

Bhatt, S., Weiss, D.J., Cameron, E., Bisanzio, D., Mappin, B., Dalrymple, U., Battle, K.E., Moyes, C.L., Henry, A., Penny, M.A., Smith, T.A., Bennett, A., Yukich, J., Eisele, T.P., Eckhoff, P.A., Wenger, E.A., Brie, O., Griffin, J.T., Fergus, C.A., Lynch, M., Lindgren, F., Cohen, J.M., Murray, C.L.J., Smith, D.L., Hay, S.I., Cibulskis, R.E. & Gething, P.W. (2015). The effect of malaria control on Plasmodium falciparum in Africa between 2000 and 2015. Nature. p.pp. 1–9.

Bian, G., Shin, S.W., Cheon, H.-M., Kokoza, V. & Raikhel, A.S. (2005). Transgenic alteration of Toll immune pathway in the female mosquito Aedes aegypti. Proceedings of the National Academy of Sciences of the United States of America. 102 (38). p.pp. 13568–73.

Biedler, J.K., Qi, Y., Pledger, D., Macias, V.M., James, A.A., Tu, Z. & Tu, Z. (2014). Maternal germline-specific genes in the Asian malaria mosquito Anopheles stephensi: characterization and application for disease control. G3 (Bethesda, Md.). 5 (2). p.pp. 157–66.

Blandin, S., Moita, L.F., Köcher, T., Wilm, M., Kafatos, F.C. & Levashina, E. a (2002). EMBO reports Reverse genetics in the mosquito Anopheles gambiae: targeted disruption of the Defensin gene. 3 (9). p.pp. 852–856.

Blandin, S., Shiao, S.H., Moita, L.F., Janse, C.J., Waters, A.P., Kafatos, F.C. & Levashina, E.A. (2004). Complement-like protein TEP1 is a determinant of vectorial capacity in the malaria vector Anopheles gambiae. Cell. 116 (5). p.pp. 661–670.

Boisson, B., Jacques, J.C., Choumet, V., Martin, E., Xu, J., Vernick, K. & Bourgouin, C. (2006). Gene silencing in mosquito salivary glands by RNAi. FEBS Letters. 580 (8). p.pp. 1988–1992.

Bonizzoni, M., Ochomo, E., Dunn, W.A., Britton, M., Afrane, Y., Zhou, G., Hartsel, J., Lee, M.-C., Xu, J., Githeko, A., Fass, J. & Yan, G. (2015). RNA-seq analyses of changes in the Anopheles gambiae transcriptome associated with resistance to pyrethroids in Kenya: identification of candidate-resistance genes and candidate-resistance SNPs. Parasites & Vectors. 8 (1). p.p. 474.

Brand, A.H. & Perrimon, N. (1993). Targeted gene expression as a means of altering cell fates and generating dominant phenotypes. Development (Cambridge, England). 118 (2). p.pp. 401–15.

Brogdon, W.G. & McAllister, J.C. (1998). Simplification of adult mosquito bioassays through use of time-mortality determinations in glass bottles. Journal of the American Mosquito Control Association. 14 (2). p.pp. 159–164.

Brown, A.E. (2003a). Comparative analysis of DNA vectors at mediating RNAi in Anopheles mosquito cells and larvae. Journal of Experimental Biology. 206 (11). p.pp. 1817–1823.

Brown, A.E. (2003b). Stable and heritable gene silencing in the malaria vector Anopheles stephensi. Nucleic Acids Research. 31 (15). p.p. 85e–85.

Brun, A., Cuany, A., Le Mouel, T., Berge, J. & Amichot, M. (1996). Inducibility of the Drosophila melanogaster cytochrome P450 gene, CYP6A2, by phenobarbital in insecticide susceptible or resistant strains. Insect Biochemistry and Molecular Biology. 26 (7). p.pp. 697–703.

Bryan, G.J., Jacobson, J.W. & Hartl, D.L. (1987). Heritable somatic excision of a Drosophila transposon. Science (New York, N.Y.). 235 (4796). p.pp. 1636–8.

Campbell, P.M., Newcomb, R.D., Russell, R.J. & Oakeshott, J.G. (1998). Two different amino acid substitutions in the ali-esterase, E3, confer alternative types of organophosphorus insecticide resistance in the sheep blowfly, Lucilia cuprina. Insect Biochemistry and Molecular Biology. 28 (3). p.pp. 139–150.

Carballar-Lejarazú, R., Jasinskiene, N. & James, A. a (2013). Exogenous gypsy insulator sequences modulate transgene expression in the malaria vector mosquito, Anopheles stephensi. Proceedings of the National Academy of Sciences of the United States of America. 110 (18). p.pp. 7176–7181.

Cariño, F.A., Koener, J.F., Plapp, F.W. & Feyereisen, R. (1994). Constitutive overexpression of the cytochrome P450 gene CYP6A1 in a house fly strain with metabolic resistance to insecticides. Insect Biochemistry and Molecular Biology. 24 (4). p.pp. 411–418.

Carvalho, D.O., McKemey, A.R., Garziera, L., Lacroix, R., Donnelly, C.A., Alphey, L., Malavasi, A. & Capurro, M.L. (2015). Suppression of a field population of Aedes aegypti in Brazil by sustained release of transgenic male mosquitoes. PLoS Neglected Tropical Diseases. 9 (7).

Cary, L.C., Goebel, M., Corsaro, B.G., Wang, H.G., Rosen, E. & Fraser, M.J. (1989). Transposon mutagenesis of baculoviruses: Analysis of Trichoplusia ni transposon IFP2 insertions within the FP-locus of nuclear polyhedrosis viruses. Virology. 172 (1). p.pp. 156–169.

Catteruccia, F., Nolan, T., Loukeris, T.G., Blass, C., Savakis, C., Kafatos, F.C. & Crisanti, a (2000). Stable germline transformation of the malaria mosquito Anopheles stephensi. Nature. 405 (6789). p.pp. 959–962.

Catteruccia, F., Benton, J.P. & Crisanti, A. (2005). An Anopheles transgenic sexing strain for vector control. Nature Biotechnology. 23 (11). p.pp. 1414–1417.

CDC (2012). Guideline for Evaluating Insecticide Resistance in Vectors Using the CDC Bottle Bioassay. CDC Methods. p.pp. 1–28.

CDC (2015a) 'Anopheles Mosquitoes', retrieved 29th June 2017 from https://www.cdc.gov/malaria/about/biology/mosquitoes/.

CDC (2015b) 'Ecology of Malaria', retrieved 1st July 2017 from https://www.cdc.gov/malaria/about/biology/ecology.html.

Chagas, A.C., Ramirez, J.L., Jasinskiene, N., James, A.A., Ribeiro, J.M.C., Marinotti, O. & Calvo, E. (2014). Collagen-binding protein, Aegyptin, regulates probing time and blood feeding success in the dengue vector mosquito, Aedes aegypti. Proceedings of the National Academy of Sciences. 111 (19). p.pp. 6946–6951.

Chandor-Proust, A., Bibby, J., Régent-Kloeckner, M., Roux, J., Guittard-Crilat, E., Poupardin, R., Riaz, M.A., Paine, M., Dauphin-Villemant, C., Reynaud, S. & David, J.-P. (2013). The central role of mosquito cytochrome P450 CYP6Zs in insecticide detoxification revealed by functional expression and structural modelling. Biochemical Journal. 455 (1). p.pp. 75–85.

Chen, X.G., Marinotti, O., Whitman, L., Jasinskiene, N. & James, A.A. (2007). The Anopheles gambiae vitellogenin gene (VGT2) promoter directs persistent accumulation of a reporter gene product in transgenic Anopheles stephensi following multiple bloodmeals. American Journal of Tropical Medicine and Hygiene. 76 (6). p.pp. 1118–1124.

Chiu, T.-L., Wen, Z., Rupasinghe, S.G. & Schuler, M. a (2008). Comparative molecular modeling of Anopheles gambiae CYP6Z1, a mosquito P450 capable of metabolizing DDT. Proc. Natl. Acad. Sci. U. S. A. 105 (26). p.pp. 8855–8860.

Chouaibou, M.S., Chabi, J., Bingham, G. V, Knox, T.B., N'Dri, L., Kesse, N.B., Bonfoh, B. & Jamet, H.V.P. (2012). Increase in susceptibility to insecticides with aging of wild Anopheles gambiaemosquitoes from Côte d'Ivoire. BMC Infectious Diseases. 12 (1). p.p. 214.

Chung, H., Bogwitz, M.R., McCart, C., Andrianopoulos, A., Ffrench-Constant, R.H., Batterham, P. & Daborn, P.J. (2007). Cis-regulatory elements in the accord retrotransposon result in tissue-specific expression of the Drosophila melanogaster insecticide resistance gene Cyp6g1. Genetics. 175 (3). p.pp. 1071–1077.

Chung, H., Boey, A., Lumb, C., Willoughby, L., Batterham, P. & Daborn, P.J. (2011). Induction of a detoxification gene in Drosophila melanogaster requires an interaction between tissue specific enhancers and a novel cis-regulatory element. Insect Biochemistry and Molecular Biology. 41 (11). p.pp. 863–871.

Clark, M.K. & Dahm, P.A. (1973). Phenobarbital-induced, membrane-like scrolls in the oenocytes of Musca domestica linnaeus. The Journal of Cell Biology. 56 (3). p.pp. 870-875.

Claudianos, C., Russell, R.J. & Oakeshott, J.G. (1999). The same amino acid substitution in orthologous esterases confers organophosphate resistance on the house fly and a blowfly. Insect Biochemistry and Molecular Biology. 29 (8). p.pp. 675–686.

Claudianos, C., Crone, E., Coppin, C., Russell, R. & Oakeshott, J. (2002). A genomics perspective on mutant aliesterases and metabolic resistance to organophosphates. In: Marshall Clark, J., Yamaguchi, I. (Eds.), Agrochemical Resistance: Extent, Mechanism and Detection. American Chemical Society, Washington, DC.

Coats, J.R. (1990). Mechanisms of toxic action and structure-activity relationships for organochlorine and synthetic pyrethroid insecticides. In: Environmental Health Perspectives. 1990, pp. 255–262.

Cohen, S.D. (1984). Mechanisms of toxicological interactions involving organophosphate insecticides. Fundamental and Applied Toxicology. 4 (3 PART 1). p.pp. 315–324.

Corby-Harris, V., Drexler, A., de Jong, L.W., Antonova, Y., Pakpour, N., Ziegler, R., Ramberg, F., Lewis, E.E., Brown, J.M., Luckhart, S. & Riehle, M.A. (2010). Activation of akt signaling reduces the prevalence and intensity of malaria parasite infection and lifespan in anopheles stephensi mosquitoes. PLoS Pathogens. 6 (7). p.pp. 1–10.

Dabiré, K.R., Diabaté, A., Djogbenou, L., Ouari, A., N'Guessan, R., Ouédraogo, J.-B., Hougard, J.-M., Chandre, F. & Baldet, T. (2008). Dynamics of multiple insecticide resistance in the malaria vector Anopheles gambiae in a rice growing area in South-Western Burkina Faso. Malaria Journal. 7. p.p. 188.

Dabiré, R.K., Namountougou, M., Diabaté, A., Soma, D.D., Bado, J., Toé, H.K., Bass, C. & Combary, P. (2014). Distribution and Frequency of kdr Mutations within Anopheles gambiae s.l. Populations and First Report of the Ace.1 G119S Mutation in Anopheles arabiensis from Burkina Faso (West Africa). PLoS ONE. 9 (7). p.p. e101484.

Daborn, P., Boundy, S., Yen, J., Pittendrigh, B. & Ffrench-Constant, R. (2001). DDT resistance in Drosophila correlates with Cyp6g1 over-expression and confers cross-resistance to the neonicotinoid imidacloprid. Molecular Genetics and Genomics. 266 (4). p.pp. 556–563.

Daborn, P.J. (2002). A Single P450 Allele Associated with Insecticide Resistance in Drosophila. Science. 297 (5590). p.pp. 2253–2256.

Daborn, P.J., Lumb, C., Boey, A., Wong, W., ffrench-Constant, R.H. & Batterham, P. (2007). Evaluating the insecticide resistance potential of eight Drosophila melanogaster cytochrome P450 genes by transgenic over-expression. Insect Biochemistry and Molecular Biology. 37 (5). p.pp. 512–519.

Daborn, P.J., Lumb, C., Harrop, T.W.R., Blasetti, A., Pasricha, S., Morin, S., Mitchell, S.N., Donnelly, M.J., Müller, P. & Batterham, P. (2012). Using Drosophila melanogaster to validate metabolism-based insecticide resistance from insect pests. Insect Biochemistry and Molecular Biology. 42 (12). p.pp. 918–924.

David, J.-P., Strode, C., Vontas, J., Nikou, D., Vaughan, A., Pignatelli, P.M., Louis, C., Hemingway, J. & Ranson, H. (2005). The Anopheles gambiae detoxification chip: a highly specific microarray to study metabolic-based insecticide resistance in malaria vectors. Proceedings of the National Academy of Sciences of the United States of America. 102 (11). p.pp. 4080–4.

David, J.-P., Ismail, H.M., Chandor-Proust, A. & Paine, M.J.I. (2013). Role of cytochrome P450s in insecticide resistance: impact on the control of mosquito-borne diseases and use of insecticides on Earth. Philosophical Transactions of the Royal Society B: Biological Sciences. 368 (1612). p.pp. 20120429–20120429.

Davies, T.G.E., Field, L.M., Usherwood, P.N.R. & Williamson, M.S. (2007). DDT, pyrethrins, pyrethroids and insect sodium channels. IUBMB Life. 59 (3). p.pp. 151–162.

De Lara Capurro, M., Coleman, J., Beerntsen, B.T., Myles, K.M., Olson, K.E., Rocha, E., Krettli, A.U. & James, A.A. (2000). Virus-expressed, recombinant single-chain antibody blocks sporozoite infection of salivary glands in Plasmodium gallinaceum-infected Aedes aegypti. American Journal of Tropical Medicine and Hygiene. 62 (4). p.pp. 427–433.

DeGennaro, M., McBride, C.S., Seeholzer, L., Nakagawa, T., Dennis, E.J., Goldman, C., Jasinskiene, N., James, A.A. & Vosshall, L.B. (2013). orco mutant mosquitoes lose strong preference for humans and are not repelled by volatile DEET. Nature. 498 (7455). p.pp. 487–491.

Ding, Y., Ortelli, F., Rossiter, L.C., Hemingway, J. & Ranson, H. (2003). The Anopheles gambiae glutathione transferase supergene family: annotation, phylogeny and expression profiles. BMC genomics. 4 (1). p.p. 35.

Dissanayake, S.N., Marinotti, O., Ribeiro, J.M.C. & James, A. a (2006). angaGEDUCI: Anopheles gambiae gene expression database with integrated comparative algorithms for identifying conserved DNA motifs in promoter sequences. BMC genomics. 7. p.p. 116.

Djègbè, I., Agossa, F.R., Jones, C.M., Poupardin, R., Cornelie, S., Akogbéto, M., Ranson, H. & Corbel, V. (2014). Molecular characterization of DDT resistance in Anopheles gambiae from Benin. Parasites & Vectors. 7 (1). p.p. 409.

Djogbénou, L., Dabiré, R., Diabaté, A., Kengne, P., Akogbéto, M., Hougard, J.M. & Chandre, F. (2008). Identification and geographic distribution of the ACE-1R mutation in the malaria vector Anopheles gambiae in South-Western Burkina Faso, West Africa. American Journal of Tropical Medicine and Hygiene. 78 (2). p.pp. 298–302.

Djouaka, R.F., Bakare, A.A., Coulibaly, O.N., Akogbeto, M.C., Ranson, H., Hemingway, J. & Strode, C. (2008). Expression of the cytochrome P450s, CYP6P3 and CYP6M2 are significantly elevated in multiple pyrethroid resistant populations of Anopheles gambiae s.s. from Southern Benin and Nigeria. BMC Genomics. 9 (1). p.p. 538.

Dong, Y., Das, S., Cirimotich, C., Souza-Neto, J.A., McLean, K.J. & Dimopoulos, G. (2011). Engineered Anopheles immunity to plasmodium infection. PLoS Pathogens. 7 (12).

Dow, J.A., Davies, S.A., Guo, Y., Graham, S., Finbow, M.E. & Kaiser, K. (1997). Molecular genetic analysis of V-ATPase function in Drosophila melanogaster. The Journal of experimental biology. 200 (Pt 2). p.pp. 237–45.

Dow, J.A. (1999). The multifunctional Drosophila melanogaster V-ATPase is encoded by a multigene family. Journal of Bioenergetics and Biomembranes. 1. p.pp. 75-83.

Du, W., Awolola, T.S., Howell, P., Koekemoer, L.L., Brooke, B.D., Benedict, M.Q., Coetzee, M. & Zheng, L. (2005). Independent mutations in the Rdl locus confer dieldrin resistance to Anopheles gambiae and An. arabiensis. Insect Molecular Biology. 14 (2). p.pp. 179–183.

Duangkaew, P., Kaewpa, D. & Rongnoparut, P. (2011). Protective efficacy of Anopheles minimus CYP6p7 and CYP6AA3 against cytotoxicity of pyrethroid insecticides in Spodoptera frugiperda (Sf9) insect cells. Tropical Biomedicine. 28 (2). p.pp. 293–301.

Dunkov, B.C., Guzov, V.M., Mocelin, G., Shotkoski, F., Brun, A., Amichot, M., Ffrench-Constant, R.H. & Feyereisen, R. (1997). The Drosophila cytochrome P450 gene Cyp6a2: structure, localization, heterologous expression, and induction by phenobarbital. DNA Cell Biol. 16 (11). p.pp. 1345–1356.

Edi, C.V.A., Koudou, B.G., Jones, C.M., Weetman, D. & Ranson, H., (2012). Multiple-insecticide resistance in anopheles gambiae mosquitoes, southern Côte d'Ivoire. Emerging Infectious Diseases. 18 (9). p.pp. 1508–1511.

Edi, C.V.A., Djogbénou, L., Jenkins, A.M., Regna, K., Muskavitch, M.A.T., Poupardin, R., Jones, C.M., Essandoh, J., Kétoh, G.K., Paine, M.J.I., Koudou, B.G., Donnelly, M.J., Ranson, H. & Weetman, D. (2014). CYP6 P450 Enzymes and ACE-1 Duplication Produce Extreme and Multiple Insecticide Resistance in the Malaria Mosquito Anopheles gambiae. PLoS Genetics. 10 (3).

Elick, T. a, Bauser, C. a & Fraser, M.J. (1996). Excision of the piggyBac transposable element in vitro is a precise event that is enhanced by the expression of its encoded transposase. Genetica. 98 (1). p.pp. 33–41.

Essandoh, J., Yawson, A.E. & Weetman, D. (2013). Acetylcholinesterase (Ace-1) target site mutation 119S is strongly diagnostic of carbamate and organophosphate resistance in Anopheles gambiae s.s. and Anopheles coluzzii across southern Ghana. Malaria Journal. 12 (1). p.p. 404.

Feyereisen, R. (1999). Insect P450 Enzymes. Annual Review of Entomology. 44 (1). p.pp. 507–533.

Feyereisen, R. (2015). Insect P450 inhibitors and insecticides: Challenges and opportunities. Pest Management Science. 71 (6). p.pp. 793–800.

Fossog Tene, B., Poupardin, R., Costantini, C., Awono-Ambene, P., Wondji, C.S., Ranson, H. & Antonio-Nkondjio, C. (2013). Resistance to DDT in an Urban Setting: Common Mechanisms Implicated in Both M and S Forms of Anopheles gambiae in the City of Yaoundé Cameroon. PLoS ONE. 8 (4).

Franz, G. & Savakis, C. (1991) Minos, a new transposable element from Drosophila hydei, is a member of the Tc1-like family of transposons. Nucleic Acids Research. 19 (23). pp. 6646.

Franz, A.W.E., Jasinskiene, N., Sanchez-Vargas, I., Isaacs, A.T., Smith, M.R., Khoo, C.C.H., Heersink, M.S., James, A.A. & Olson, K.E. (2011). Comparison of transgene expression in Aedes aegypti generated by mariner Mos1 transposition and Phic31 site-directed recombination. Insect Molecular Biology. 20 (5). p.pp. 587–598.

Fraser, M.J., Brusca, J.S., Smith, G.E. & Summers, M.D. (1985). Transposon-mediated mutagenesis of a baculovirus. Virology. 145 (2). p.pp. 356–361.

Fraser, M.J., Cary, L., Boonvisudhi, K. & Wang, H.G.H. (1995). Assay for movement of Lepidopteran transposon IFP2 in insect cells using a baculovirus genome as a target DNA. Virology. 211 (2) p.pp. 397–407.

Fraser, M.J., Clszczon, T., Elick, T. & Bauser, C. (1996). Precise excision of TTAA-specific lepidopteran transposons piggyBac (IFP2) and tagalong (TFP3) from the baculovirus genome in cell lines from two species of Lepidoptera. Insect Molecular Biology. 5 (2). p.pp. 141–151.

Fraser, M.J. (2012). Insect Transgenesis: Current Applications and Future Prospects. Annual Review of Entomology. 57 (1). p.pp. 267–289.

Fukuto, T.R. (1990). Mechanism of action of organophosphorus and carbamate insecticides. In: Environmental Health Perspectives. 1990, pp. 245–254.

Gabrieli, P., Smidler, A. & Catteruccia, F. (2014). Engineering the control of mosquito-borne infectious diseases. Genome Biology. 15 (11). p.p. 535.

Gaj, T. (2014). ZFN, TALEN and CRISPR/Cas based methods for genome engineering. 2013. 31 (7). p.pp. 397–405.

Galizi, R., Doyle, L.A., Menichelli, M., Bernardini, F., Deredec, A., Burt, A., Stoddard, B.L., Windbichler, N. & Crisanti, A. (2014). A synthetic sex ratio distortion system for the control of the human malaria mosquito. Nature Communications. 5. p.pp. 1–8.

Galizi, R., Hammond, A., Kyrou, K., Taxiarchi, C., Bernardini, F., O'Loughlin, S.M., Papathanos, P.-A., Nolan, T., Windbichler, N. & Crisanti, A. (2016). A CRISPR-Cas9 sex-ratio distortion system for genetic control. Scientific Reports. 6 (1). p.p. 31139.

Gantz, V.M., Jasinskiene, N., Tatarenkova, O., Fazekas, A., Macias, V.M., Bier, E. & James, A.A. (2015). Highly efficient Cas9-mediated gene drive for population modification of the malaria vector mosquito Anopheles stephensi. Proceedings of the National Academy of Sciences. 112 (49). p.pp. E6736–E6743.

Gatton, M.L., Chitnis, N., Churcher, T., Donnelly, M.J., Ghani, A.C., Godfray, H.C.J., Gould, F., Hastings, I., Marshall, J., Ranson, H., Rowland, M., Shaman, J. & Lindsay, S.W. (2013). The importance of mosquito behavioural adaptations to malaria control in Africa. Evolution. 67 (4). p.pp. 1218–1230.

Geurts, A.M., Yang, Y., Clark, K.J., Liu, G., Cui, Z., Dupuy, A.J., Bell, J.B., Largaespada, D.A. & Hackett, P.B. (2003). Gene transfer into genomes of human cells by the Sleeping Beauty transposon system. Molecular Therapy. 8 (1). p.pp. 108–117.

Gibson, D.G., Young, L., Chuang, R.-Y., Venter, J.C., Hutchison, C.A. & Smith, H.O. (2009). Enzymatic assembly of DNA molecules up to several hundred kilobases. Nature Methods. 6 (5). p.pp. 343–345.

Gibson, D.G., Smith, H.O., Hutchison 3rd, C.A., Venter, J.C. & Merryman, C. (2010). Chemical synthesis of the mouse mitochondrial genome. Nature methods. 7 (11). p.pp. 901–903.

Giniger, E., Varnum, S.M. & Ptashne, M. (1985). Specific DNA binding of GAL4, a positive regulatory protein of yeast. Cell. 40 (4). p.pp. 767–774.

Giraldo-Calderón, G.I., Emrich, S.J., MacCallum, R.M., Maslen, G., Emrich, S., Collins, F., Dialynas, E., Topalis, P., Ho, N., Gesing, S., Madey, G., Collins, F.H., Lawson, D., Kersey, P., Allen, J., Christensen, M., Hughes, D., Koscielny, G., Langridge, N., Gallego, E.L., Megy, K., Wilson, D., Gelbart, B., Emmert, D., Russo, S., Zhou, P., Christophides, G., Brockman, A., Kirmitzoglou, I., MacCallum, B., Tiirikka, T., Louis, K., Dritsou, V., Mitraka, E., Werner-Washburn, M., Baker, P., Platero, H., Aguilar, A., Bogol, S., Campbell, D., Carmichael, R., Cieslak, D., Davis, G., Konopinski, N., Nabrzyski, J., Reinking, C., Sheehan, A., Szakonyi, S. & Wieck, R. (2015). VectorBase: An updated Bioinformatics Resource for invertebrate vectors and other organisms related with human diseases. Nucleic Acids Research. 43 (D1). p.pp. D707–D713.

Giraudo, M., Unnithan, G.C., Le Goff, G. & Feyereisen, R. (2010). Regulation of cytochrome P450 expression in Drosophila: Genomic insights. Pesticide Biochemistry and Physiology. 97 (2). p.pp. 115–122.

Gould, F. (1984). Mixed function oxidases and herbivore polyphagy: the devil's advocate position. Ecological Entomology. 9. p.pp 29-34.

Grant, D.F., Dietze, E.C. & Hammock, B.D. (1991). Glutathione S-transferase isozymes in Aedes aegypti: Purification, characterization, and isozyme-specific regulation. Insect Biochemistry. 21 (4). p.pp. 421–433.

Greenbaum, D., Colangelo, C., Williams, K. & Gerstein, M. (2003). Comparing protein abundance and mRNA expression levels on a genomic scale. Genome Biology. 4 (9). p.p. 117.

Gregory, R., Darby, A.C., Irving, H., Coulibaly, M.B., Hughes, M., Koekemoer, L.L., Coetzee, M., Ranson, H., Hemingway, J., Hall, N. & Wondji, C.S. (2011). A De Novo expression profiling of Anopheles funestus, malaria vector in Africa, using 454 pyrosequencing. PLoS ONE. 6 (2).

Grigoraki, L., Lagnel, J., Kioulos, I., Kampouraki, A., Morou, E., Labbé, P., Weill, M. & Vontas, J. (2015). Transcriptome Profiling and Genetic Study Reveal Amplified Carboxylesterase Genes Implicated in Temephos Resistance, in the Asian Tiger Mosquito Aedes albopictus. PLoS Neglected Tropical Diseases. 9 (5).

Grigoraki, L., Balabanidou, V., Meristoudis, C., Miridakis, A., Ranson, H., Swevers, L. & Vontas, J. (2016). Functional and immunohistochemical characterization of CCEae3a, a carboxylesterase associated with temephos resistance in the major arbovirus vectors Aedes aegypti and Ae. albopictus. Insect Biochemistry and Molecular Biology. 74. p.pp. 61–67.

Grossman, G.L., Rafferty, C.S., Clayton, J.R., Stevens, T.K., Mukabayire, O. & Benedict, M.Q. (2001). Germline transformation of the malaria vector, Anopheles gambiae, with the piggyBac transposable element. Insect Molecular Biology. 10 (6). p.pp. 597–604.

Groth, A.C., Fish, M., Nusse, R. & Calos, M.P. (2004). Construction of Transgenic Drosophila by Using the Site-Specific Integrase from Phage PhiC31. Genetics. 166 (4). p.pp. 1775–1782.

Guengerich, F.P. (2001). Common and uncommon cytochrome P450 reactions related to metabolism and chemical toxicity. Chemical Research in Toxicology. 14 (6). p.pp. 611–50.

Gutierrez, E., Wiggins, D., Fielding, B. & Gould, A.P. (2007). Specialized hepatocyte-like cells regulate Drosophila lipid metabolism. Nature. 445 (7125). p.pp. 275–280.

Haghighat-Khah, R.E., Scaife, S., Martins, S., St. John, O., Matzen, K.J., Morrison, N. & Alphey, L. (2015). Site-specific cassette exchange systems in the aedes aegypti mosquito and the plutella xylostella moth. PLoS ONE. 10 (4).

Hammond, A., Galizi, R., Kyrou, K., Simoni, A., Siniscalchi, C., Katsanos, D., Gribble, M., Baker, D., Marois, E., Russell, S., Burt, A., Windbichler, N., Crisanti, A. & Nolan, T. (2016). A CRISPR-Cas9 gene drive system targeting female reproduction in the malaria mosquito vector Anopheles gambiae. Nature Biotechnology. 34 (1). p.pp. 78–83.

Handler, A.M., McCombs, S.D., Fraser, M.J. & Saul, S.H. (1998). The lepidopteran transposon vector, piggyBac, mediates germ-line transformation in the Mediterranean fruit fly. Proceedings of the National Academy of Sciences of the United States of America. 95 (June). p.pp. 7520–7525.

Handler, A.M. & Harrell, R.A. (1999). Germline transformation of Drosophila melanogaster with the piggyBac transposon vector. Insect Molecular Biology. 8 (4). p.pp. 449–457.

Handler, A.M. & Harrell, R.A. (2001). Transformation of the Caribbean fruit fly, Anastrepha suspensa, with a piggyBac vector marked with polyubiquitin-regulated GFP. Insect Biochemistry and Molecular Biology. 31 (2) p.pp. 199–205.

Handler, A.M. (2002). Use of the piggyBac transposon for germ-line transformation of insects. In: Insect Biochemistry and Molecular Biology. 2002, pp. 1211–1220.

Handler, A.M. (2004). Understanding and improving transgene stability and expression in insects for SIT and conditional lethal release programs. Insect Biochemistry and Molecular Biology. 34 (2). p.pp. 121–130.

Handler, A.M. & O'Brochta, D.A. (2012). Transposable Elements for Insect Transformation. Elsevier Inc.

Harrop, T.W.R., Sztal, T., Lumb, C., Good, R.T., Daborn, P.J., Batterham, P. & Chung, H. (2014). Evolutionary changes in gene expression, coding sequence and

copy-number at the Cyp6g1 locus contribute to resistance to multiple insecticides in Drosophila. PLoS ONE. 9 (1).

Hauck, E.S., Antonova-Koch, Y., Drexler, A., Pietri, J., Pakpour, N., Liu, D., Blacutt, J., Riehle, M.A. & Luckhart, S. (2013). Overexpression of phosphatase and tensin homolog improves fitness and decreases Plasmodium falciparum development in Anopheles stephensi. Microbes and Infection. 15 (12). p.pp. 775–787.

Hay, S.I., Sinka, M.E., Okara, R.M., Kabaria, C.W., Mbithi, P.M., Tago, C.C., Benz, D., Gething, P.W., Howes, R.E., Patil, A.P., Temperley, W.H., Bangs, M.J., Chareonviriyaphap, T., Elyazar, I.R.F., Harbach, R.E., Hemingway, J., Manguin, S., Mbogo, C.M., Rubio-Palis, Y. & Godfray, H.C.J. (2010). Developing global maps of the dominant Anopheles vectors of human malaria. PLoS Medicine. 7 (2).

Heinrich, J.C., Li, X., Henry, R.A., Haack, N., Stringfellow, L., Heath, A.C.G. & Scott, M.J. (2002). Germ-line transformation of the Australian sheep blowfly Lucilia cuprina. Insect Molecular Biology. 11 (1). p.pp. 1–10.

Helvig, C., Tijet, N., Feyereisen, R., Walker, F.A. & Restifo, L.L. (2004). Drosophila melanogaster CYP6A8, an insect P450 that catalyzes lauric acid (omega-1)-hydroxylation. Biochemical and Biophysical Research Communications. 325 (4). p.pp. 1495–1502.

Hemingway, J. (1982a). Genetics of organophosphate and carbamate resistance in Anopheles atroparvus (Diptera: Culicidae). Journal of Economic Entomology. 75. p.pp. 1055-1058.

Hemingway, J. (1982b). The biochemical nature of malathion resistance in Anopheles stephensi from Pakistan. Pesticide Biochemistry and Physiology. 17. p.pp. 149–155.

Hemingway, J. & Georghiou, G.P. (1983). Studies on the acetylcholinesterase of Anopheles albimanus resistant and susceptible to organophosphate and carbamate insecticides. Pesticide Biochemistry and Physiology. 19. p.pp. 167–171.

Hemingway, J., Miyamoto, J. & Herath, P.R.J. (1991). A possible novel link between organophosphorus and DDT insecticide resistance genes in Anopheles: Supporting evidence from fenitrothion metabolism studies. Pesticide Biochemistry and Physiology. 39 (1). p.pp. 49–56.

Hemingway, J. & Karunaratne, S.H. (1998). Mosquito carboxylesterases: a review of the molecular biology and biochemistry of a major insecticide resistance mechanism. Medical and veterinary entomology. 12 (1). p.pp. 1–12.

Hemingway, J., Hawkes, N.J., McCarroll, L. & Ranson, H. (2004). The molecular basis of insecticide resistance in mosquitoes. In: Insect Biochemistry and Molecular Biology. 2004, pp. 653–665.

Herath, P.R.J., Hemingway, J., Weerasinghe, I.S. & Jayawardena, K.G.I. (1987). The detection and characterization of malathion resistance in field populations of Anopheles culicifacies B in Sri Lanka. Pesticide Biochemistry and Physiology. 29 (2). p.pp. 157–162.

Hoang, K.P., Teo, T.M., Ho, T.X. & Le, V.S. (2016). Mechanisms of sex determination and transmission ratio distortion in Aedes aegypti. Parasites & Vectors. 9 (1). p.p. 49.

Hoi, K.K., Daborn, P.J., Battlay, P., Robin, C., Batterham, P., O'Hair, R.A.J. & Donald, W.A. (2014). Dissecting the insect metabolic machinery using twin ion mass spectrometry: A single P450 enzyme metabolizing the insecticide imidacloprid in vivo. Analytical Chemistry. 86 (7). p.pp. 3525–3532.

Holt, R. a, Subramanian, G.M., Halpern, A., Sutton, G.G., Charlab, R., Nusskern, D.R., Wincker, P., Clark, A.G., Ribeiro, J.M.C., Wides, R., Salzberg, S.L., Loftus, B., Yandell, M., Majoros, W.H., Rusch, D.B., Lai, Z., Kraft, C.L., Abril, J.F., Anthouard, V., Arensburger, P., Atkinson, P.W., Baden, H., de Berardinis, V., Baldwin, D., Benes, V., Biedler, J., Blass, C., Bolanos, R., Boscus, D., Barnstead, M., Cai, S., Center, A., Chaturverdi, K., Christophides, G.K., Chrystal, M. a, Clamp, M., Cravchik, A., Curwen, V., Dana, A., Delcher, A., Dew, I., Evans, C. a, Flanigan, M., Grundschober-Freimoser, A., Friedli, L., Gu, Z., Guan, P., Guigo, R., Hillenmeyer, M.E., Hladun, S.L., Hogan, J.R., Hong, Y.S., Hoover, J., Jaillon, O., Ke, Z., Kodira, C., Kokoza, E., Koutsos, A., Letunic, I., Levitsky, A., Liang, Y., Lin, J.-J., Lobo, N.F., Lopez, J.R., Malek, J. a, McIntosh, T.C., Meister, S., Miller, J., Mobarry, C., Mongin, E., Murphy, S.D., O'Brochta, D. a, Pfannkoch, C., Qi, R., Regier, M. a, Remington, K., Shao, H., Sharakhova, M. V, Sitter, C.D., Shetty, J., Smith, T.J., Strong, R., Sun, J., Thomasova, D., Ton, L.Q., Topalis, P., Tu, Z., Unger, M.F., Walenz, B., Wang, A., Wang, J., Wang, M., Wang, X., Woodford, K.J., Wortman, J.R., Wu, M., Yao, A., Zdobnov, E.M., Zhang, H., Zhao, Q., Zhao, S., Zhu, S.C., Zhimulev, I., Coluzzi, M., della Torre, A., Roth, C.W., Louis, C., Kalush, F., Mural, R.J., Myers, E.W., Adams, M.D., Smith, H.O., Broder, S., Gardner, M.J., Fraser, C.M., Birney, E., Bork, P., Brey, P.T., Venter, J.C., Weissenbach, J., Kafatos, F.C., Collins, F.H. & Hoffman, S.L. (2002). The genome sequence of the malaria mosquito Anopheles gambiae. Science. 298 (5591). p.pp. 129–49.

Hong, M., Fitzgerald, M.X., Harper, S., Luo, C., Speicher, D.W. & Marmorstein, R. (2008). Structural Basis for Dimerization in DNA Recognition by Gal4. Structure. 16 (7). p.pp. 1019–1026.

Horn, C., Offen, N., Nystedt, S., Häckert, U. & Wimmer, E.A. (2003). piggyBac-based insertional mutagenesis and enhancer detection as a tool for functional insect genomics. Genetics. 163 (2). p.pp. 647–661.

Huynh, C.Q. & Zieler, H. (1999). Construction of modular and versatile plasmid vectors for the high- level expression of single or multiple genes in insects and insect cell lines. J.Mol.Biol. 288 (0022–2836 SB–M SB–X). p.pp. 13–20.

Ibrahim, S.S., Ndula, M., Riveron, J.M., Irving, H. & Wondji, C.S. (2016a). The P450 CYP6Z1 confers carbamate/pyrethroid cross-resistance in a major African malaria vector beside a novel carbamate-insensitive N485I acetylcholinesterase-1 mutation. Molecular Ecology. 25 (14). p.pp. 3436–3452.

Ibrahim, S.S., Riveron, J.M., Stott, R., Irving, H. & Wondji, C.S. (2016b). The cytochrome P450 CYP6P4 is responsible for the high pyrethroid resistance in knockdown resistance-free Anopheles arabiensis. Insect Biochemistry and Molecular Biology. 68. p.pp. 23–32.

Imamura, M., Nakai, J., Inoue, S., Quan, G.X., Kanda, T. & Tamura, T. (2003). Targeted gene expression using the GAL4/UAS system in the silkworm _Bombyx mori_. Genetics. 165 (3). p.pp. 1329–1340.

Ingham, V.A., Jones, C.M., Pignatelli, P., Balabanidou, V., Vontas, J., Wagstaff, S.C., Moore, J.D. & Ranson, H. (2014). Dissecting the organ specificity of insecticide resistance candidate genes in Anopheles gambiae: known and novel candidate genes. BMC genomics. 15 (1). p.p. 1018.

Ingham, V.A. (2016). Identification of novel transcripts involved in insecticide resistance in African malaria vectors. Ph.D. Thesis. Systems Biology DTC, University of Warwick, in collaboration with the Vector Biology Department at the Liverpool School of Tropical Medicine, UK.

Irving, H., Riveron, J.M., Ibrahim, S.S., Lobo, N.F. & Wondji, C.S. (2012). Positional cloning of rp2 QTL associates the P450 genes CYP6Z1, CYP6Z3 and CYP6M7 with pyrethroid resistance in the malaria vector Anopheles funestus. Heredity. 109 (6). p.pp. 383–392.

Isaacs, A.T., Li, F., Jasinskiene, N., Chen, X., Nirmala, X., Marinotti, O., Vinetz, J.M. & James, A.A. (2011). Engineered resistance to Plasmodium falciparum development in transgenic Anopheles stephensi. PLoS Pathog. 7 (4). p.p. e1002017.

Isaacs, A.T., Jasinskiene, N., Tretiakov, M., Thiery, I., Zettor, A., Bourgouin, C. & James, A.A. (2012). Transgenic Anopheles stephensi coexpressing single-chain antibodies resist Plasmodium falciparum development. Proceedings of the National Academy of Sciences. 109 (28). p.pp. E1922–E1930.

Ismail, H.M., O'Neill, P.M., Hong, D.W., Finn, R.D., Henderson, C.J., Wright, A.T., Cravatt, B.F., Hemingway, J. & Paine, M.J.I. (2013). Pyrethroid activity-based probes for profiling cytochrome P450 activities associated with insecticide interactions. Proceedings of the National Academy of Sciences. 110 (49). p.pp. 19766–19771.

Itokawa, K., Komagata, O., Kasai, S., Ogawa, K., & Tomita, T. (2016). Testing the causality between CYP9M10 and pyrethroid resistance using the TALEN and CRISPR/Cas9 technologies. Scientific Reports. 6. p.p. 24652.

Jacobson, J.W. & Hartl, D.L. (1985). Coupled instability of two X-linked genes in Drosophila mauritiana: germinal and somatic mutability. Genetics. 111 (1). p.pp. 57–65.

Jones, C.M., Liyanapathirana, M., Agossa, F.R., Weetman, D., Ranson, H., Donnelly, M.J., & Wilding, C.S. (2012). Footprints of positive selection associated with a mutation (N1575Y) in the voltage-gated sodium channel of Anopheles gambiae. Proceedings of the National Academy of Sciences. 109. p.pp. 6614–6619.

Jones, C.M., Haji, K.A., Khatib, B.O., Bagi, J., Mcha, J., Devine, G.J., Daley, M., Kabula, B., Ali, A.S., Majambere, S. & Ranson, H. (2013). The dynamics of pyrethroid resistance in Anopheles arabiensis from Zanzibar and an assessment of the underlying genetic basis. Parasites & Vectors. 6. p.p. 343.

Joussen, N., Heckel, D.G., Haas, M., Schuphan, I., & Schmidt, B. (2008). Metabolism of imidacloprid and DDT by P450 CYP6G1 expressed in cell cultures of Nicotiana tabacum suggests detoxification of these insecticides in Cyp6g1-overexpressing strains of Drosophila melanogaster, leading to resistance. Pest Management Science. 64 (1). p.pp. 65-73.

Karunaratne, S.H., Jayawardena, K.G., Hemingway, J. & Ketterman, A.J. (1993). Characterization of a B-type esterase involved in insecticide resistance from the mosquito Culex quinquefasciatus. The Biochemical journal. 294 (Pt 2. p.pp. 575–579.

Karunker, I., Benting, J., Lueke, B., Ponge, T., Nauen, R., Roditakis, E., Vontas, J., Gorman, K., Denholm, I. & Morin, S. (2008). Over-expression of cytochrome P450 CYP6CM1 is associated with high resistance to imidacloprid in the B and

Q biotypes of Bemisia tabaci (Hemiptera: Aleyrodidae). Insect Biochemistry and Molecular Biology. 38 (6). p.pp. 634–644.

Kawada, H., Ohashi, K., Dida, G.O., Sonye, G., Njenga, S.M., Mwandawiro, C. & Minakawa, N. (2014). Preventive effect of permethrin-impregnated long-lasting insecticidal nets on the blood feeding of three major pyrethroid-resistant malaria vectors in western Kenya. Parasit Vectors. 7 (1). p.p. 383.

Kennerdell, J.R. & Carthew, R.W. (2000). Heritable gene silencing in Drosophila using double-stranded RNA. Nature Biotechnology. 18 (8). p.pp. 896–898.

Ketterman, A.J., Jayawardena, K.G. & Hemingway, J. (1992). Purification and characterization of a carboxylesterase involved in insecticide resistance from the mosquito Culex quinquefasciatus. The Biochemical journal. 287 (2). p.pp. 355–360.

Khot, A.C., Bingham, G., Field, L.M. & Moores, G.D. (2008). A novel assay reveals the blockade of esterases by piperonyl butoxide. Pest Management Science. 64 (11). p.pp. 1139–1142.

Kidwell, M.G., Kidwell, J.F. & Sved JA. (1977). Hybrid Dysgenesis in Drosophila Melanogaster: A Syndrome of Aberrant Traits Including Mutation, Sterility and Male Recombination. Genetics. 86 (4). p.pp. 813-33.

Killeen, G.F., Masalu, J.P., Chinula, D., Fotakis, E.A., Kavishe, D.R., Malone, D. & Okumu, F. (2017). Control of Malaria Vector Mosquitoes by Insecticide-Treated Combinations of Window Screens and Eave Baffles. 23 (5).

Kim, W., Koo, H., Richman, A.M., Seeley, D., Vizioli, J., Klocko, A.D. & O'Brochta, D.A. (2004). Ectopic expression of a Cecropin transgene in the human malaria vector Anopheles gambie (Diptera: Culicidae): Effects on susceptibility to Plasmodium. Med. entomol. 41 (3). p.pp. 447–455.

Kistler, K.E., Vosshall, L.B. & Matthews, B.J. (2015). Genome engineering with CRISPR-Cas9 in the mosquito aedes aegypti. Cell Reports. 11 (1). p.pp. 51–60.

Knipling, E.F. (1955). Possibilities of insect control or eradication through the use of sexually sterile males. Journal of Economic Entomology. 48. p.pp. 459-469.

Kokoza, V., Ahmed, A., Wimmer, E.A. & Raikhel, A.S. (2001). Efficient transformation of the yellow fever mosquito Aedes aegypti using the piggyBac transposable element vector pBac[3xP3-EGFP afm]. Insect Biochemistry and Molecular Biology. 31 (12). p.pp. 1137–1143.

Kokoza, V.A. & Raikhel, A.S. (2011). Targeted gene expression in the transgenic Aedes aegypti using the binary Gal4-UAS system. Insect Biochemistry and Molecular Biology. 41 (8). p.pp. 637–644.

Komagata, O., Kasai, S. & Tomita, T. (2010). Overexpression of cytochrome P450 genes in pyrethroid-resistant Culex quinquefasciatus. Insect Biochemistry and Molecular Biology. 40 (2). p.pp. 146–152.

Kostaropoulos, I., Papadopoulos, A.I., Metaxakis, A., Boukouvala, E. & Papadopoulou-Mourkidou, E. (2001). Glutathione S-transferase in the defence against pyrethroids in insects. Insect Biochemistry and Molecular Biology. 31 (4–5). p.pp. 313–319.

Koutsos, A.C., Blass, C., Meister, S., Schmidt, S., MacCallum, R.M., Soares, M.B., Collins, F.H., Benes, V., Zdobnov, E., Kafatos, F.C. & Christophides, G.K.

(2007). Life cycle transcriptome of the malaria mosquito Anopheles gambiae and comparison with the fruitfly Drosophila melanogaster. Proceedings of the National Academy of Sciences of the United States of America. 104 (27). p.pp. 11304–9.

Kwiatkowska, R.M., Platt, N., Poupardin, R., Irving, H., Dabire, R.K., Mitchell, S., Jones, C.M., Diabaté, A., Ranson, H. & Wondji, C.S. (2013). Dissecting the mechanisms responsible for the multiple insecticide resistance phenotype in Anopheles gambiae s.s., M form, from Vallée du Kou, Burkina Faso. Gene. 519 (1). p.pp. 98–106.

Labbé, P., Berthomieu, A., Berticat, C., Alout, H., Raymond, M., Lenormand, T. & Weill, M. (2007). Independent duplications of the acetylcholinesterase gene conferring insecticide resistance in the mosquito Culex pipiens. Molecular Biology and Evolution. 24 (4). p.pp. 1056–1067.

Labbé, G., Nimmo, D. & Alphey, L. (2010). piggybac-and PhiC31-Mediated Genetic Transformation of the Asian Tiger Mosquito, Aedes albopictus (Skuse). PLoS Neglected Tropical.

Lai, S.-L. & Lee, T. (2006). Genetic mosaic with dual binary transcriptional systems in Drosophila. Nature Neuroscience. 9 (5). p.pp. 703–709.

Lapied, B., Pennetier, C., Apaire-Marchais, V., Licznar, P., & Corbel, V. (2009). Innovative applications for insect viruses: towards insecticide sensitization. Trends in Biotechnology. 27 (4). p.pp. 190–8.

Laughon, A. & Gesteland, R.F. (1982). Isolation and preliminary characterization of the GAL4 gene, a positive regulator of transcription in yeast. Proceedings of the National Academy of Sciences of the United States of America. 79 (22). p.pp. 6827–31.

Lawniczak, M.K.N., Emrich, S.J., Holloway, A.K., Regier, A.P., Olson, M., White, B., Redmond, S., Fulton, L., Appelbaum, E., Godfrey, J., Farmer, C., Chinwalla, A., Yang, S.-P., Minx, P., Nelson, J., Kyung, K., Walenz, B.P., Garcia-Hernandez, E., Aguiar, M., Viswanathan, L.D., Rogers, Y.-H., Strausberg, R.L., Saski, C.A., Lawson, D., Collins, F.H., Kafatos, F.C., Christophides, G.K., Clifton, S.W., Kirkness, E.F. & Besansky, N.J. (2010). Widespread Divergence Between Incipient Anopheles gambiae Species Revealed by Whole Genome Sequences. Science. 330 (6003). p.pp. 512–514.

Lee T, Lee A, & Luo L. (1999). Development of the Drosophila mushroom bodies: sequential generation of three distinct types of neurons from a neuroblast. Development (Cambridge, England). 126 (18). p.pp. 4065–76.

Li, T., Liu, L., Zhang, L. & Liu, N. (2014). Role of G-protein-coupled Receptor-related Genes in Insecticide Resistance of the Mosquito, Culex quinquefasciatus. Scientific Reports. 4. p.p. 6474.

Li, T., Cao, C., Yang, T., Zhang, L., He, L., Xi, Z., Bian, G. & Liu, N. (2015). A G-protein-coupled receptor regulation pathway in cytochrome P450-mediated permethrin-resistance in mosquitoes, Culex quinquefasciatus. Scientific Reports. 5 (December). p.p. 17772.

Liu, N., Liu, H., Zhu, F. & Zhang, L. (2007). Differential expression of genes in pyrethroid resistant and susceptible mosquitoes, Culex quinquefasciatus (S.). Gene. 394 (1–2). p.pp. 61–68.

Liu, N. (2015). Insecticide Resistance in Mosquitoes: Impact, Mechanisms, and Research Directions. Annual Review of Entomology. 60 (1). p.pp. 537–559.

Liu, N., Li, M., Gong, Y., Liu, F. & Li, T. (2015). Cytochrome P450s - Their expression, regulation, and role in insecticide resistance. Pesticide Biochemistry and Physiology. 120. p.pp. 77–81.

Livak, K.J. & Schmittgen, T.D. (2001). Analysis of Relative Gene Expression Data Using Real-Time Quantitative PCR and the 2-ddCt method. Methods. 25. p.pp. 402–8.

Lobo, N.F., Clayton, J.R., Fraser, M.J., Kafatos, F.C. & Collins, F.H. (2006). High efficiency germ-line transformation of mosquitoes. Nature protocols. 1 (3). p.pp. 1312–1317.

Lombardo, F., Di Cristina, M., Spanos, L., Louis, C., Coluzzi, M. & Arcà, B. (2000). Promoter sequences of the putative Anopheles gambiae apyrase confer salivary gland expression in Drosophila melanogaster. Journal of Biological Chemistry. 275 (31). p.pp. 23861–23868.

Lombardo, F., Nolan, T., Lycett, G., Lanfrancotti, A., Stich, N., Catteruccia, F., Louis, C., Coluzzi, M. & Arcà, B. (2005). An Anopheles gambiae salivary gland promoter analysis in Drosophila melanogaster and Anopheles stephensi. Insect Molecular Biology. 14 (2). p.pp. 207–216.

Lombardo, F., Lycett, G.J., Lanfrancotti, A., Coluzzi, M. & Arcà, B. (2009). Analysis of apyrase 5' upstream region validates improved Anopheles gambiae transformation technique. BMC research notes. 2. p.p. 24.

Lombardo, F., Ghani, Y., Kafatos, F.C. & Christophides, G.K. (2013). Comprehensive genetic dissection of the hemocyte immune response in the malaria mosquito Anopheles gambiae. PLoS Pathog. 9 (1). p.p. e1003145.

Lombardo, F. & Christophides, G.K. (2016). Novel factors of Anopheles gambiae haemocyte immune response to Plasmodium berghei infection. Parasites & Vectors. 9 (1). p.p. 78. Long, D., Lu, W., Zhang, Y., Bi, L., Xiang, Z. & Zhao, A. (2015). An efficient strategy for producing a stable, replaceable, highly efficient transgene expression system in silkworm, Bombyx mori. Scientific Reports. 5 (1). p.p. 8802.

Lorenzen, M.D., Brown, S.J., Denell, R.E. & Beeman, R.W. (2002). Transgene expression from the Tribolium castaneum Polyubiquitin promoter. Insect Molecular Biology. 11 (5). p.pp. 399–407.

Luckhart, S., Giulivi, C., Drexler, A.L., Antonova-Koch, Y., Sakaguchi, D., Napoli, E., Wong, S., Price, M.S., Eigenheer, R., Phinney, B.S., Pakpour, N., Pietri, J.E., Cheung, K., Georgis, M. & Riehle, M. (2013). Sustained Activation of Akt Elicits Mitochondrial Dysfunction to Block Plasmodium falciparum Infection in the Mosquito Host. PLoS Pathogens. 9 (2).

Lumjuan, N., McCarroll, L., Prapanthadara, L.A., Hemingway, J. & Ranson, H. (2005). Elevated activity of an Epsilon class glutathione transferase confers DDT resistance in the dengue vector, Aedes aegypti White star. Insect Biochemistry and Molecular Biology. 35 (8). p.pp. 861–871.

Lumjuan, N., Rajatileka, S., Changsom, D., Wicheer, J., Leelapat, P., Prapanthadara, L. aied, Somboon, P., Lycett, G. & Ranson, H. (2011). The role of the Aedes aegypti Epsilon glutathione transferases in conferring resistance to DDT and

pyrethroid insecticides. Insect Biochemistry and Molecular Biology. 41 (3). p.pp. 203–209.

Lycett, G.J., McLaughlin, L.A., Ranson, H., Hemingway, J., Kafatos, F.C., Loukeris, T.G. & Paine, M.J.I. (2006). Anopheles gambiae P450 reductase is highly expressed in oenocytes and in vivo knockdown increases permethrin susceptibility. Insect Molecular Biology. 15 (3). p.pp. 321–327.

Lycett, G.J., Amenya, D. & Lynd, A. (2012). The Anopheles gambiae alpha-tubulin-1b promoter directs neuronal, testes and developing imaginal tissue specific expression and is a sensitive enhancer detector. Insect Molecular Biology. 21 (1). p.pp. 79–88.

Lynd, A. & Lycett, G.J. (2011). Optimization of the Gal4-UAS system in an Anopheles gambiae cell line. Insect Molecular Biology. 20 (5). p.pp. 599–608.

Lynd, A. & Lycett, G.J. (2012). Development of the bi-partite Gal4-UAS system in the African malaria mosquito, Anopheles gambiae. PLoS ONE. 7 (2).

MacCallum, R.M., Redmond, S.N. & Christophides, G.K. (2011). An expression map for Anopheles gambiae. BMC Genomics. 12 (1). p.p. 620.

Makki, R., Cinnamon, E. & Gould, A.P. (2014). The Development and Functions of Oenocytes. Annual Review of Entomology. 59 (1). p.pp. 405–425.

Marcombe, S., Mathieu Blanc, R., Pocquet, N., Riaz, M.-A., Poupardin, R., Sélior, S., Darriet, F., Reynaud, S., Yébakima, A., Corbel, V., David, J.-P. & Chandre, F. (2AD). Insecticide Resistance in the Dengue Vector <italic>Aedes aegypti</italic> from Martinique: Distribution, Mechanisms and Relations with Environmental Factors. PLoS ONE. 7 (2). p.p. e30989.

Marinotti, O., Calvo, E., Dissanayake, S., Ribeiro, J. & James, A. (2006). Genome-wide analysis of gene expression in adult Anopheles gambiae. Insect Mol.Biol. 15 (1). p.pp. 1–12.

Marinotti, O., Jasinskiene, N., Fazekas, A., Scaife, S., Fu, G., Mattingly, S.T., Chow, K., Brown, D.M., Alphey, L. & James, A.A. (2013). Development of a population suppression strain of the human malaria vector mosquito, Anopheles stephensi. Malaria Journal. 12 (1). p.p. 142.

Markstein, M., Pitsouli, C., Villalta, C., Celniker, S.E. & Perrimon, N. (2008). Exploiting position effects and the gypsy retrovirus insulator to engineer precisely expressed transgenes. Nature Genetics. 40 (4). p.pp. 476–483.

Marois, E., Scali, C., Soichot, J., Kappler, C., Levashina, E.A. & Catteruccia, F. (2012). High-throughput sorting of mosquito larvae for laboratory studies and for future vector control interventions. Malaria Journal. 11 (1). p.p. 302.

Martin, T., Ochou, O.G., Vaissayre, M. & Fournier, D. (2003). Organophosphorus insecticides synergize pyrethroids in the resistant strain of cotton bollworm, Helicoverpa armigera (Hübner) (Lepidoptera: Noctuidae) from West Africa. Journal of economic entomology. 96 (2). p.pp. 468–474.

Martinez-Torres, D., Chandre, F., Williamson, M.S., Darriet, F., Bergé, J.B., Devonshire, A.L., Guillet, P., Pasteur, N. & Pauron, D. (1998). Molecular characterization of pyrethroid knockdown resistance (kdr) in the major malaria vector Anopheles gambiae s.s. Insect Molecular Biology. 7 (2). p.pp. 179–184.

Martins, G.F., Ramalho-Ortigão, J.M., Lobo, N.F., Severson, D.W., Mcdowell, M.A. & Pimenta, P.F.P. (2011). Insights into the transcriptome of oenocytes from aedes aegypti pupae. Memorias do Instituto Oswaldo Cruz. 106 (3). p.pp. 308–315.

Masumoto, M., Ohde, T., Shiomi, K., Yaginuma, T. & Niimi, T. (2012). A Baculovirus Immediate-Early Gene, ie1, Promoter Drives Efficient Expression of a Transgene in Both Drosophila melanogaster and Bombyx mori. PLoS ONE. 7 (11).

Matolcsy, G., Nadasy, M. & Andriska, V. (1988). Pesticide chemistry. Elsevier Science Publishing Co, NJ.

Matowo, J., Jones, C.M., Kabula, B., Ranson, H., Steen, K., Mosha, F., Rowland, M. & Weetman, D. (2014). Genetic basis of pyrethroid resistance in a population of Anopheles arabiensis, the primary malaria vector in Lower Moshi, north-eastern Tanzania. Parasites & Vectors. 7 (1). p.p. 274.

Matthews, B.J., McBride, C.S., DeGennaro, M., Despo, O. & Vosshall, L.B. (2016). The neurotranscriptome of the Aedes aegypti mosquito. BMC Genomics. 17 (1). p.p. 32.

McLaughlin, L.A., Niazi, U., Bibby, J., David, J.P., Vontas, J., Hemingway, J., Ranson, H., Sutcliffe, M.J. & Paine, M.J.I. (2008). Characterization of inhibitors and substrates of Anopheles gambiae CYP6Z2. Insect Molecular Biology. 17 (2). p.pp. 125–135.

McMeniman, C.J., Lane, R. V., Cass, B.N., Fong, A.W.C., Sidhu, M., Wang, Y.-F. & O'Neill, S.L. (2009). Stable Introduction of a Life-Shortening Wolbachia Infection into the Mosquito Aedes aegypti. Science. 323 (5910). p.pp. 141–144.

Mellanby, K. (1992). The DDT Story. British Crop Protection Council (CCPC), Unwin Brothers, Old Woking, Surrey, UK.

Menze, B.D., Riveron, J.M., Ibrahim, S.S., Irving, H., Antonio-Nkondjio, C., Awono-Ambene, P.H. & Wondji, C.S. (2016). Multiple Insecticide Resistance in the Malaria Vector Anopheles funestus from Northern Cameroon Is Mediated by Metabolic Resistance Alongside Potential Target Site Insensitivity Mutations. PLoS One. 11 (10):e0163261.

Meredith, J.M., Basu, S., Nimmo, D.D., Larget-Thiery, I., Warr, E.L., Underhill, A., McArthur, C.C., Carter, V., Hurd, H., Bourgouin, C. & Eggleston, P. (2011). Site-specific integration and expression of an anti-malarial gene in transgenic Anopheles gambiae significantly reduces Plasmodium infections. PLoS ONE. 6 (1). p.pp. 1–9.

Meredith, J.M., Underhill, A., McArthur, C.C. & Eggleston, P. (2013). Next-Generation Site-Directed Transgenesis in the Malaria Vector Mosquito Anopheles gambiae: Self-Docking Strains Expressing Germline-Specific phiC31 Integrase. PLoS ONE. 8 (3).

Messenger, L.A. & Rowland, M. (2017). Insecticide-treated durable wall lining (ITWL): future prospects for control of malaria and other vector-borne diseases. Malaria Journal. 16 (1). p.p. 213.

Meyers, J.I., Pathikonda, S., Popkin-Hall, Z.R., Medeiros, M.C., Fuseini, G., Matias, A., Garcia, G., Overgaard, H.J., Kulkarni, V., Reddy, V.P., Schwabe, C., Lines, J., Kleinschmidt, I. & Slotman, M.A. (2016). Increasing outdoor host-seeking in Anopheles gambiae over 6 years of vector control on Bioko Island. Malaria Journal. 15 (1). p.p. 239.

Misra, J.R., Horner, M.A., Lam, G. & Thummel, C.S. (2011). Transcriptional regulation of xenobiotic detoxification in Drosophila. Genes and Development. 25 (17). p.pp. 1796–1806.

Mitchell, S.N., Stevenson, B.J., Muller, P., Wilding, C.S., Egyir-Yawson, A., Field, S.G., Hemingway, J., Paine, M.J.I., Ranson, H. & Donnelly, M.J. (2012). Identification and validation of a gene causing cross-resistance between insecticide classes in Anopheles gambiae from Ghana. Proceedings of the National Academy of Sciences. 109 (16). p.pp. 6147–6152.

Mitchell, S.N., Rigden, D.J., Dowd, A.J., Lu, F., Wilding, C.S., Weetman, D., Dadzie, S., Jenkins, A.M., Regna, K., Boko, P., Djogbenou, L., Muskavitch, M.A.T., Ranson, H., Paine, M.J.I., Mayans, O. & Donnelly, M.J. (2014). Metabolic and target-site mechanisms combine to confer strong DDT resistance in Anopheles gambiae. PLoS ONE. 9 (3).

Mitra, R., Fain-Thornton, J. & Craig, N.L. (2008). piggyBac can bypass DNA synthesis during cut and paste transposition. The EMBO Journal. 27 (7). p.pp. 1097–1109.

Moreira, L.A., Iturbe-Ormaetxe, I., Jeffery, J.A., Lu, G., Pyke, A.T., Hedges, L.M., Rocha, B.C., Hall-Mendelin, S., Day, A., Riegler, M., Hugo, L.E., Johnson, K.N., Kay, B.H., McGraw, E.A., van den Hurk, A.F., Ryan, P.A. & O'Neill, S.L. (2009). A Wolbachia Symbiont in Aedes aegypti Limits Infection with Dengue, Chikungunya, and Plasmodium. Cell. 139 (7). p.pp. 1268–1278.

Morris, A.C., Eggleston, P. & Crampton, J.M. (1989). Genetic transformation of the mosquito Aedes aegypti by microinjection of DNA. Medical and Veterinary Entomology. 3 (1). p.pp. 1–7.

Mulamba, C., Riveron, J.M., Ibrahim, S.S., Irving, H., Barnes, K.G., Mukwaya, L.G., Birungi, J. & Wondji, C.S. (2014). Widespread pyrethroid and DDT resistance in the major malaria vector anopheles funestus in East Africa is driven by metabolic resistance mechanisms. PLoS ONE. 9 (10).

Müller, H.M., Catteruccia, F., Vizioli, J., della Torre, A. & Crisanti, A. (1995). Constitutive and blood meal-induced trypsin genes in Anopheles gambiae. Exp Parasitol. 81 (3). p.pp. 371–85.

Müller, P., Donnelly, M.J. & Ranson, H. (2007). Transcription profiling of a recently colonised pyrethroid resistant Anopheles gambiae strain from Ghana. BMC genomics. 8. p.p. 36.

Müller, P., Chouaïbou, M., Pignatelli, P., Etang, J., Walker, E.D., Donnelly, M.J., Simard, F. & Ranson, H. (2008a). Pyrethroid tolerance is associated with elevated expression of antioxidants and agricultural practice in Anopheles arabiensis sampled from an area of cotton fields in Northern Cameroon. Molecular Ecology. 17 (4). p.pp. 1145–1155.

Müller, P., Warr, E., Stevenson, B.J., Pignatelli, P.M., Morgan, J.C., Steven, A., Yawson, A.E., Mitchell, S.N., Ranson, H., Hemingway, J., Paine, M.J.I. & Donnelly, M.J. (2008b). Field-caught permethrin-resistant Anopheles gambiae overexpress CYP6P3, a P450 that metabolises pyrethroids. PLoS Genetics. 4 (11).

Najarro, M.A., Hackett, J.L., Smith, B.R., Highfill, C.A., King, E.G., Long, A.D. & Macdonald, S.J. (2015). Identifying Loci Contributing to Natural Variation in Xenobiotic Resistance in Drosophila. PLoS Genetics. 11 (11).

Nardini, L., Christian, R.N., Coetzer, N. & Koekemoer, L.L. (2013). DDT and pyrethroid resistance in Anopheles arabiensis from South Africa. Parasites & vectors. 6 (1). p.p. 229.

Newcomb, R.D., Campbell, P.M., Ollis, D.L., Cheah, E., Russell, R.J. & Oakeshott, J.G. (1997). A single amino acid substitution converts a carboxylesterase to an organophosphorus hydrolase and confers insecticide resistance on a blowfly. Proceedings of the National Academy of Sciences. 94 (14). p.pp. 7464–7468.

Nimmo, D.D., Alphey, L., Meredith, J.M. & Eggleston, P. (2006). High efficiency site-specific genetic engineering of the mosquito genome. Insect Molecular Biology. 15 (2). p.pp. 129–136.

Nirmala, X., Marinotti, O., Sandoval, J.M., Phin, S., Gakhar, S., Jasinskiene, N. & James, A.A. (2006). Functional characterization of the promoter of the vitellogenin gene, AsVg1, of the malaria vector, Anopheles stephensi. Insect Biochem Mol Biol. 36 (9). p.pp. 694–700.

Nkya, T.E., Akhouayri, I., Kisinza, W. & David, J.P. (2013). Impact of environment on mosquito response to pyrethroid insecticides: Facts, evidences and prospects. Insect Biochemistry and Molecular Biology. 43 (4). p.pp. 407–416.

Nolan, T., Bower, T.M., Brown, A.E., Crisanti, A. & Catteruccia, F. (2002). piggyBac-mediated germline transformation of the malaria mosquito Anopheles stephensi using the red fluorescent protein dsRED as a selectable marker. Journal of Biological Chemistry. 277 (11). p.pp. 8759–8762.

Nolan, T., Petris, E., Müller, H.M., Cronin, A., Catteruccia, F. & Crisanti, A. (2011). Analysis of two novel midgut-specific promoters driving transgene expression in Anopheles stephensi mosquitoes. PLoS ONE. 6 (2).

O'Brochta, D.A., Alford, R.T., Pilitt, K.L., Aluvihare, C.U. & Harrell, R.A. (2011). piggyBac transposon remobilization and enhancer detection in Anopheles mosquitoes. Proceedings of the National Academy of Sciences. 108 (39). p.pp. 16339–16344.

O'Brochta, D.A., Pilitt, K.L., Harrell 2nd, R.A., Aluvihare, C. & Alford, R.T. (2012). Gal4-based enhancer-trapping in the malaria mosquito Anopheles stephensi. G3 (Bethesda). 2 (11). p.pp. 1305–1315.

O'Brochta, D., A., George, K. & Xu, H. (2014). Transposons for Insect Transformation. In: Benedict, M.Q. (Ed). Transgenic Insects Techniques and Applications, CAB International, Boston, USA.

Olé Sangba, M.L., Sidick, A., Govoetchan, R., Dide-Agossou, C., Ossè, R.A., Akogbeto, M. & Ndiath, M.O. (2017). Evidence of multiple insecticide resistance mechanisms in Anopheles gambiae populations in Bangui, Central African Republic. Parasites & Vectors. 10 (1). p.p. 23.

Ortelli, F., Rossiter, L.C., Vontas, J., Ranson, H. & Hemingway, J. (2003). Heterologous expression of four glutathione transferase genes genetically linked to a major insecticide-resistance locus from the malaria vector Anopheles gambiae. Biochemical Journal. 373 (3). p.pp. 957–963.

Overend, G., Cabrero, P., Halberg, K.A., Ranford-Cartwright, L.C., Woods, D.J., Davies, S.A. & Dow, J.A.T. (2015). A comprehensive transcriptomic view of renal function in the malaria vector, Anopheles gambiae. Insect Biochemistry and Molecular Biology. 67. p.pp. 47–58.

Pachecho, C.A., Chaboli Alevi, K.C., Ravazi, A. & de Azeredo Oliveira, M.T.V. (2014). Review: Malpighian Tubule, an Essential Organ for Insects. Entomology, Ornithology & Herpetology: Current Research. 3 (2). p.pp. 1–3.

Padrón, A., Molina-Cruz, A., Quinones, M., Ribeiro, J.M., Ramphul, U., Rodrigues, J., Shen, K., Haile, A., Ramirez, J. & Barillas-Mury, C. (2014). In depth annotation of the Anopheles gambiae mosquito midgut transcriptome. BMC Genomics. 15 (1). p.p. 636.

Panini, M., Manicardi, G., Moores, G. & Mazzoni, E. (2016). An overview of the main pathways of metabolic resistance in insects. Isj. 13. p.pp. 326–335.

Papathanos, P.A., Bossin, H.C., Benedict, M.Q., Catteruccia, F., Malcolm, C.A., Alphey, L. & Crisanti, A. (2009a). Sex separation strategies: past experience and new approaches. Malaria Journal. 8 (Suppl 2). p.p. S5.

Papathanos, P.A., Windbichler, N., Menichelli, M., Burt, A. & Crisanti, A. (2009b). The vasa regulatory region mediates germline expression and maternal transmission of proteins in the malaria mosquito Anopheles gambiae: a versatile tool for genetic control strategies. BMC Molecular Biology. 10 (1). p.p. 65.

Perera, O.P., Harrell, R.A. & Handler, A.M. (2002). Germ-line transformation of the South American malaria vector, Anopheles albimanus, with a piggyBac/EGFP transposon vector is routine and highly efficient. Insect Molecular Biology. 11 (4). p.pp. 291–297.

Phuc, H., Andreasen, M.H., Burton, R.S., Vass, C., Epton, M.J., Pape, G., Fu, G., Condon, K.C., Scaife, S., Donnelly, C.A., Coleman, P.G., White-Cooper, H. & Alphey, L. (2007). Late-acting dominant lethal genetic systems and mosquito control. BMC Biology. 5 (1). p.p. 11.

Piccin, A., Salameh, A., Benna, C., Sandrelli, F., Mazzotta, G., Zordan, M., Rosato, E., Kyriacou, C.P. & Costa, R. (2001). Efficient and heritable functional knock-out of an adult phenotype in Drosophila using a GAL4-driven hairpin RNA incorporating a heterologous spacer. Nucleic acids research. 29 (12). p.pp. E55–E55.

Pondeville, E., David, J.P., Guittard, E., Maria, A., Jacques, J.C., Ranson, H., Bourgouin, C. & Dauphin-Villemant, C. (2013). Microarray and RNAi analysis of P450s in Anopheles gambiae male and female steroidogenic tissues: CYP307A1 is required for ecdysteroid synthesis. PLoS ONE. 8 (12).

Pondeville, E., Puchot, N., Meredith, J.M., Lynd, A., Vernick, K.D., Lycett, G.J., Eggleston, P. & Bourgouin, C. (2014). Efficient ΦC31 integrase–mediated site-specific germline transformation of Anopheles gambiae. Nature Protocols. 9 (7). p.pp. 1698–1712.

Poupardin, R., Riaz, M.A., Jones, C.M., Chandor-Proust, A., Reynaud, S. & David, J.P. (2012). Do pollutants affect insecticide-driven gene selection in mosquitoes? Experimental evidence from transcriptomics. Aquatic Toxicology. 114–115. p.pp. 49–57.

Poupardin, R., Riaz, M.A., Vontas, J., David, J.P. & Reynaud, S. (2010). Transcription profiling of eleven cytochrome p450s potentially involved in xenobiotic metabolism in the mosquito aedes aegypti. Insect Molecular Biology. 19 (2). p.pp. 185–193.

Poupardin, R., Srisukontarat, W., Yunta, C. & Ranson, H. (2014). Identification of Carboxylesterase Genes Implicated in Temephos Resistance in the Dengue Vector Aedes aegypti. PLoS Neglected Tropical Diseases. 8 (3).

Prapanthadara, L.A. & Ketterman, A.J. (1993). Qualitative and quantitative changes in glutathione S-transferases in the mosquito Anopheles gambiae confer DDT-resistance. Biochemical Society Transactions. 21 (Pt 3) (3):304S.

Pullikuth, A.K., Filippov, V. & Gill, S.S. (2003). Phylogeny and cloning of ion transporters in mosquitoes. J Exp Biol. 206 (21). p.pp. 3857–3868.

Raghavendra, K., Barik, T.K., Reddy, B.P.N., Sharma, P. & Dash, A.P. (2011). Malaria vector control: From past to future. Parasitology Research. 108 (4). p.pp. 757–779.

Ranson, H., Jensen, B., Vulule, J.M., Wang, X., Hemingway, J. & Collins, F.H. (2000). Identification of a point mutation in the voltage-gated sodium channel gene of Kenyan Anopheles gambiae associated with resistance to DDT and pyrethroids. Insect Molecular Biology. 9 (5). p.pp. 491–497.

Ranson, H., Rossiter, L., Ortelli, F., Jensen, B., Wang, X., Roth, C.W., Collins, F.H. & Hemingway, J. (2001). Identification of a novel class of insect glutathione S-transferases involved in resistance to DDT in the malaria vector Anopheles gambiae. Biochemical Journal. 359 (2). p.pp. 295–304.

Ranson, H., Nikou, D., Hutchinson, M., Wang, X., Roth, C.W., Hemingway, J. & Collins, F.H. (2002). Molecular analysis of multiple cytochrome P450 genes from the malaria vector, Anopheles gambiae. Insect Mol. Biol. 11 (5). p.pp. 409–418.

Ranson, H., N'Guessan, R., Lines, J., Moiroux, N., Nkuni, Z. & Corbel, V. (2011). Pyrethroid resistance in African anopheline mosquitoes: What are the implications for malaria control? Trends in Parasitology. 27 (2). p.pp. 91–98.

Ranson, H. & Lissenden, N. (2016). Insecticide Resistance in African Anopheles Mosquitoes: A Worsening Situation that Needs Urgent Action to Maintain Malaria Control. Trends in Parasitology. 32 (3) p.pp. 187–196.

Reddy, M.R., Overgaard, H.J., Abaga, S., Reddy, V.P., Caccone, A., Kiszewski, A.E. & Slotman, M.A. (2011). Outdoor host seeking behaviour of Anopheles gambiae mosquitoes following initiation of malaria vector control on Bioko Island, Equatorial Guinea. Malaria Journal. 10 (1). p.p. 184.

Remnant, E.J., Good, R.T., Schmidt, J.M., Lumb, C., Robin, C., Daborn, P.J. & Batterham, P. (2013). Gene duplication in the major insecticide target site, Rdl, in Drosophila melanogaster. Proceedings of the National Academy of Sciences. 110 (36). p.pp. 14705–14710.

Riabinina, O., Task, D., Marr, E., Lin, C.-C., Alford, R., O'Brochta, D.A. & Potter, C.J. (2016). Organization of olfactory centres in the malaria mosquito Anopheles gambiae. Nature Communications. 7. p.p. 13010.

Riaz, M.A., Chandor-Proust, A., Dauphin-Villemant, C., Poupardin, R., Jones, C.M., Strode, C., Régent-Kloeckner, M., David, J.P. & Reynaud, S. (2013). Molecular mechanisms associated with increased tolerance to the neonicotinoid insecticide imidacloprid in the dengue vector Aedes aegypti. Aquatic Toxicology. 126. p.pp. 326–337.

Ringrose, L. (2009). Transgenesis in Drosophila melanogaster' in Transgenesis Techniques. Volume 561 of the series Methods in Molecular Biology p.pp. 3-19.

Riveron, J.M., Irving, H., Ndula, M., Barnes, K.G., Ibrahim, S.S., Paine, M.J.I. & Wondji, C.S. (2013). Directionally selected cytochrome P450 alleles are driving the spread of pyrethroid resistance in the major malaria vector Anopheles funestus. Proceedings of the National Academy of Sciences. 110 (1). p.pp. 252–257.

Riveron, J.M., Ibrahim, S.S., Chanda, E., Mzilahowa, T., Cuamba, N., Irving, H., Barnes, K.G., Ndula, M. & Wondji, C.S. (2014a). The highly polymorphic CYP6M7 cytochrome P450 gene partners with the directionally selected CYP6P9a and CYP6P9b genes to expand the pyrethroid resistance front in the malaria vector Anopheles funestus in Africa. BMC genomics. 15 (1). p.p. 817.

Riveron, J.M., Yunta, C., Ibrahim, S.S., Djouaka, R., Irving, H., Menze, B.D., Ismail, H.M., Hemingway, J., Ranson, H., Albert, A. & Wondji, C.S. (2014b). A single mutation in the GSTe2 gene allows tracking of metabolically based insecticide resistance in a major malaria vector. Genome Biology. 15 (2). p.p. R27.

Riveron, J.M., Chiumia, M., Menze, B.D., Barnes, K.G., Irving, H., Ibrahim, S.S., Weedall, G.D., Mzilahowa, T. & Wondji, C.S. (2015). Rise of multiple insecticide resistance in Anopheles funestus in Malawi: a major concern for malaria vector control. Malaria Journal. 14 (1). p.p. 344.

Riveron, J.M., Ibrahim, S.S., Mulamba, C., Djouaka, R., Irving, H., Wondji, M.J., Ishak, I.H. & Wondji, C.S. (2017). Genome-Wide Transcription and Functional Analyses Reveal Heterogeneous Molecular Mechanisms Driving Pyrethroids Resistance in the Major Malaria Vector Anopheles funestus Across Africa. Genes|Genomes|Genetics. 7 (6). p.pp. 1819-1832.

Rodrigues, F.G., Oliveira, S.B., Rocha, B.C. & Moreira, L.A. (2006). Germline transformation of Aedes fluviatilis (Diptera: Culicidae) with the piggyBac transposable element. Memorias do Instituto Oswaldo Cruz. 101 (7). p.pp. 755–757.

Ronis, M.J. & Hodgson, E. (1989). Cytochrome P-450 monooxygenases in insects. Xenobiotica; the fate of foreign compounds in biological systems. 19 (10). p.pp. 1077–92.

Roseman, R.R., Pirrotta, V. & Geyer, P.K. (1993). The su(Hw) protein insulates expression of the Drosophila melanogaster white gene from chromosomal position-effects. The EMBO journal. 12 (2). p.pp. 435–42.

Rozhkov, N. V., Aravin, A.A., Zelentsova, E.S., Schostak, N.G., Sachidanandam, R., McCombie, W.R., Hannon, G.J. & Evgen'ev, M.B. (2010). Small RNA-based silencing strategies for transposons in the process of invading Drosophila species. RNA. 16 (8). p.pp. 1634–1645.

Rubin, G. & Spradling, A. (1982). Genetic transformation of Drosophila with transposable element vectors. Science. 218 (4570). p.pp. 348–353.

Russell, T.L., Govella, N.J., Azizi, S., Drakeley, C.J., Kachur, S.P. & Killeen, G.F. (2011). Increased proportions of outdoor feeding among residual malaria vector populations following increased use of insecticide-treated nets in rural Tanzania. Malaria Journal. 10 (1). p.p. 80.

Saner, C., Weibel, B., Würgler, F.E. & Sengstag, C. (1996). Metabolism of promutagens catalyzed by Drosophila melanogaster CYP6A2 enzyme in Saccharomyces cerevisiae. Environmental and Molecular Mutagenesis. 27 (1). p.pp. 46–58.

Sarkar, A., Atapattu, A., Belikoff, E.J., Heinrich, J.C., Li, X., Horn, C., Wimmer, E. a & Scott, M.J. (2006). Insulated piggyBac vectors for insect transgenesis. BMC biotechnology. 6. p.p. 27.

Schinko, J.B., Weber, M., Viktorinova, I., Kiupakis, A., Averof, M., Klingler, M., Wimmer, E.A. & Bucher, G. (2010). Functionality of the GAL4/UAS system in Tribolium requires the use of endogenous core promoters. BMC Developmental Biology. 10 (1). p.p. 53.

Schmidt, J.M., Good, R.T., Appleton, B., Sherrard, J., Raymant, G.C., Bogwitz, M.R., Martin, J., Daborn, P.J., Goddard, M.E., Batterham, P. & Robin, C. (2010). Copy number variation and transposable elements feature in recent, ongoing adaptation at the Cyp6g1 locus. PLoS Genetics. 6 (6). p.pp. 1–11.

Schmittgen, T.D. & Livak, K.J. (2008). Analyzing real-time PCR data by the comparative C T method. Nature Protocols. 3 (6). p.pp. 1101–1108.

Scott, J.G. (2008). Insect cytochrome P450s: thinking beyond detoxification. Recent advances in insect physiology, toxicology and molecular biology. 661 (2). p.pp. 117–124.

Shaw, M. (1991). Lipoproteins as Carriers of Pharmacological Agents. CRC Press

Sieglaff, D.H., Dunn, W.A., Xie, X.S., Megy, K., Marinotti, O. & James, A.A. (2009). Comparative genomics allows the discovery of cis-regulatory elements in mosquitoes. Proceedings of the National Academy of Sciences of the United States of America. 106 (9). p.pp. 3053–3058.

Sinka, M.E., Bangs, M.J., Manguin, S., Coetzee, M., Mbogo, C.M., Hemingway, J., Patil, A.P., Temperley, W.H., Gething, P.W., Kabaria, C.W., Okara, R.M., Van Boeckel, T., Godfray, H.C.J., Harbach, R.E. & Hay, S.I. (2010a). The dominant Anopheles vectors of human malaria in Africa, Europe and the Middle East: occurrence data, distribution maps and bionomic précis. Parasites & Vectors. 3 (1). p.p. 117.

Sinka, M.E., Rubio-Palis, Y., Manguin, S., Patil, A.P., Temperley, W.H., Gething, P.W., Van Boeckel, T., Kabaria, C.W., Harbach, R.E. & Hay, S.I. (2010b). The dominant Anopheles vectors of human malaria in the Americas: occurrence data, distribution maps and bionomic précis. Parasites & Vectors. 3 (1). p.p. 72.

Sinka, M.E., Bangs, M.J., Manguin, S., Chareonviriyaphap, T., Patil, A.P., Temperley, W.H., Gething, P.W., Elyazar, I.R., Kabaria, C.W., Harbach, R.E. & Hay, S.I. (2011). The dominant Anopheles vectors of human malaria in the Asia-Pacific region: occurrence data, distribution maps and bionomic précis. Parasites & Vectors. 4 (1). p.p. 89.

Sinka, M.E., Bangs, M.J., Manguin, S., Rubio-Palis, Y., Chareonviriyaphap, T., Coetzee, M., Mbogo, C.M., Hemingway, J., Patil, A.P., Temperley, W.H., Gething, P.W., Kabaria, C.W., Burkot, T.R., Harbach, R.E. & Hay, S.I. (2012). A global map of dominant malaria vectors. Parasites & Vectors. 5 (1). p.p. 69.

Sinkins, S. P. & Gould, F. (2006). Gene drive systems for insect disease vectors, Nature Reviews Genetics. 7. p.pp. 427–435.

Smidler, A.L., Terenzi, O., Soichot, J., Levashina, E.A. & Marois, E. (2013). Targeted Mutagenesis in the Malaria Mosquito Using TALE Nucleases. PLoS ONE. 8 (8). p.pp. 1–10.

Sokhna, C., Ndiath, M.O. & Rogier, C. (2013). The changes in mosquito vector behaviour and the emerging resistance to insecticides will challenge the decline of malaria. Clinical Microbiology and Infection. 19 (10) p.pp. 902–907.

Sougoufara, S., Diédhiou, S., Doucouré, S., Diagne, N., Sembène, P., Harry, M., Trape, J.-F., Sokhna, C. & Ndiath, M. (2014). Biting by Anopheles funestus in broad daylight after use of long-lasting insecticidal nets: a new challenge to malaria elimination. Malaria Journal. 13 (1). p.p. 125.

Stevenson, B.J., Bibby, J., Pignatelli, P., Muangnoicharoen, S., O'Neill, P.M., Lian, L.Y., Müller, P., Nikou, D., Steven, A., Hemingway, J., Sutcliffe, M.J. & Paine, M.J.I. (2011). Cytochrome P450 6M2 from the malaria vector Anopheles gambiae metabolizes pyrethroids: Sequential metabolism of deltamethrin revealed. Insect Biochemistry and Molecular Biology. 41 (7). p.pp. 492–502.

Stevenson, B.J., Pignatelli, P., Nikou, D. & Paine, M.J.I. (2012). Pinpointing P450s associated with pyrethroid metabolism in the dengue vector, Aedes aegypti: Developing new tools to combat insecticide resistance. PLoS Neglected Tropical Diseases. 6 (3).

Strode, C., Wondji, C.S., David, J.P., Hawkes, N.J., Lumjuan, N., Nelson, D.R., Drane, D.R., Karunaratne, S.H.P.P., Hemingway, J., Black IV, W.C. & Ranson, H. (2008). Genomic analysis of detoxification genes in the mosquito Aedes aegypti. Insect Biochemistry and Molecular Biology. 38 (1). p.pp. 113–123.

Tamura, T., Thibert, C., Royer, C., Kanda, T., Eappen, A., Kamba, M., Kômoto, N., Thomas, J.-L., Mauchamp, B., Chavancy, G., Shirk, P., Fraser, M., Prudhomme, J.-C. & Couble, P. (2000). Germline transformation of the silkworm Bombyx mori L. using a piggyBac transposon-derived vector. Nature Biotechnology. 18 (1). p.pp. 81–84.

Thomas, D.D. (2000). Insect Population Control Using a Dominant, Repressible, Lethal Genetic System. Science. 287 (5462). p.pp. 2474–2476.

Thorpe, H.M. & Smith, M.C.M. (1998). In vitro site-specific integration of bacteriophage DNA catalyzed by a recombinase of the resolvase/invertase family. Proceedings of the National Academy of Sciences. 95 (10). p.pp. 5505–5510.

Tiono, A.B., Pinder, M., N'Fale, S., Faragher, B., Smith, T., Silkey, M., Ranson, H. & Lindsay, S.W. (2015). The AvecNet Trial to assess whether addition of pyriproxyfen, an insect juvenile hormone mimic, to long-lasting insecticidal mosquito nets provides additional protection against clinical malaria over current best practice in an area with pyrethroid-resistant vectors in rural Burkina Faso: study protocol for a randomised controlled trial. Trials. 16. pp. 113.

Toé, K.H., Jones, C.M., N'fale, S., Ismai, H.M., Dabiré, R.K. & Ranson, H. (2014). Increased pyrethroid resistance in malaria vectors and decreased bed net effectiveness Burkina Faso. Emerging Infectious Diseases. 20 (10). p.pp. 1691–1696.

Tomita, T., Liu, N., Smith, F.F., Sridhar, P. & Scott, J.G. (1995). Molecular mechanisms involved in increased expression of a cytochrome P450 responsible for pyrethroid resistance in the housefly, Musca domestica. Insect Molecular Biology. 4 (3). p.pp. 135–140.

Tomoyasu, Y., Miller, S.C., Tomita, S., Schoppmeier, M., Grossmann, D. & Bucher, G. (2008). Exploring systemic RNA interference in insects: a genome-wide survey for RNAi genes in Tribolium. Genome Biology. 9 (1). p.p. R10.

Tu, Z. (2012). Insect Transposable Elements. Elsevier B.V.

Venken, K.J.T., He, Y., Hoskins, R.A. & Bellen, H.J. (2006). P[acman]: A BAC Transgenic Platform for Targeted Insertion of Large DNA Fragments in D. melanogaster. Science. 314 (5806). p.pp. 1747–1751.

Vijverberg, H., van der Zalm, J. & van den Bercken, J. (1982). Similar mode of action of pyrethroids and DDT on sodium channel gating in myelinated nerves. Nature. 295 (5850). p.pp. 601–603.

Volohonsky, G., Hopp, A.K., Saenger, M., Soichot, J., Scholze, H., Boch, J., Blandin, S.A. & Marois, E. (2017). Transgenic Expression of the Anti-parasitic Factor TEP1 in the Malaria Mosquito Anopheles gambiae. PLoS Pathogens. 13 (1). p.pp. 1–26.

Volohonsky, G., Terenzi, O., Soichot, J., Naujoks, D.A., Nolan, T., Windbichler, N., Kapps, D., Smidler, A.L., Vittu, A., Costa, G., Steinert, S., Levashina, E.A., Blandin, S.A. & Marois, E. (2015). Tools for Anopheles gambiae Transgenesis. Genes|Genomes|Genetics. 5 (6). p.pp. 1151–1163.

Vontas, J.G., Small, G.J. & Hemingway, J. (2001). Glutathione S-transferases as antioxidant defence agents confer pyrethroid resistance in Nilaparvata lugens. Biochemical Journal. 357 (1). p.pp. 65–72.

Vontas, J., Blass, C., Koutsos, A.C., David, J.P., Kafatos, F.C., Louis, C., Hemingway, J., Christophides, G.K. & Ranson, H. (2005). Gene expression in insecticide resistant and susceptible Anopheles gambiae strains constitutively or after insecticide exposure. Insect Molecular Biology. 14 (5). p.pp. 509–521.

Wang, J., Kean, L., Yang, J., Allan, A.K., Davies, S.A., Herzyk, P. & Dow, J.A.T. (2004). Function-informed transcriptome analysis of Drosophila renal tubule. Genome biology. 5 (9). p.p. R69.

Wang, L., Nomura, Y., Du, Y., Liu, N., Zhorov, B.S., Dong, K. (2015). A mutation in the intracellular loop III/IV of mosquito sodium channel synergizes the effect of mutations in helix IIS6 on pyrethroid resistance. Moleculat Pharmacology. 87 (3). p.pp. 421–9.

Warren, W.D., Atkinson, P.W. & O'Brochta, D.A. (1994). The Hermes transposable element from the house fly, Musca domestica, is a short inverted repeat-type element of the hobo, Ac, and Tam3 (hAT) element family. Genet Res. 64 (2). p.pp. 87–97.

Weill, M., Malcolm, C., Chandre, F., Mogensen, K., Berthomieu, A., Marquine, M. & Raymond, M. (2004). The unique mutation in ace-1 giving high insecticide resistance is easily detectable in mosquito vectors. Insect Molecular Biology. 13 (1). p.pp. 1–7.

White, M.T., Conteh, L., Cibulskis, R. & Ghani, A.C. (2011). Costs and cost-effectiveness of malaria control interventions - a systematic review. Malaria Journal. 10 (1). p.p. 337.

WHO (2006). Pesticides and their application for the control of vectors and pests of public health importance. World Health Organization. 1 (6). p.pp. 1–104.

WHO (2009). 'WHO recommended insecticides for indoor residual spraying against malaria vectors'. http://www.who.int/whopes/Insecticides_IRS_Malaria_09.pdf.

WHO (2011). Guidelines for monitoring the durability of long-lasting insecticidal mosquito nets under operational conditions. WHO/HTM/NTD/WHOPES/2011.5. p.p. 44.

WHO (2012a). 'WHO recommended long-lasting insecticidal mosquito nets' http://www.who.int/whopes/Long_lasting_insecticidal_nets_Jul_2012.pdf.

WHO (2012b). Global plan for insecticide resistance management (GPIRM) in malaria vectors. World Health Organization press. p.p. 13.

WHO (2015a). 'Indoor residual spraying: An operational manual for IRS for malaria transmission, control and elimination. Second edition'.

WHO (2015b). 'Conditions for use of long-lasting insecticidal nets treated with a pyrethroid and piperonyl butoxide'.

WHO (2016a). World Malaria Report.

WHO (2016b). 'Test procedures for insecticide resistance monitoring in malaria vector mosquitoes, Second Edition'. Geneva, World Health Organization.

Wilding, C.S., Smith, I., Lynd, A., Yawson, A.E., Weetman, D., Paine, M.J.I. & Donnelly, M.J. (2012). A cis-regulatory sequence driving metabolic insecticide resistance in mosquitoes: Functional characterisation and signatures of selection. Insect Biochemistry and Molecular Biology. 42 (9). p.pp. 699–707.

Williamson, A. & Lehmann, R. (1996). Germ cell development in Drosophila. Annual review of cell and developmental biology. 12. p.pp. 365–391.

Williamson, M.S., Denholm, I., Bell, C.A. & Devonshire, A.L. (1993). Knockdown resistance (kdr) to DDT and pyrethroid insecticides maps to a sodium channel gene locus in the housefly (Musca domestica). MGG Molecular & General Genetics. 240 (1). p.pp. 17–22.

Wimmer, E.A. (2005). Insect transgenesis by site-specific recombination. Nature Methods. 2 (8). p.pp. 580–582.

Windbichler, N., Papathanos, P.A. & Crisanti, A. (2008). Targeting the X chromosome during spermatogenesis induces Y chromosome transmission ratio distortion and early dominant embryo lethality in Anopheles gambiae. PLoS Genetics. 4 (12).

Wondji, C.S., Irving, H., Morgan, J., Lobo, N.F., Collins, F.H., Hunt, R.H., Coetzee, M., Hemingway, J. & Ranson, H. (2009). Two duplicated P450 genes are associated with pyrethroid resistance in Anopheles funestus, a major malaria vector. Genome Research. 19 (3). p.pp. 452–459.

Wondji, C.S., Dabire, R.K., Tukur, Z., Irving, H., Djouaka, R. & Morgan, J.C. (2011). Identification and distribution of a GABA receptor mutation conferring dieldrin resistance in the malaria vector Anopheles funestus in Africa. Insect Biochemistry and Molecular Biology. 41 (7). p.pp. 484–491.

Wood, O.R., Hanrahan, S., Coetzee, M., Koekemoer, L.L. & Brooke, B.D. (2010). Cuticle thickening associated with pyrethroid resistance in the major malaria vector Anopheles funestus. Parasites & Vectors. 3 (1). p.p. 67.

Wright, A.T. & Cravatt, B.F. (2007). Chemical Proteomic Probes for Profiling Cytochrome P450 Activities and Drug Interactions In Vivo. Chemistry and Biology. 14 (9). p.pp. 1043–1051.

Xu, C., Li, C.Y.-T. & Kong, A.-N.T. (2005). Induction of phase I, II and III drug metabolism/transport by xenobiotics. Archives of Pharmacal Research. 28 (3). p.pp. 249–268.

Xue, Z., Wu, M., Wen, K., Ren, M., Long, L., Zhang, X. & Gao, G. (2014). CRISPR/Cas9 Mediates Efficient Conditional Mutagenesis in Drosophila. Genes|Genomes|Genetics. 4 (11). p.pp. 2167–2173.

Yahouédo, G.A., Cornelie, S., Djègbè, I., Ahlonsou, J., Aboubakar, S., Soares, C., Akogbéto, M. & Corbel, V. (2016). Dynamics of pyrethroid resistance in malaria vectors in southern Benin following a large scale implementation of vector control interventions. Parasites & Vectors. 9 (1). p.p. 385.

Yang, J., McCart, C., Woods, D.J., Terhzaz, S., Greenwood, K.G., Ffrench-Constant, R.H. & Dow, J.A.T. (2007). A Drosophila systems approach to xenobiotic metabolism. Physiological genomics. 30 (3). p.pp. 223–31.

Yang, T. & Liu N. (2011). Genome analysis of cytochrome P450s and their expression profiles in insecticide resistant mosquitoes, Culex quinquefasciatus. PLoS One. 6 (12):e29418.

Yewhalaw, D., Wassie, F., Steurbaut, W., Spanoghe, P., Van Bortel, W., Denis, L., Tessema, D.A., Getachew, Y., Coosemans, M., Duchateau, L. & Speybroeck, N. (2011). Multiple Insecticide Resistance: An Impediment to Insecticide-Based Malaria Vector Control Program. PLoS ONE. 6 (1). p.p. e16066.

Yoshida, S. & Watanabe, H. (2006). Robust salivary gland-specific transgene expression in Anopheles stephensi mosquito. Insect Molecular Biology. 15 (4). p.pp. 403–410.

Young, S.J., Gunning, R. V. & Moores, G.D. (2005). The effect of piperonyl butoxide on pyrethroid-resistance-associated esterases in Helicoverpa armigera (Hubner) (Lepidoptera: Noctuidae). Pest Management Science. 61 (4). p.pp. 397–401.

Yu, Z., Zhang, X., Wang, Y., Moussian, B., Zhu, K.Y., Li, S., Ma, E. & Zhang, J. (2016). LmCYP4G102: An oenocyte-specific cytochrome P450 gene required for cuticular waterproofing in the migratory locust, Locusta migratoria. Scientific Reports, 6:29980.

Yunta, C., Grisales, N., Nász, S., Hemmings, K., Pignatelli, P., Voice, M., Ranson, H. & Paine, M.J.I. (2016). Pyriproxyfen is metabolized by P450s associated with pyrethroid resistance in An. gambiae. Insect Biochemistry and Molecular Biology. 78. p.pp. 50–57.

Zhu, F., Parthasarathy, R., Bai, H., Woithe, K., Kaussmann, M., Nauen, R., Harrison, D.A. & Palli, S.R. (2010). A brain-specific cytochrome P450 responsible for the majority of deltamethrin resistance in the QTC279 strain of Tribolium castaneum. Proceedings of the National Academy of Sciences. 107 (19). p.pp. 8557–8562.

Zhu, G., Zhong, D., Cao, J., Zhou, H., Li, J., Liu, Y., Bai, L., Xu, S., Wang, M.-H., Zhou, G., Chang, X., Gao, Q. & Yan, G. (2014). Transcriptome profiling of pyrethroid resistant and susceptible mosquitoes in the malaria vector, Anopheles sinensis. BMC Genomics. 15 (1). p.p. 448.

Zimmer, C.T, Garrood, W.T., Puinean, A.M., Eckel-Zimmer, M., Williamson, M.S., Davies, T.G.E., & Bass, C. (2016). A CRISPR/Cas9 mediated point mutation in the alpha 6 subunit of the nicotinic acetylcholine receptor confers resistance to

spinosad in Drosophila melanogaster. Insect Biochemistry and Molecular Biology. 73. p.pp. 62–69.